

ORGANOCATALYTIC APPROACHES TO ASYMMETRIC OXIDATION:

Epoxidation of α -Branched Enals

and α -Benzoyloxylation of Carbonyl Compounds

In a u g u r a l - D i s s e r t a t i o n

zur

Erlangung des Doktorgrades

der Mathematisch-Naturwissenschaftlichen Fakultät

der Universität zu Köln

vorgelegt von

Olga Lifchits

aus Minusinsk (Russland)

Köln 2012

Berichterstatter: Prof. Dr. Benjamin List

Prof. Dr. Hans-Günther Schmalz

Prof. Dr. Axel Klein

Tag der mündlichen Prüfung: 3 April 2012

Table of Contents

ABSTRACT	IV
LIST OF ABBREVIATIONS	V
ACKNOWLEDGEMENTS	VIII
1. INTRODUCTION	1
2. BACKGROUND	4
2.1. Asymmetric Organocatalysis	4
2.1.1 Introduction	4
2.1.2 Classification of Modern Organocatalysis	5
2.1.2 Aminocatalysis	6
2.1.2.1 Asymmetric Counteranion-Directed Catalysis (ACDC)	8
2.1.2.2 Primary Amine Salt Catalysis	9
2.1.2.3 Primary Amine Catalysts Derived from the Cinchona Alkaloids	12
2.1.2.4 Dienamine Catalysis: A Special Case of Selectivity	15
2.2 Catalytic Asymmetric Epoxidation of Electron-Deficient Olefins	18
2.2.1 Overview of Catalytic Asymmetric Epoxidation	18
2.2.2 <i>Weitz-Scheffer</i> Epoxidation	19
2.2.3 Organocatalytic (Lewis Base) Approaches to Epoxidation	21
2.2.4 Enantioselective Epoxidation of α -Branched Enals	25
2.2.5 Synthetic Versatility of α -Substituted α,β -Epoxyaldehydes	27
2.3 Catalytic Asymmetric α-Oxidation of Carbonyl Compounds	29
2.3.1 Historical Overview	29
2.3.2 Organocatalytic Approaches	31
2.3.2.1 Benzoyl Peroxide as the Electrophilic Oxidant	33
2.3.3 Primary Aminocatalysis in the α -Oxidation of Carbonyl Compounds	34
3. OBJECTIVES OF THIS PH.D. WORK	36
4. RESULTS AND DISCUSSION	40
4.1 Catalytic Asymmetric Epoxidation of α-Branched Enals	40
4.1.1. Identification of a Model System	40
4.1.2 Optimization of the Reaction Parameters.....	41
4.1.3 The Fate of Excess Hydrogen Peroxide and Optimization of Workup.....	49
4.1.4 Optimization of Reaction Conditions for α -Substituted Acroleins	51
4.1.5 Reaction Scope and Discussion.....	54

Table of Contents

4.1.5.1 Preparation of the Starting Materials.....	54
4.1.5.2 The Scope of α,β -Disubstituted Enals	56
4.1.5.3 The Scope of α -Substituted Acroleins.....	60
4.1.6 Mechanistic Studies.....	63
4.1.6.1 Investigation of Catalytic Intermediates.....	63
4.1.6.2 Investigation of Absolute Stereochemistry in the Epoxidation of Substrates 53	70
4.2 Catalytic Asymmetric α-Benzoyloxylation of Carbonyl Compounds.....	89
4.2.1 α -Benzoyloxylation of Cyclic Ketones	89
4.2.1.1 Identification of a Model System	89
4.2.1.2 Optimization of the Reaction Parameters.....	93
4.2.1.3 Reaction Scope and Discussion.....	101
4.2.1.4 Asymmetric Total Synthesis of Cineole Monoterpenoids.....	105
4.2.1.5 Mechanistic Considerations.....	108
4.2.2 α -Benzoyloxylation of α -Branched Aldehydes.....	116
4.2.2.1 Development and Optimization of the Catalytic System	116
4.2.2.2 Preliminary Reaction Scope and Discussion.....	122
4.2.3 α -Benzoyloxylation of α -Branched Enals	125
4.2.3.1 Development and Optimization of the Catalytic System	126
4.2.3.2 Investigations on α/γ Selectivity	130
5. SUMMARY.....	132
6. OUTLOOK	140
6.1 Epoxidation of Sterically Hindered Electron-Deficient Olefins	140
6.2 Benzoyloxylation of Carbonyl Compounds.....	144
7. EXPERIMENTAL SECTION	146
7.1 General Experimental Conditions.....	146
7.2 Catalytic Asymmetric Epoxidation of α-Branched Enals.....	150
7.2.1 Preparation of the Starting Materials	150
7.2.2 General Epoxidation Procedures.....	157
7.2.2.1 Epoxidation of α,β -Disubstituted Enals 53	157
7.2.2.2 Epoxidation of α -Substituted Acroleins 66	158
7.2.3 Scope of Enantioenriched α,β -Epoxyaldehydes.....	159
7.2.3.1 α,β -Disubstituted Epoxyaldehydes 54	159
7.2.3.2 α -Substituted Epoxyaldehydes 67	168
7.2.4 Studies on the <i>N</i> -oxidation of catalyst 9	172

Table of Contents

7.2.4.1. Synthesis of 9-amino(9-deoxy) <i>epiquinine N</i> -oxide (78).....	172
7.2.4.2 Kinetic studies	173
7.2.4.3 Reduction of 9-amino(9-deoxy) <i>epiquinine N</i> -oxide 78 to 9-amino(9-deoxy) <i>epiquinine</i> 9	174
7.2.5 NMR Investigations of Imine Salts 80	175
7.2.6 Synthesis of 9-hydroxylamino(9-deoxy) <i>epiquinine</i> 140	187
7.3 Catalytic Asymmetric α-Benzoyloxylaton of Carbonyl Compounds.....	188
7.3.1 Preparation of the Starting Materials	188
7.3.2 General α -Benzoyloxylaton Procedures.....	193
7.3.2.1 α -Benzoyloxylaton of Cyclic Ketones 83	193
7.3.2.2 α -Benzoyloxylaton of α -Branched Aldehydes 117	194
7.3.2.3 α -Benzoyloxylaton of α -Branched Enals 53b-c	195
7.3.3 Scope of Enantioenriched α -Benzoyloxylated Carbonyl Compounds.....	196
7.3.3.1 α -Benzoyloxylated Cyclic Ketones 84	196
7.3.3.2 α -Benzoyloxylated α -Substituted Aldehydes 118	205
7.3.3.3 Benzoyloxylaton of Enals	211
7.3.4 Asymmetric Synthesis of Cineole Derivatives 108 and 114	214
7.3.5 Synthesis and Characterization of 115	219
7.3.6 α - Chlorination and α -Fluorination of α -Branched Enal 53c	220
7.3.6.1 General Procedures.....	220
7.3.6.1 Product Characterization	221
7.4 Catalytic Asymmetric α-Amination of α-Branched Enal 53c^[25e]	223
7.4.1 Synthesis and Characterization	223
7.4.2 Crystallographic Data.....	224
8. BIBLIOGRAPHY	228
9. APPENDIX	235
9.1 Structure Index	235
9.2 Erklärung.....	240
9.3 Lebenslauf.....	241

Abstract

This work describes the development of enantioselective oxidation reactions of carbonyl compounds using covalent organocatalysis. In the first part, asymmetric epoxidation of α -branched α,β -unsaturated aldehydes with aqueous hydrogen peroxide is presented. An exceptionally synergistic combination of a primary cinchona alkaloid-derived amine and a chiral BINOL-derived phosphoric acid was found to promote the reaction with excellent enantiocontrol for a wide variety of α,β -disubstituted and α -monosubstituted enals. Conformational analysis of catalytically relevant intermediates using NMR and computational techniques enabled the rationalization of the absolute stereochemistry of products. The second part of this thesis describes a highly efficient direct catalytic asymmetric α -benzoyloxylation of cyclic ketones. The same primary amine paired with an inorganic acid was found to be an effective catalyst for a wide range of substrates. The methodology was applied to the first asymmetric synthesis of (+)-2 β ,4-dihydroxy-1,8-cineole, a predicted terpenoid metabolite in mammals. Preliminary investigations on the α -benzoyloxylation of α -branched aldehydes and α -branched enals using this catalytic system demonstrated significant potential of the method for the enantioselective formation of oxygenated quaternary stereocenters.

Die vorliegende Arbeit beschreibt die Entwicklung enantioselektiver Oxidationsreaktionen von Carbonylverbindungen durch kovalente Organokatalyse. Der erste Teil behandelt die asymmetrische Epoxidierung von α -verzweigten α,β -ungesättigten Aldehyden mit wässrigem Wasserstoffperoxid. Unter Einsatz eines äußerst kooperativen Katalysatorsystems, bestehend aus einem primären Amin mit Cinchona-Grundgerüst und einer BINOL-Phosphorsäure, verläuft die Reaktion mit exzellenter Enantioselektivität und hoher Variabilität der Ausgangsverbindungen. Durch Konformationsanalyse der katalytisch relevanten Intermediate mittels NMR-Spektroskopie und DFT-Berechnungen wurde die absolute Konfiguration der Produkte nachvollzogen. Im zweiten Teil dieser Arbeit wird die Entwicklung der katalytischen asymmetrischen α -Benzoyloxylierung von cyclischen Ketonen beschrieben. Hierbei ermöglicht das selbe primäre Amin als Katalysator einen direkten Zugang zu den wertvollen Benzoyl-geschützten 2-Hydroxyketonen. Die entwickelte Methode wurde in einer asymmetrischen Totalsynthese von (+)-2 β ,4-dihydroxy-1,8-Cineol angewendet. Eine Übertragung dieser Methode auf die α -Benzoyloxylierung von α -verzweigten Aldehyden und α -verzweigten Enalen zeigte ein hohes Potenzial für die enantioselektive Herstellung oxygenierter quarternärer Stereozentren.

List of Abbreviations

Ac	acetyl
ACDC	asymmetric counteranion-directed catalysis
AcO	acetate
Alk	alkyl
Aliph	aliphatic
app.	apparent
Ar	aryl, aromatic
aq.	Aqueous
ax	axial
calcd	calculated
BINAM	2,2'-diamino-1,1'-binaphthalene
BINAP	2,2'-bis(diphenylphosphino)-1,1'-binaphthyl
BINOL	1,1'-bi-2-naphthol
BIPP	3,3'-bis-phenyl-1,1'-binaphthyl-2,2'-diyl hydrogen phosphate
Bn	benzyl
Boc	<i>tert</i> -butyloxycarbonyl
brsm	based on the recovered starting material
Bu	butyl
c.	centered
C	cinchonine
Calcd	calculated
cat.	catalyst/catalytic
CD	cinchonidine
CHP	cumene hydroperoxide
conv.	Conversion
CSA	camphorsulfonic acid
Cy	cyclohexyl
cycl.	cyclic
d	doublet
d	day(s)
DET	diethyl tartrate
DFT	density functional theory
DIAD	diisopropyl azodicarboxylate
DKR	dynamic kinetic resolution
DME	dimethyl ether
DMF	dimethylformamide
DMM	dimethoxymethane
DMSO	dimethylsulfoxide
DOSY	diffusion ordered spectroscopy
DPEN	1,2-diphenylethylenediamine
DPPA	diphenylphosphoryl azide
DPP	diphenyl phosphoric acid
dr	diastereomeric ratio
E	electrophile
EI	electron impact
ee	enantiomeric excess
EM	exact mass
<i>ent</i>	enantiomer(ic)
epox	epoxide

List of Abbreviations

eq	equatorial
equiv	equivalent(s)
er	enantiomeric ratio
Et	ethyl
ESI	electrospray ionization
GC (GC-MS)	gas chromatography (gas chromatography coupled with mass detection)
h	hour(s)
HMDS	hexamethyldisilazane
HOESY	heteronuclear Overhauser effect spectroscopy
HOMO	highest occupied molecular orbital
HPLC	high performance liquid chromatography
HRMS	high resolution mass spectrometry
<i>i</i>	iso
IPC	ion pair chromatography
iso	isocratic (temperature regime in GC)
KMDS	potassium hexamethyldisilazane (potassium bis(trimethylsilyl amide))
KR	kinetic resolution
LA	Lewis acid
LDA	lithium diisopropylamide
Lit.	literature
LUMO	lowest unoccupied molecular orbital
<i>m</i>	<i>meta</i>
m	multiplet
M	molar (concentration)
<i>m</i> -CPBA	<i>meta</i> -chloroperbenzoic acid
Me	methyl
Mes	mesityl (2,4,6-trimethylphenyl)
MM	molecular mechanics
MS	mass spectrometry, molecular sieves
Ms	methylsulfonyl
MTBE	methyl <i>tert</i> -butyl ether
MW	molecular weight
<i>m/z</i>	atomic mass units per charge
<i>n</i>	normal
N	normal (concentration)
n.a.	not available
NaHMDS	sodium hexamethyldisilazane (sodium bis(trimethylsilyl amide))
NCS	<i>N</i> -chlorosuccinimide
n.d.	not determined
NFSI	<i>N</i> -fluorobenzenesulfonimide
NHC	<i>N</i> -heterocyclic carbene
9-NH ₂ -Q	9-amino(9-deoxy)quinine
9-NH ₂ - <i>epi</i> Q	9-amino(9-deoxy) <i>epi</i> quinine
9-NH ₂ - <i>epi</i> QD	9-amino(9-deoxy) <i>epi</i> quinidine
NMO	
NMR	nuclear magnetic resonance spectroscopy
NOE(SY)	nuclear Overhauser effect (spectroscopy)
Nu-H/Nu	nucleophile
Ns	nosyl, 4-nitrobenzenesulfonyl
<i>o</i>	<i>ortho</i>
P	product

List of Abbreviations

<i>p</i>	<i>para</i>
PCC	pyridinium chloro chromate
Ph	phenyl
PHK	peroxyhemiketal
Pr	propyl
pTSA	<i>para</i> -toluenesulfonic acid
Py	pyridine
quint	quintet
<i>rac.</i>	racemic
r.t.	room temperature
S	substrate
sept	septet
sext	sextet
SM	starting material
SOMO	singly occupied molecular orbital
5-SSA	5-sulfosalicylic acid
<i>t</i>	<i>tert, tertiary</i>
t	triplet
TBDPS	<i>tert</i> -butyl-diphenylsilyl
TBHP	<i>tert</i> -butyl hydroperoxide
TBS	<i>tert</i> -butyl-dimethylsilyl
TCA	trichloroacetic acid
TEMPO	2,2,6,6-tetramethylpiperidine N-oxyl
TEP	triethylphosphite
Tf	trifluoromethylsulfonyl
TFA	trifluoroacetic acid
THF	tetrahydrofuran
THP	tetrahydropyran-2-yl
TLC	thin layer chromatography
TMS	trimethylsilyl
TRIP	3,3'-bis(2,4,6-triisopropylphenyl)-1,1'-binaphthyl-2,2'-diyl hydrogen phosphate
Ts	<i>para</i> -toluenesulfonyl
TsOH	<i>para</i> -toluene sulfonic acid
UHP	urea hydrogen peroxide
wt	weight

Acknowledgements

I would like to extend my sincerest thanks to Prof. Dr. Benjamin List for the opportunity to work in his talented research group and to experience some of the most exciting and forefront chemistry. I am indebted to him for the exceptional trust and freedom given to me, for the academic support and the eagerness to discuss results, however trivial, at any time of the day. His wonderful sense of humour and activities outside of work ensured a truly enjoyable time in Mülheim that I will cherish.

I would also like to thank assistant professors Dr. Nuno Maulide and Dr. Martin Klußman who have volunteered their time and knowledge by leading various Ph.D. seminars, total synthesis exercises and competitions. These seminars were an enormously important part of my Ph.D. education, and for their dedication and teaching prowess I am truly thankful.

I am grateful to Prof. Dr. Hans-Günther Schmalz for accepting to review this thesis, and to Prof. Dr. Axel Klein and Dr. Martin Klußman for serving on my defence committee. I also thank Nathalie Dupré, Nicolas Demoulin and Niklas Schöne for kindly proofreading this work and for their valuable suggestions.

I am extremely grateful to those who worked directly with me, including my talented and by now graduated apprentice Natascha Wippich, Dr. Nicolas Demoulin for our productive collaboration on the benzyloxylation chemistry and Dr. Corinna Reisinger for her valuable insight and ideas on the epoxidation chemistry. It was truly a pleasure to collaborate with Dr. Christophe Farès from the NMR department on the mechanistic studies of epoxidation. I am also grateful to Iakov Polyak and Dr. Gopakumar Gopinadhanpillai from the Thiel group for their valuable computational work, Dominique Bock for investing her time into a very difficult crystallization project, and Manuel Mahlau together with Melanie Gossens for their kind help with experimental work.

I thank Adrienne Hermes for her advice and support in various forms, and all of the technician staff for providing me with valuable catalysts and their routine assistance in the lab, especially Marianne Hannappel, Simone Marcus, Hendrik van Thienen, Pascal Wallkamp and Arno Döring. I thank our GC department, and especially Sylvia Ruthe, Frank Kohler and Stefanie Dehn for their friendly, helpful and prompt work, as well as the HPLC and mass departments for their support. I am indebted to my labmates from the List, Klußman and Maulide groups for sharing chemicals, catalysts, ideas and insight. For all the valuable discussions, I'd like to thank especially Ilija Čorić, Jiwoong Lee, Steffen Müller, Dr. Matthew Webber, Lars Ratjen, Dr. Nuno Maulide and Dr. Martin Klußman whose creativity and chemical intuition have been a source of great help and inspiration.

Acknowledgements

I owe my best memories of Mülheim to my labmates and officemates who have made all the difference in the world through their friendship. I thank Teresa Oliveira, Viviana Valerio, Claire Madelaine, Desi Petkova and Caroline Souris for bringing life to every event, my box-buddy Jiwoong Lee for his help, advice and encouragement in the lab and outside, Matthew Webber, Nicolas Demoulin and Alberto Martinez for their amazing friendship, and Lars Ratjen, Kostas Rampalakos and Tjostil Vlaar for sharing my very eclectic sense of humour. I thank all my past and present officemates Quinggang Wang, Alberto Martinez, Nicolas Demoulin, Caterina Gruenwald, Kristina Zumbansen, Artur Pinto and Guillaume Bordeau for the wonderful times and the necessary distraction, as well as my football “coaches” Frédéric Frébault, Marco Luparia and Ilija Čorić for all the laughter and ball-chasing. I am grateful to all of my MPI colleagues for their talent, humour and unforgettable personalities which have made my stay in Mülheim so special.

Finally, I would like to thank the closest people in my life for their love, encouragement and support: my parents Alla and Alex, my sister Julia and brother Andrei, my “German parents” Marie-Anne and Ulrich, and my Niklas.

1. INTRODUCTION

Chirality, a geometric property which describes all rigid objects that cannot be superimposed on their mirror images, is one of the most fundamental attributes of living systems. An inevitable consequence of chirality is the additional dimension of physical uniqueness that it imparts to chemically identical structures. Though the reasons are still debatable,^[1] it is a fact that life has chosen to differentiate enantiomers by keeping to enantiopure, homochiral molecules in biological processes. This is particularly evident when considering amino acids, sugars, lipids and nucleotides which, barring rare exceptions, are all produced as single enantiomers. Since homochirality of these basic building blocks translates into stereodefined macroscopic environments, a pair of enantiomers often has dramatically different and easily observable biological effects. A common example of this phenomenon is the perception of odours by the human brain, which is triggered by an odorant fitting into a complementary chiral receptor. Depending on the absolute configuration of the odorant, it can fit into different receptors, so that the two mirror images of the same molecule may elicit different responses. Indeed, in 2003, more than 285 enantiomeric pairs of compounds (570 enantiomers) had been described which exhibit either different odours or odour intensities.^[2] Perhaps even more important is the enantiomer-specific bioactivity of drugs and agrochemicals, which can also be highly polarized. For instance, all phenoxypropionic acid herbicides, including dichlorprop shown in Figure 1.1, display the desired weed-killing activity in their (*R*)-(+)-form, but have are inactive in their (*S*)-(-)-form.^[3]

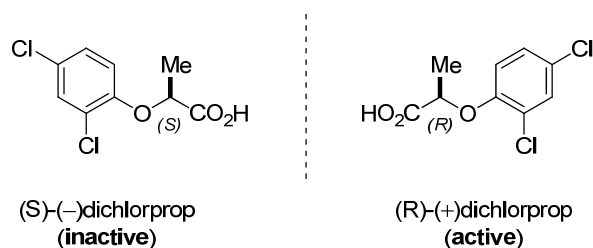


Figure 1.1 Enantiomers of herbicide dichlorprop and their activity

In organic chemistry, the concept of chirality had already been recognized in the mid 1870's with the pioneering studies of *LeBel*^[4] and *van't Hoff*,^[5] who independently identified carbon atoms possessing four different substituents as chiral units. Yet despite extensive systematization and refinement of the concept of chirality, and an advent of asymmetric synthesis, its importance in the pharmaceutical industry did not gain much attention until about two decades ago.^[6] In fact, a survey of nearly 1700 drugs in the early 1980's revealed that of

1. Introduction

the synthetic, chiral compounds, only 12% were marketed as single enantiomers, the remainder being racemic mixtures.^[7] Some twenty years later, this number changed to 75% and many of the established racemic drugs are now being reinvestigated as single enantiomers in a process known as “chiral switching.”^[8] This change in attitude came about after the widespread recognition that the wrong “handedness” of an otherwise identical chemical compound can sometimes strip it of its bioactivity or even impart toxic or mutagenic properties. Hence, the synthesis and biological testing of single-enantiomer compounds (provided they do not racemize under physiological conditions) have become of crucial importance to the pharmaceutical, agrochemical and food industries.^[8]

Several methods exist to obtain enantiopure materials, which include optical resolution *via* the formation of diastereomers, chromatographic separation of enantiomers, enzymatic resolution, chemical kinetic resolution and asymmetric synthesis. Asymmetric synthesis, which does not resolve, but creates stereogenic centres, can in turn be divided into stoichiometric and catalytic approaches. Of all these processes, asymmetric catalysis, in which “a small amount of an enantiomerically pure catalyst [...] is used to produce large quantities of an optically active compound from a precursor that may be chiral or achiral”^[9] clearly emerges as the optimal solution in terms of atom- and often step- and redox economy,^[10] with the potential of offering significant economic advantages. Possessing both practical value and interesting challenges, asymmetric catalysis has fittingly enjoyed extensive studies by various branches of chemical research. Until recently, asymmetric catalysis was heavily dominated by metal-mediated processes, with biocatalysis representing a complementary branch. In 2000, simultaneous publications by *List*^[11] and *MacMillan*^[12] defined a new area of asymmetric catalysis, mediated by small organic molecules. These reports triggered an avalanche of synthetic work in this area in the immediate years, and just over a decade later, organocatalysis has already been extended into virtually every area and type of organic chemistry. From polymer synthesis to total synthesis, employing ionic and radical intermediates, photochemical and thermal activation modes, homogeneous and solid-supported reactions, organocatalysis seems to know no limit, mediating addition, substitution, elimination and rearrangement reactions in a myriad of processes.^[13]

One area of asymmetric catalysis that has been particularly influenced by metals is the enantioselective oxidation. Indeed, it was the Nobel Prize-winning studies of *Sharpless* in the 1980's on the asymmetric epoxidation of allylic alcohols using chiral titanium complexes that set the stage for the development of enantioselective C-O bond-forming reactions.^[14] In

1. Introduction

comparison, it was not until 2005, halfway into its lifetime, that modern organocatalysisⁱ tackled a comparable catalytic asymmetric transformation, the epoxidation of α,β -unsaturated aldehydes.^[15] Given the prevalence of chiral oxygenated compounds in natural products and the utility of oxygen functionalities as handles for (stereospecific) chemical transformation, asymmetric oxidation represents an important area of research that continuously demands improvement and innovation. The focus of this Ph.D. work has been to expand organocatalysis to oxidative processes. In particular, this thesis describes the use of primary amine catalysts for highly enantioselective epoxidation of α -branched α,β -unsaturated aldehydes and for asymmetric α -benzoyloxylation of cyclic ketones and other carbonyl compounds. Apart from the obvious advantages of organocatalysis, such as the readily available, cheap and bench-stable amine catalysts and reaction conditions which are not sensitive to air and moisture, it is important to note that organocatalysis was used to solve long-standing challenges, in which metal-mediated and other approaches proved to be only moderately effective or failed altogether.

Amid the discussion of organocatalysis and its advantages, it is nevertheless important to acknowledge that organocatalysis probably cannot, nor strives to, replace metal catalysis. The common assumption that organocatalysis solves the problems associated with the toxicity of transition metals in the pharmaceutical industry may well be dispelled by suitable studies on the metabolism of modern synthetic organocatalysts in biological systems. Indeed, as one of the most prominent figures in organocatalysis expressed, “organocatalysis seems to complement rather than compete with metal and enzyme catalysis. For example, certain recently developed reactions such as the exceptionally important transition metal-catalyzed cross-coupling and metathesis reactions are unlikely candidates for organocatalysis. Yet other processes, for example, those using aldehydes as nucleophiles in asymmetric catalysis, seem to only work within the realm of organocatalysis. Both transition metal catalysis and organocatalysis have allowed the realization of catalytic asymmetric processes that were considered extremely challenging if not impossible before.”^[16]

In the following chapters, an overview of organocatalysis, and in particular aminocatalysis, is presented, followed by the discussion of asymmetric epoxidation and α -oxygenation strategies. This is succeeded by the description and discussion of our own results on asymmetric organocatalytic oxidation reactions, which include asymmetric epoxidation of α -branched enals using a combination of iminium ion and enamine catalysis and α -benzoyloxylation of various carbonyl compounds *via* enamine and dienamine catalysis.

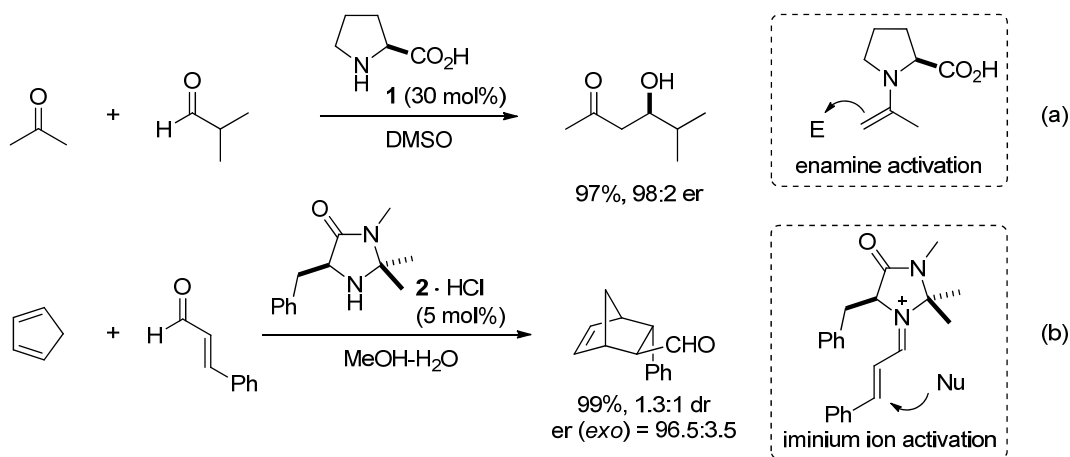
ⁱ An important exception to the metal-based approaches prior to modern organocatalysis is the *Shi* epoxidation of unfunctionalized olefins using chiral ketones as catalysts, although metal salts are typically used as oxidants (cf. Section 2.2.1)

2. BACKGROUND

2.1. Asymmetric Organocatalysis

2.1.1 Introduction

Although the use of small organic molecules to effect enantioselective processes can be traced back to the studies of *van Liebig* in the 1800's,^[17] and the more systematic work of *Bredig* starting in 1908,^[18] it was not until a whole century later that the full potential of organocatalysis was realized with the seminal reports of *List* and *MacMillan*. The success of these studies in galvanizing the chemical community toward extensive exploration of the subject probably lies in their simultaneous demonstration of two extremely general and powerful modes of organocatalysis. In particular, *List* showed that the amino acid L-proline (**1**) can activate acetone as an enamine toward an aldol reaction with various aldehydes,^[11] while *MacMillan* reported that enals can be activated with the chiral imidazolidinone **2** as iminium ions toward a *Diels-Alder* reaction with dienes (Scheme 2.1).^[12] It is noteworthy that both of the original publications presented well defined mechanistic insight, which was undoubtedly crucial for the widespread recognition of the concept.



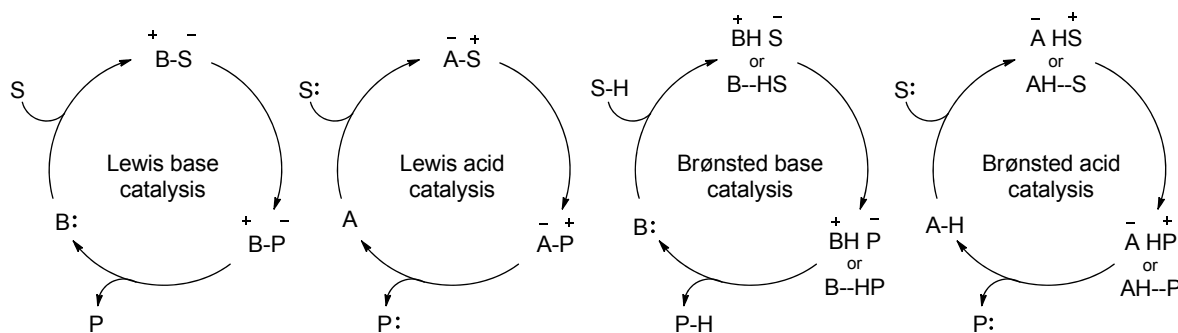
Scheme 2.1 (a) Enamine activation in proline-catalyzed aldol reaction; (b) Iminium activation in Diels-Alder reaction catalyzed by **2**.

Following these studies, a myriad of reports on iminium and enamine-catalyzed reactions, as well as other catalytic modes relying on small to medium-sized organic molecules which lack metals in their reactive centres have appeared, defining what has now become a broad and multifaceted field of organocatalysis.

2. Background

2.1.2 Classification of Modern Organocatalysis

In an effort to organize the extensive and ever-growing field of organocatalysis, in 2004 *Seayad* and *List* introduced a mechanism-based classification system.^[19] Accordingly, organocatalysis can be broadly divided into four major areas: Lewis base catalysis, Lewis acid catalysis, Brønsted base catalysis and Brønsted acid catalysis (Scheme 2.2).



Scheme 2.2 Four major areas of asymmetric organocatalysis and their simplified mechanisms (S = Substrate, P = Product, B = Base, A = Acid).

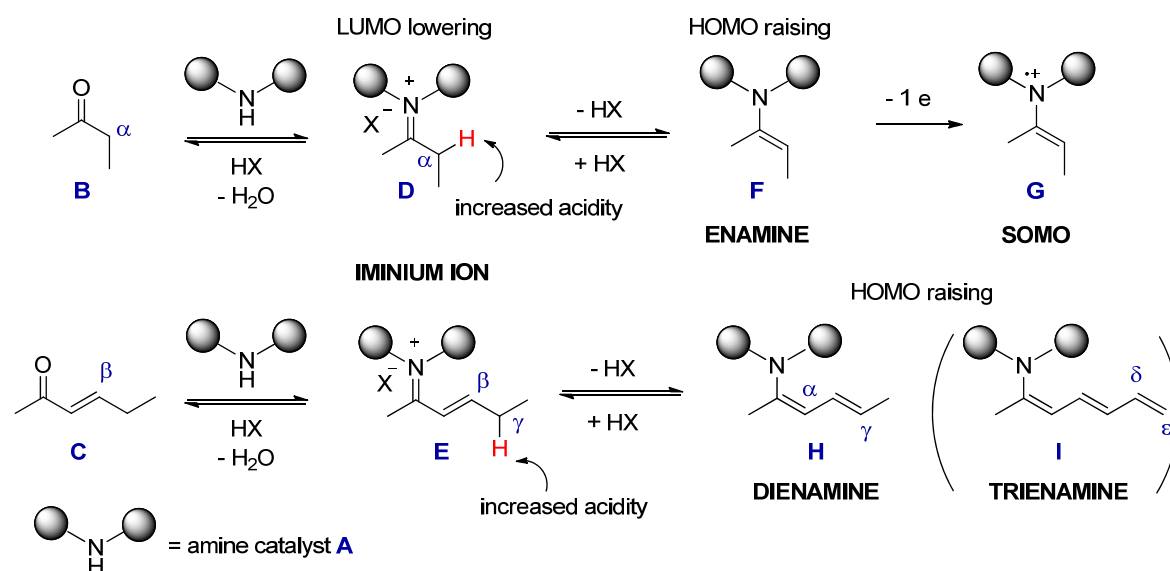
Lewis base catalysis encompasses all reactions in which the catalyst donates a pair of electrons to form a covalent bond with the substrate. These catalysts are generally N-, C-, O-, P- and S-based Lewis bases which can reversibly activate the substrate either as a nucleophile or an electrophile in the form of iminium ions, enamines, acyl ammonium ions, 1-, 2-, or 3-ammonium enolates, and others. After the reactive intermediate has undergone a reaction, the bond between the product and the catalyst is broken, allowing the catalytic cycle to repeat. Catalysis mediated by nucleophilic amines, or aminocatalysis, belongs to this mechanistic class and describes the seminal publications of *List* and *MacMillan* (Section 2.1) as well as the work presented in this thesis (Chapter 4). In Lewis acid catalysis, the catalyst activates neutral or negatively charged substrates by accepting a pair of electrons. The recently introduced organosilicon catalysis^[20] and the extensive field of phase-transfer catalysis^[21] can be considered examples of such activation. Brønsted base catalysis and Brønsted acid catalysis are conceptually related catalytic modes which involve (partial) deprotonation and protonation, respectively, for the activation of the substrate. It is important to note that more than one catalytic regime may operate in the same reaction. As will be discussed in the subsequent sections, primary amine catalysts, for example, cannot easily activate substrates as iminium ions in the absence of Brønsted acid additives and hence such reactions rely on the synergistic combination of Lewis base catalysis and Brønsted acid catalysis.

2. Background

2.1.2 Aminocatalysis

The fact that amines can activate carbonyl compounds toward nucleophilic addition was already recognized in the late 1800's by *Knoevenagel*, who studied the aldol condensation of β -ketoesters and malonates with aldehydes and ketones in the presence of amines, and even proposed the intermediacy of imine and enamine species.^[22] His work was followed by very important, albeit sporadic and mechanistically poorly understood discoveries, which include some examples of asymmetric catalysis.^[23] The real explosion of aminocatalysis in asymmetric transformations, however, occurred in recent years followed by the widespread recognition of the generality of the concept.

Aminocatalysis today deserves its own classification system. The original iminium and enamine mechanistic paradigms^[24] have now been expanded to new activation modes, which include extended enamine catalysis (dienamine^[25] and trienamine^[26]) and SOMO (singly occupied molecular orbital) catalysis characterized by the formation of enamine radical cations (Scheme 2.3).^[27]



Scheme 2.3 Classification of aminocatalysis based on the reactive intermediates (iminium, enamine, SOMO and dienamine/trienamine).

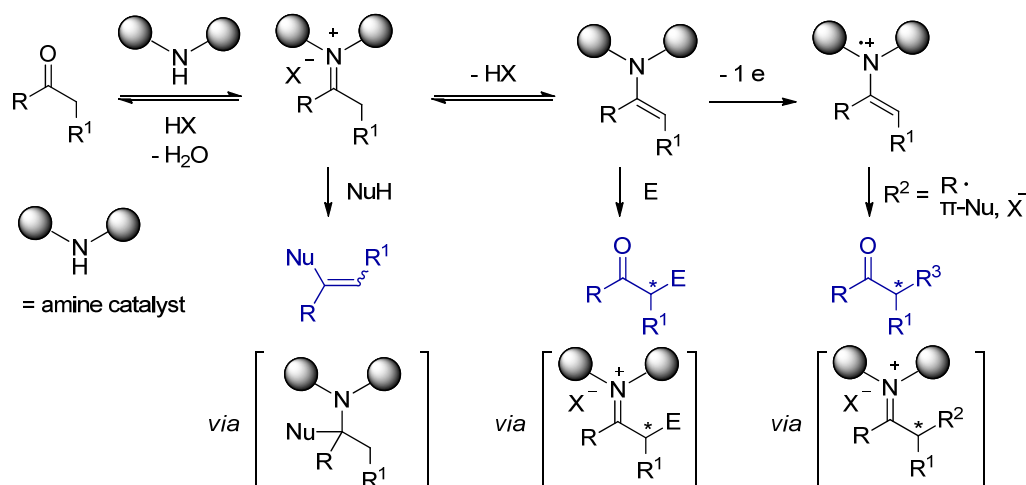
As the Scheme 2.3 illustrates, all of these reaction modes are interrelated and start by the reversible condensation of the amine catalyst **A** with the carbonyl substrate to form an iminium ion (**D/E**). Transforming a neutral carbonyl compound into an iminium ion effectively lowers the LUMO energy of the system, activating it for a nucleophilic attack as well as increasing the acidity of the α -protons. With saturated carbonyl substrates like **B**, deprotonation in the α -

2. Background

position forms enamine **F**. Compared to the enol form of the parent carbonyl compound, enamines possess a higher HOMO energy of the system, resulting in an overall activation of **B** toward nucleophilic additions at the α -carbon. The group of *MacMillan* recently identified a further type of catalytic activation based on the oxidation of enamines **F** to radical cations **G**.^[28] This so-called SOMO activation allows the substrate to react with previously inaccessible reagents like radicals, π -nucleophiles and halides. In the case of unsaturated substrates such as **C**, the LUMO energy-lowering effect induced by the formation of iminium **E** activates the system as an electrophile toward conjugate additions at the β -carbon and pericyclic reactions. Alternatively, loss of the γ -proton forms dienamine **H** which can act as a normal α -carbon nucleophile or a vinylogous γ -carbon nucleophile. Most recently, *Chen, Jørgensen* and *Melchiorre*^[26] demonstrated that this vinylogy can be extended even further by using $\alpha,\beta,\gamma,\delta$ -unsaturated carbonyl compounds which form trienamines **I** upon condensation with the amine catalyst and the loss of an ε -proton.

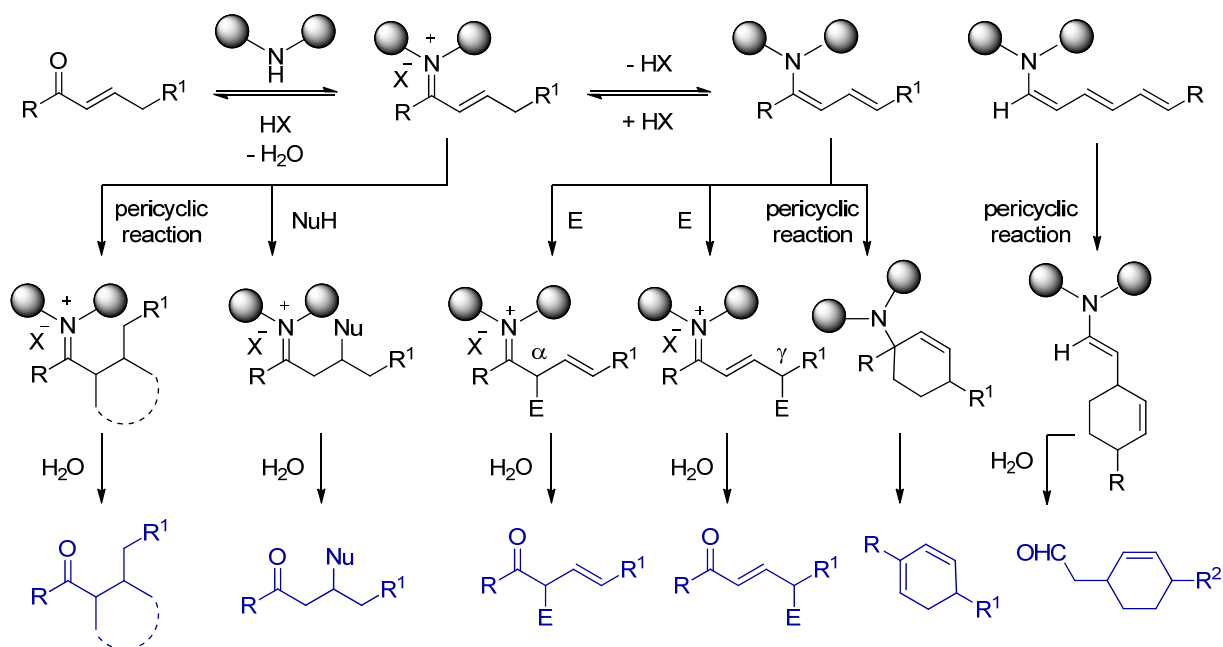
Although the activation modes discussed above are conceptually related to Lewis acid activation of carbonyls by metals, aminocatalysis often significantly outperforms metals in enantiodiscrimination. This is because chiral Lewis acidic metals must discriminate between two similar lone electron pairs of the carbonyl compound to achieve enantioselectivity, while aminocatalysis replaces this process with a much more selective π -bond formation with the aminocatalyst, which is governed by the *E/Z* geometry of the iminium.^[29]

Schemes 2.4 and 2.5 give an overview of the types of products that can be obtained with the various modes of aminocatalysis. It is important to note that many of these mechanistic pathways have been combined into domino and cascade reaction processes, which constitute an extensively studied branch of organocatalysis.^[30]



Scheme 2.4 Types of products obtained with aminocatalysis from ketones and aldehydes.

2. Background



Scheme 2.5 Types of products obtained with aminocatalysis from enones and enals.

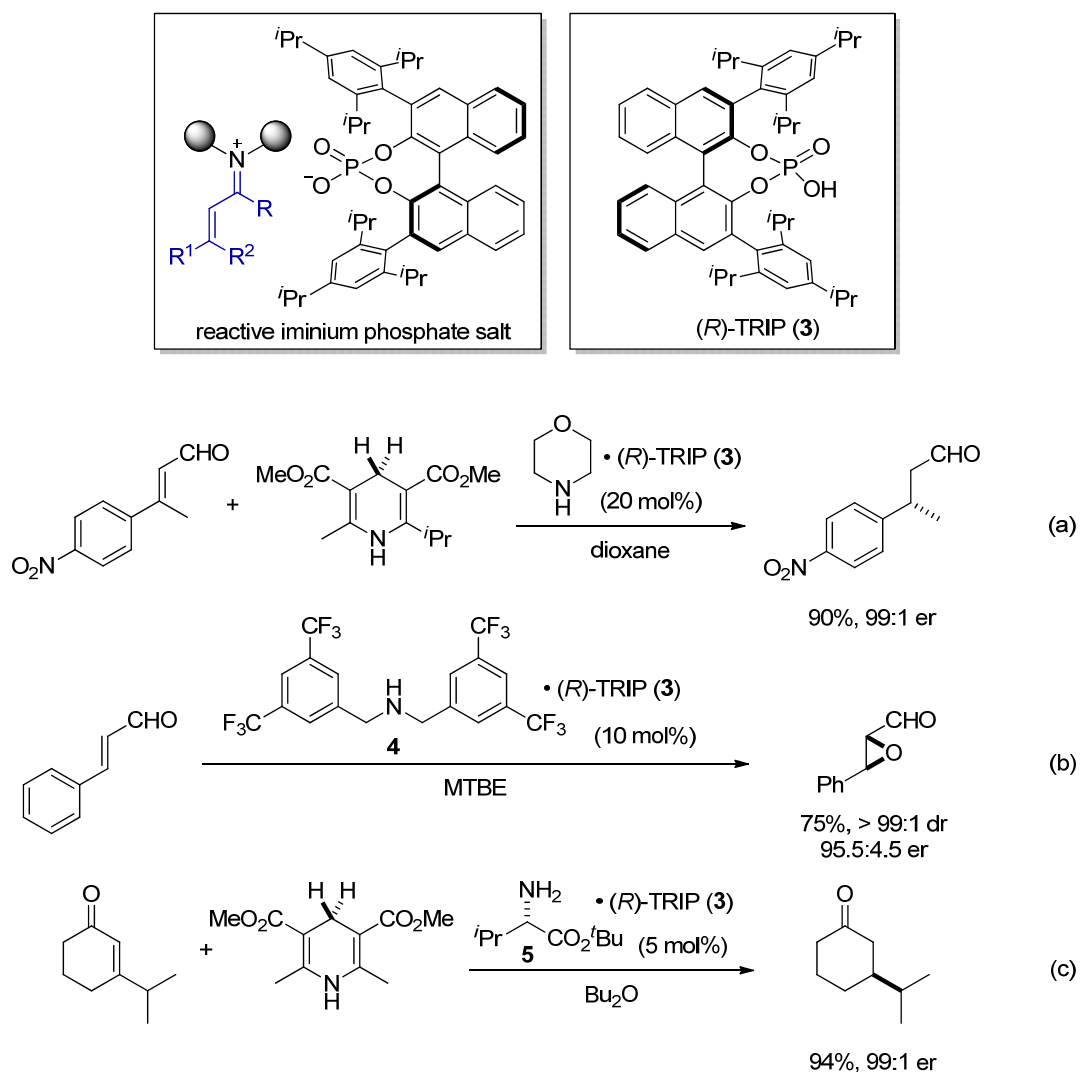
2.1.2.1 Asymmetric Counteranion-Directed Catalysis (ACDC)

When considering iminium catalysis, one readily notices that the positively charged iminium ion always involves a counteranion as part of the reactive intermediate. Provided that the ion association is close, it is reasonable to assume that the counteranion may have a strong influence on the reaction outcome.^[31] Indeed, such were the observations of *List* and co-workers while studying iminium-catalyzed transfer hydrogenation of enals in 2006.^[32] Following these observations, and inspired by the reports on chiral phosphates as asymmetric Brønsted acid catalysts, the authors hypothesized and successfully demonstrated that catalytic salts of *achiral* amines and chiral phosphoric acids could induce impressive asymmetry in the reaction (Scheme 2.6 (a)). This led to the generalization of the concept of “asymmetric counteranion-directed catalysis” or ACDC, with has since been extended beyond aminocatalysis (Scheme 2.6) to Brønsted acid and metal-mediated processes as well.^[33]

ACDC, in which the counteranion is the only source of chirality, is a powerful demonstration that the Brønsted acid co-catalyst, often employed in aminocatalysis to facilitate the initial condensation of the carbonyl and the amine, may play more than a passive spectator role in the subsequent enantioselective step of the reaction. In fact, carefully chosen combinations of *chiral* amine catalysts and *chiral* Brønsted acid co-catalysts may lead to unprecedented levels of enantioselectivity in a given transformation. This observation, first made in 2006 in our group

2. Background

(Scheme 2.6 (c)),^[34] gained popularity in the chemical community over the past several years^[35] and also found application in this Ph.D. work (cf. Section 4.1).



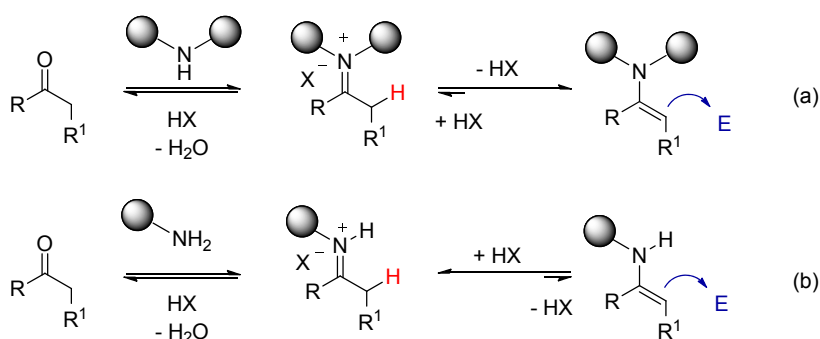
Scheme 2.6 Examples of ACDC (a, b) and chiral Brønsted acid co-catalyst paired with a chiral amine catalyst (c) in iminium-catalyzed reactions.^[32, 34, 36]

2.1.2.2 Primary Amine Salt Catalysis

Although primary amines were already established as competent catalysts in 1910 by *Dakin* in the *Knoevenagel* condensation,^[37] modern organocatalysis was overwhelmingly dominated by the use of secondary amines until about 2005.^[38] The reason for neglecting primary amines at the outset of organocatalysis may lie in the generally unfavourable imine-enamine equilibrium,^[38-39] i.e. the fact that while secondary amine-derived iminium ions readily

2. Background

tautomerize to catalytically relevant enamines if an α -proton is present, most primary amine-derived imines prefer to keep the carbon-nitrogen double bond (Scheme 2.7).^[40]



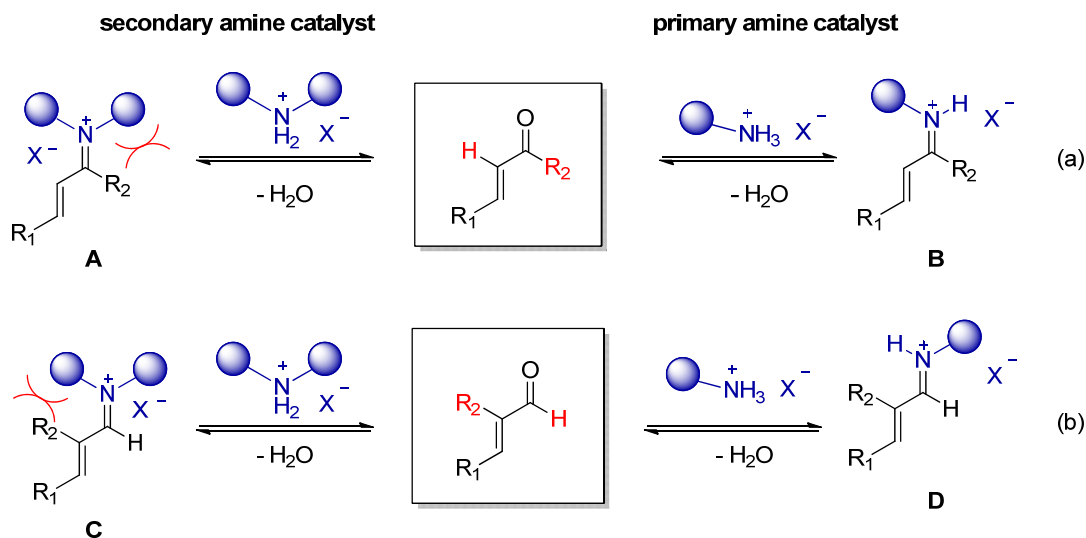
Scheme 2.7 Imine-enamine equilibria of primary and secondary amines.

Nevertheless, primary aminocatalysis has experienced a renaissance in recent years as witnessed by the ever-growing number of reviews devoted to this topic.^[38-39, 41] A survey of recently established reactions catalyzed by primary amines quickly reveals the reason. The initial success of classical secondary amines catalysts (in particular proline and imidazolidinone derivatives) has largely been in the activation of relatively unencumbered aldehydes and enals; yet when the same reactions were attempted on less sterically accessible ketones, α -branched enals and enones, the result has typicallyⁱⁱ been poor conversion and enantioselectivity.^[38, 41c] On the other hand, primary amines have consistently proven to be superior catalysts for iminium and even enamine activation of challenging substrates in terms of reactivity and enantioselectivity.

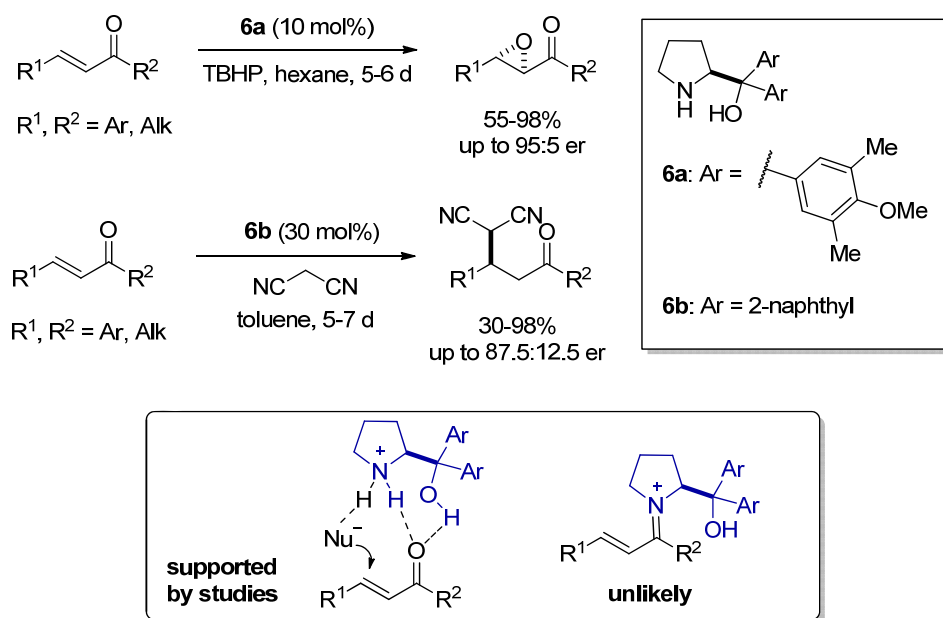
These results may be explained by a simple mechanistic rationale: the formation of covalent iminium intermediates is disfavoured between *secondary* amines and sterically encumbered substrates, while the reduced steric requirements of *primary* amines make this process more feasible (Scheme 2.8). In other words, primary amines may provide a higher concentration of requisite iminium ions **B/D** under acidic conditions compared to secondary amine-derived iminium ions **A/C**, facilitating catalytic turnover (Scheme 2.8). Moreover, the N-H group in primary amines (as opposed to another alkyl group in secondary amines) may help to better control iminium/enamine geometry, a crucial parameter for enantioselectivity.^[38] This hypothesis is supported by recent experimental and computational studies of *Lattanzi* and colleagues, who have shown that certain reactions of enones which were reasonably successful with secondary amine catalysts proceed *via* cooperative Brønsted acid/Brønsted base catalysis rather than covalent iminium catalysis (Scheme 2.9).^[42]

ⁱⁱ α -Substituted acroleins and cyclic carbaldehydes often appear to be an exception in recent studies (see e.g. Sections 2.2.3 and 2.2.4)

2. Background



Scheme 2.8 Secondary and primary amine catalysis in the iminium activation of enones (a) and α -branched enals (b).

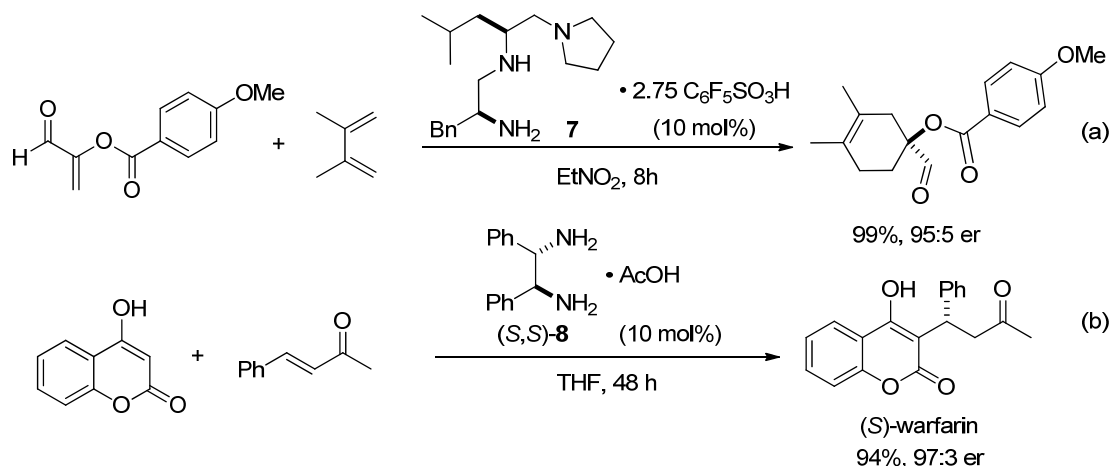


Scheme 2.9 Secondary amine catalysis in the conjugate addition to enones.^[42]

An important characteristic of successful primary aminocatalysts is *bifunctionality*, i.e. the presence of another site in the catalyst which can interact with, and organize substrates in the transition state. This is typically achieved by the inclusion of a second amine functionality: indeed, chiral diamines have proven to be extremely versatile catalysts.^[38-39] In addition, as discussed in Section 2.1.3.1, the choice of the Brønsted acid co-catalyst often has a significant effect on the efficiency and enantioselectivity of the reaction, and provides a further handle for reaction optimization.

2. Background

Seminal examples of iminium catalysis using primary amines include the work of *Ishihara* on the *Diels-Alder* reaction of α -branched enals,^[43] *Chin* on the *Michael* addition to enones for the synthesis of the anticoagulant warfarin^[44] (Scheme 2.10), and that of our group on transfer hydrogenation (Scheme 2.6 (c)). These studies were shortly followed by the introduction of the cinchona alkaloid-derived primary amines in 2007, which were used in this work and which remain to be some of the most popular primary amine catalysts to date (cf. Section 2.1.3.3).



Scheme 2.10 Seminal examples of iminium catalysis using primary amines: (a) Diel-Alder reaction developed by *Ishihara*^[43], and (b) *Michael* reaction developed by *Chin*.^[44]

Enamine catalysis employing primary amines has similarly been widely investigated since 2005 and applied in aldol, *Mannich*, *Michael*, amination, alkylation^[38-39, 41] and most recently fluorination^[45] reactions of challenging substrates. Presumably, the ability of primary amines to condense with sterically hindered substrates is a powerful enough factor for driving the reactions forward in spite of the less favourable iminium/enamine tautomerization that follows.

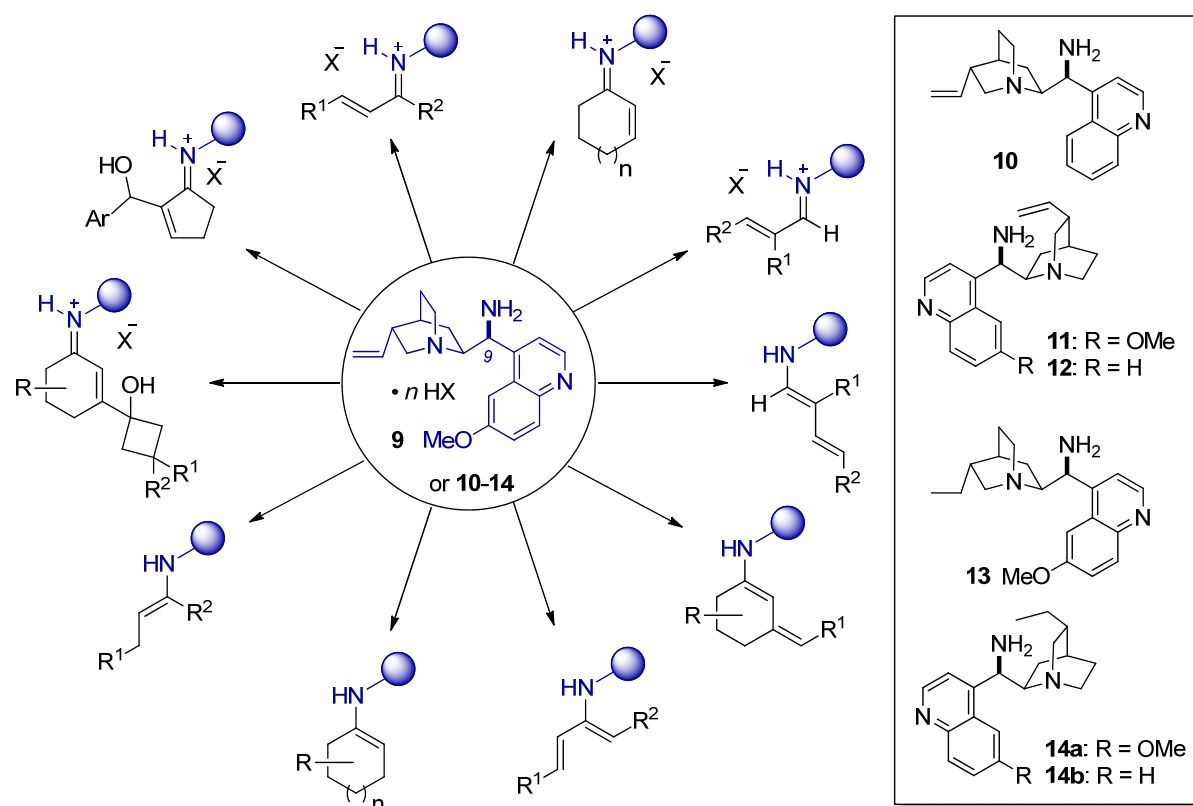
In the context of organocatalytic oxidative transformations, primary amine catalysts may possess a further advantage. Since primary amines have lower reactivity toward oxidation than their secondary amine counterparts,^[46] they may display higher stability and therefore higher turnover numbers under oxidative conditions.

2.1.2.3 Primary Amine Catalysts Derived from the Cinchona Alkaloids

Since the extensive studies of *Wynberg* in the late 1970's,^[47] cinchona alkaloids and their derivatives have enjoyed a status of a privileged catalytic motif, mediating a myriad of chemical transformations.^[48] The 9-amino(9-deoxy)-*epiquinine* derivative **9** (Scheme 2.11), introduced in 1995 by the group of *Brunner* in the context of metal ligand synthesis,^[49] was rediscovered in

2. Background

2007 by the groups of *Chen and Deng*^[50] and *Melchiorre*^[51] as a highly efficient aminocatalyst. The following years have witnessed an explosion of synthetic work employing **9** and closely related catalysts **10-14**. Using these catalysts, pericyclic, rearrangement, substitution, addition, and other reactions have been carried out with various carbonyl compounds using enamine, iminium, and dienamine activation modes (Scheme 2.11).^[41a, 41b]



Scheme 2.11 Scope of substrates activated by cinchona alkaloid-derived primary amine **9** and its closely related congeners **10-14**.^[41a, 41b]

In contrast to the wealth of synthetic work, the mechanism by which cinchona-derived amine catalysts and their salts operate has been virtually unexplored. To date, no X-ray structure of the corresponding imine, iminium or enamine intermediates exists to rationalize the absolute stereochemistry imparted to products, which shows remarkable consistency among mechanistically similar reactions. Due to the scarcity of computational^[52] and/or NMR studies on this catalyst, mechanisms proposed in the literature are only speculative, and generally fail to answer the important questions outlined in Figure 2.1.

2. Background

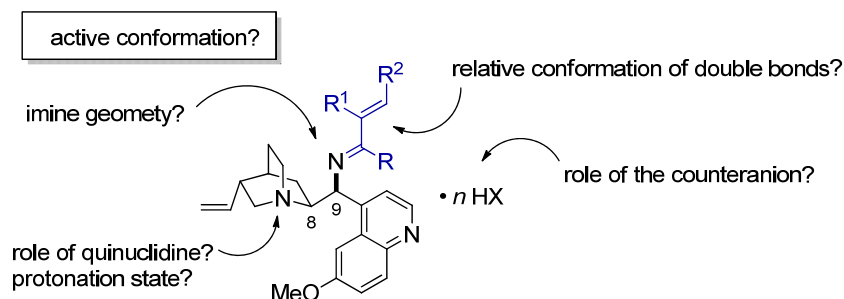
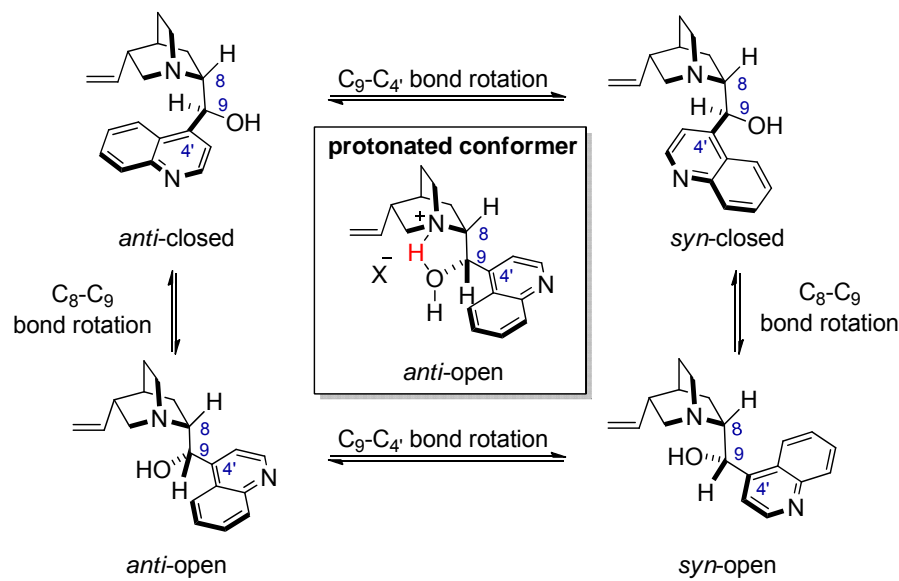


Figure 2.1 Important (and unanswered) mechanistic questions in reactions catalyzed by **9**.

Some information can be drawn from the abundant structural information that exists for the parent cinchona alkaloid scaffold.^[48] Through NMR studies and molecular mechanics calculations, it has been recognized that cinchona alkaloids display a strong conformational preference in solution.^[53] In particular, C₈-C₉ and C_{4'}-C₉ bonds were found to be most important in determining the overall conformation, resulting in four lowest-energy conformers: *syn*-closed, *syn*-open, *anti*-closed and *anti*-open (Scheme 2.12). Importantly, factors such as protonation can significantly shift these equilibria. It was found that cinchonidine, for example, exists exclusively in the *anti*-open conformation when protonated.^[54] Depending on the counteranion, this rigidification has been explained by a hydrogen bond that forms between the two central heteroatoms (N, O)^[55] (Scheme 2.12), or hydrogen bonding of both heteroatoms to the same bidentate anion.^[56] In general, protonation of cinchona alkaloids tends to hinder the rotation around the C₉-C₈ and C_{4'}-C₉ bonds, favouring a narrow range of the conformational space.^[57]



Scheme 2.12 The four lowest-energy conformers of cinchona alkaloids (shown: cinchonidine) and the conformational effect of protonation.^[53, 55, 57]

2. Background

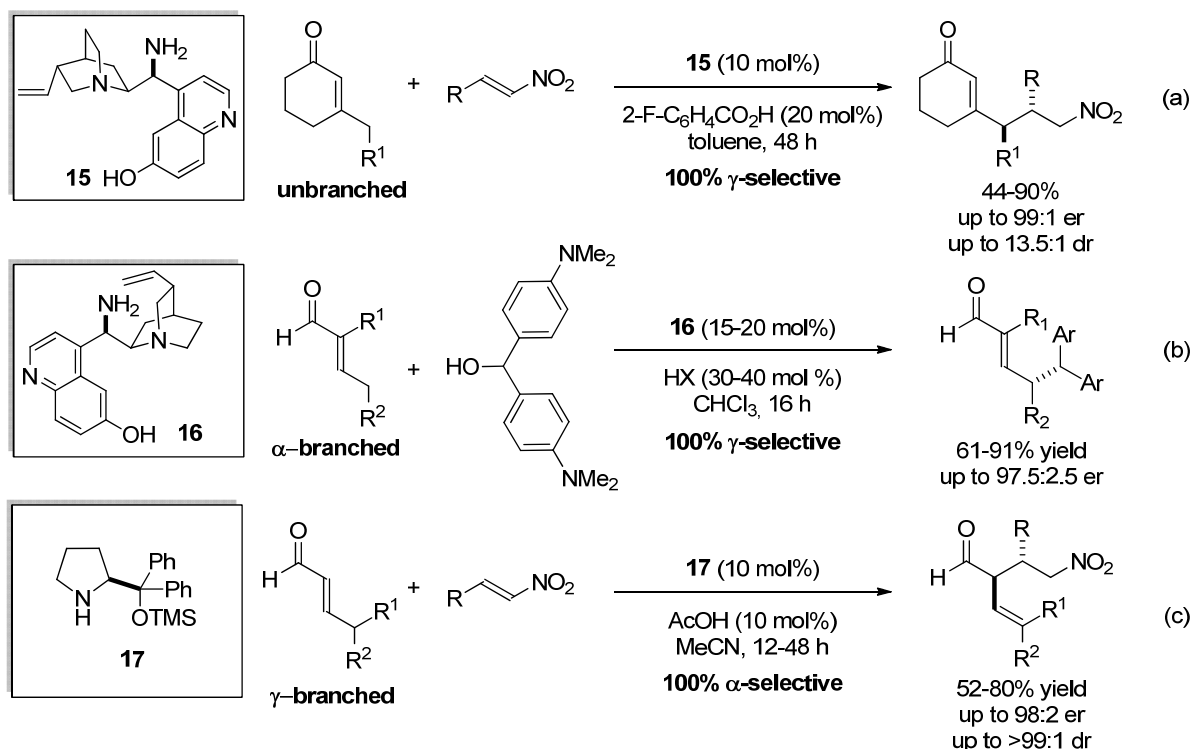
Significantly, using cinchonidine-platinum complex to hydrogenate ketopantolactone, *Baiker* has demonstrated a direct relationship between the observed conformational behaviour of the cinchona alkaloid in solution and the enantioselectivity of the reaction.^[54] Driven by the same logic, *Olah* and co-workers synthesized 9-dehydro-9-trifluoromethyl derivatives of cinchona alkaloids to inhibit C₈-C₉ rotation forming a conformationally rigid structure.^[58] These results hint at the possibility that the commonly used salts of cinchona-derived amines **9-14** may also display strong conformational preferences, especially when protonated, forming a rigid and well-defined iminium/enamine adducts with substrates. Furthermore, the role of the Brønsted acid in imine activation^[59] to form the reactive iminium species is intriguing since the counteranion has been shown numerous times to have a strong effect on the enantioselectivity of reactions.^[35a] Some NMR and computational studies to address these questions were performed within the framework of this Ph.D. thesis, and are presented in Section 4.1.6.2.

2.1.2.4 Dienamine Catalysis: A Special Case of Selectivity

Within the realm of extended enamine catalysis, dienamine synthons represent a particularly interesting case of reactivity. As mentioned in Section 2.1.3, they can act either as normal α -carbon nucleophiles or as vinylogous γ -carbon nucleophiles. Although one frequently encounters examples of both in aminocatalytic reactions, factors which govern this dual behaviour are poorly understood and are not trivial to generalize. As this Ph.D. work covers an example of rather unusual dienamine reactivity (Section 4.2.3), this section aims to provide an overview of what is known in this area.^[60]

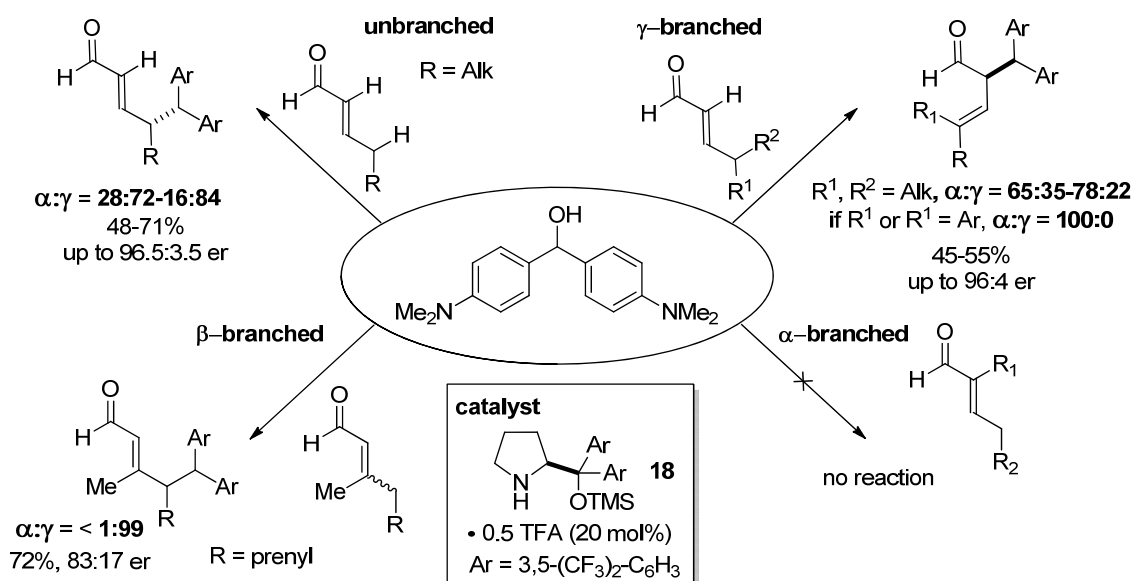
Studies on dienamine catalysis can be broadly divided into reactions which form a single new carbon-carbon bond, a single new carbon-heteroatom bond, and reactions which form multiple bonds *via* pericyclic or stepwise processes. For reasons of simplicity, only the first two reaction classes are discussed here. The group of *Melchiorre* has recently reported a *Michael* reaction of enones^[25c] and an S_N1 type substitution reaction of α -branched enals^[25a] using primary amine catalysts **15** and **16**, respectively (Scheme 2.13 (a) and (b)). In both cases, despite rather different electrophilic partners, exclusive γ -selectivity was reported. Interestingly, *Chen* and co-workers used the secondary amine catalyst **17** to effect the same *Michael* reaction with α -unbranched, γ -branched enals and obtained exclusive α -selectivity (Scheme 2.13 (c)).^[25c] Considering the two latter cases, it is tempting to speculate that, given a choice, the system prefers to avoid forming a quaternary stereocenter and selects the most unencumbered position for a nucleophilic attack.

2. Background



Scheme 2.13 Studies of dienamine catalysis for C-C bond formation by *Melchiorre* (a, b)^[25a, 25c] and *Chen* (c).^[25c] HX = **63a**, **63e** (cf. Structure Index, Section 9.1).

Christmann and colleagues performed a systematic study on the S_N1 type substitution reaction with various enals, including unbranched, α -, β - and γ -branched enals, and a secondary amine catalyst **18** (Scheme 2.14).

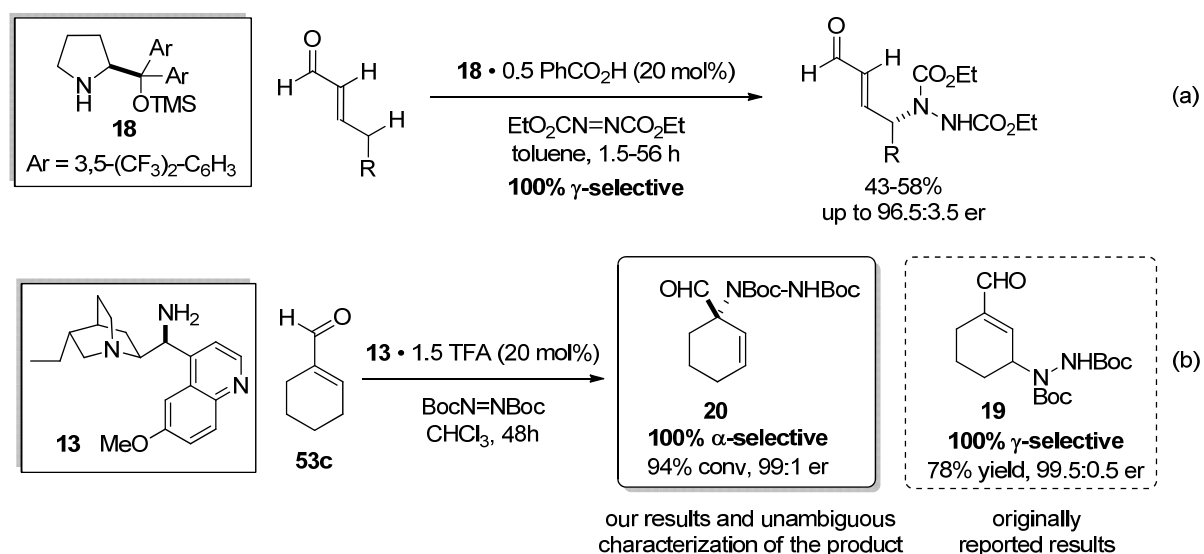


Scheme 2.14 Systematic studies of dienamine catalysis by *Christmann*.^[25d]

2. Background

Although their findings were less clear-cut, as mixtures of both α - and γ -regioisomers were generally obtained, the formation of a quaternary carbon stereocenter was still consistently avoided in all cases, as judged by the corresponding ratios of the α - and γ -products.^{iii,[61]}

The situation becomes more complicated, however, when one considers reactions in which a carbon-heteroatom bond is formed. The seminal report of *Jørgensen* on dienamine catalysis discloses that unbranched enals undergo exclusive γ -amination in the presence of secondary amine catalysts (Scheme 2.15 (a)).^[25b] When *Melchiorre et al.* tried an analogous reaction on α -branched enal **53c** using the primary amine catalyst **13**, the authors also reported the formation of the expected γ -regioisomer **19**.^[25e] However, subsequent re-characterization of the product by us using 2D-NMR and X-ray crystallography unambiguously confirmed that in fact the α -regioisomer **20** was formed as the exclusive product (Scheme 2.15 (b), cf. Section 4.2.3.2).



Scheme 2.15 Studies of dienamine catalysis for carbon-nitrogen bond formation by *Jørgensen* (a)^[25b] and *Melchiorre* (b).^[25e]

None of the various factors like the type of the reaction (addition vs. substitution), the nature of the electrophile (hard vs. soft), the type of the aminocatalyst (primary vs. secondary) or the type of bond being formed (carbon-carbon vs. carbon-heteroatom) allows for a simple rationalization of α - vs. γ -selectivity. The last example discussed in this section as well as the results obtained in this Ph.D. work (Section 4.2.3), similarly dispel the trend of preferentially reacting at the least substituted carbon. At this time, clarification of this intriguing topic must await further detailed studies.

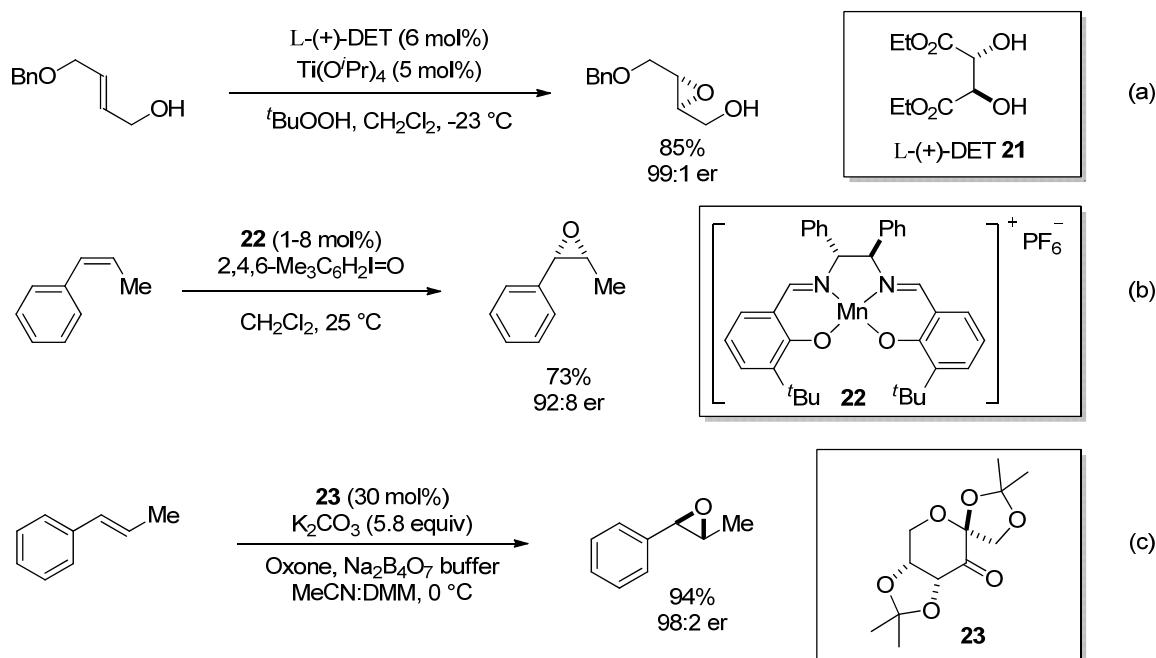
ⁱⁱⁱ To complicate matters, the studies of *Barbas* on unbranched enals with *Mannich* electrophiles report exclusive α -selectivity, unlike *Christmann's* findings of predominant γ -selectivity for this substrate class. See reference in text.

2. Background

2.2 Catalytic Asymmetric Epoxidation of Electron-Deficient Olefins

2.2.1 Overview of Catalytic Asymmetric Epoxidation

Since the Nobel Prize winning studies of *Sharpless* in the 1980's on the enantioselective epoxidation of allylic alcohols using titanium tartrate complexes (Scheme 2.16 (a)),^[14] advances in catalytic olefin epoxidation have continued to define the state of the art in asymmetric synthesis.^[62] Following the seminal work of *Sharpless*, many other important contributions appeared, which have not only provided reliable routes to synthetically valuable epoxides but also identified entirely novel catalytic motifs. In 1990, *Jacobsen* and *Katsuki* independently reported the first highly enantioselective epoxidation of unfunctionalized (and primarily *cis*-configured) olefins using chiral salen-manganese (III) complex **22** ((Scheme 2.16 (b)).^[63] Six years later, the group of *Shi* introduced the fructose-derived organocatalyst **23** which could tackle the epoxidation of unfunctionalized *trans*-configured olefins with excellent enantioselectivity (Scheme 2.16 (c)).^[64]



Scheme 2.16 Early milestones in the catalytic asymmetric epoxidation of olefins: *Sharpless* epoxidation (a),^[14] *Jacobsen-Katsuki* epoxidation (b),^[63] and *Shi* epoxidation (c).^[64]

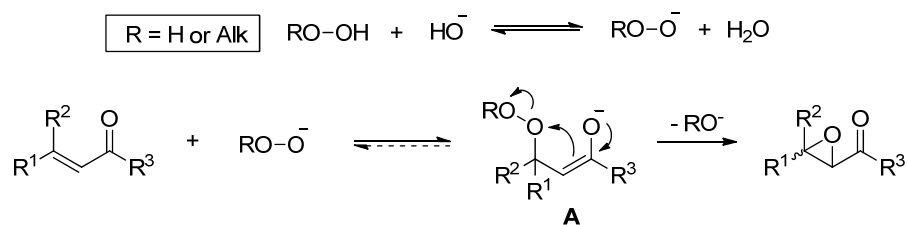
Many other important catalytic asymmetric methodologies associated with the names of *Enders*,^[65] *Jackson*,^[66] *Juliá* and *Colonna*,^[67] *Maruoka*,^[68] *Shibasaki*^[69] and *Wynberg*^[47a, 47b, 70] deal with the broad class of unsaturated carbonyl compounds, and follow the common mechanistic regime involving a conjugate addition of the oxygen nucleophile to the electron-

2. Background

poor olefin. These reactions can all be described as the asymmetric variants of the *Weitz-Scheffer* epoxidation which is covered in the next section.

2.2.2 *Weitz-Scheffer* Epoxidation

First described in 1921 by *Weitz* and *Scheffer*,^[71] the epoxidation of α,β -unsaturated ketones and aldehydes by treatment with basic hydrogen peroxide represents one of the most fundamental ways of forming an oxirane ring. Kinetic studies of this transformation by *Bunton* and *Minkoff*^[72] established it to be a two-step addition-elimination process, common to many syntheses of three-membered rings. In particular, hydrogen (or alkyl) peroxide, which is deprotonated under basic conditions, adds to the β -carbon of the unsaturated carbonyl compound in a *Michael* fashion, forming the β -peroxyenolate intermediate **A** (Scheme 2.17). This is followed by an intramolecular ring-closure, in which the weak O-O bond is broken and a second C-O bond is formed, expelling a hydroxide or an alkoxide anion as the leaving group.



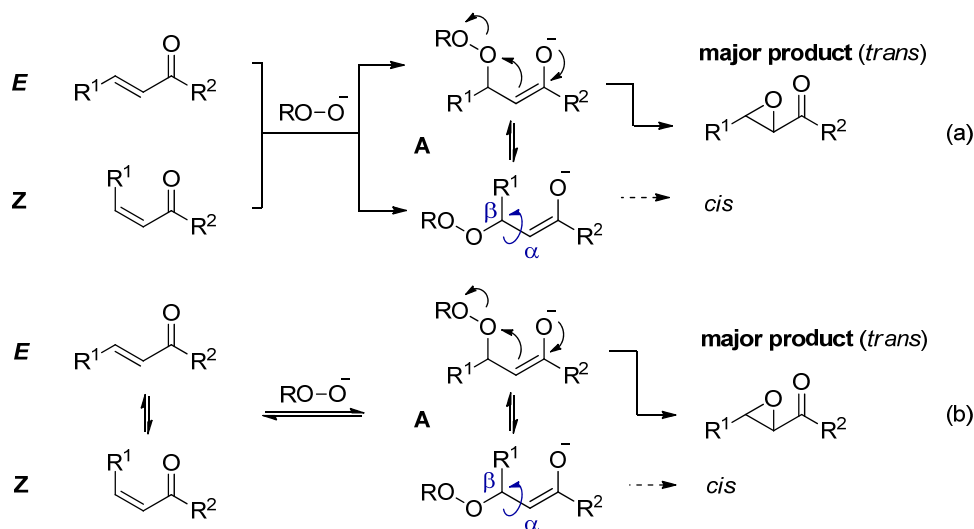
Scheme 2.17 The mechanism of the *Weitz-Scheffer* epoxidation.^[72]

The reaction mechanism proceeding *via* a nucleophilic addition of a peroxyanion was supported by kinetic measurements, which showed that replacing a methyl group at the β -position of the substrate by a smaller and less electron-donating hydrogen ($\text{R}^2 = \text{Me}$ vs. H , $\text{R}^1 = \text{Alk}$, Scheme 2.17) increased the reaction rate 5-6 fold.^[72] This effect is in direct contrast to reactions between olefins and electrophilic peracid oxidants such as *m*-CPBA in which the reaction is accelerated by alkyl substituents on the double bond.^[73] Furthermore, unlike the concerted additions of peracids across a double bond, the *Weitz-Scheffer* reaction is non-stereospecific, as both *E*- and *Z*-configured enones and enals predominantly furnish *trans*-epoxides. This lack of stereospecificity supports the existence of the intermediate **A** which would effect isomerization by rotation about the $\text{C}_\alpha\text{-C}_\beta$ bond.

The mechanism of this isomerization has been the subject of numerous studies. In principle, peroxyanion addition could be irreversible, and the formation of *trans*-epoxides from both *E*- and *Z*-configured olefins could be explained by a strong rotational preference of $\text{C}_\alpha\text{-C}_\beta$ bond in

2. Background

the long-lived intermediate **A** (Scheme 2.18 (a)). Alternatively, the initial peroxyanion addition could be reversible and rapid, causing fast isomerization of the olefin to the more stable *E*-isomer, followed by stereospecific epoxidation (Scheme 2.18 (b)).



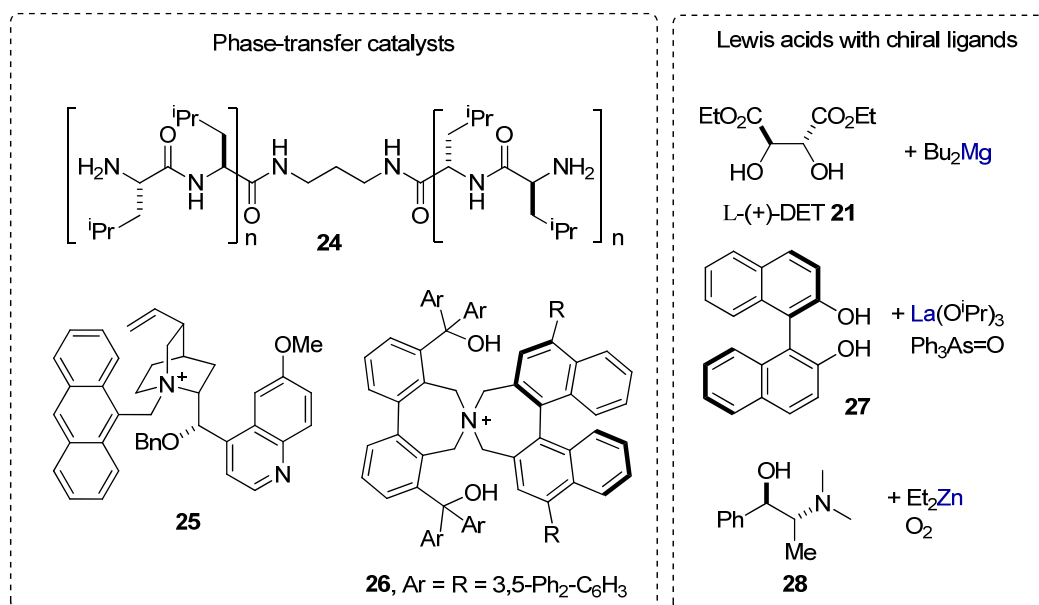
Scheme 2.18 Possible mechanisms that explain the non-stereospecificity of the *Weitz-Scheffer* epoxidation.

Bunton and *Minkoff* found that the rate of epoxide formation was first order with respect to the concentration of both peroxyanion and the unsaturated ketone, but had no definite order with respect to hydroxide or hydrogen peroxide concentration,^[72] which can be equally well rationalized by either a slow and rate-limiting addition of the peroxyanion followed by fast cyclization, or a fast addition followed by slow and rate-limiting cyclization.^[74] Similar results were obtained for the *Weitz-Scheffer* epoxidation of cinnamaldehyde.^[75] Several studies sought to resolve this ambiguity. *House* and *Ro* found that *Z*-chalcones isomerize to the *E* isomer under *Weitz-Scheffer* conditions, and showed through kinetic studies that this isomerization occurred *via* rapid and reversible formation of the intermediate **A**, in line with the mechanistic scenario shown in Scheme 2.18 (b).^[76] This was further supported by the recent studies of *Kelly*, *Roberts* and colleagues who studied *Weitz-Scheffer* epoxidation of phenyl vinyl ketone and found that the addition of hydroperoxide anion was rapid and reversible, with the ring-closure being the rate-limiting step.^[74]

Although a rather clear picture exists for the *Weitz-Scheffer* epoxidation, its asymmetric variants do not necessarily follow the same mechanistic pathway. Recent experimental and computational studies of *Singleton* suggest that the rate-limiting step and the reversibility of peroxide addition may vary depending on the specific reaction conditions, such as the nature of the catalyst present in the asymmetric transformations.^[77]

2. Background

Numerous enantioselective variants of the *Weitz-Scheffer* epoxidation have been developed to date, which rely on the catalytic activation of the substrate and/or the peroxide reagent. The most widely used catalyst classes developed for this purpose before the advent of modern organocatalysis are summarized in Scheme 2.19.^[62] Metal-free methods include the *Juliá-Colonna* epoxidation of chalcones derivatives using polypeptide catalysts such as the poly-(*S*)-alanine **24**,^[67] and phase transfer catalysis (PTC). The most established examples of PTC include quaternized cinchona alkaloids such as **25**, originally introduced by *Wynberg*^[47a, 47b, 70] and the recently developed axially chiral quaternary *N*-spiroammonium salts (e.g. **26**) pioneered by *Maruoka*.^[68] Metal Lewis acids with chiral organic ligands have also been extensively investigated and include magnesium and lithium complexes of diethyltartrate (**21**) first developed by *Jackson*,^[66] lanthanide complexes of BINOL derivatives (e.g. **27**) developed by *Shibasaki*^[69] and others, and aminoalcohol complexes of zinc (**28**) originally developed by *Enders*.^[65]



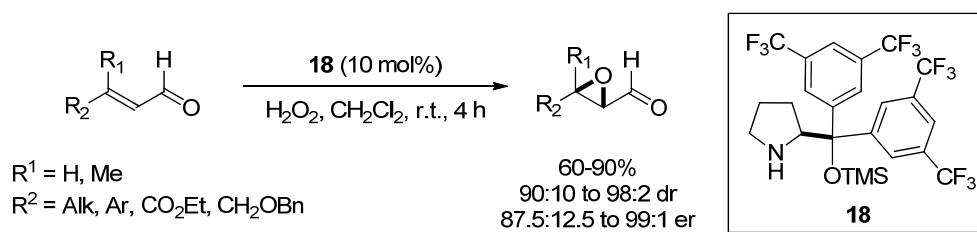
Scheme 2.19 Typical examples of the major catalyst classes used for the *Weitz-Scheffer* epoxidation before the advent of modern organocatalysis.

2.2.3 Organocatalytic (Lewis Base) Approaches to Epoxidation

Although nucleophilic amine catalysts were initially thought to be incompatible with epoxidation conditions given the well-known susceptibility of secondary amines to oxidation, in 2005 *Jørgensen* and colleagues demonstrated that the silylated prolinol catalyst **18** can

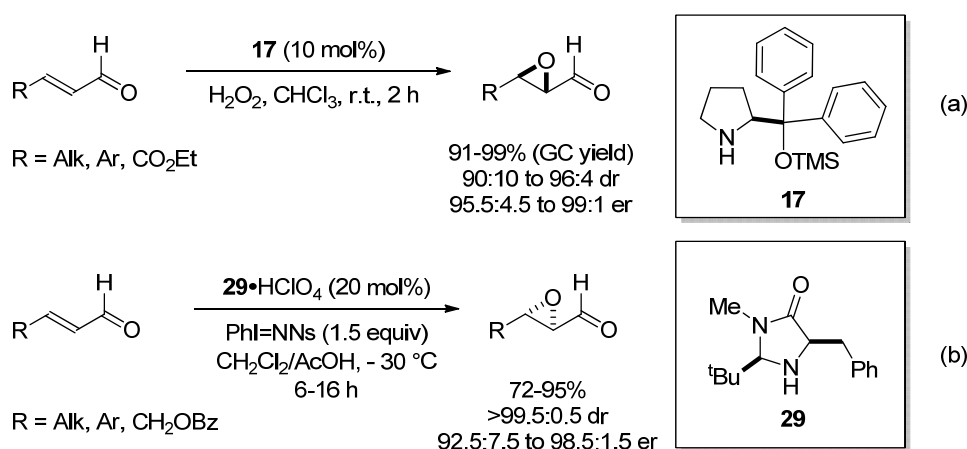
2. Background

efficiently activate α,β -unsaturated aldehydes as iminium ions toward epoxidation by aqueous hydrogen peroxide with excellent yields and enantioselectivity (Scheme 2.20).^[15]



Scheme 2.20 Seminal example of aminocatalytic epoxidation by *Jørgensen*^[15]

Shortly following this work, *Cordova* and colleagues disclosed a very similar approach using silylated prolinol **17** and aqueous hydrogen peroxide (Scheme 2.21 (a)).^[78] A complementary methodology was offered by the group of *MacMillan* in the following year, which employs imidazolidinone **29** as the chiral secondary amine catalyst and iodosobenzene as the oxidant, formed *in situ* from the slow reaction of [(*N*-Nosylimino)iodo]benzene ($\text{PhI}=\text{NNs}$) and acetic acid.^[79] The slow internal release of the oxidant was argued to provide higher levels of reaction efficiency and enantiocontrol by preventing catalyst degradation (Scheme 2.21 (b)).

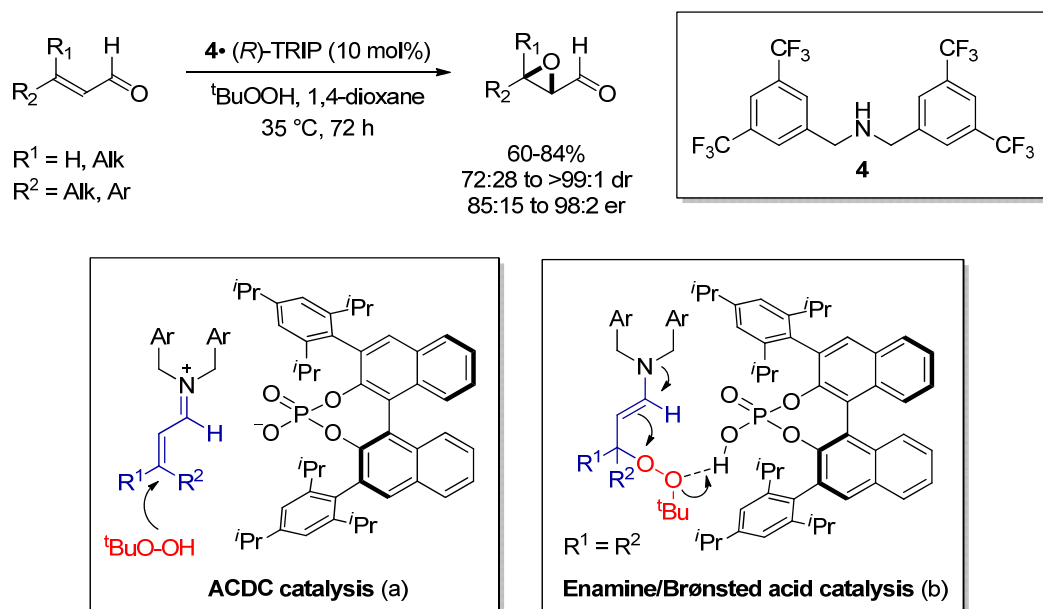


Scheme 2.21 Aminocatalytic epoxidation of enals by *Cordova* (a),^[78] and *MacMillan* (b).^[79]

List and *Wang* achieved an aminocatalytic asymmetric epoxidation of enals *via* asymmetric counteranion directed catalysis (ACDC).^[36] In contrast to previous studies, the authors used an *achiral* secondary amine catalyst **4** together with the chiral Brønsted acid TRIP (**3**). As discussed in Section 2.1.3.1, under this mechanistic regime the achiral iminium species exists as a tight ion pair with the chiral conjugate base of TRIP (**3**), allowing for enantiodiscrimination during the nucleophilic attack of the oxidant (Scheme 2.22, box (a)). Importantly, this method also gave excellent enantioselectivities with trisubstituted α,β -unsaturated aldehydes ($\text{R}^1 = \text{R}^2 =$

2. Background

Alk, Scheme 2.22), which had previously been elusive to highly enantioselective epoxidation. These findings are particularly intriguing since the enantioselective step in the epoxidation of such substrates no longer falls under the ACDC mechanistic regime. Indeed, the initial nucleophilic addition of the peroxide reagent to symmetrically substituted substrates does not create a stereogenic centre, and it is the subsequent, enamine-catalyzed cyclization that is enantiodiscriminating (Scheme 2.22, box (b). This mechanistic mode can be best described as a synergistic enamine/chiral Brønsted acid catalysis, and has been surprisingly underexplored to date.^[35b]

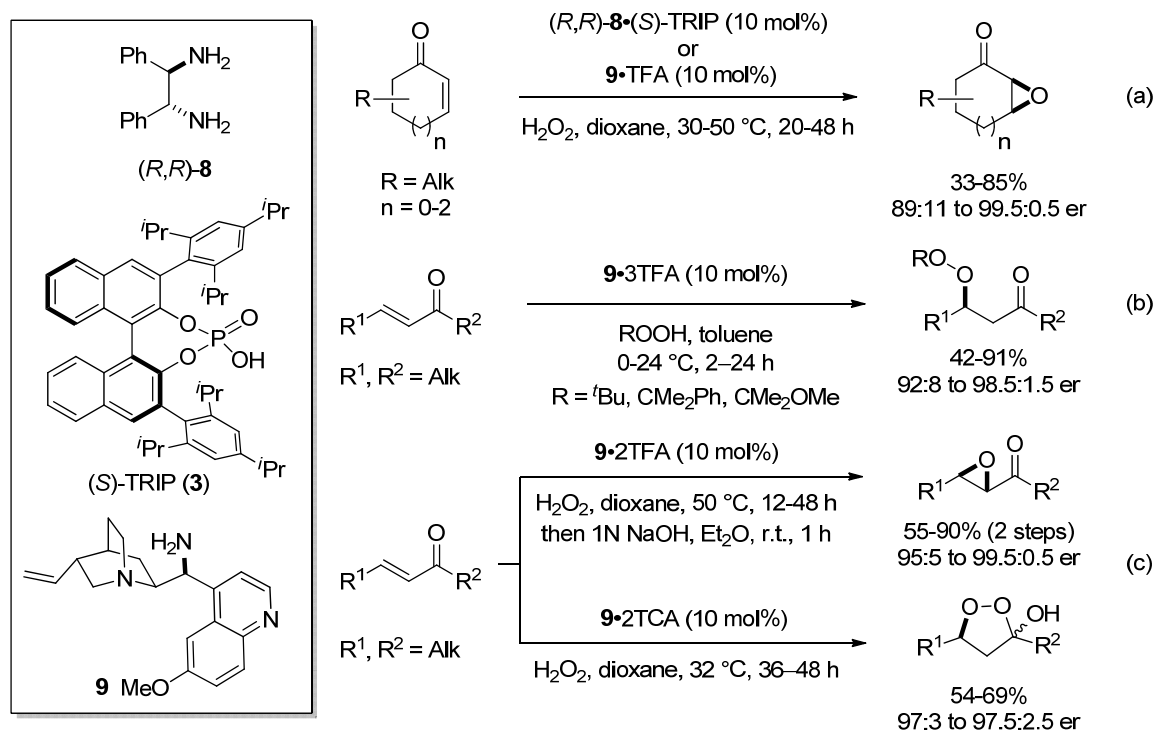


Scheme 2.22 Aminocatalytic epoxidation of enals by *List*.^[36]

Following the seminal discoveries on the epoxidation of α -unbranched enals with secondary amine catalysts, *List* and colleagues successfully expanded the methodology to cyclic α,β -unsaturated ketones.^[80] This time the most efficient catalysts proved to be primary amines, and two equally powerful catalytic salts were identified, consisting of a primary diamine (*R,R*)-**8** and (*S*)-TRIP, and primary cinchona-derived amine **9** with trifluoroacetic acid (TFA) (Scheme 2.23 (a)). The latter catalyst combination also proved to be extremely effective in the epoxidation and peroxidation of acyclic α,β -unsaturated ketones, which was simultaneously developed by the groups of *Deng* and *List* in 2008. In particular, *Deng* and colleagues used catalytic **9**·TFA salt and *tert*-butyl hydroperoxide for the asymmetric peroxidation of acyclic enones (Scheme 2.23 (b)),^[81] while *List et al.* used the same catalyst system with aqueous hydrogen peroxide to effect

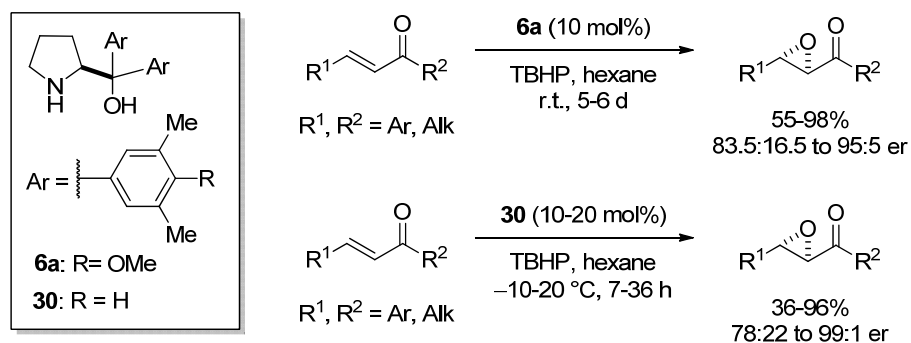
2. Background

both asymmetric hydroperoxidation and epoxidation of acyclic α,β -unsaturated ketones, depending on the reaction conditions (Scheme 2.23 (c)).^[82]



Scheme 2.23 Aminocatalytic hydroperoxidation and epoxidation of enones by *List*^[80, 82] and *Deng*.^[81]

It should be noted that the groups of *Lattanzi*^[42b] and *Zhao*^[83] also developed methodologies for the enantioselective epoxidation of enals using prolinol catalysts **6a** and **30**, respectively (Scheme 2.24). However, as mentioned in Section 2.1.3.2 these reactions were found to proceed *via* general Brønsted acid/Brønsted base catalysis, rather than iminium/enamine activation that belongs to the Lewis base catalysis discussed in this section.

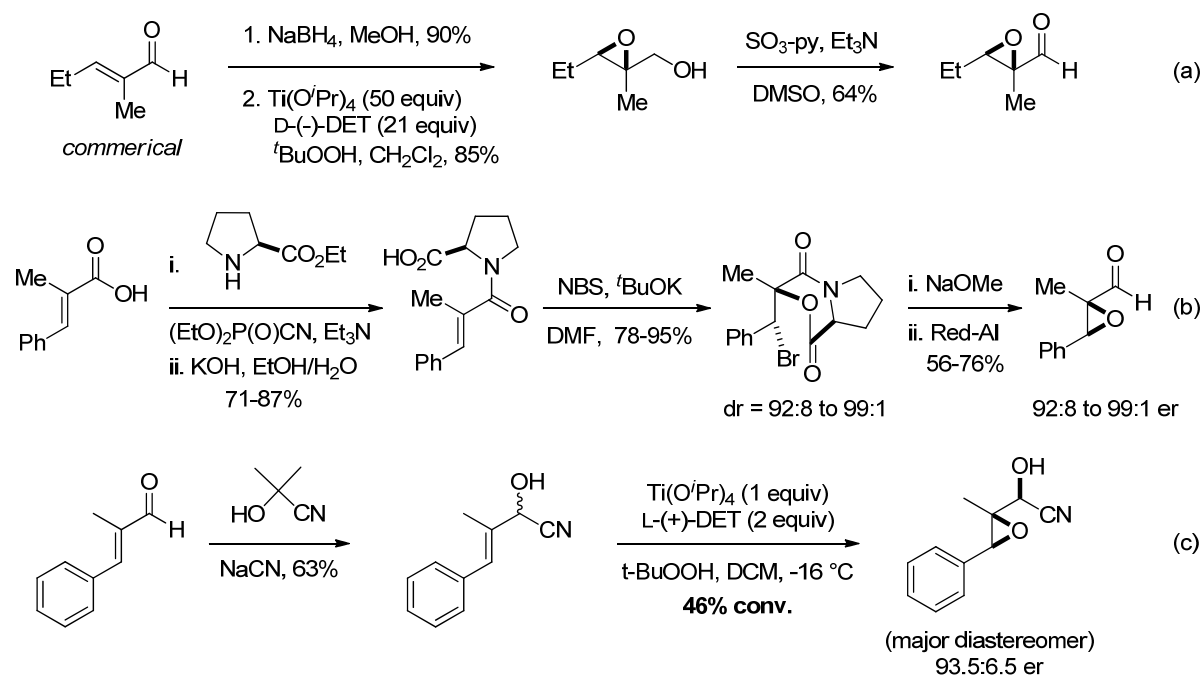


Scheme 2.24 Epoxidation of enals by *Lattanzi* (a),^[42b] and *Zhao* (b)^[83] using non-covalent catalysis.

2. Background

2.2.4 Enantioselective Epoxidation of α -Branched Enals

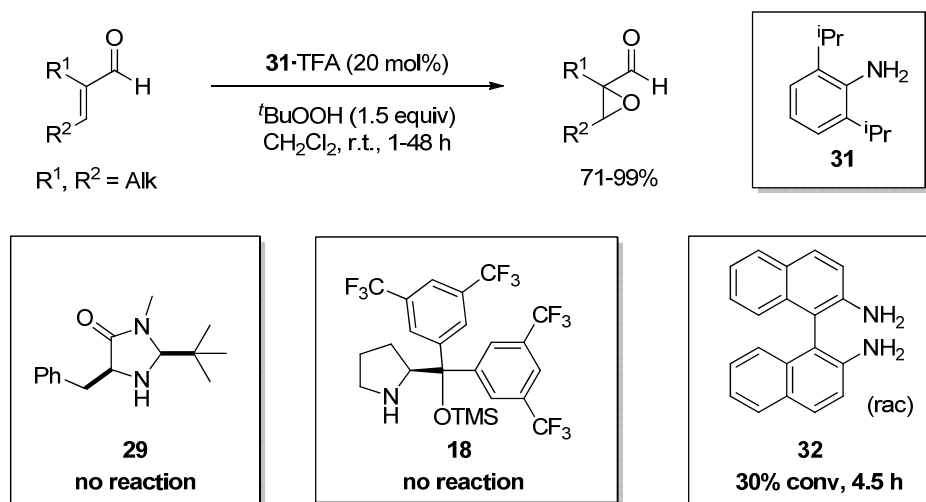
At the outset of this Ph.D. work, no general and direct approaches for the epoxidation of α -branched enals existed, as asymmetric methodologies invariably utilized substrates of higher or lower oxidation state.^[84] The most commonly used route to access the corresponding epoxyaldehydes still remains to be the *Sharpless* epoxidation of allylic alcohols, followed by the oxidation of the alcohol moiety to an aldehyde. However, since the requisite allylic alcohols often have to be prepared from carbonyl or carboxyl starting materials, the overall approach often involves three or more iterative redox operations, of which only one achieves the desired increase in the oxidation state (Scheme 2.25 (a)). Similar problems of redox and atom economy exist in the chiral auxiliary approaches, such as the one developed by *Terashima* in the 1980's (Scheme 2.25 (b)). A conceptually elegant strategy was pursued by the group of *Williams*, who reversibly masked α -branched enals as cyanohydrins, making them substrates for the *Sharpless* epoxidation (Scheme 2.25 (c)).^[85] Unfortunately, the authors were only able to effect kinetic resolution of the racemic cyanohydrins, which effectively reduces the theoretical yield to a maximum of 50%. Perhaps due to difficulties in activating aldehydes by Lewis acids, catalytic enantioselective strategies discussed in Section 2.2.2 did not find application with enals, whether linear or branched.



Scheme 2.25 Typical approaches to asymmetric epoxidation of α -branched enals at the outset of this Ph.D. work: *Sharpless* epoxidation-oxidation sequence (a),^[86] an auxiliary approach (b),^[87] and indirect *Sharpless* epoxidation of cyanohydrins.^[85]

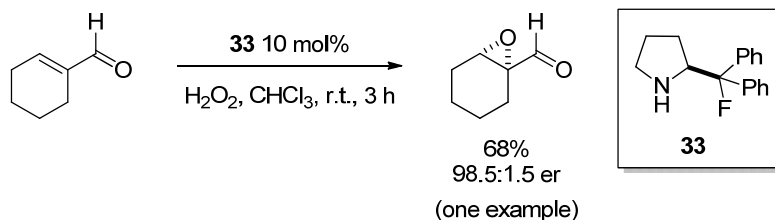
2. Background

Within the realm of organocatalysis, α -branched enals remained to be a notoriously difficult substrate for iminium activation. Nevertheless, already in 2007 *Pihko* and colleagues recognized that primary amine catalysts can efficiently activate this class of compounds for epoxidation, and developed an elegant non-asymmetric methodology (Scheme 2.26).^[88] Unfortunately, their efforts to extend this method to an asymmetric variant did not meet with success, as the commonly used secondary amine catalysts **29** and **18** provided no conversion. The axially chiral primary diamine BINAM **32** used in racemic form provided only 30% conversion, discouraging the authors from testing the enantiopure version of this catalyst.



Scheme 2.26 Non-asymmetric epoxidation of α -branched enals by *Pihko* and early attempts at asymmetric catalysis.^[88]

An isolated example of an enantioselective epoxidation of cyclohexene-1-carboxaldehyde was reported by *Gilmour* and co-workers in 2009 in their studies of the fluorinated secondary aminocatalyst **33** (Scheme 2.27).^[89] While the scope of this epoxidation was not tested on other α -branched enals, cyclic carboxaldehydes often appear to be exceptionally amenable to secondary amine activation, unlike their acyclic counterparts.^[90]

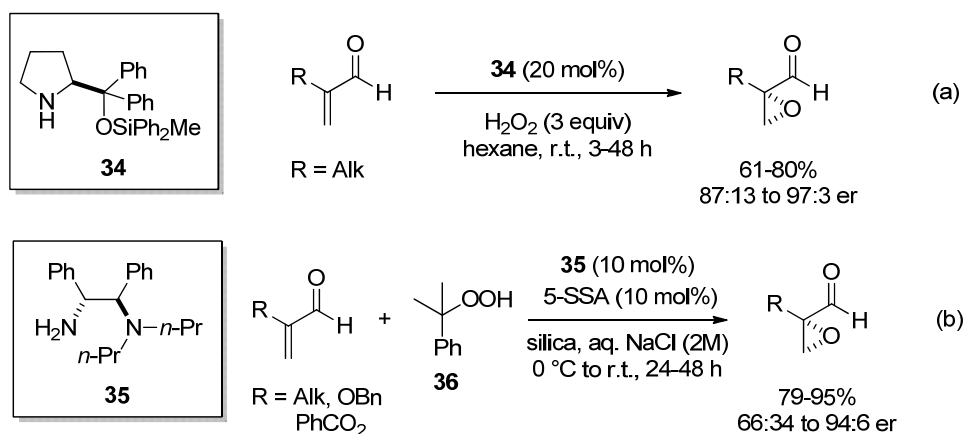


Scheme 2.27 An isolated example of asymmetric epoxidation of a cyclic carbaldehyde by *Gilmour*.^[89]

2. Background

Inspired by the seminal works of *Ishihara*, *Pihko* and *Melchiorre* on establishing primary aminocatalysis for the activation of α -branched enals (cf. Section 2.1.3.2), we have identified new salts that consist of a chiral primary ammonium cation and a chiral phosphate anion that catalyze the epoxidation of a variety of branched enals with excellent enantioselectivity.^[91] These results constitute a part of this Ph.D. work, and will be discussed in full in Section 4.1.

Shortly following our report, two further independent studies by the groups of *Hayashi*^[92] and *Luo*^[93] appeared, which described the asymmetric epoxidation of α -substituted acroleins using aminocatalysis (Scheme 2.28). In particular, *Hayashi* and colleagues used aqueous hydrogen peroxide and the silylated prolinol **34** as catalyst – a rather surprising result, given *Pihko's* earlier studies^[88] (see Scheme 2.26). The group of *Luo* used cumene hydroperoxide (CHP) **36** and a salt of the primary aminocatalyst **35** to achieve the same transformation. Mechanistically, both of the methods rely on iminium catalysis for the activation of the substrate toward the nucleophilic addition of the peroxide, although this step does not create a stereogenic centre. Instead, it is the subsequent enamine-catalyzed intramolecular ring-closure that governs the enantioselectivity of the reaction, similar to the mechanism discussed in Section 2.2.3 (Scheme 2.22, box (b)).



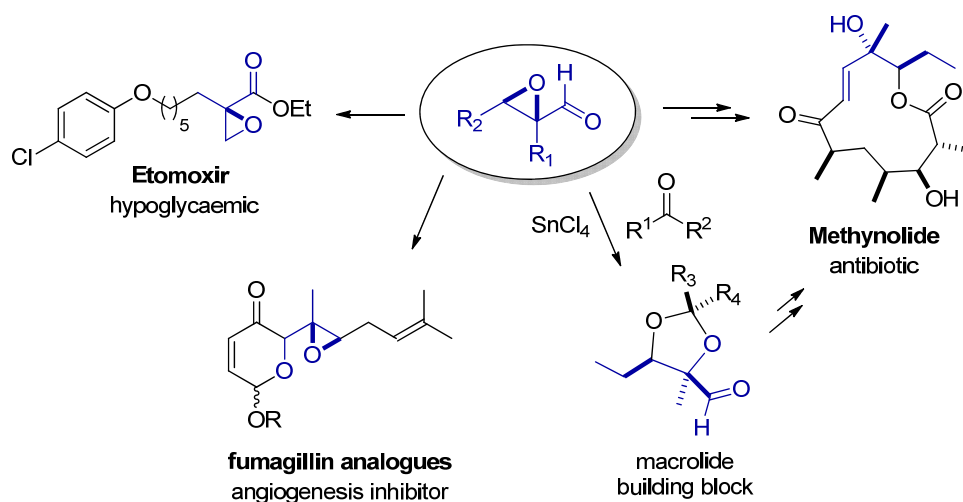
Scheme 2.28 Catalytic asymmetric epoxidation of α -substituted acroleins by *Hayashi* (a),^[92] and *Luo* (b).^[93] 5-SSA = 5-sulfosalicylic acid.

2.2.5 Synthetic Versatility of α -Substituted α,β -Epoxyaldehydes

Due to their useful pattern of functionalization, enantioenriched α -substituted α,β -epoxyaldehydes serve as some of the most commonly used synthons in total synthesis. Scheme 2.29 shows some examples where α -substituted α,β -epoxyaldehydes were used as direct precursors to bioactive compounds (Etomoxir and Fumagillin analogues), as well as a starting

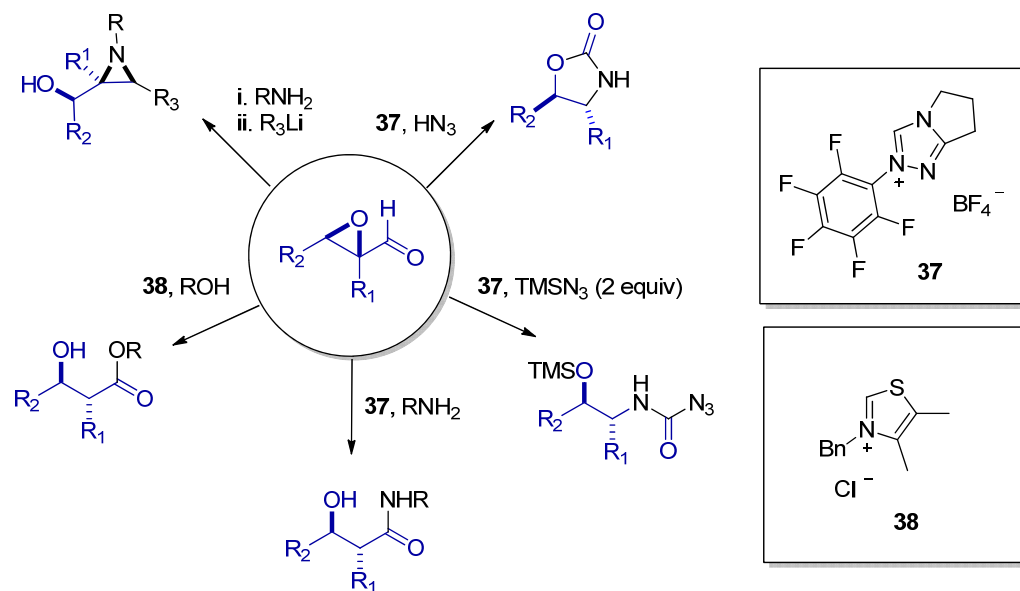
2. Background

material for macrolide building blocks, which are used to construct a variety of compounds, including the antibiotic Methynolide.^[94]



Scheme 2.29 The use of α -substituted α,β -epoxyaldehydes in total synthesis.^[94]

Apart from direct use, enantioenriched α -substituted α,β -epoxyaldehydes can also be converted into many valuable derivatives with full retention of the stereochemical information. Such derivatization methods include NHC-catalyzed internal redox reactions and *Payne* type rearrangements, among others (Scheme 2.30).^[95]



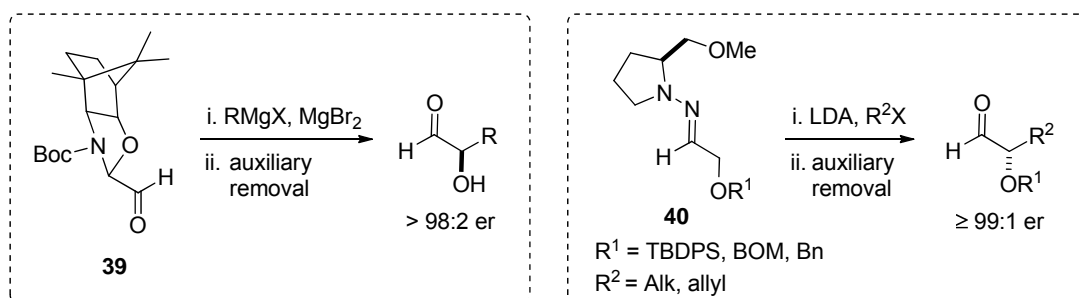
Scheme 2.30 Synthetic versatility of α -substituted α,β -epoxyaldehydes.^[95]

2.3 Catalytic Asymmetric α -Oxidation of Carbonyl Compounds

2.3.1 Historical Overview

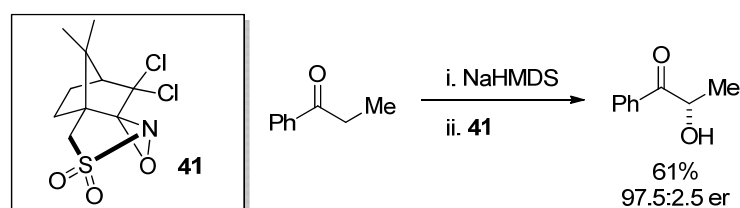
Enantioselective α -oxidation of carbonyl compounds represents one of the most fundamental transformations in organic synthesis, and extensive research efforts have been directed to this area since the early 1980's.^[96] Remarkably, it was not until 2004 that the first general and *direct* catalytic methodology was developed using aminocatalysis.^[97]

Before organocatalysis, catalytic asymmetric α -hydroxylation of aldehydes was particularly challenging and the synthesis of the corresponding products mainly relied on the transformations of chiral pool reagents, including amino acids,^[98] sugars^[99] and chiral α -hydroxy acids.^[100] Indirect auxiliary approaches, including diastereoselective reactions of glyoxal derivatives such as **39**^[101] and *Enders* hydrazones **40**,^[102] were also commonly employed (Scheme 2.31)



Scheme 2.31 Auxiliary approaches to enantioenriched α -oxygenated aldehydes.^[101-102]

In contrast, ketones and esters were found to be amenable to enantioselective α -hydroxylation, albeit only after prefunctionalization to enolates, or (silyl) enol ethers/ketene acetals. In the 1990's, electrophilic α -hydroxylation of enolates was dominated by the use of chiral oxaziridine reagents such as **41**, pioneered by the group of *Davis* (Scheme 2.32).^[103]

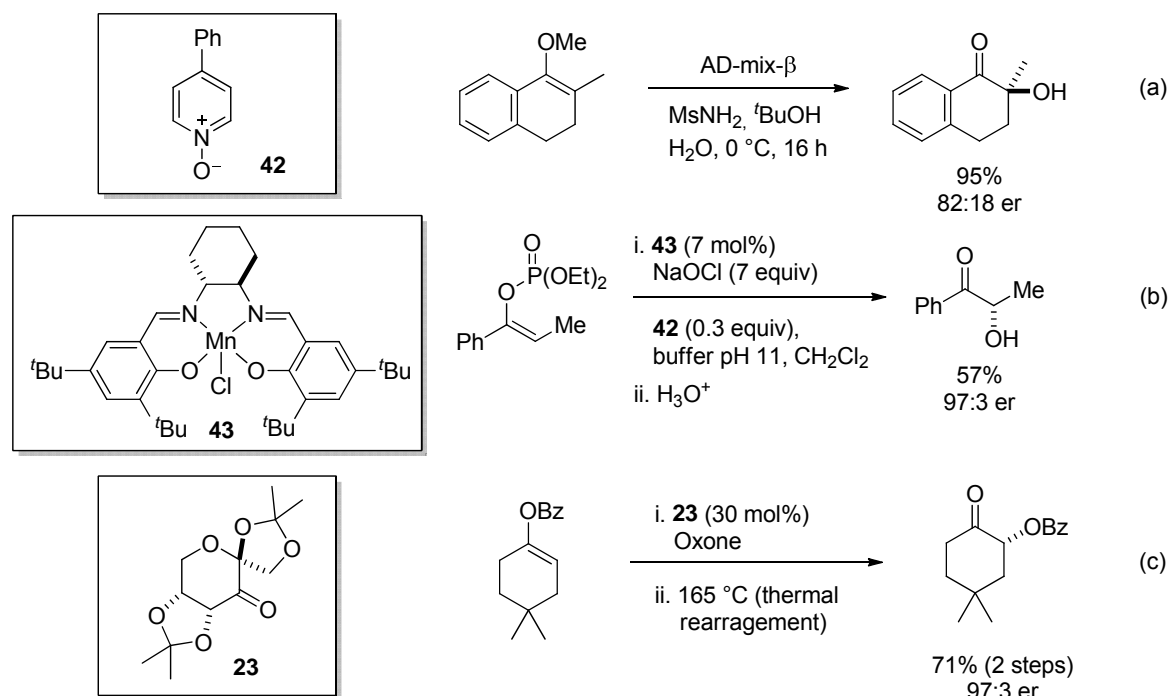


Scheme 2.32 Enolate hydroxylation of ketones with *Davis* oxaziridine.^[103]

Subsequently, catalytic methodologies based on the *Sharpless* dihydroxylation of enol ethers^[104] (Scheme 2.33, (a)) and epoxidation of enol ethers and esters^[96] (Scheme 2.33, (b)-(c)) were

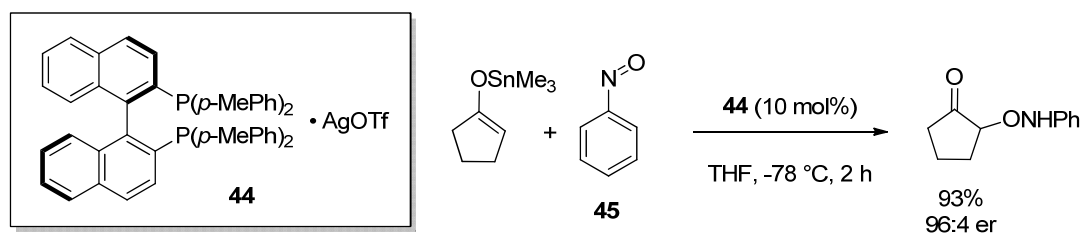
2. Background

developed. Not surprisingly, in the latter two cases the most successful enol epoxidation methods rely on catalysts established for regular olefins, including *Jacobsen-Katsuki* Mn(III) salen complexes of type **43** for silyl enol ethers^[105] and enol phosphonates^[106] and the *Shi* catalyst **23** for silyl enol ethers^[107] and enol esters.^[108]



Scheme 2.33 Sharpless dihydroxylation of enol ethers (b),^[104] enol phosphonate epoxidation with Mn-salen complex (c),^[106] *Shi* epoxidation of enol esters (d).^[108]

Most recently, *Momiyama* and *Yamamoto* developed a very efficient aminoxylation of tin enolates and silyl enol ethers with nitrosobenzene using *tol*-BINAP/AgOTf complex **44** as the catalyst (Scheme 2.34).^[109] The use of nitrosobenzene **45** as the electrophilic oxygen source inspired the early organocatalytic approaches, which are discussed in the next section.



Scheme 2.34 *Yamamoto's* α -hydroxylation of tin enolates with nitrosobenzene.^[109]

2. Background

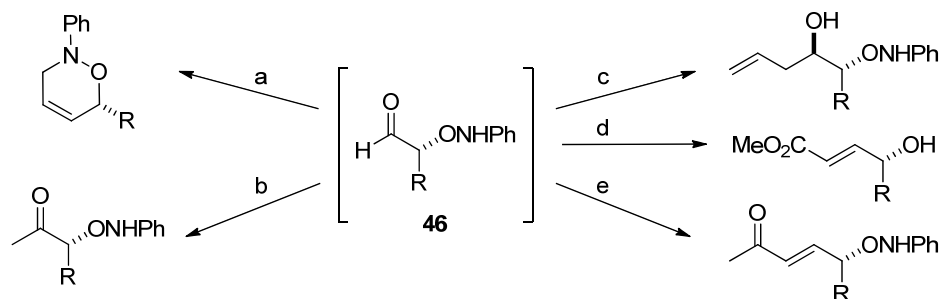
2.3.2 Organocatalytic Approaches

Organocatalytic activation of aldehydes and ketones as enamines particularly influenced the field of enantioselective carbonyl α -functionalization by providing methodologies which, for the first time, did not require prefunctionalization of the carbonyl group. The first organocatalyzed enantioselective α -aminoxylation of aldehydes was independently reported by the groups of Hayashi,^[110] MacMillan^[111] and Zhong^[112] in 2003 (Table 2.1). All of these methods employed simple α -unbranched aldehydes and L-proline as the catalyst. Nitrosobenzene, which can act as an oxygen- or a nitrogen electrophile underwent exclusive *O*-attack in these reactions.

Table 2.1 Catalytic asymmetric α -aminoxylation of aldehydes: seminal reports.^[110-112]

Reference	Conditions	yield, % (46a)	er (46a)
Hayashi <i>et al.</i>	30 mol% 1 , MeCN, -20 °C, 24 h	62-99	97.5:2.5 to 99.5:0.5
MacMillan <i>et al.</i>	5 mol% 1 , CHCl ₃ , 4 °C, 4 h	60-88	98.5:1.5 to 99.5:0.5
Zhong	20 mol% 1 , DMSO, r.t., 10-20 min	54-86	97:3 to 99.5:0.5

Excellent enantioselectivity and good yields were obtained for a variety of unbranched aliphatic, benzylic and allylic substrates. It should be noted that α -oxygenated aldehydes **46** which exist as oligomers in solution,^[111] are never isolated, but typically reduced *in situ* to afford diols (**46a**). However, even in oligomeric form, the aldehyde moiety smoothly undergoes a variety of reactions *in situ*, and a number of reports have demonstrated the synthetic utility of products **46** (Scheme 2.35).^[113]

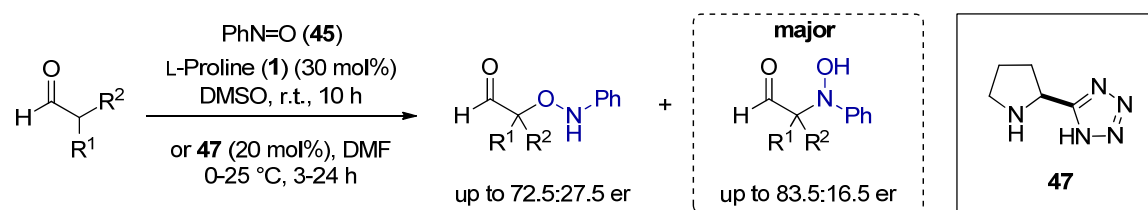


(a) CH₂=CHPh₃⁺ Br⁻, NaH, 0 °C; (b) CH₂N₂, MgCl₂, Et₂O, r.t.; (c) In, allyl bromide, r.t.; (d) LiCl, DBU, NH₄Cl, MeO₂CCH₂P(O)(OEt)₂, -15 °C; (e) diethyl (2-oxopropyl)phosphonate, Cs₂CO₃, r.t.

Scheme 2.35 Synthetic utility of products **46** (references in same order).^[113]

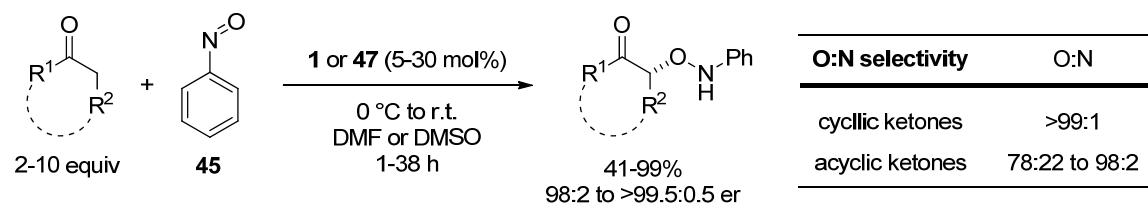
2. Background

Despite its high enantioselectivity and versatility, the method suffers from two important limitations. Firstly, a several-fold excess of the aldehyde substrate (typically 3 equiv) is required to secure good yields, thus limiting the method to inexpensive starting materials and the early stages of a multistep synthesis. Although *MacMillan* has used the procedure in a convergent total synthesis of natural products brasoside and littoralisone on a relatively advanced intermediate, reaction-specific optimization and higher catalyst loading was required to achieve a method which is stoichiometric in the aldehyde reagent.^[113d] Secondly, reactions with α -branched aldehydes invariably afford inseparable mixtures of aminoxylation and nitroso aldol products (i.e. both *O*- and *N*-attack on nitrosobenzene), favouring the latter and resulting in only moderate enantioselectivity for the α -oxygenated product (up to 72.5:27.5 er, Scheme 2.36).^[114]



Scheme 2.36 The reactivity of α -branched aldehydes with nitrosobenzene under secondary amine catalysis.^[114]

Shortly after the seminal reports on the α -aminooxylation of aldehydes, the method was extended to aliphatic ketone substrates. Once again, several groups independently reported this transformation in the same year, using L-proline (**1**) or the *Ley* tetrazole **47** as the catalyst (Scheme 2.37).^[115]

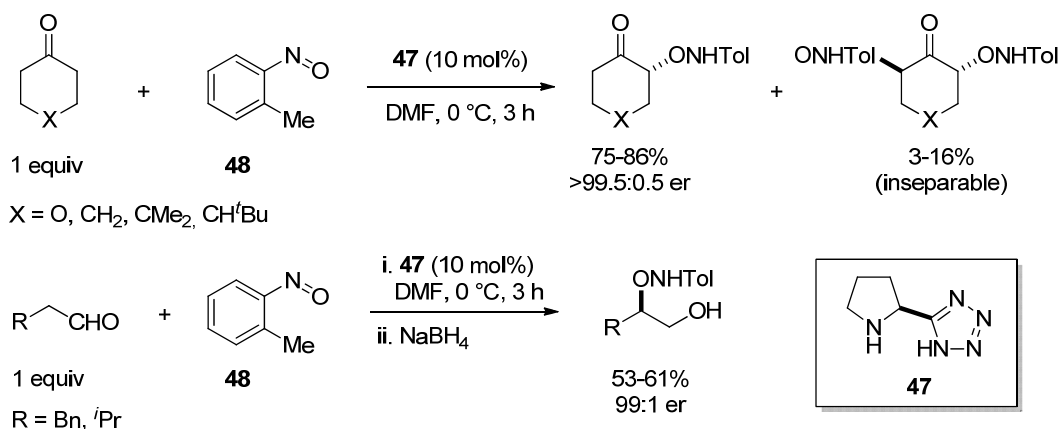


Scheme 2.37 Catalytic asymmetric α -aminooxylation of ketones.^[115]

While excellent O:N selectivity was again observed for cyclic ketones, it was somewhat diminished for acyclic ketones (Scheme 2.37). Moreover, two available α -positions of ketones and the high reactivity of nitrosobenzene made bis-aminooxylation a competitive process, which could be suppressed with a large excess of ketone (up to 10 equiv) and a slow addition of nitrosobenzene by a syringe pump. Unlike with the aldehydes, the α -aminooxylated ketones can be isolated and the weak O-N bond cleaved by simple treatment with $\text{CuSO}_4 \cdot 5\text{H}_2\text{O}$.^[115a]

2. Background

Although α -aminoxylation of ketones is highly enantioselective and amenable to kinetic resolution^[115c, 115e] and desymmetrization reactions,^[116] the problem of ketone stoichiometry is once again the major disadvantage of the method. Several approaches have been explored to circumvent the problem. The group of *Yamamoto* found that the use of 2-nitrosotoluene **48** instead of nitrosobenzene, together with the tetrazole catalyst **47** enabled asymmetric aminoxylation of a stoichiometric amount of ketone and aldehyde reagents (Scheme 2.38).^[117] Nevertheless, slow addition of 2-nitrosotoluene over hours is still required, and the minor amounts (3-16%) of the bis-aminoxylated product were found to be inseparable in all cases.



Scheme 2.38 Catalytic asymmetric α -aminoxylation of ketones: *Yamamoto* modification.^[117]

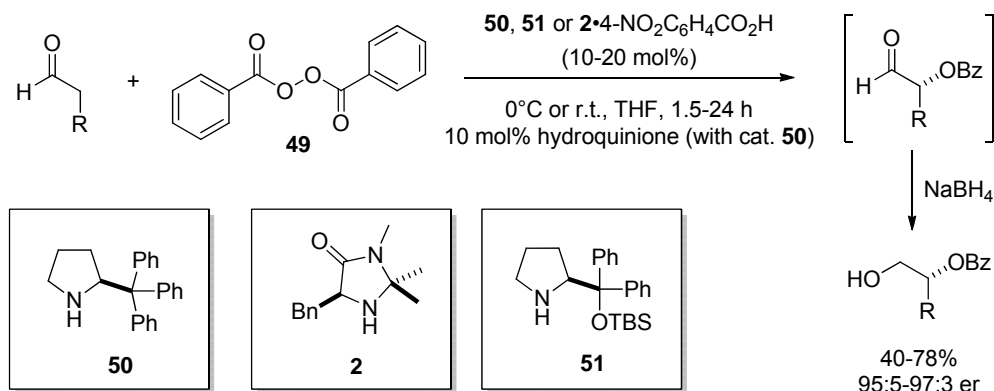
Other organocatalytic α -oxygenation strategies of aldehydes and ketones have also been pursued including the use of singlet oxygen, hypervalent iodine reagents, hydroperoxides, oxaziridines and benzoyl peroxide as the oxygen source, and reaction of enamine radical cations (SOMO activation) with TEMPO.^[97] Of these methodologies, the use of benzoyl peroxide to effect α -benzoyloxylation has been the most promising methodology in terms of both reactivity and enantioselectivity, and is covered in detail in the next section.

2.3.2.1 Benzoyl Peroxide as the Electrophilic Oxidant

Although early organocatalytic approaches were heavily dominated by the use of the highly reactive nitrosobenzene, it is not the only electrophilic reagent that can effectively promote α -oxidation of carbonyl compounds. Indeed, in 2009 the groups of *Maruoka*,^[118] *Tomkinson*^[119] and *Hayashi*^[120] independently reported the use of benzoyl peroxide **49** for the enantioselective α -benzoyloxylation of aldehydes (Scheme 2.39). Not only inexpensive, readily available and easy-to-handle, benzoyl peroxide also proved to have another very important advantage: it could

2. Background

be used with stoichiometric amounts of the aldehyde. Good yields and excellent enantioselectivities could be obtained using catalytic amounts of *Maruoka's* trityl-substituted pyrrolidine **50**, *MacMillan's* imidazolidinone **2** (used with an acid co-catalyst), or the silylated prolinol **51**. Radical inhibitor hydroquinone was used as a substoichiometric additive under *Maruoka's* conditions to prevent possible benzoyl radical side reactions.



Scheme 2.39 Catalytic asymmetric α -benzoyloxylation of aldehydes.^[118-120]

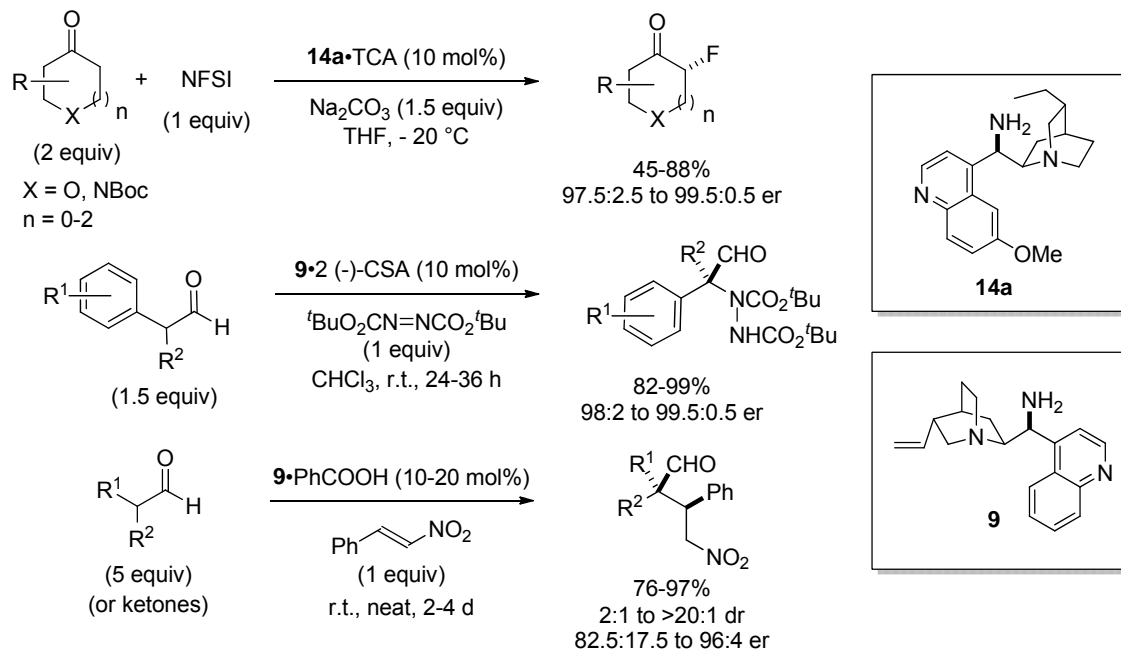
When considering the catalysts shown in Scheme 2.39, it becomes apparent that they all bear particularly bulky groups around the reactive nitrogen centre. In fact, *Maruoka* and colleagues specifically designed the trityl-substituted pyrrolidine **50** for the α -benzoyloxylation reaction,^[118] and in their catalyst screening, *Hayashi* and co-workers found that the TBS protecting group in catalyst **51** was necessary to achieve a higher yield compared to the commonly used TMS group.^[120] This steric bulk has been rationalized to prevent the attack of the catalyst on benzoyl peroxide, resulting in a catalyst decomposition pathway.^[118, 121] This feature of the catalysts may also well be the reason why no other, more sterically demanding substrate classes such as ketones and α -branched aldehydes had been applied to this catalyst system. We rationalized that the less nucleophilic primary amines would be simultaneously less susceptible to decomposition by oxidation and amenable to activation of sterically demanding substrates. This hypothesis led to the development of an enantioselective α -benzoyloxylation methodology of cyclic ketones^[122] and α -branched aldehydes, which is discussed in full detail in Section 4.2.

2.3.3 Primary Aminocatalysis in the α -Oxidation of Carbonyl Compounds

As discussed in Section 2.1.3.2, the use of primary amines in enamine catalysis has been extensively developed since 2005. Among methods for the α -functionalization of carbonyl

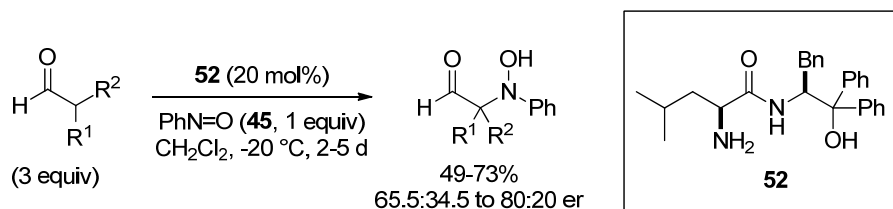
2. Background

compounds, cinchona-derived amines **9-14** have been particularly effective in catalyzing highly enantioselective transformations, including fluorination, amination and C-C bond formation *via* *Michael* additions (Scheme 2.40).^[35b, 45, 123]



Scheme 2.40 Examples of carbonyl α -functionalization catalyzed by cinchona-derived amines.^[35b, 45, 123]

Nevertheless, neither cinchona-derived amines nor any other primary amine catalysts found application in the α -oxidation of carbonyl compounds, even though aminocatalytic epoxidation methodologies attest to the oxidative stability of primary amines (cf. Section 2.2.3 and 2.2.4). Prior to our report,^[122] a single publication described the use of a primary amine in a reaction between α -branched aldehydes and nitrosobenzene, but reported exclusive *N*-selectivity (Scheme 2.41).^[124]

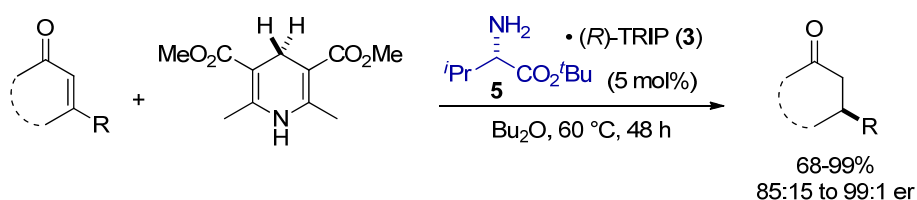


Scheme 2.41 Primary amine catalysis in a reaction between α -branched aldehydes and nitrosobenzene.^[124]

3. OBJECTIVES OF THIS PH.D. WORK

The ubiquity of oxygenated functional groups in organic molecules places asymmetric C-O bond formation among the most fundamental transformations in chemical synthesis. Despite the myriad of metal-based and enzymatic methodologies that have been developed over the years, continuous demand for improvement stimulates the search for new methods, which are general, operationally simple and utilize inexpensive, readily available and environmentally benign materials. The recently established field of organocatalysis has supplied new tools for enantioselective C-O bond-forming reactions, providing solutions to long-standing synthetic challenges. One such example is the organocatalytic asymmetric epoxidation of α,β -unsaturated aldehydes, first disclosed by *Jørgensen* and colleagues in 2005, for which no general approaches existed before (cf. Section 2.2.3).^[15]

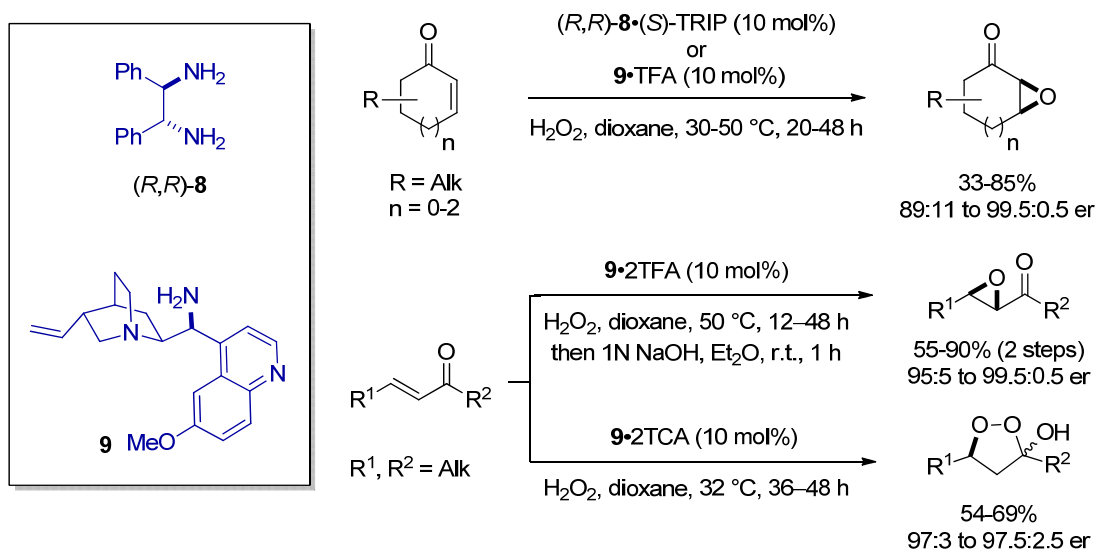
Following the report of *Jørgensen* and others,^[78-79] our group made important contributions to expand the substrate scope of epoxidation to other challenging substrates,^[36, 80, 82] including cyclic and acyclic α,β -unsaturated ketones. Key to the success of these methodologies was the identification of a competent catalytic system: in particular, the activation of less reactive and more sterically encumbered α,β -unsaturated ketones required a switch from the classically used secondary amine catalysis to primary amine catalysis (cf. Section 2.1.3.2). This observation was first made in our group in 2006 during the studies on transfer hydrogenation of cyclic enones, in which the primary amine catalyst **5** (used as a salt with a Brønsted acid co-catalyst) proved to be superior over various established secondary amines (Scheme 3.1).



Scheme 3.1 Primary amine catalysis in the transfer hydrogenation of α,β -unsaturated ketones.^[34]

The application of primary aminocatalysis to the epoxidation of α,β -unsaturated ketones identified two highly efficient catalyst systems consisting of primary ammonium salts (*R,R*)-**8**·(*S*)-TRIP and **9**·TFA, which could mediate the epoxidation of cyclic enones and hydroperoxidation and epoxidation of acyclic enones (Scheme 3.2, cf. Section 2.2.3).^[80, 82] Apart from using readily available amine catalysts, the method also employed hydrogen peroxide as an environmentally benign and atom-economic oxidant.

3. Objectives of this Ph.D. Work



Scheme 3.2 Primary amine-catalyzed epoxidation and hydroperoxidation of enones.^[80, 82]

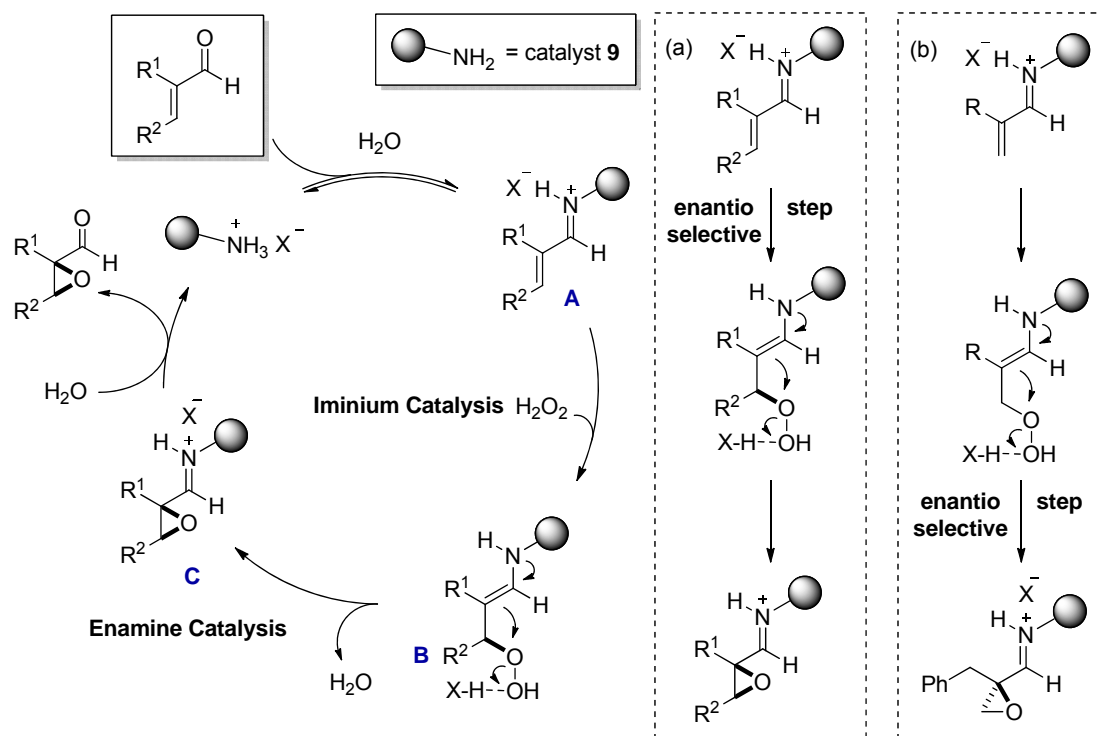
The establishment of primary amine catalysts in epoxidation reactions encouraged us to explore their ability to activate other previously inaccessible substrates. In particular, α -branched enals still posed a formidable challenge to synthetic chemists, with neither metal catalysis nor organocatalysis offering methodologies for their enantioselective epoxidation. Instead, multistep approaches were commonly utilized, employing substrates of a higher or lower oxidation level for epoxidation followed by redox adjustment (cf. Section 2.2.4). We recognized that a more step-, atom- and redox-economic approach which operates at the oxidation level of an aldehyde would not only be highly desirable, but also perfectly suited to amine-mediated catalysis.

*The goal of this Ph.D. work was to develop a direct, efficient and enantioselective epoxidation methodology for α -branched α,β -unsaturated aldehydes using environmentally benign, inexpensive and easily available hydrogen peroxide as the oxidant. In particular, primary amine catalysts, such as the cinchona alkaloid derivative **9**, were envisioned to provide a suitable catalytic platform. Over the course of this work, a further goal became the rationalization of the absolute stereochemistry of the epoxide products by structural and computational investigations of the reaction intermediates.*

In general terms, the desired epoxidation was envisioned to proceed *via* iminium ion activation of α -branched enals by primary ammonium salts (Scheme 3.3). This activation would encourage conjugate addition of hydrogen peroxide, forming the enamine intermediate **B**. The intermediate **B** would then undergo an intramolecular ring-closure, breaking the weak O-O bond and forming the epoxide moiety while regenerating an iminium ion (structure **C**). Hydrolysis of **C** would release the product and the catalyst for turnover. It is important to point out that,

3. Objectives of this Ph.D. Work

depending on the substitution pattern of the α -branched enal, the enantioselective step of the reaction could either be the iminium-catalyzed conjugate addition of hydrogen peroxide (α,β -disubstituted enals, Scheme 3.3 (a)) or the enamine-catalyzed ring-closure (α -monosubstituted enals, Scheme 3.3 (b)).



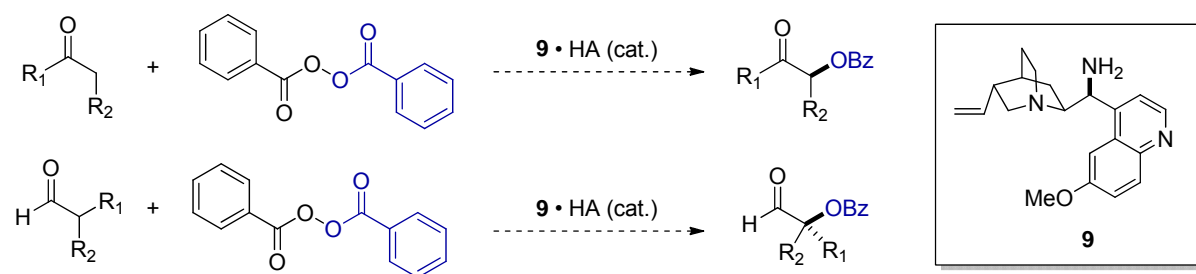
Scheme 3.3 Proposed mechanistic models of epoxidation of α,β -disubstituted enals (a), and α -monosubstituted enals (b).

Over the course of this work, both mechanistic scenarios outlined in Scheme 3.3 were successfully realized using the cinchona alkaloid-derived catalyst **9** (cf. Section 4.1). The high activity of **9** under oxidative conditions and in particular, its success in effecting an enantioselective epoxidation *via enamine catalysis* (Scheme 3.3 (b)) inspired us to turn our attention to a mechanistically related transformation – oxidative α -functionalization of ketones and α -branched aldehydes. Organocatalytic approaches to this transformation are based on enamine activation of the carbonyl toward an attack on electrophilic oxidants, and possess the advantage of not requiring carbonyl prefunctionalization to an enolate equivalent compared to metal catalysis (cf. Section 2.3.2). Highly enantioselective α -oxidation of ketones has been developed using nitrosobenzene, but the method requires a large excess of the ketone substrate (up to 10 equiv) limiting the method's practicability.^[115] Moreover, no useful methodology, organocatalytic or metal-based, exists for α -branched aldehydes to date (cf. Section 2.3.2). The

3. Objectives of this Ph.D. Work

recently developed asymmetric α -oxidation using benzoyl peroxide as the electrophilic oxidant operates with stoichiometric amounts of the carbonyl component but had not been extended beyond simple unbranched aldehydes for possible reasons discussed in Section 2.3.2.1.

On the basis of these considerations, we envisioned that the readily available primary amines of type **9** could catalyze a direct enantioselective α -benzoyloxylation of ketones and α -branched aldehydes. Thus, the second goal of this Ph.D. work was to develop an efficient method for the α -benzoyloxylation of previously inaccessible carbonyl compounds that is stoichiometric in the carbonyl reagent and introduces a protected oxygen functionality using primary aminocatalysis (Scheme 3.4).



Scheme 3.4 Envisioned α -benzoyloxylation of ketones and α -branched aldehydes using primary amine catalyst **9**.

4. RESULTS AND DISCUSSION

4.1 Catalytic Asymmetric Epoxidation of α -Branched Enals

4.1.1. Identification of a Model System

The catalytic efficiency of 9-amino(9-deoxy)*epi*quinine TFA salt ([**9**·2TFA]) in promoting the enantioselective epoxidation of various α,β -unsaturated ketones^[80, 82] encouraged us to test this catalytic platform in the asymmetric epoxidation α -substituted α,β -unsaturated aldehydes **53**, a previously unsolved substrate class. Following the enone studies,^[82] aqueous hydrogen peroxide (50 wt. %) was selected as the second most atom economic and environmentally benign oxidant, and reactions were conducted in water-miscible 1,4-dioxane at 50 °C. A brief screen of several commercially available (*E*)-configured α -substituted enals **53a-c** revealed that 2-methyl-2-pentenal **53c** afforded the desired product with an encouraging conversion and stereoselectivity (Table 4.1, entry 3). In contrast, the epoxidation of α -methyl-cinnamaldehyde **53a** gave only traces of the desired product even after several days (entry 1). It is noteworthy that the same detrimental effect of an aromatic β -substituent was observed in the epoxidation of acyclic α,β -unsaturated ketones, where chalcones proved to be unreactive.^[82] The epoxidation of the cyclic aliphatic substrate **53b** was found to be feasible but only sluggish under these reaction conditions (entry 2).

Table 4.1 Catalytic asymmetric epoxidation of various α -substituted enals: preliminary study.

Entry	Time	Substrate	Conv., % ^a	dr ^a	er (<i>trans</i>) ^b	er (<i>cis</i>) ^b	
1	4 d		53a	6	88:12	<i>nd</i>	<i>nd</i>
2	48 h		53b	20	>99:1	<i>nd</i>	<i>nd</i>
3	22 h		53c	47	75:25	93:7	60:40

^a Determined by GC. ^b Determined by chiral-phase GC

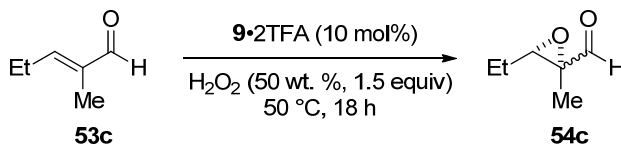
4. Results and Discussion

As seen from Table 4.1, both of the acyclic (*E*)-configured enal substrates (entries 1, 3) afforded the desired product as mixtures of diastereomers, with moderate selectivity for the *trans*-isomer. This lack of stereospecificity is in accord with the stepwise mechanism typical for *Weitz-Scheffer* type epoxidations (cf. Section 2.2.2). Interestingly, significant difference was observed in the enantiomeric excess of the two diastereomers of **54c** (entry 3). Assuming a sequential formation of the two epoxide stereogenic centres *via* a catalyst-controlled enantioselective step, followed by a diastereoselective step (cf. Chapter 3 for proposed mechanism), enantiomeric enrichment of the *trans*-diastereomer at the expense of the *cis*-diastereomer is possible. Due to the encouraging conversion and enantioselectivity observed in its epoxidation, 2-methyl-2-pentenal **53c** was chosen as the model substrate for further optimization. The absolute configuration (*2R,3S*) of *trans*-**54c** was assigned by comparing the optical rotation of the corresponding epoxyalcohol after NaBH₄ reduction, to the literature value.^[125]

4.1.2 Optimization of the Reaction Parameters

To understand the general effect of the reaction medium, a preliminary screen of various chlorinated, aromatic and ethereal solvents was performed, keeping the other reaction parameters as before (Table 4.2). Compared to the control in 1,4-dioxane (entry 1), every tested solvent resulted in diminished stereoselectivity, with acetonitrile (entry 5) affording a completely non-diastereoselective and only slightly enantioselective reaction.

Table 4.2 Preliminary solvent screen.



Entry	Solvent (0.125 M)	Conversion, % ^a	dr ^a	er (<i>trans</i>) ^b
1	1,4-dioxane	40	75:25	93:7
2 ^c	CH ₂ Cl ₂	96	73:27	83:17
3	CHCl ₃	48	68:32	84:16
4	toluene	41	62:38	78:22
5	MeCN	23	51:49	64:36

^a Determined by GC. ^b Determined by chiral-phase GC. ^c Performed at 32 °C.

All of the solvents gave a similar conversion of approximately 40% after 18 hours with two exceptions. Acetonitrile significantly retarded the reaction rate (entry 5), while dichloromethane

4. Results and Discussion

improved the conversion to nearly complete (96%, entry 2). However, the volatility of dichloromethane required lowering of the reaction temperature to 32 °C from the standard 50 °C, and even at this temperature significant solvent loss was observed. It was hypothesized that the success of dichloromethane may simply have been due to the increased reaction concentration, which was tested next (Table 4.3). Indeed, increasing the concentration under the standard reaction conditions (1,4-dioxane at 50 °C) led to some improvement of conversion (entries 2-3 vs. 1). However, increased concentration also compromised the stereoselectivity of the reaction, discouraging us from changing this parameter.

Table 4.3 Optimization of the reaction concentration.

CC=CC(=O)O $\xrightarrow[\text{1,4-dioxane, 50 }^\circ\text{C, 18 h}]{\text{9}\cdot\text{2TFA (10 mol\%)}\text{, H}_2\text{O}_2 \text{ (50 wt. \%, 1.5 equiv)}}$ CC[C@H](C)C(=O)O

53c **54c**

Entry	Concentration, [M]	Conversion, % ^a	dr ^a	er (<i>trans</i>) ^b
1	0.125	40	75:25	93:7
2	0.25	48	75:25	89:11
3	0.50	50	70:30	84:16

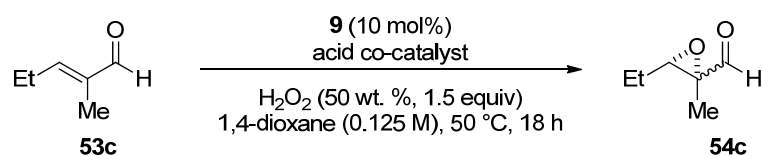
^a Determined by GC. ^b Determined by chiral-phase GC.

We next turned our attention to the catalytic system, and in particular the Brønsted acid co-catalyst, which often plays an important role in iminium catalysis (cf. Section 2.1.3.1). A screen of various achiral and chiral acids is summarized in Table 4.4. As expected, the structure of the Brønsted acid had a significant impact on the conversion and stereoselectivity of the reaction, although no clear trend with respect to the acid strength (pK_a)^[126] was observed. Thus, good conversion and stereoselectivity was observed over a wide range of pK_a values, including very strong acids (entry 7), strong acids (entries 1-4) and weak acids (entries 6, 10-13). At the same time, subtle electronic and/or structural properties of some Brønsted acids resulted in severe loss of yield (entries 5 and 8). Although TFA performed equally well at 10-30 mol% loading (entries 1-3), reducing the catalyst loading of H₃PO₄ from 20 to 7 mol% dramatically reduced the conversion (entries 9-10). Among the achiral acids tried, those containing a phosphate group had a positive effect on both the conversion and the stereoselectivity of the reaction (entries 5 and 9). To our delight, the chiral phosphoric acid (*R*)-TRIP (**3**) used at 20 mol% loading further improved the stereoselectivity of the reaction to nearly perfect enantioselectivity (99.5:0.5 er) and very good diastereoselectivity of 92:8 dr, demonstrating a dramatic case of “matched” chiral induction (entry 12). Furthermore, the (*S*) enantiomer of TRIP resulted in the loss of this

4. Results and Discussion

synergism, giving a completely reversed but only modest enantioselectivity and diastereoselectivity (entry 13).

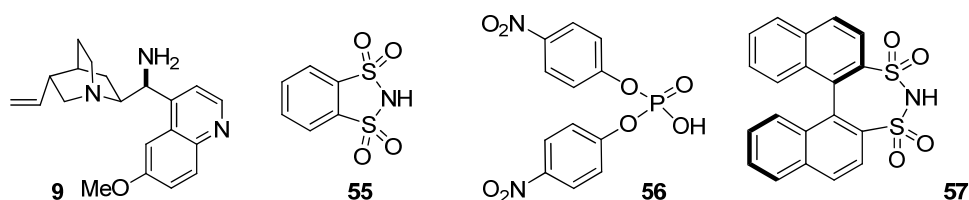
Table 4.4 Screen of various chiral and achiral Brønsted acid co-catalysts with primary amine **9**.



Entry	Acid co-catalyst	pKa (H ₂ O) ^a	[mol%]	Conversion,% ^b	dr ^b	er (<i>trans</i>) ^c
1	TFA	-0.25	10	38	78:22	93:7
2	TFA	-0.25	20	41	78:22	93:7
3	TFA	-0.25	30	40	79:21	93:7
4	TCA	0.65	20	34	76:24	91:9
5	<i>p</i> -nitrobenzoic acid	3.44	20	6	54:46	84.5:15.5
6	(PhO) ₂ P(O)OH	3.72	20	69	82:18	93:7
7	<i>p</i> TSA+H ₂ O	-2.80	20	63	80:20	90.5:9.5
8	55	1.77 ^d	20	25	67:33	74:26
9	56	n.a.	20	8	77:23	83:17
10	H ₃ PO ₄	2.15 ^e	20	77	80:20	93:7
11	H ₃ PO ₄	2.15 ^e	7	7	80:20	90:10
12	(<i>R</i>)-TRIP	4.22 ^f	20	52	92:8	99.5:0.5
13	(<i>S</i>)-TRIP	4.22 ^f	20	45	71:29	30.5:69.5

^a See references in text ^b Determined by GC. ^c Determined by chiral-phase GC. ^d pKa of **57** in DMSO.

^e pKa of first proton dissociation. ^f pKa in DMSO



To assess the contribution of the amine catalyst **9** in the outstanding enantioselectivity of the [**9**·2(*R*)-TRIP] salt, we screened other achiral and chiral primary amines with TRIP (**3**) as the acid co-catalyst (Table 4.5) All *achiral* primary amines (entries 4-7) afforded the product with a very similar enantioselectivity (approximately 70:30 er), highlighting the contribution of the chiral Brønsted acid in the enantiomeric induction. Chiral amines (entries 8-13) partly afforded high enantioselectivities, especially when paired with the “matched” enantiomer of TRIP, but none of the salts proved comparable to the original [**9**·2(*R*)-TRIP] combination (entry 1).

4. Results and Discussion

Interestingly, catalyst **61** which lacks the quinoline moiety displayed no “match/mismatch” relationship with TRIP (entries 12-13) and afforded the product with the opposite sense of selectivity compared to catalyst **9** when paired with TFA (see footnote). In line with the mechanistic rationale discussed in Section 2.1.3.2, the secondary amine catalyst **4**, which had been found optimal for the epoxidation of α -unbranched enals,^[36] was inactive with the α -branched enal **53c** (entry 6). At this stage we also tested the pseudoenantiomer of **9**, 9-amino(9-deoxy)*epi*quinidine^{iv} **11** in combination with (*S*)-TRIP (entry 2). As expected, the opposite (*2S,3R*)-enantiomer of the corresponding product *ent*-**54c** was obtained with a comparable 57% conversion and 93:7 er, albeit with a low diastereomeric ratio of 59:41. Using (*R*)-TRIP alone as the catalyst (entry 14) resulted in the formation of only traces of the racemic product, in accordance with a mechanism which involves covalent aminocatalysis.

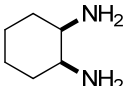
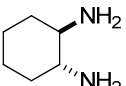
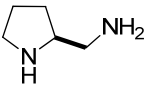
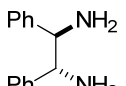
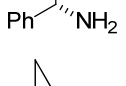
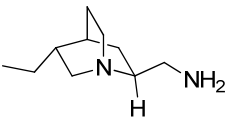
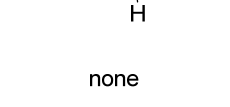
Table 4.5 Screen of primary amine catalysts with the acid co-catalyst TRIP (**3**).

Entry	Amine catalyst	TRIP	Conv., % ^a	dr ^a	er (<i>trans</i>) ^b	
1		9	(<i>R</i>)	52	92:8	99.5:0.5
2		11	(<i>S</i>)	45	71:29	30.5:69.5
3		11	(<i>S</i>)	57	59:41	7:93
4		58	(<i>R</i>)	13	59:41	68:32
5		meso-8	(<i>R</i>)	46	58:42	69:31
6		4	(<i>R</i>)	<10	n.d.	n.d.

(Ar = 3,5-(CF₃)₂C₆H₃)

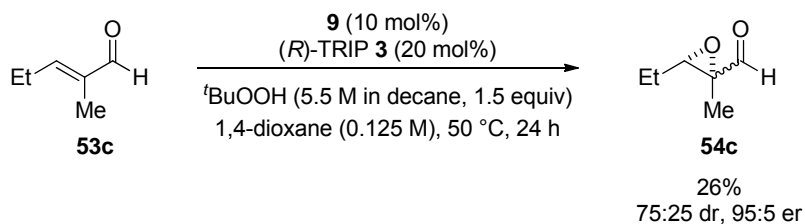
^{iv} Because catalysts **9-14** are derived from naturally occurring cinchona alkaloids, there are no direct routes to obtain their enantiomers. However, pseudoenantiomeric pairs such as **9** and **11** generally afford products with the opposite configuration and comparable enantioselectivity.

4. Results and Discussion

Entry	Amine catalyst	TRIP	Conv., % ^a	dr ^a	er (<i>trans</i>) ^b	
7		<i>meso</i> - 59	(<i>R</i>)	19	71:20	66:34
8		(<i>R,R</i>)- 59	(<i>R</i>)	28	72:28	58:42
9		60	(<i>R</i>)	18	83:17	88:12
10		(<i>R,R</i>)- 8	(<i>R</i>)	25	75:25	14:86
11		(<i>S,S</i>)- 8	(<i>S</i>)	32	81:19	6.5:93.5
12		61^c	(<i>R</i>)	48	71:29	90:10
13		61^c	(<i>S</i>)	35	74:26	6:94
14	none	(<i>R</i>)	<10	n.d.	49:51	

^a Determined by GC. ^b Determined by chiral-phase GC. ^c With 20 mol% TFA: 18% conv., 35:65 er, 62:38 dr

Given the generally low conversion observed in the epoxidation reactions of the model substrate **53c** with aqueous hydrogen peroxide, we tested a more nucleophilic organic peroxide reagent, *tert*-butyl hydroperoxide, which has been employed in a number of organocatalytic epoxidations [36, 42b, 81, 83, 88] (Scheme 4.1).



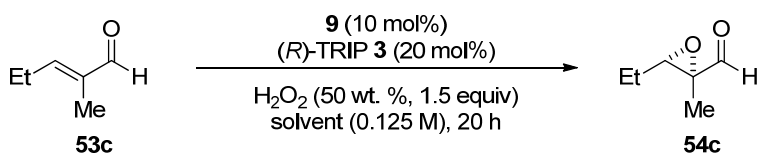
Scheme 4.1 Evaluating *tert*-butyl peroxide in the epoxidation of **53c**.

However, despite higher nucleophilicity, *tert*-butyl peroxide afforded only 26% conversion after 24 hours. In addition, compared to hydrogen peroxide, the stereoselectivity of the reaction was also diminished.

Having identified a highly stereoselective catalyst salt [**9**·2(*R*)-TRIP] and aqueous hydrogen peroxide as the optimal oxidant, we decided to re-evaluate the solvent, this time focusing on various ethers (Table 4.6). For solvents with low boiling points (entries 3 and 7), the reaction temperature was lowered to r.t. so that all reactions could proceed at atmospheric pressure.

4. Results and Discussion

Table 4.6 Re-evaluation of the reaction medium: screen of ethereal solvents.



Entry	Solvent	T, °C	Conversion,% ^a	dr ^a	er (<i>trans</i>) ^b
1	1,4-dioxane	50	45	92:8	99.5:0.5
2	THF	50	74	92:8	99.5:0.5
3	Et ₂ O	r.t.	47	83:17	98:2
4	DME	50	57	92:8	99.5:0.5
5	Bu ₂ O	50	0	n.a.	n.a.
6	<i>i</i> Pr ₂ O	50	31	79:21	96.5:3.5
7	MTBE	r.t.	55	88:12	99.5:0.5

^a Determined by GC. ^b Determined by chiral-phase GC.

While the enantioselectivity of the reactions remained very high for all of the solvents tried, a range of conversions was observed. Notably, the reaction was completely shut down when dibutyl ether was used as solvent (entry 5), presumably due to the insolubility of the catalyst in this medium (a precipitate was observed). No clear trend could be observed among the other water miscible and immiscible ethereal solvents, but THF emerged as the superior reaction medium, improving the conversion by almost 30% compared to 1,4-dioxane (entry 2).

With the optimal solvent in hand, we examined the effect of changing the catalyst loading by varying the amount of both the amine and the Brønsted acid component (Table 4.7). Decreasing the loading of the amine catalyst **9** to 5 mol% (1:4 amine:acid ratio) resulted in a significant drop in conversion (entry 2). A similar effect was observed when increasing the loading of **9** to 20 mol% (1:1 amine:acid ratio), which also significantly reduced the diastereoselectivity of the reaction (entry 4). Keeping the amine loading constant at 10 mol%, but increasing the amount of the Brønsted acid to 25 mol% (1: 2.5 amine:acid ratio) did not improve the conversion, but only diminished it, although stereoselectivity remained unchanged.

At this point, we decided to keep the original ratio and loading of the catalysts and opted for the fine-tuning of the Brønsted acid component in order to improve conversion. Since the axially chiral BINOL-scaffold proved to be particularly promising in our initial investigations and in previous reports from our group,^[34, 36, 80] corresponding bis-sulfonic and phosphoric acids, synthesized by *F. Lay*, *S. Marcus* and *M. Hannappel* in our group, were screened (Table 4.8).

4. Results and Discussion

Table 4.7 A screen of different stoichiometries of the catalytic salt [9·(*R*)-TRIP].

Entry	9, mol%	(<i>R</i>)-TRIP, mol%	Conversion,% ^a	dr ^a	er (<i>trans</i>) ^b
1	10	20	74	92:8	99.5:0.5
2	5	20	39	92:8	99:1
3	10	25	60	92:8	99.5:0.5
4	20	20	56	80:20	99:1

^a Determined by GC. ^b Determined by chiral-phase GC.

Table 4.8 Evaluation of BINOL-derived Brønsted acid co-catalysts with primary amine 9.

Entry	Brønsted acid	R	mol%	Conv.,% ^a	dr ^a	er (<i>trans</i>) ^b
1		3,5-(CF ₃) ₂ C ₆ H ₃	62a (<i>R</i>)	10	14	94:6 98.5:1.5
2		3,5-(CF ₃) ₂ C ₆ H ₃	62a (<i>R</i>)	20	14	53:47 83:17
3		4- ^t Bu-C ₆ H ₄	62b (<i>R</i>)	10	21	91:9 97.5:2.5
4		4- ^t Bu-C ₆ H ₄	62b (<i>R</i>)	20	23	31:69 87:13
5		2,4,6- ⁱ Pr ₃ C ₆ H ₂	62c (<i>S</i>)	10	30	89:11 96.5:3.5
6		2,4,6- ⁱ Pr ₃ C ₆ H ₂	62c (<i>S</i>)	20	30	56:44 95:5

7		H	63a (<i>R</i>)	20	78	85:15 95:5
8		H	63a (<i>S</i>)	20	64	80:20 93.5:6.5
9		Ph	63b (<i>R</i>)	20	84	96:4 99.5:0.5
10		Ph	63b (<i>S</i>)	20	84	87:13 81:19
11		4-Ph-C ₆ H ₄	63c (<i>R</i>)	20	71	80:20 85:15
12		3,5-(CF ₃) ₂ C ₆ H ₃	63d (<i>S</i>)	20	72	96:4 99:1

^a Determined by GC. ^b Determined by chiral-phase GC.

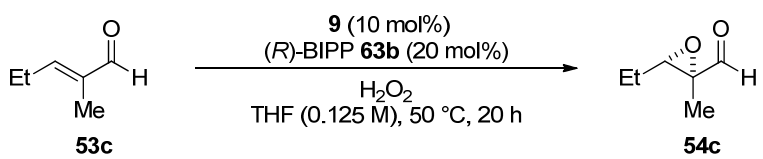
As can be seen from Table 4.8, all BINOL-derived bis-sulfonic acids **62** (entries 1-6) afforded the product with only very low conversion, which was unchanged at 10 and 20 mol% loading

4. Results and Discussion

(since bis-sulfonic acids **62** possess two acidic moieties per molecule, the effective acid loading should be considered as 20 and 40 mol%, respectively). However, 20 mol% loading of **62** (entries 2, 4 and 6) decreased the enantioselectivity of the reaction in all cases, and even more dramatically eroded the diastereoselectivity. BINOL-derived phosphoric acids **63** fared better in comparison, giving considerably higher conversions and generally high stereoselectivity (entries 7-12). In particular, the bis-phenyl substituted BINOL-derived phosphoric acid **63b** (abbreviated BIPP in this work) gave the highest conversion of 84% (entries 9-10). Intriguingly, in contrast to bulkier (*S*)-TRIP, a much less pronounced mismatch was observed with (*S*)-BIPP (entry 10 vs. 9) and essentially no mismatch was observed with BINOL-phosphoric acid which lacks any 3,3'-substituents (entry 8 vs. 7) in terms of enantioselectivity. Gratifyingly, (*R*)-BIPP proved to be just as stereoselective as the (*R*)-TRIP co-catalyst, while being more catalytically active (entry 9).

Using the more active catalyst salt [**9**·2(*R*)-BIPP], we next evaluated oxidant stoichiometry. As summarized in Table 4.9, various amounts of commercially available 30 wt. % and 50 wt. % hydrogen peroxide solutions were screened. To our delight, increasing the amount of the peroxide readily improved the conversion. The best conditions were found to be 5 equiv of 50 wt. % hydrogen peroxide (entry 5), which afforded the product with 97% conversion and only slightly diminished stereoselectivity. Using these optimal conditions with (*R*)-TRIP as the Brønsted acid co-catalyst (entry 6) also resulted in improved conversion but the stereoselectivity was too compromised to be useful.

Table 4.9 Optimization of the oxidant stoichiometry.



Reaction scheme showing the oxidation of 3-methyl-2-pentenal (**53c**) to 3-methyl-2-pentanoic acid (**54c**) using catalyst **9** (10 mol%) and (*R*)-BIPP **63b** (20 mol%) in THF (0.125 M) at 50 °C for 20 h with H₂O₂.

Entry	H ₂ O ₂	equiv	Conversion, % ^a	dr ^a	er (<i>trans</i>) ^b
1	30 wt. %	2	90	95:5	99.5:0.5
2	30 wt. %	3	94	94:6	99.5:0.5
3	30 wt. %	5	98	93:7	98.5:1.5
4	50 wt. %	3	89	95:5	99.5:0.5
5	50 wt. %	5	97	93:7	99:1
6 ^c	50 wt. %	5	88	85:15	98:2

^a Determined by GC. ^b Determined by chiral-phase GC. ^c Using (*R*)-TRIP (20 mol%) as the Brønsted acid co-catalyst

4. Results and Discussion

Having secured conditions which give an excellent conversion and stereoselectivity, we wished to test if the loading of the Brønsted acid co-catalyst (*R*)-BIPP (**63b**) could be reduced. In particular, we wondered if the amount of BIPP could be lowered by a compensative addition of an achiral Brønsted acid additive. To this end, we screened the achiral phosphoric acid H₃PO₄, together with various amounts of (*R*)-BIPP (Table 4.10).

Table 4.10 Optimization of the oxidant stoichiometry.

Reaction scheme showing the epoxidation of 2-methyl-2-pentenal (**53c**) to 2-methyl-2-oxiranecarbaldehyde (**54c**). The reaction conditions are: **9** (10 mol%), cat. (*R*)-BIPP (**63b**), cat. H₃PO₄, H₂O₂ (50 wt. %, 5 equiv), THF (0.125 M), 50 °C, 24 h.

Entry	Acid	mol%	H ₃ PO ₄ , mol%	Conversion, % ^a	dr ^a	er (<i>trans</i>) ^b
1	(<i>R</i>)-BIPP	20	0	98	92:8	99:1
2	(<i>R</i>)-BIPP	15	0	94	94:6	99:1
3	(<i>R</i>)-BIPP	10	0	89	90:10	98:2
4	(<i>R</i>)-BIPP	15	5	96	93:7	99:1
5	(<i>R</i>)-BIPP	10	5	94	91:9	99:1

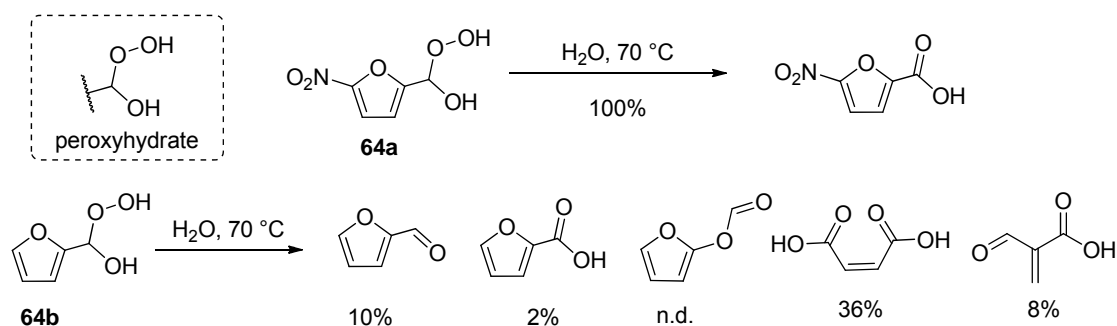
^a Determined by GC. ^b Determined by chiral-phase GC.

Unfortunately, reducing the loading of (*R*)-BIPP led to diminished conversion and stereoselectivity (entries 1-3). Although the compensative addition of H₃PO₄ appeared to restore conversion (entries 4-5), it had no beneficial effect on the stereoselectivity of the reaction.

4.1.3 The Fate of Excess Hydrogen Peroxide and Optimization of Workup

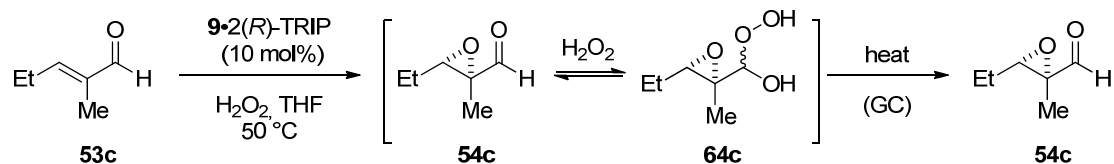
Having established optimal conditions at 50 °C, we tested the epoxidation of 2-methyl-2-pentenal **53c** at a higher temperature (70 °C) in hopes of improving the reaction rate. However, increased temperature resulted in the formation of previously undetected side products, signifying that 50 °C represented a threshold for decomposition pathways. Intrigued by such thermal behaviour, we decided to investigate its possible origins. A survey of the literature revealed that hydroperoxy adducts of aldehydes (i.e. peroxyhydrate species of type **64**, Scheme 4.2) can decompose into a variety of oxidation products under aqueous conditions at 70 °C.^[127] Peroxyhydrates represent the products of reversible addition of hydrogen peroxide to aldehydes, similar to the rapid and reversible formation of *gem*-diols (hydrates) by the addition of water to a carbonyl group.

4. Results and Discussion



Scheme 4.2 Decomposition of furyl peroxyacetals at 70 °C in the presence of water.^[127]

The possibility of the aldehyde products being reversibly masked as peroxyhydrates by the excess of hydrogen peroxide under our reaction conditions was corroborated by a further observation. The epoxidation product **54c** could never be detected by TLC analysis of the crude reaction mixture, even though crude GC analysis indicated the formation of the desired product and the disappearance of the starting material. Instead, a baseline spot corresponding to a highly polar species was observed by TLC. These results could be easily explained by the formation of peroxyhydrate **64c** under the reaction conditions which reverts to the expected product **54c** under the high-temperature (and anhydrous) conditions of GC (Scheme 4.3).



Scheme 4.3 Hypothesized formation of peroxyhydrate **64c** in the epoxidation of **53c**.

In order to test this hypothesis, we performed ¹H NMR studies using the epoxidation of substrate **53g** (cf. Section 4.1.5.1 for synthesis) as a non-volatile model system. Figure 4.1 shows the ¹H NMR spectrum of the crude reaction mixture after consumption of the starting material (a), superimposed with the spectrum of the isolated epoxide product **54g** (b). In accordance with our expectations, the crude reaction mixture showed the presence of a ca. 1:1 diastereomeric mixture of a new compound, together with small amounts of the expected epoxide **54g**. The characteristic acetal proton of the literature-known heptanal-derived peroxyacetal **65** (Figure 4.1) has a chemical shift of 5.11 ppm.^[128] The two singlets at 4.78 ppm and 4.83 ppm belonging to the new compound thus correspond well to peroxyacetal protons **1b-H** of the diastereomeric pair **64g**. Furthermore, the crude reaction mixture was found to quantitatively yield **54g** upon a reductive workup with sodium thiosulfate, but not after a normal aqueous workup, suggesting that a peroxyacetal and not a simple hydrate formation was

4. Results and Discussion

responsible for masking the aldehyde product in the reaction. It is noteworthy that in their kinetic studies on the epoxidation of unbranched enals with hydrogen peroxide,^[15] Jørgensen and colleagues also identified peroxyacetal species of type **64**, which were responsible for autocatalytic behaviour of the reaction (unpublished results).

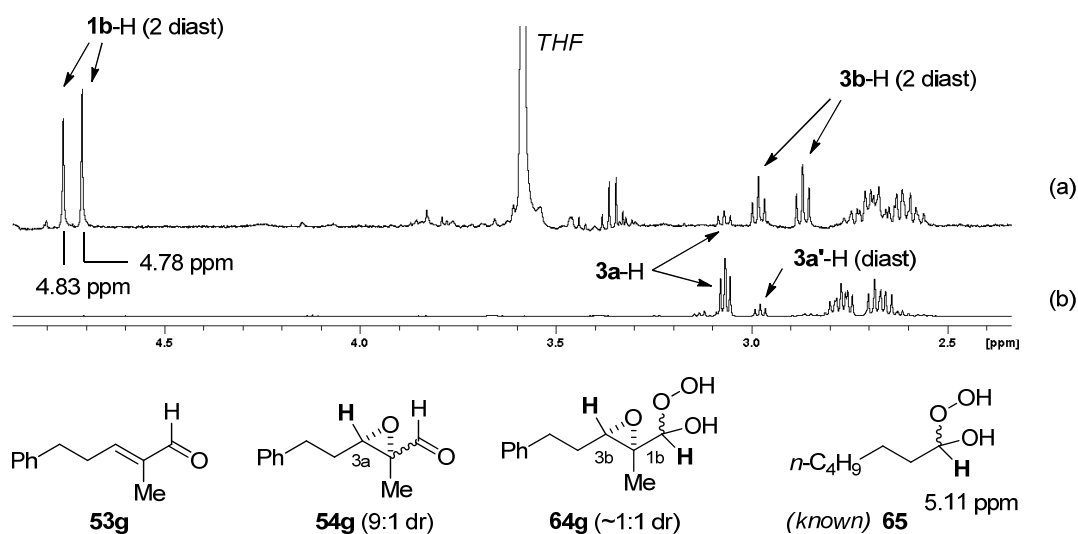


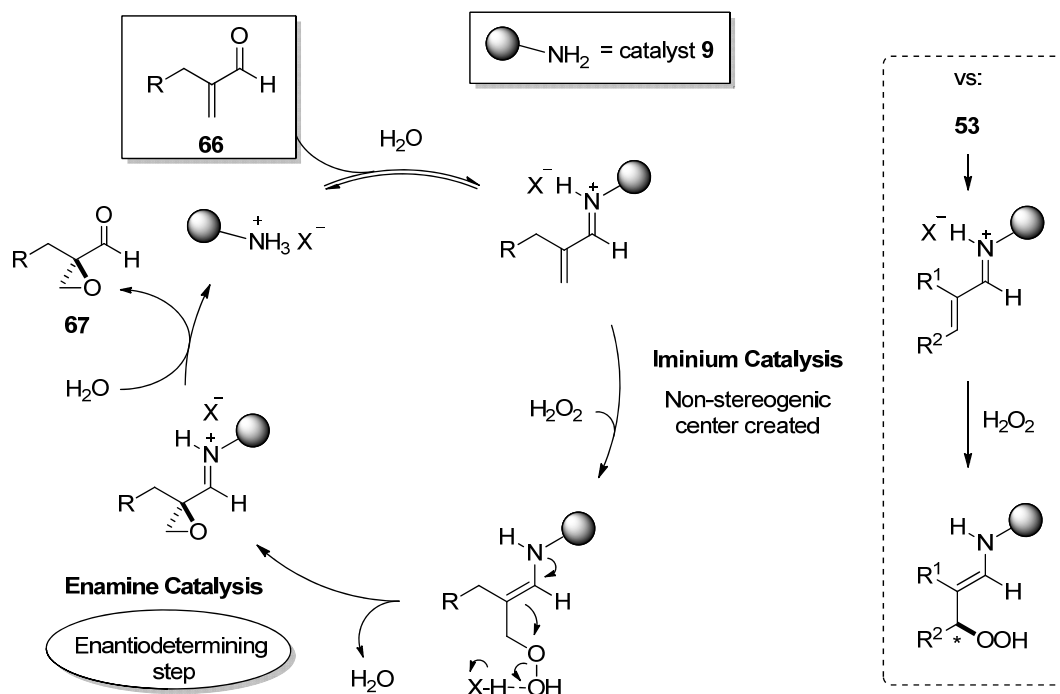
Figure 4.1 Selected regions of the ¹H NMR spectra showing the crude reaction mixture after 15 h for the epoxidation of **53g** (a), and the isolated epoxide product **54g** (b) (NMR in CDCl₃).

The findings that excess hydrogen peroxide was reversibly taken up by the product as a peroxyacetal **64** suggested that an efficient isolation of the product must involve a complete reduction of any residual peroxide bonds. After a screen of conditions, two suitable workup procedures were identified, which involve stirring the reaction with saturated aqueous sodium thiosulfate for 5 min followed by an aqueous extraction, or adding solid sodium thiosulfate to the crude reaction mixture and stirring the suspension for 1 hour followed by filtration.

4.1.4 Optimization of Reaction Conditions for α-Substituted Acroleins

Having secured optimal conditions for the epoxidation of α,β-disubstituted enals **53**, we next turned our attention to a similar substrate class, α-substituted acroleins **66**. As discussed in Chapter 3, due to mechanistic dissimilarities in the epoxidation of **66** vs. **53** we expected factors governing the enantioselectivity to differ for these substrate classes. In particular, in contrast enals **53**, the initial iminium-catalyzed hydrogen peroxide addition to acroleins **66** no longer generates a stereogenic centre, making the subsequent, enamine-catalyzed ring-closure the enantiodetermining step of the reaction (Scheme 4.4).

4. Results and Discussion



Scheme 4.4 Proposed mechanistic model for the epoxidation α -monosubstituted enals.

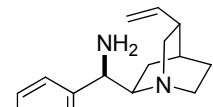
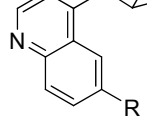
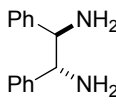
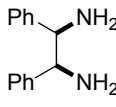
In optimizing the reaction conditions for α -substituted acroleins, we decided to adopt the previously optimized solvent, concentration, temperature and oxidant loading, but re-evaluate both the amine and the Brønsted acid catalysts (Table 4.11). Readily available^[129] α -benzyl derivative **66a** synthesized by *C. Rampalakos* in our group was chosen as the model substrate.

Table 4.11 Evaluation of the catalytic salt in the epoxidation of α -substituted acroleins **66a**.

Entry	Amine catalyst	Acid co-catalyst	mol%	Conv., % ^a	er ^b
1		TFA	20	21	59:41
2		(PhO) ₂ P(O)OH	20	52	63:37
3		(<i>R</i>)-BIPP (63b)	20	92	91:9
4		(<i>R</i>)-TRIP (3)	20	100	99:1
5		(<i>S</i>)-TRIP (3)	20	40	32:68
6		(<i>R</i>)-TRIP (3)	10	67	94:6

^a Determined by GC. ^b Determined by chiral-phase GC

4. Results and Discussion

Entry	Amine catalyst	Acid co-catalyst	mol%	Conv., % ^a	er ^b
7		R = OMe (S)-TRIP (3)	20	44	29:71
8		R = H (S)-TRIP (3)	20	28	34:66
9		(R,R)-8 (S)-TRIP (3)	20	100	18:82
10		meso-8 (R)-TRIP (3)	20	75	57:43

^a Determined by GC. ^b Determined by chiral-phase GC

In stark contrast to the α,β -disubstituted enals **53**, 9-amino(9-deoxy)epiquinine TFA salt ([**9**-2TFA]) mediated the epoxidation of **66a** with only modest conversion and enantioselectivity, giving the product **67a** with 59:41 er (entry 1). The absolute (*R*)-configuration of **67a** was assigned by comparing the optical rotation of the corresponding epoxyalcohol after NaBH₄ reduction, to the literature value.^[130]

Using phosphoric acid diphenyl ester ((PhO)₂P(O)OH) instead of TFA resulted in improved conversion, but the enantioselectivity remained low (entry 2). Fortunately, the axially chiral BINOL-derived phosphoric acids once again proved to be powerful co-catalysts. Using 20 mol% of (*R*)-BIPP (entry 3) dramatically increased both the conversion and the enantioselectivity of the reaction, which was further improved to full conversion and an excellent er of 99:1 with the more bulky acid (*R*)-TRIP (entry 4). As with 2-methyl-2-pentenal **53a**, a significant drop and reversal of enantioselectivity was observed when (*S*)-TRIP was used as the co-catalyst (entry 5). Lowering the catalyst loading of (*R*)-TRIP to 10 mol% resulted in diminished conversion and enantioselectivity (entry 6). Wishing to obtain the opposite (*S*)-enantiomer of the product **67a**, we also tried the pseudoenantiomeric amine catalyst **11** together with (*S*)-TRIP. Although the desired switch in enantioselectivity was observed, both the conversion and the enantiomeric ratio were only modest (entry 7). The selectivity was not improved by using a related cinchonine-derived catalyst **12** (entry 8), but chiral diamine (*R,R*)-**8** together with (*S*)-TRIP was found to give full conversion and an improved enantioselectivity of 82:18 er for the (*S*)-configured product **67a**. The importance of both chiral components in the highly enantioselective catalyst salt [**9**-2(*R*)-TRIP] was tested by substituting **9** with an achiral primary diamine *meso*-**8** (entry 10). Although the conversion was good, only poor

4. Results and Discussion

enantioselectivity was observed, signifying that both the chiral amine **9** and the chiral Brønsted acid (*R*)-TRIP were crucial for optimal enantioselectivity.

4.1.5 Reaction Scope and Discussion

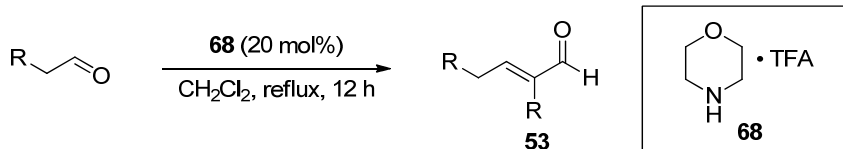
With the optimized conditions for both α,β -disubstituted enals **53** and α -substituted acroleins **66** in hand, we wished to explore the scope of the novel epoxidation procedure. The following protocol was applied for both substrate classes: the catalytic salt [9·2(*R*)-BIPP] or [9·2(*R*)-TRIP] was generated *in situ* by mixing the primary amine **9** (10 mol%) and the respective Brønsted acid (*R*)-BIPP or (*R*)-TRIP (20 mol%) in THF for 5 min. The substrate **53** or **66** (0.125M) was then added and stirred for an additional 5 min. Finally, aqueous hydrogen peroxide (50 wt. %, 5 equiv) was added, the reaction vessel sealed under ambient atmosphere and stirred at 50 °C for 24 hours.

4.1.5.1 Preparation of the Starting Materials

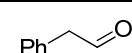
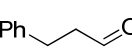
Although few substrates for the enantioselective epoxidation were commercially available, all of the required (*E*)-configured α -branched enals could be easily prepared *via* one-step redox-neutral methodologies from aldehyde precursors. The substrate synthesis was carried out following three general strategies: self-aldol condensation developed in our group by Zumbansen and List,^[131] Grubbs cross-metathesis of acroleins with terminal olefins^[132] and crossed-aldol condensation with formaldehyde developed by Pihko and colleagues.^[129]

Self-aldol condensation of aldehydes was performed using catalytic morpholine TFA salt **68** in refluxing dichloromethane^[131] which afforded the products with very good yields and complete *E/Z* selectivity (Table 4.12).

Table 4.12 Preparation of α -branched enals **53** by cross self-aldol condensation.^[131]



Reaction scheme: $\text{R-CH}_2\text{-CHO} \xrightarrow[\text{CH}_2\text{Cl}_2, \text{ reflux, 12 h}]{\text{68 (20 mol\%)}} \text{R-CH}_2\text{-CH=C(R)-CHO}$ (**53**). Catalyst **68** is morpholine · TFA.

Entry	Terminal olefin	Enal	Yield, % ^a	<i>E/Z</i> ratio ^b
1		53k	91	>99:1
2		53e	86	97:3

^a Isolated yield. ^b Determined by crude ¹H NMR analysis.

4. Results and Discussion

Cross-metathesis between various terminal olefins and methacrylaldehyde was performed using *Grubbs* second-generation catalyst **69** (Table 4.13). This procedure afforded the products **53** with complete *E/Z* selectivity except for the cyclohexyl-substituted enal **53i** (entry 3). Yields were generally low due to the homocoupling of the terminal enone (major product in the formation of **53f**, entry 2) and/or the instability of the aldehyde products which were prone to spontaneous aerobic oxidation, especially in the crude reaction mixture (entry 3). This procedure was not optimized.

Table 4.13 Preparation of α -branched enals **53** by cross metathesis. ^[132]

Entry	Terminal olefin	Enal	Yield, % ^a	<i>E/Z</i> ratio ^b
1		53g	65	>20:1
2		53f	30 ^c	>20:1
3		53i	55 ^d	6:1

^a Isolated yield. ^b Determined by crude ¹H NMR analysis ^c Homocoupling of the terminal olefin observed as a side product. ^d Product unstable, prone to oxidation even at 0 °C.

Pihko's methylenation of aldehydes by crossed-aldol condensation with aqueous formaldehyde was performed using catalytic pyrrolidine salt with the carboxylic acid **70**.^[129] Various α -substituted acroleins **66** were obtained in good yields except when highly volatile (Table 4.14).

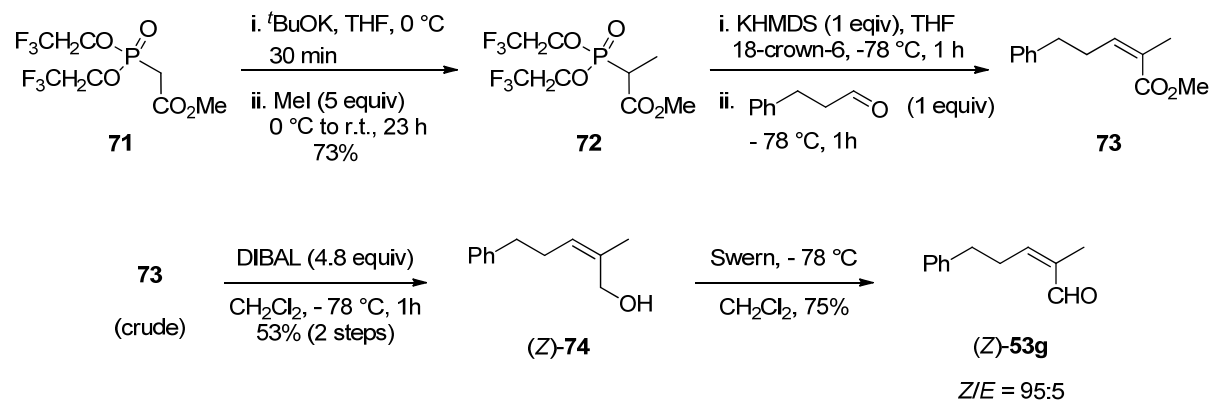
Table 4.14 Preparation of α -branched acroleins **66** by *Pihko's* methylenation. ^[129]

Entry	R	Enal	Yield, % ^a	Entry	R	Enal	Yield, % ^a
1		66b	69	4		66e	60
2		66c	39 ^b	5		66f	44 ^b
3		66d	71				

^a Isolated yield. ^b Highly volatile product.

4. Results and Discussion

To test the effect of enal geometry, we also synthesized (*Z*)-configured enal (*Z*)-**53g**, which required a multistep procedure involving a *Still-Gennari* olefination^[133] of hydrocinnamaldehyde (product **73**), followed by oxidation state adjustment^[134] (Scheme 4.5).



Scheme 4.5 Synthesis of (*Z*)-**53g** by *Still-Gennari* olefination followed by oxidation state adjustment.

4.1.5.2 The Scope of α,β -Disubstituted Enals

A range of α,β -disubstituted enals was screened in the asymmetric epoxidation (Table 4.15). Due to the sensitive nature of the aldehyde group, the products were reduced to the corresponding epoxyalcohols *in situ* using NaBH_4 for yield and *er* determination. To our delight, good yields and excellent enantioselectivities were observed regardless of the size of the α -substituent, with methyl, ethyl, benzyl and phenyl groups being well tolerated (entries 1-3, 8). The reduced yield obtained for the model substrate **53c** (entry 1) reflects the difficulty of isolating the highly volatile product **54c**. Good diastereoselectivity favouring the *trans*-isomer was also observed in all cases, except for the α -phenyl-substituted enal **53h** (entry 7). It is noteworthy that the *trans*-diastereoselectivity was not always inherent to the substrate, but rather reflected catalyst control. The diastereoselectivity obtained in the non-asymmetric epoxidation of **53d** using alkaline H_2O_2 in methanol, for example, actually strongly favoured the *cis* diastereomer (*cis/trans* dr 72:28).^v We were pleased to find that under the optimized conditions, cyclic substrate **53b** could now be smoothly converted to the corresponding epoxide **54b** with excellent enantioselectivity (entry 4). Surprisingly, even α -methyl cinnamaldehyde **53a** which afforded only traces of product at the outset of our investigations (Section 4.1.1) could be converted to the corresponding product with a moderate yield and very good enantioselectivity

^v Relative configuration was assigned using *NOE* and ^{13}C NMR analysis (γ effect). See Chapter 7 for further details.

4. Results and Discussion

by extending the reaction time to 48 h (entry 5). Non-conjugated aromatic group (entry 6) and an ester group (entry 7) were also well tolerated. Interestingly, applying the optimal conditions to the epoxidation of a non-branched enal **53i** gave the corresponding product with only a modest yield and enantioselectivity and an opposite sense of enantioinduction. Although difficult to rationalize, this result underscores the intricate complementarity that must be achieved between the steric and electronic requirements of the substrate and those of the catalyst to obtain a viable catalytic system.

Table 4.15 Substrate scope of the epoxidation of α,β -disubstituted enals **53**.

Reaction scheme: $\text{R}^1\text{-CH=CH(R}^2\text{)-CHO} \xrightarrow[\text{THF (0.125 M), 50 }^\circ\text{C, 24 h}]{\text{9 (10 mol\%), (R)-BIPP (20 mol\%), H}_2\text{O}_2 \text{ (50 wt. \%, 5 equiv)}} \text{R}^1\text{-CH(O)}\text{-CH(R}^2\text{)-CHO}$

Entry	Substrate	Product	Yield, % ^a	dr ^b	er (<i>trans</i>) ^c
1	53c	54c	43	92:8	98.5:1.5
2	53d	54d	64	83:17 ^d	99:1
3	53e	54e	77	90:10	99:1
4	53b	54b	70	>99:1	98.5:1.5
5 ^e	53a	54a	49	97:3	98:2
6	53f	54f	66	93:7	99:1
7	53g	54g	75	95:5	98.5:1.5
8	53h	54h	49 ^f	56:44	95:5
9	53i	54i	30	95:5	70:30

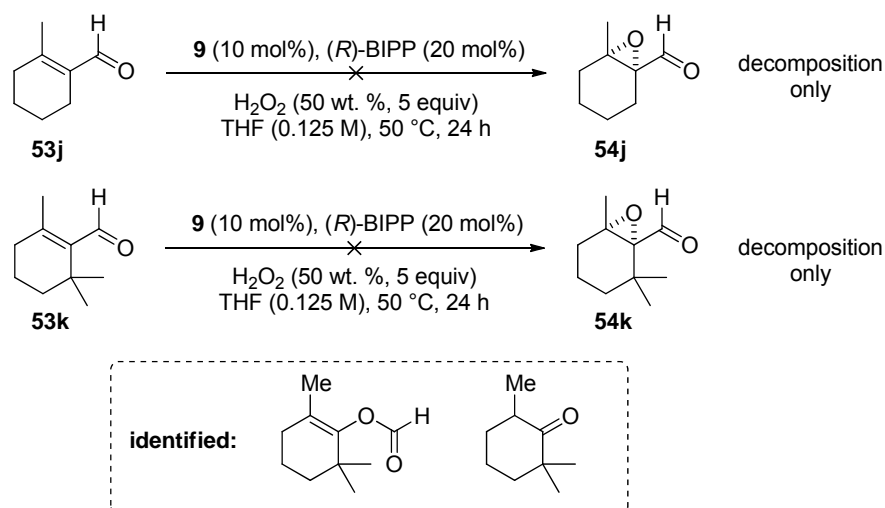
^a Isolated yield after reduction with NaBH₄. ^b Determined by GC of the crude reaction mixture.

^c Determined by chiral-phase GC ^d Opposite diastereoselectivity (28:72 dr) in racemic reaction.

^e 48 h reaction time. ^f Unidentified side product also isolated.

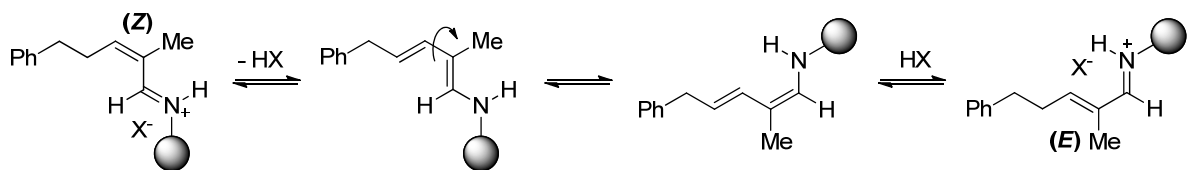
4. Results and Discussion

Unfortunately, substrates possessing a tetrasubstituted double bond were found to be resistant to epoxidation. Thus, both 2-methylcyclohex-1-enecarbaldehyde **53j** and β -cyclocitral **53k** failed to furnish the corresponding epoxide products, presumably due to the difficulty of the amine catalyst **9** in condensing with the sterically hindered aldehyde moiety (Scheme 4.6). After nearly complete conversion of the starting material, only decomposition products *via* the *Baeyer-Villiger* reaction were identified by GC-MS and NMR analyses in the reaction of **53k**.



Scheme 4.6 Decomposition of substrates **53j** and **53k** under the conditions of asymmetric epoxidation catalyzed by [**9**·2(*R*)-BIPP].

We also tested the effect of enal geometry by submitting the (*Z*)-configured enal **53g** to the epoxidation conditions (Table 4.16). Based on the previous studies in our group using acyclic enones^[82] and unbranched enals,^[36] we expected the reaction to be diastereoconvergent, or independent of the *E/Z* ratio of the starting material, due to rapid *Z*→*E* isomerization of the double bond under the conditions of aminocatalysis. A plausible mechanism for such isomerization *via* reversible formation of a dienamine species is shown in Scheme 4.7.



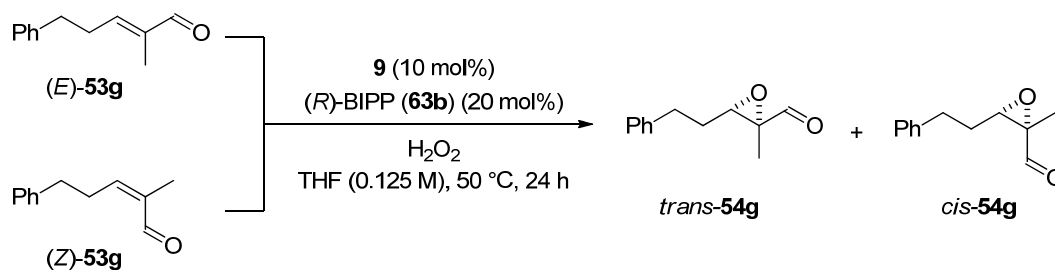
Scheme 4.7 Possible mechanism of the *Z*-*E* isomerization of enals under aminocatalysis.

When we tested the isomerization of (*Z*)-**53g** in the absence of hydrogen peroxide, full isomerization to (*E*)-**53g** was indeed observed within 24 hours (Table 4.16, entry 1). Similarly,

4. Results and Discussion

subjecting the more thermodynamically stable (*E*)-**53g** to the reaction conditions in the absence of hydrogen peroxide did not yield any detectable amounts of (*Z*)-**53g** (entry 2). However, when (*Z*)-**53g** was subjected to the reaction conditions in the presence of hydrogen peroxide (entry 4), only partial diastereoconvergence was observed. That is, although *trans*-**54g** was still formed as the major product, its diastereomeric and enantiomeric ratios were diminished, whereas *cis*-**54g** was formed with the opposite and higher enantioselectivity,^{vi} when one compares the epoxidation of (*Z*)-configured starting material (entry 4) with that of the (*E*)-configured starting material (entry 3). In addition, incomplete *Z*→*E* isomerization of the recovered starting material was observed even after 24 hours (entry 4). These results suggest that the *Z*→*E* isomerization does not precede, but occurs at the same time as, enal epoxidation, so that the products **54g** are simultaneously formed from both (*E*) and (*Z*)-configured starting materials. The fact that diastereoconvergence, even if only partial, is observed, combined with the incomplete *Z*→*E* isomerization of the starting material suggests that the epoxidation of (*E*)-**53g** is predominant over the epoxidation of (*Z*)-**53g**. This implies that the enantiomeric excess of the major product should be directly dependent on the *E/Z* ratio of the substrate, but in general always compromised by the presence of the (*Z*)-configured starting material.

Table 4.16 Partial diastereoconvergence of (*E*) and (*Z*)-configured enals in the catalytic asymmetric epoxidation.



Entry	<i>E</i> : <i>Z</i> of 53g	H ₂ O ₂ equiv	Conversion % ^a	dr ^a	er (<i>trans</i> - 54g) ^b	er (<i>cis</i> - 54g) ^b	<i>E</i> : <i>Z</i> of remaining 53g ^c
1	>95:5	none	-	-	-	-	>95:5
2	5:95	none	-	-	-	-	>95:5
3	>95:5	5	93:5	95:5	98.5:1.5	65:35	>95:5
4	5:95	5	85	76:24	85:15	14:86	76:24

^a Determined by GC. ^b Determined by chiral-phase GC. ^c Determined by crude ¹H NMR analysis

^{vi} The absolute (*2S*, *3R*) configuration of the minor diastereomer *cis*-**54g** was determined by comparing the corresponding epoxyalcohol after NaBH₄ reduction to an authentic sample, synthesized by the *Sharpless* epoxidation of the appropriate (*Z*)-configured allylic alcohol. See Chapter 7 for further details.

4. Results and Discussion

4.1.5.3 The Scope of α -Substituted Acroleins

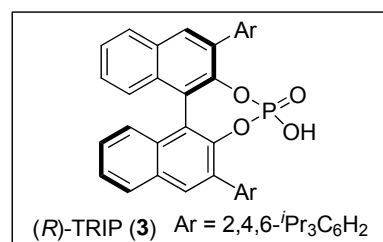
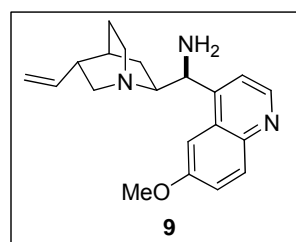
Several aliphatic α -substituted acroleins were subjected to the optimized catalytic asymmetric epoxidation protocol, and the results are summarized in Table 4.17. It is noteworthy that α -aryl acroleins are absent from the scope due to their extreme instability: attempts at the synthesis of 2-phenylacrylaldehyde resulted in the rapid decomposition of the purified product even at $-20\text{ }^{\circ}\text{C}$. Gratifyingly, all of the tested substrates **66** afforded the products with good isolated yields and consistently excellent enantioselectivities. The reaction proved chemoselective in the presence of an isolated double bond (substrate **66b**), with the corresponding epoxide product **67b** being formed without any side products (entry 2). Excellent enantiodiscrimination was achieved even with the small substrate **66c**, although the high volatility of the product **67c** resulted in a diminished yield (entry 3). In comparison, a longer aliphatic chain of **66d** enabled the isolation of the corresponding non-volatile product **67d** with a very good 84% yield and 99:1 er (entry 4).

Table 4.17 Substrate scope of the epoxidation of α -substituted acroleins **66**.

66 $\xrightarrow[\text{THF (0.125 M), 50 }^{\circ}\text{C, 24 h}]{\text{9 (10 mol\%), (R)-TRIP (20 mol\%), H}_2\text{O}_2 \text{ (50 wt. \%, 5 equiv)}}$ **67**

Entry	Substrate	Product	Yield, % ^a	er ^b
1	66a	67a	78	99:1
2	66b	67b	74	98.5:1.5
3	66c	67c	29 ^c	98:2
4	66d	67d	84	99:1

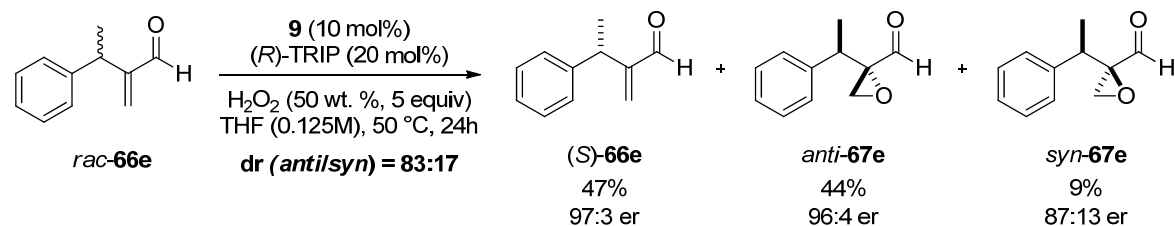
^a Isolated yield after reduction with NaBH_4 . ^b Determined by chiral-phase GC. ^c Reflects the high volatility of the product.



4. Results and Discussion

Although we were unable to identify an efficient catalytic system to furnish epoxide products **67** with the opposite (*S*) configuration (cf. Section 4.1.4, Table 4.11), these products can be accessed by the recently reported complementary approaches of Luo^[93] and Hayashi.^[92]

We also tested the catalytic system in a kinetic resolution of a β' -substituted enal *rac*-**66e** (Scheme 4.8). Under the standard conditions, the reaction proceeded to 53% conversion, whereby (*R*)-**66e** underwent epoxidation with good diastereoselectivity and excellent enantioselectivity for the major diastereomer *anti*-**67e**, while (*S*)-**66e** was recovered with 97:3 er. The absolute configuration of recovered (*S*)-**66e** was established by comparison of the optical rotation to the literature value.^[135] Because both diastereomers of racemic **67e** have been described in the literature,^[88] it was possible to assign their relative configuration. Combining this information, the epoxide products were assigned as (*2S,3R*)-**67e** (*anti*-**67e**) and (*2R,3R*)-**67e** (*syn*-**67e**). Interestingly, it follows that the major product *anti*-**67e** has the opposite absolute configuration of the epoxide moiety, compared to that normally preferred by the catalyst (cf. Scheme 4.8 vs. Table 4.17).

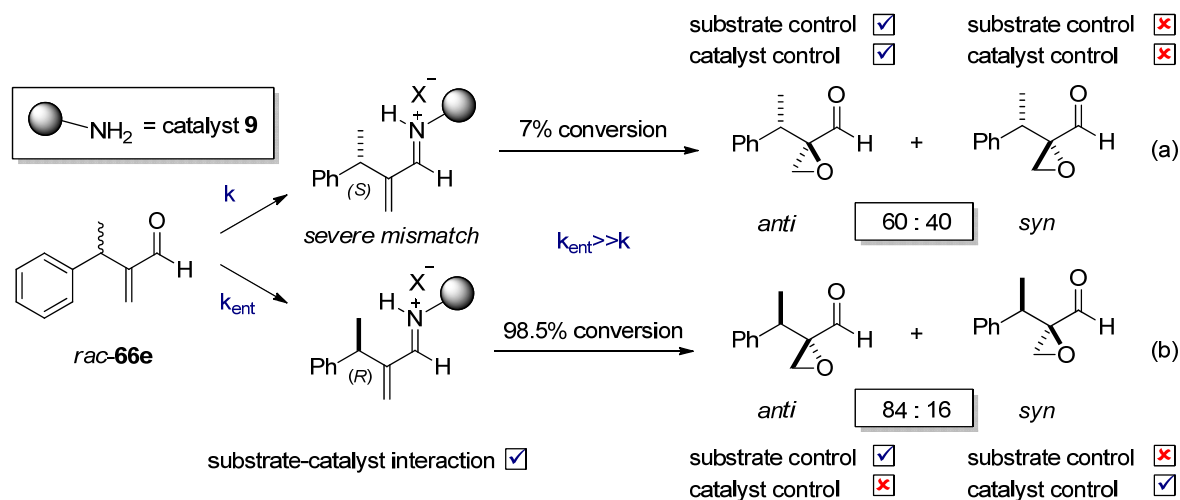


Scheme 4.8 Kinetic resolution of β' -substituted enal *rac*-**66e** under the conditions of asymmetric epoxidation.

These results can be interpreted in the following way: excellent kinetic resolution of *rac*-**66e** suggests that the β' -substituent has a significant match/mismatch relationship with the catalyst at the stage of iminium activation (Scheme 4.9). This leads to (*S*)-**66e** being essentially unreactive and undergoing only 7% conversion after 24 hours. On the other hand, (*R*)-**66e** readily condenses with the catalyst and undergoes epoxidation with 98.5% conversion. At the stage of epoxidation, however, the intrinsic biases of the catalyst **9** and the (*R*)-configured substrate diverge (Scheme 4.9, (b)). While the steric hindrance by the β' -substituent of the substrate directs the enantiodetermining epoxide ring-closure to occur from the opposite side, leading to an *anti*-relationship, the bias of the chiral catalyst demands the opposite, as evidenced from the absolute configuration imparted by the catalyst to achiral substrates (Table 4.17). The overall result is the prevalence of the *anti*-diastereomer (substrate control), albeit with a somewhat low selectivity (84:16) due to the opposing catalyst control. In the case of (*S*)-**66e** (Scheme 4.9, (a)),

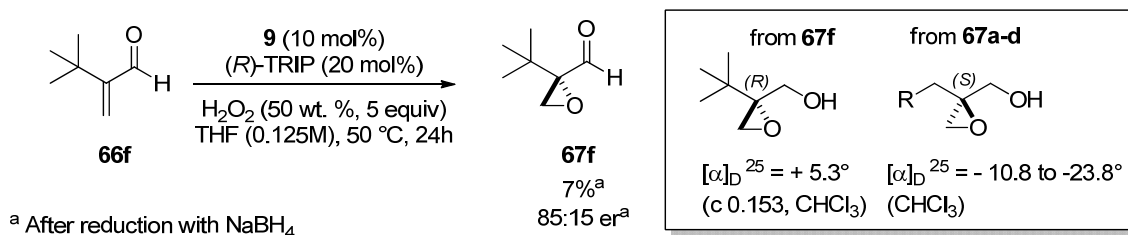
4. Results and Discussion

both the catalyst and the substrate should have the same intrinsic bias for the formation of the *anti* product. The low *anti/syn* ratio of 60:40 could be explained by the fact that catalyst condensation with (*S*)-**66e** represents a severely mismatched case which might change the catalyst's conformation thus diminishing its ability for proper enantiodiscrimination.



Scheme 4.9 Kinetic resolution of β' -substituted enal *rac*-**66e**: a possible rationalization of the product distribution.

An alternative explanation for the observed absolute configuration of the major product *anti*-**67e** cannot be excluded, however. It is possible that the β' -substituent of the substrate simply reverses the catalyst's absolute sense of enantioselectivity (and concurrently diminishes *er*) by changing an important conformational parameter, such as the *E/Z* geometry of the enamine intermediate. In fact, the epoxidation of β',β' -disubstituted achiral enal **66f** provides tentative support for this hypothesis (Scheme 4.10). Although the corresponding epoxide **67f** was obtained with only 7% yield after reduction, enough product was obtained to determine the optical rotation, which was found have the opposite sign compared to all other substrates tested (**66a-d**). This presumable reversal of enantioselectivity was accompanied by only moderate enantioselectivity of 85:15 *er*.

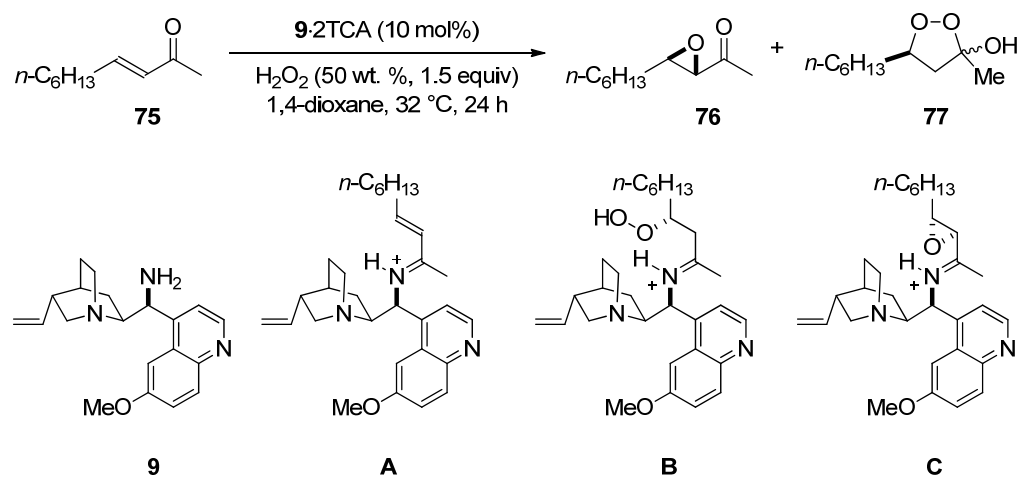


Scheme 4.10 Epoxidation of β',β' -disubstituted enal **66f**: reversal of enantioselectivity.

4.1.6 Mechanistic Studies

4.1.6.1 Investigation of Catalytic Intermediates

Mechanistic studies on the asymmetric epoxidation and hydroperoxidation of acyclic α,β -unsaturated ketones using 9-amino(9-deoxy)*epi*quinine **9**^[82] were initiated by *C. Reisinger* in our group, who investigated the reaction intermediates using ESI-MS (Electrospray Ionization Mass Spectroscopy).^[136] In these studies, oxidation of the model enone substrate **75** at 32 °C was investigated by taking samples at various time points over 24 h and submitting them to ESI-MS and MS/MS analysis. Significantly, the analysis revealed the presence of the expected protonated reaction intermediates **A-C** and catalyst **[9+H]⁺** by mass (Scheme 4.11). These intermediates are thought to be common to all aminocatalyzed epoxidation reactions of α,β -unsaturated carbonyl compounds, and include the protonated imine species **A** formed by the initial condensation of the amine catalyst with the carbonyl substrate, the hydroperoxy adduct **B** formed by the conjugate addition of hydrogen peroxide to the iminium ion **A**, and the epoxide **C** formed from **B** *via* enamine-catalyzed intramolecular ring-closure (see also Scheme 4.12).

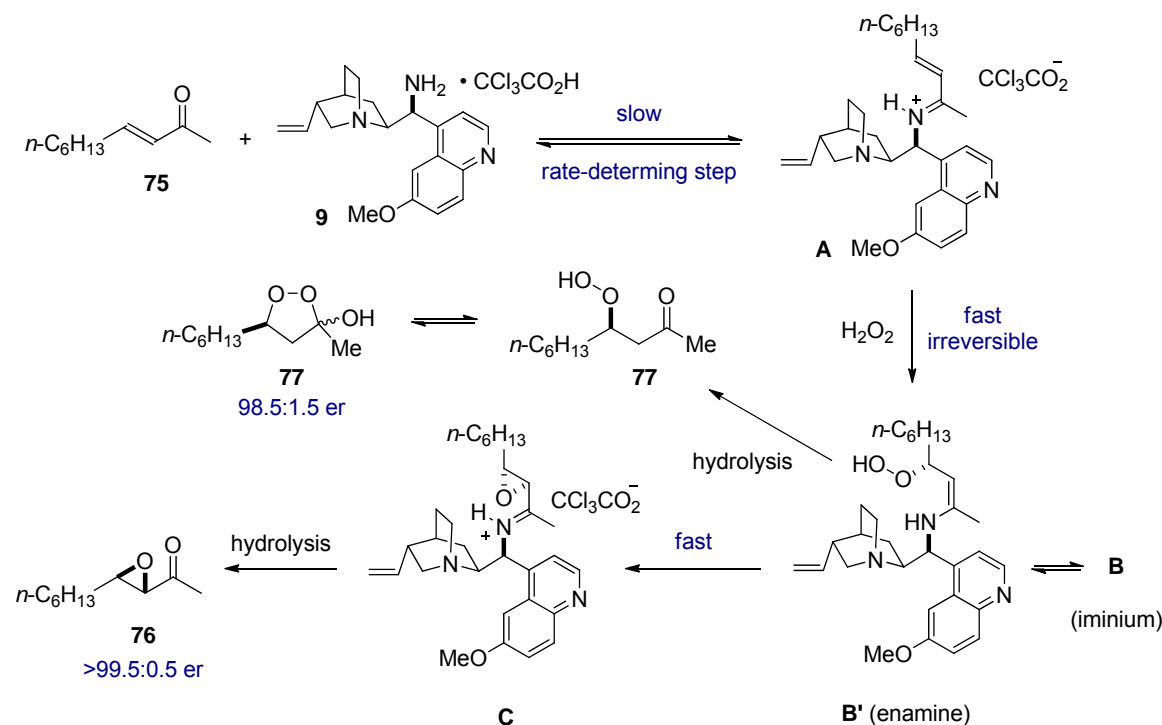


	[9 + H]	A	B	C
formula	$\text{C}_{20}\text{H}_{26}\text{N}_3\text{O}$	$\text{C}_{30}\text{H}_{42}\text{N}_3\text{O}$	$\text{C}_{30}\text{H}_{44}\text{N}_3\text{O}_3$	$\text{C}_{30}\text{H}_{42}\text{N}_3\text{O}_2$
LRMS	324.1	460.3	494.3	476
HRMS: found	324.207039	460.332803	494.338147	476.327879
calcd	324.206741	460.332238	494.337720	476.327145
error [ppm]	0.92	1.23	0.86	1.52

Scheme 4.11 ESI-MS studies by *C. Reisinger* on the asymmetric epoxidation and hydroperoxidation of acyclic α,β -unsaturated ketones using **9**.^[136]

4. Results and Discussion

Another significant finding of the studies was the reactivity of the iminium ion **A**, which could only be detected prior to the addition of hydrogen peroxide. Upon H_2O_2 addition, the iminium ion **A** could no longer be detected, suggesting its rapid consumption by hydrogen peroxide, although the signal for the free catalyst **9** remained. Furthermore, already after 1 hour of the reaction time, the peaks for both oxidation products **B** and **C** could be detected. The fact that the free catalyst **9** as well as the iminium products of hydroperoxidation (**B**) and intramolecular epoxide closure (**C**) could be easily detected in the crude reaction mixture, but that the iminium ion **A** remained below the detection limit, suggested that the initial formation of the iminium intermediate **A** is the rate-limiting step of the reaction, whereas hydrogen peroxide addition is rapid (Scheme 4.12). Isolation of highly enantioenriched hydroperoxy adducts of type **77**^[82] further suggested that the addition of hydrogen peroxide is irreversible.



Scheme 4.12 Putative reaction mechanism of the asymmetric epoxidation and hydroperoxidation of acyclic α,β -unsaturated ketones using amine catalyst **9**.^[136]

When analyzing the reaction at 50 °C, *C. Reisinger* further found the appearance of additional signals at m/z 340, 492 and 510, which presumably correspond to the oxidized version of the catalyst (species $\mathbf{9}_{+O}$) and iminium ions \mathbf{B}_{+O} and \mathbf{C}_{+O} which incorporate this oxygenated catalyst (Figure 4.2, tentative assignment). After 12 h of reaction time, these peaks gained in intensity, while the parent peaks **9**, **B** and **C** (m/z 324, 476 and 494, respectively) showed considerable loss of intensity, suggesting extensive catalyst oxidation. A doubly oxidized catalyst species, i.e.

4. Results and Discussion

a mass incorporating two oxygens (m/z 356) could not be detected. This oxidation behaviour, though less rapid, was also present at 32 °C, suggesting that oxidation of the catalyst **9** was a relatively facile process in the presence of aqueous hydrogen peroxide.

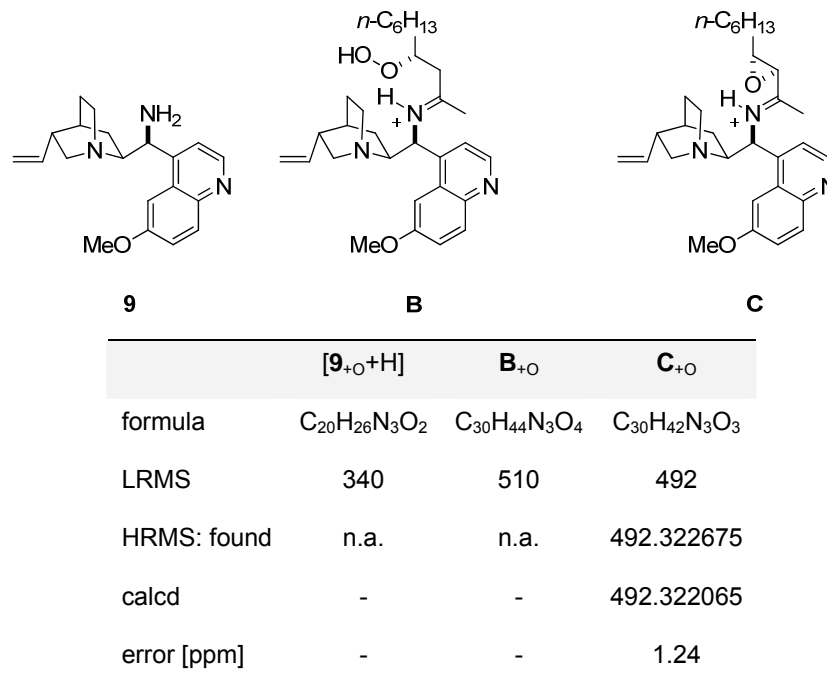


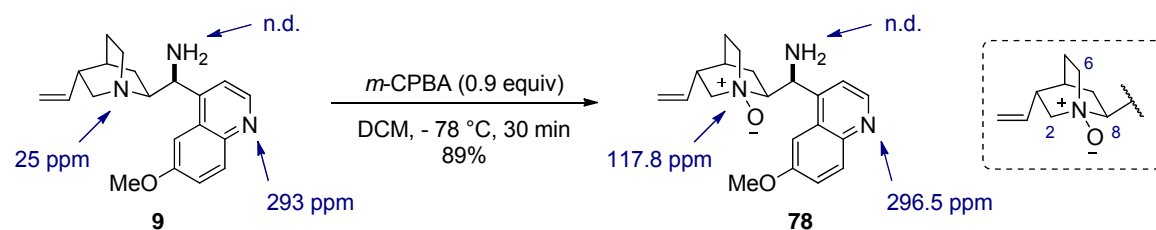
Figure 4.2 Evidence for catalyst oxidation through ESI-MS studies on the asymmetric epoxidation and hydroperoxidation of acyclic α,β -unsaturated ketones using catalyst **9**.^[136]

The fact that the 12-hour hydroperoxidation reactions catalyzed by **9** proceed to completion and with excellent enantioselectivity despite the apparent catalyst oxidation which already manifests itself after 1 hour, raised interesting mechanistic questions. As part of this Ph.D. work, we sought to continue the investigations of *C. Reisinger* and expand them to the related epoxidation of α -branched enals.

The nature of catalyst oxidation, i.e. the exact structure of **9**_{+O} was investigated first. The observation that the epoxidation reactions are apparently undisturbed by catalyst oxidation, and the formation of iminium species **B**_{+O} and **C**_{+O} suggested that the primary amine moiety cannot be involved in the oxidation **9** → **9**_{+O}. We therefore hypothesized that species **9**_{+O} most likely arises from the *N*-oxidation of the most reactive quinuclidine nitrogen. Toward this end, we synthesized 9-amino(9-deoxy)*epi*quinine *N*-oxide **78** from **9** using substoichiometric amounts of *m*-CPBA at -78 °C to ensure mono-oxidation (Scheme 4.13). The structure of **78** was unambiguously confirmed by extensive NMR analysis. In particular, characterization of the nitrogen atoms by ¹H-¹⁵N HMBC experiments in MeOD demonstrated the presence of an unchanged aromatic (quinoline) nitrogen^[137] at 296.5 ppm, and an oxidized quinuclidine

4. Results and Discussion

nitrogen at 117.8 ppm, as well as a typical deshielding^[138] of protons and carbons 2, 6 and 8 which immediately surround the *N*-oxide moiety (Scheme 4.13).



Scheme 4.13 Synthesis of 9-amino(9-deoxy)epiquinine *N*-oxide **78** using *m*-CPBA and ¹⁵N NMR characterization (in MeOD, NH₃ = 0 ppm, primary amine not detected).

With an authentic sample of **78** in hand, we carried out the model reaction of enone **75** (Scheme 4.11) to recover and analyze the catalyst species which remained at end of the 12 hour reaction period. Crude ¹H NMR analysis without an aqueous workup^{vii} showed a complex mixture (Figure 4.3, (c)), which presumably corresponds to various catalytic intermediates **9**, **A**, **B**, **B'** and **C** as well as the related oxidized species (cf. Schemes 4.12 and Figure 4.2).

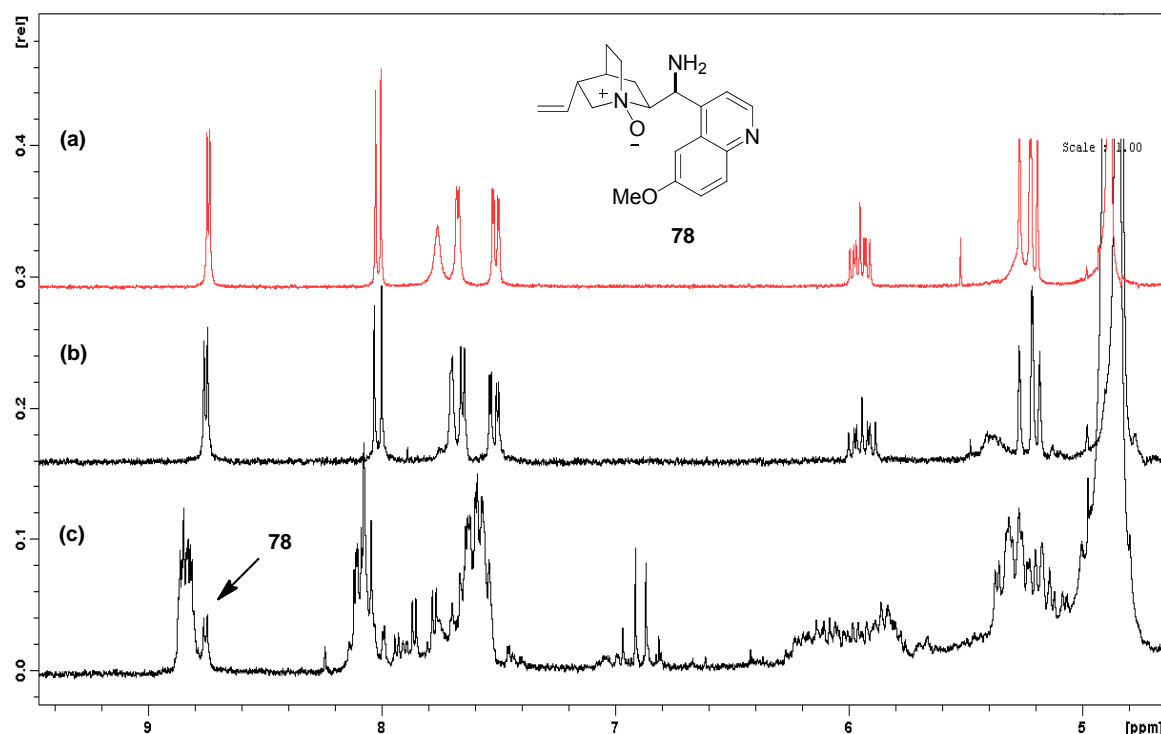


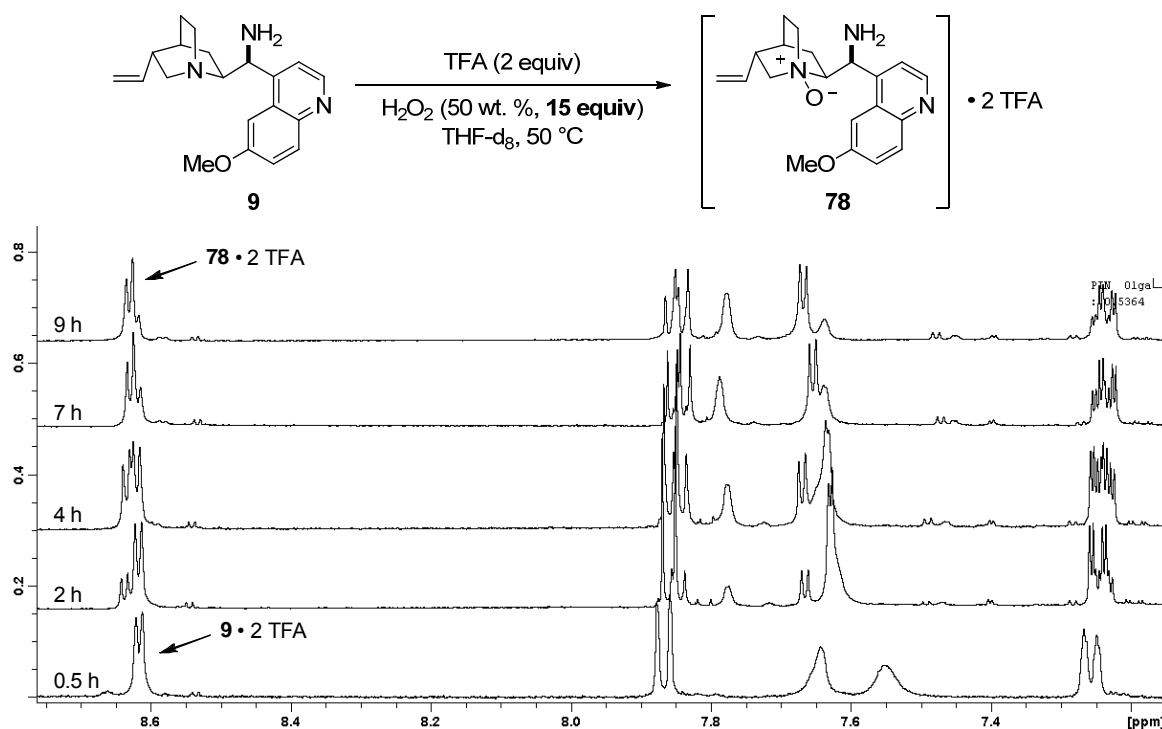
Figure 4.3 ¹H NMR analysis (CD₃OD) showing an authentic sample of **78** (a), the same product isolated at the end of epoxidation of enone **75** (b), and the crude reaction mixture at the end of epoxidation of enone **75** containing **78** and other unidentified catalytic species (c).

^{vii} Although an aqueous workup would liberate the catalyst from any covalent intermediates **A-C** and presumably simplify the spectrum, it had to be avoided because *N*-oxidized species **78** was found to be water-soluble.

4. Results and Discussion

However, TLC analysis clearly indicated the formation of a new and more polar species which eluted separately from **9** and other closely related compounds. Isolation of this species by flash column chromatography showed it to be a single compound (Figure 4.3 (b)), which was identical in all respects to the authentic sample of **78** (Figure 4.3, (a)). Thus, we established that quinuclidine *N*-oxidation occurs *in-situ* and that **78** presumably corresponds to **9**_{+O} observed by mass spectrometry. Unfortunately, other catalytic species present in the crude reaction mixture could not be separated by column chromatography or reliably characterized.

To ensure that other potential products of oxidation were not being overlooked due to the complexity of the crude reaction mixture, we subjected **9** to the epoxidation conditions in the absence of substrate **75** (Scheme 4.14). Gratifyingly, in this simplified system we could observe clean and complete oxidation of amine **9** to a single new species within 18 hours, which could be easily monitored by NMR and IPC techniques over time. Characterization of the product confirmed it to be the TFA salt of *N*-oxide **78**. No other constitutional isomers or products of multiple oxidation could be detected, in agreement with ESI-MS studies.

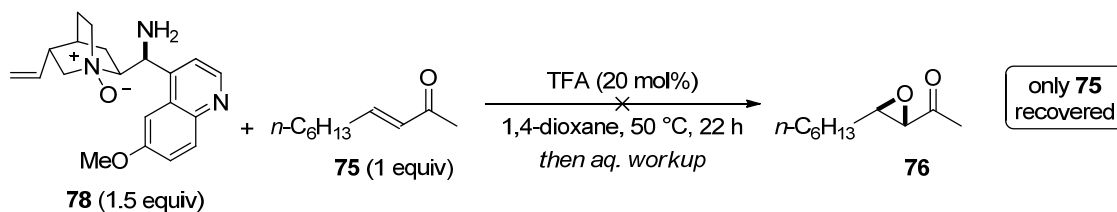


Scheme 4.14 Oxidation of the catalyst **9** to **78** under standard conditions for epoxidation but in the absence of substrate and ¹H NMR analysis (THF-d₈) of the process over time (only selected time points shown).

Examining the kinetics of the oxidation under these simplified conditions showed a standard conversion curve with no apparent autocatalytic effect (cf. Section 7.2.4).

4. Results and Discussion

Having confidently established the identity of **9**_{+O} as the *N*-oxide **78**, we next examined its reactivity. Mixing stoichiometric amounts of **78** with enone **75** in the absence of hydrogen peroxide at 50 °C did not give any epoxidation products, ruling out the ability of **78** to act as an oxygen transfer reagent,^[139] at least at the reaction temperature employed (Scheme 4.15).



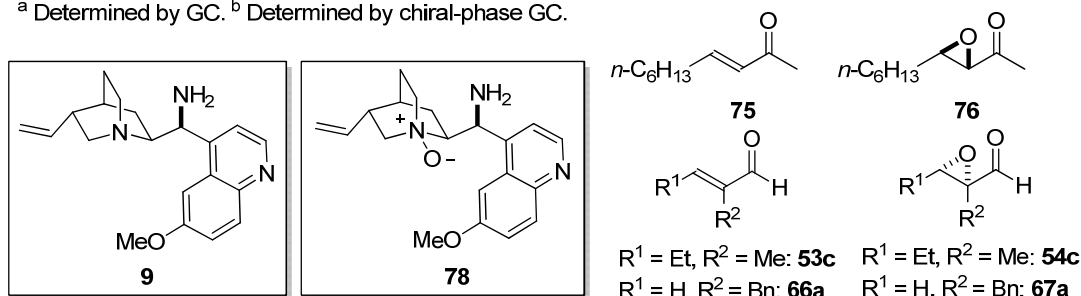
Scheme 4.15 Testing *N*-oxide **78** as an oxygen transfer reagent for the epoxidation of enone **75**.

We next examined the competence of **78** as a catalyst by testing it in the epoxidation of enone **75**, as well as enals **53c** and **66a** under the corresponding optimized conditions for each substrate class. A control reaction using the unmodified amine catalyst **9** was also performed in each case (Table 4.18).

Table 4.18 Evaluation of the *N*-oxidized catalyst **78** in the epoxidation of unsaturated carbonyl compounds.

Entry	Amine	Acid	Substrate	Product	Conditions	Conv., % ^a	dr ^a	er ^b
1	9	TFA	75	76	H ₂ O ₂ (50 wt. %, 1.5 equiv) 1,4-dioxane, 50 °C, 24 h	99	>99:1	98.5:1.5
2	78	TFA	75	76	then 1N NaOH, THF	74	>99:1	96.5:3.5
3	9	(<i>R</i>)-BIPP	53c	54c	H ₂ O ₂ (50 wt. %, 5 equiv) THF, 50 °C, 24 h	94	93:7	99:1
4	78	(<i>R</i>)-BIPP	53c	54c		99.5	86:14	97.5:2.5
5	9	(<i>R</i>)-TRIP	66a	67a	H ₂ O ₂ (50 wt. %, 5 equiv) THF, 50 °C, 24 h	99	n.a.	99:1
6	78	(<i>R</i>)-TRIP	66a	67a		84	n.a.	94:6

^a Determined by GC. ^b Determined by chiral-phase GC.



4. Results and Discussion

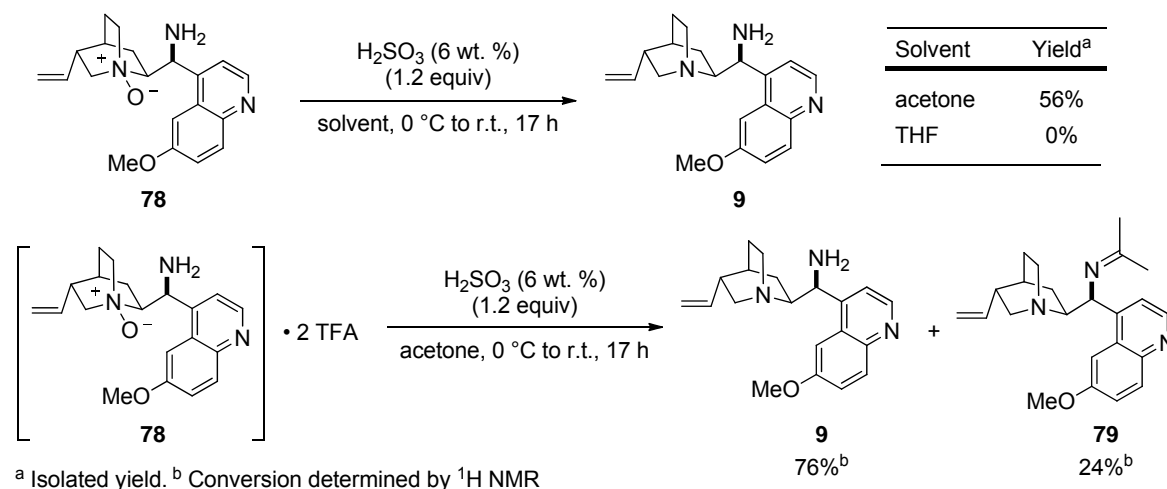
After 24 hours, all substrates underwent epoxidation with good to excellent conversion in the presence of either catalyst, indicating that the amine **78** was not only catalytically active but also comparable to the control in terms of reactivity. Furthermore, when using the amine **78**, epoxides **76**, **54c** and **67a** were formed with the same sense of stereoselection and nearly the same enantio- and diastereoselectivity as with catalyst **9** (entries 1 vs. 2, 3 vs. 4 and 5 vs. 6). These results demonstrate that the *in situ* *N*-oxidation of the catalyst **9** is not a decomposition pathway that removes the active catalyst species from the reaction, but a competing process that creates a new and nearly equally competent catalyst **78**. Remarkably, *N*-oxidation of the catalyst's quinuclidine moiety does not appear to disrupt the formation of a highly organized transition state in all of the epoxidation reactions.

Although the *N*-oxidized catalyst **78** can clearly act as a competing catalytic species, its effective contribution to the reaction is not obvious since it depends on the rate of oxidation of **9**. The observation that products are formed with slightly lower enantio- and diastereoselectivity when starting with the oxidized catalyst **78** than when starting with **9** (Table 4.18) implies that the contribution of catalyst **78** in the latter case is only minor and not enough to offset the overall enantiomeric excess of the product. Since results obtained by ESI-MS studies are only qualitative, we attempted to quantify the rate of *in situ* oxidation of catalyst **9** to **78** by NMR, HPLC and IPC techniques using the hydroperoxidation of enone **75** as a model system. Unfortunately, these studies were hindered by the presence of various catalytic intermediates (similar to Figure 4.3 (c)), which made analysis exceedingly complicated. Although a hydrolytic workup of crude samples would presumably liberate the catalytic species from any covalent associations with the product or the starting material, it could not be used due to the solubility of **78** in water. Kinetic studies performed with exclusion of the starting material (Scheme 4.14) are also not reliable. In these simplified studies, the catalyst was found to be completely oxidized after 18 hours, whereas in the presence of the substrate, oxidation of **78** was clearly only partial even after 24 hours (Figure 4.3 (c)).

Although not detrimental to activity or enantioselectivity, the oxidation of the catalyst **9** under the reaction conditions still results in slightly lowered catalytic efficiency (Table 4.18). Since this process can compromise the catalyst's recyclability, we tested the feasibility of reducing **78** back to **9**. Preliminary investigations were performed using a procedure adapted from Deng *et al.*^[140] Submitting pure **78** to a slight excess of sulfurous acid in acetone resulted in a clean reduction to afford the amine **9**, albeit with only a modest isolated yield of 56% (Scheme 4.16). Switching the solvent to THF shut down the reaction, giving only complete recovery of the starting material. Submitting a TFA salt of **78** to the same conditions gave

4. Results and Discussion

complete conversion to the desired product, albeit together with 24% of imine **79** formed by condensation of **9** with acetone. At this point, further optimization was not performed, but it appears that a clean reduction should be feasible with minor modification of conditions and/or a hydrolytic workup to recover **9** from **79**.



Scheme 4.16 Preliminary investigations of the reduction of **78** to **9** with sulphurous acid.

4.1.6.2 Investigation of Absolute Stereochemistry in the Epoxidation of Substrates **53**

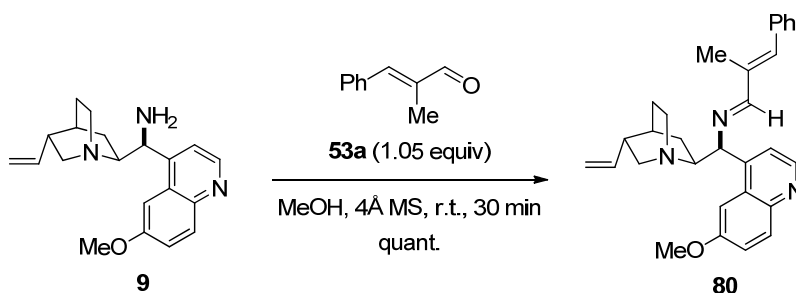
NMR investigations were performed in collaboration with Dr. Christophe Farès (NMR department, MPI Mülheim). Computational studies were performed by Dr. C. Farès and I. Polyak (AK Prof. Thiel, MPI Mülheim).

As discussed in Section 2.1.2.3, despite the myriad of synthetic transformations employing 9-amino(9-deoxy)*epi*quinine **9** and its salts as aminocatalysts, no mechanistic studies exist to date to shed light on the absolute stereochemistry imparted by the catalyst to the products. Yet, when one surveys the literature, remarkable consistency in the stereochemical outcome is observed across mechanistically similar reactions catalyzed by **9** for a variety of different substrates.^[41a, 41b, 48]

We became interested in rationalizing the absolute stereochemistry determined by the salts of catalyst **9** in the epoxidation of α -branched enals **53**. To approach this problem, we decided to perform structural studies of the iminium intermediate formed between amine **9** and enal **53**, which participates in the enantiodetermining step of the reaction. α -Methyl cinnamaldehyde **53a** was anticipated to form the most stable imine adduct with **9** due to the conjugation of the phenyl group with the unsaturated imine and chosen for the investigation. The high enantioselectivity

4. Results and Discussion

obtained in the epoxidation of **53a** (98:2 er, Section 4.1.5.2, Table 4.15) justified the choice of this α -branched enal as a representative substrate. After a brief optimization, it was found that condensation of **9** and **53a** proceeds quantitatively in methanol in the presence of 4Å molecular sieves (Scheme 4.17). A slight (5 %) excess of **53a** was used to ensure complete consumption of **9**. The resulting imine **80** was isolated as an amorphous solid without purification by a simple filtration and removal of solvent under reduced pressure, and analyzed together with the small excess of remaining **53a**. Imine **80** was found to be sufficiently stable to be handled under air and with non-dried solvents. For long-term storage, however, **80** was kept under argon at $-20\text{ }^{\circ}\text{C}$.



Scheme 4.17 Synthesis of imine **80** by the condensation of **9** with **53a**.

Unfortunately, extensive attempts at crystallizing **80** or its (*R*)-TRIP, TFA, HClO₄, TfOH, MsOH and HBF₄ salts did not meet with success. Notably, crystallization of the (*R*)-TRIP salt of **80** (in a glove box to exclude moisture) resulted in the formation of crystals of (*R*)-TRIP only, while imine **80** remained dissolved in the mother liquor. However, recent studies by the group of *Gschwind* on the mechanisms of proline and silyl prolinol organocatalysts have demonstrated that NMR spectroscopy can be used as a powerful tool for conformational analysis of catalytically relevant intermediates.^[141] Encouraged by these reports, we prepared samples of **80** and its various representative salts (cf. Section 4.1.4, Table 4.4) for NMR analysis. The salts were prepared by dissolving **80** together with the corresponding acid in a specific ratio in a deuterated solvent. The structures examined in this work are summarized in Figure 4.4.

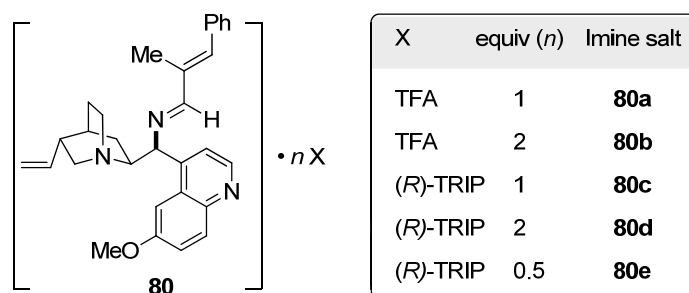


Figure 4.4 Salts of imine **80** used for structural analysis by NMR in this work.

4. Results and Discussion

It is noteworthy that iminium salts **80a-e** were found to be extremely sensitive to moisture and hydrolyzed rapidly in air. Therefore, samples had to be prepared in the presence of 4Å molecular sieves in dried glassware, filtered into flame-dried NMR tubes under argon and sealed under vacuum (cf. Chapter 7 for experimental details). When sealed, however, the samples in CDCl₃ and other solvents were found to be stable and could be stored for months.

A comparison of **80** dissolved in the reaction solvent THF-d₈ and in CDCl₃ revealed only very minor differences by NMR, so for convenience we chose deuterated chloroform as the standard polar, non-protic solvent for all samples at ca. 58 mM concentration. The numbering system shown in Figure 4.5 was adopted for all samples and is used in the following discussion.

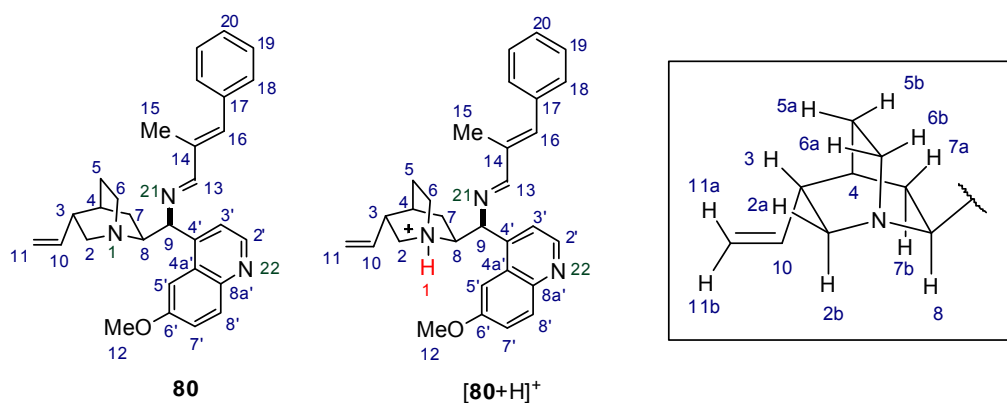


Figure 4.5 Numbering system used in the characterization of **80** and its salts.

In order to find the best conditions to characterize **80** and its salts, a range of temperatures were first screened. Figure 4.6 shows the ¹H NMR spectra of **80a** (**80**·1TFA) measured over a series of temperature spanning 100 °. Near room temperature (300 K), the majority of lines appeared sharp and well dispersed except for the peaks corresponding to protons in the vicinity of the central C₉ (H₉, H₈, H₁, H₁₃, H_{3'} and H_{5'}). The same was true for the corresponding carbons in the ¹³C NMR spectra. At this stage, the broadening was attributed to a degree of conformational freedom around the central C₈-C₉ and/or C₄'-C₉ bonds, which has been found typical for the parent cinchona alkaloids (cf. Section 2.1.3.3).

In an attempt to sharpen these peaks, both lower and higher temperatures of the sample were examined. As the temperature was lowered from 300 K, the peaks first broadened and then sharpened again near 223 K, albeit as split signals in an approximate ratio of 3:1. Presumably, at 223 K, two species reflecting a small conformational difference could be “frozen out” in a 3:1 ratio. As the temperature was increased from 300 K to 323 K, all of the peaks sharpened, except for H₁ at 12.8 ppm originating from TFA. Although the broadening of peaks was affected over

4. Results and Discussion

the temperature range, the position of the peaks did not change severely, suggesting that major conformational changes or decomposition of the sample were not occurring. Therefore, in order to obtain a full ^1H , ^{13}C and ^{15}N chemical shift assignment it was necessary to measure certain experiments at both high and low temperature, despite relaxation obstruction on the performance of some experiments.

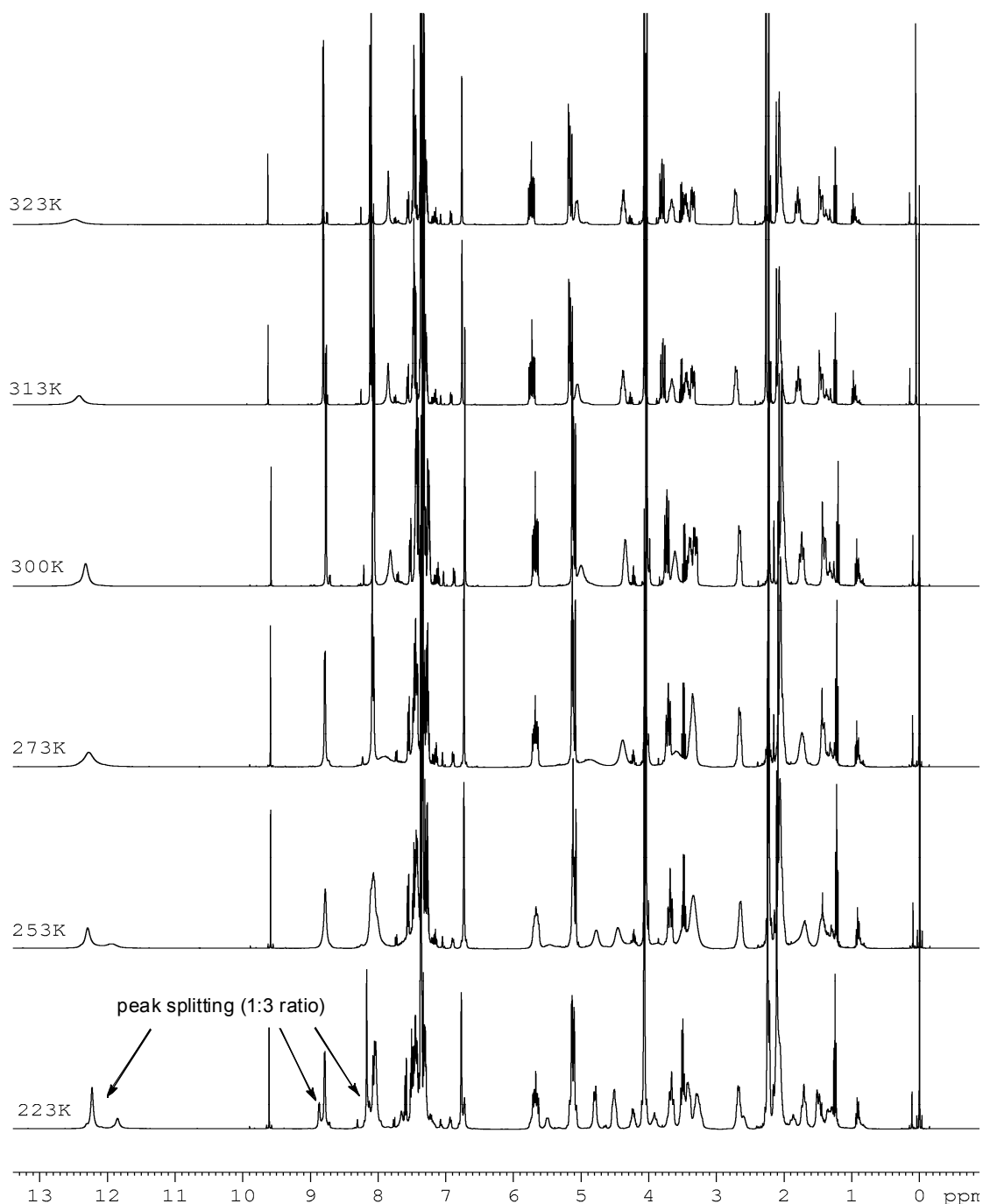


Figure 4.6 ^1H NMR analysis of **80a** over a 100° temperature range and peak splitting at 223K.

4. Results and Discussion

The relative configuration of the double bonds in the unsaturated imine moiety (aza-diene), the overall conformation of **80** and its salts, and the approximate position of the associated counteranion were analyzed by detailed NMR experiments at several temperatures in CDCl₃. In general, analysis of the chemical shifts and scalar couplings for samples **80a-e** showed that in the presence of different counteranions (TFA, TRIP) and different acid stoichiometries (0.5 - 2 equiv), the overall conformation of the iminium structure remained unchanged, although some smaller conformational adjustments are possible. Assignment of different structural elements verified for each of **80a-e** is discussed in the following text.

Configuration of the imine double bond N=C₁₃

The configuration of the imine double bond (N=C₁₃) is one of the most crucial parameters in enantioselectivity, as it determines the position of the catalyst relative to the substrate and thus has a direct influence on facial discrimination. This double bond was determined to be *E* based primarily on the signature ²*J* coupling constant between ¹H₁₃ and ¹⁵N₂₁ (Figure 4.7). The observed value of 3 Hz falls within the range of 2-5 Hz typical for *E* configuration, as opposed to -10 to -15 Hz typical for the *Z* configuration^[142].

Conformation of the single bond C₁₃-C₁₄

The conformation of the single bond between C₁₃ and C₁₄ was determined to be close to *s-trans*, based principally on *NOE* contacts indicators, namely the strong *NOE* between H₁₃ and H₁₆, in combination with the weak *NOE* between H₁₃ and H₁₅ (Me), and H₁₆ and H₁₅ (Me) (Figure 4.7). A small deviation from planarity (180°) of the aza-diene system was indicated by the coupling constant ³*J* (H₁₃-C₁₅) of 2.9 Hz, as discussed for substituted butadienes.^[143]

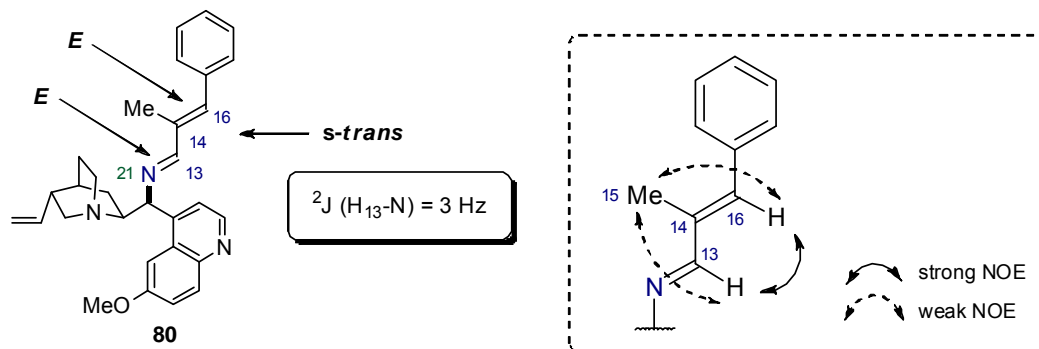


Figure 4.7 Determination of (*E,E*)-*s-trans* conformation of the unsaturated imine moiety.

Configuration of the double bond C₁₄=C₁₆

The geometry of the double bond C₁₄=C₁₆, derived from the *E*-configured enal **53a** was confirmed to be unchanged (*E*) in the imine adduct **80**. Although the smaller coupling constant of 7.6 Hz for $^3J(\text{H}_{16}\text{-C}_{15})$ compared to 10 Hz for $^3J(\text{H}_{16}\text{-C}_{13})$ would seem to indicate the opposite configuration, *Vogeli* and *von Philipsborn* have demonstrated that the vicinal $^3J_{\text{C,H}}$ coupling constants in trisubstituted alkenes strongly vary with a number of structural factors.^[144] Indeed, the authors showed that in certain cases, $^3J_{\text{C,H}}$ coupling constants for *trans*-substituents (spanning the range of 7.4 – 17.9 Hz) may be smaller than those for *cis*-substituents (4.6 – 11.1 Hz). For example, the coupling constants observed in the *E*-configured enal moiety of isomorellin **81**, an isomer of natural antibiotic morellin, reflect such a case,^[144] and are very close to ones measured for **80** (Figure 4.8). In addition, the relatively weak *NOE* existing between H₁₆ and H₁₅ (Me) as well as the very strong *NOE* (one of the strongest in the NOESY spectrum) between H₁₆ and H₁₃, strongly support the *E* configuration (Figure 4.7). Linear *NOE* build-up for both these key *NOEs* over five mixing times did not indicate the presence of spin-diffusion which could skew the intensities.

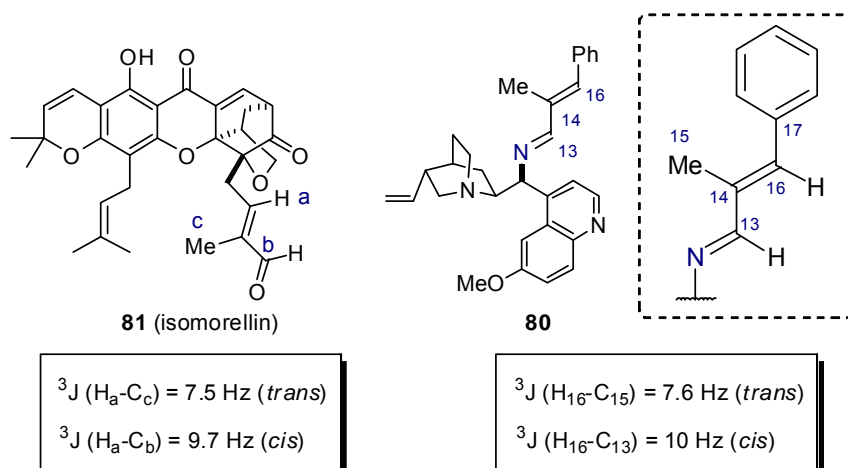


Figure 4.8 Confirmation of the (*E*)-configuration of the C₁₄-C₁₆ double bond.^[144]

Conformation of the single bond C₁₆-C₁₇

Overlap of the signals corresponding to both *ortho*- and both *meta*-substituent pairs in the aromatic ring in the ¹H and ¹³C spectra did not allow a proper *NOE* or *J*-coupling analysis of the C₁₆-C₁₇ bond conformation. The magnetic equivalence of both *ortho*- and both *meta*-proton and carbon pairs in the aromatic ring indicates that the C₁₆-C₁₇ bond is dynamic and allows for rapid ring flips, even at low temperature. It is expected, however, that due to steric hindrance with the

4. Results and Discussion

C₁₅ methyl group, a perfectly planar π -conjugated system of the phenyl ring with the unsaturated imine (aza-diene) is not possible.

Conformation of the single bond C₈-C₉

The large vicinal coupling constant $^3J_{\text{H,H}}$ of 9.3-9.5 Hz between H₈ and H₉ as well as key *NOE* from H₉ to H_{6b} (**80a-e**) and H_{7a} (**80**, **80a-e**) were found to be in accordance with this single bond adopting a conformation which places H₈ and H₉ close to a *trans* configuration ($\varphi_{\text{H}_8\text{C}_8\text{C}_9\text{H}_9} = 180^\circ$, Figure 4.9).

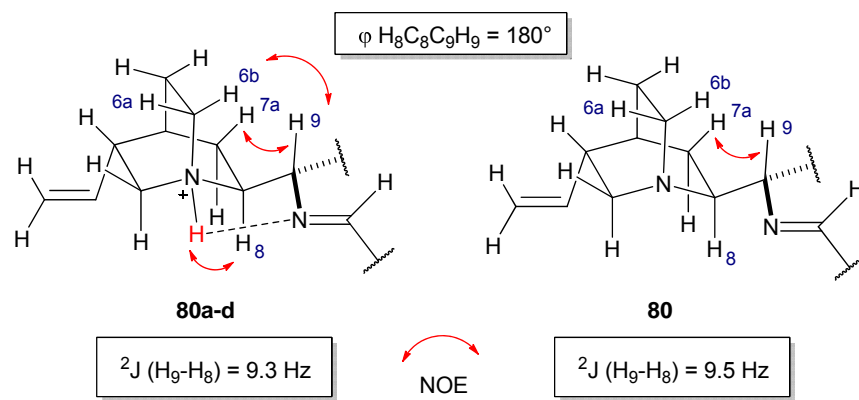


Figure 4.9 Key *NOE* correlation establishing the *trans*-relationship of H₈-H₉ (300 K).

Configuration of the single bond C₉-C_{4'}

As mentioned in Section 2.1.2.3, the quinoline group in cinchona alkaloids and derivatives exists in several energetically favored positions assumed by the rotation of the C₉-C_{4'} bond.^[53] Analysis of *NOESY* data at room temperature for the unprotonated imine **80** suggested a mixture of two rapidly exchanging conformations involving the quinoline group. This was particularly evident from the similar *NOESY* cross-peaks patterns for H_{3'} and H_{5'}, both of which showed close proximity to H₈, H₉, H₁₅ (Me) and H_{7a} (Figure 4.10 (a)). Since the H₈-H₉ coupling remained large at 10 Hz in both conformations, the C₈-C₉ bond is not likely to be involved in this conformational change. Indeed, most consistent with the NMR data is a 180° bond rotation around C₉-C_{4'} giving *syn* and *anti* conformers (Figure 4.11). In the monoprotonated salt **80a** this interchange was found to be strongly hindered to favour the *syn* conformer, as indicated by the relative ratio of the same *NOE* cross-peaks (Figure 4.10 (b)). At low temperatures down to -60°C , the protonated species **80a** displayed broadening and peak-doubling in a 3:1 ratio, which presumably corresponds to the *syn* and *anti* conformers of the quinoline group, although

4. Results and Discussion

residual slow exchange and broadening did not allow to confirm this by *NOESY*. Interestingly, the free amine **80** did not show similar peak splitting at low temperatures down to $-60\text{ }^{\circ}\text{C}$ (although broadening did occur), suggesting unhindered rotation of the quinoline group.

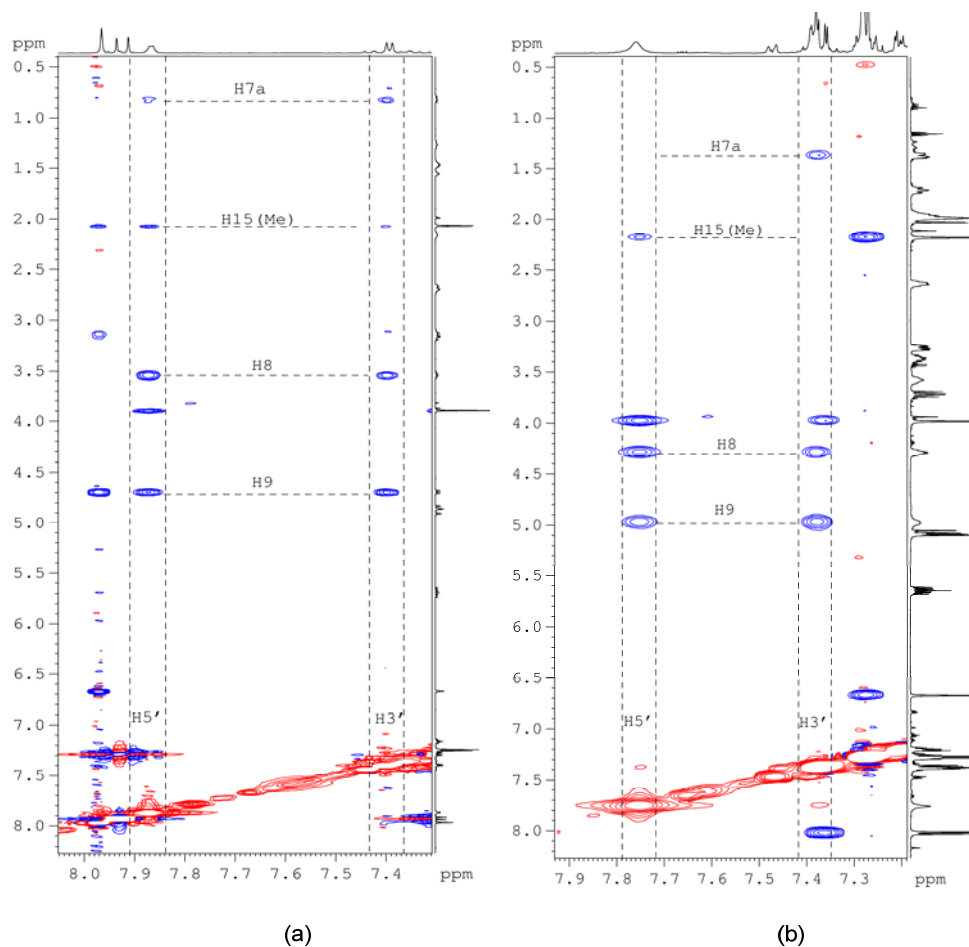


Figure 4.10 *NOESY* spectrum of **80** at 300K (r.t.) in CDCl_3 showing a mixture of quinoline rotational conformers indicated by same cross-peaks of $\text{H}_{3'}$ and $\text{H}_{5'}$ (a), and the same spectrum of the monoprotonated salt **80a** showing a preference for the *syn* conformer (b).

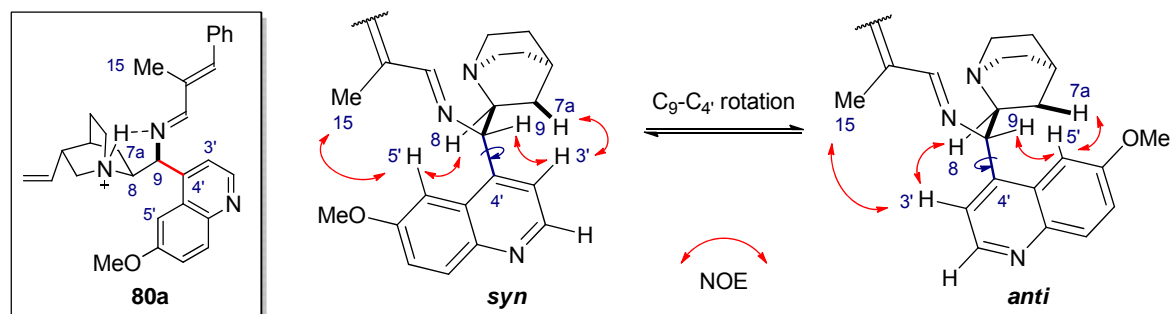


Figure 4.11 Proposed conformers originating from $\text{C}_9\text{-C}_{4'}$ bond rotation which account for the *NOESY* data.

4. Results and Discussion

Protonation site with 1 equivalent of TFA (salt **80a**) or (*R*)-TRIP (salt **80c**)

In agreement with the relative pK_a values of all three nitrogen sites,^[145] NMR analysis of the salt **80a** confirmed the most basic quinuclidine nitrogen (N₁) to be fully protonated upon the addition of 1 equivalent of TFA, forming two fully charged species ([**80**+H]⁺ and CF₃CO₂⁻). The broad peak corresponding to H₁ appeared at 12.8 ppm, and showed key *NOE* cross-peaks to H_{2a}, H_{2b}, H_{6a}, H_{6b} and H₈ (Figure 4.12). Moreover, the chemical shift of N₁ was found to move downfield from 24.3 ppm to 40.5 ppm with respect to NH₃ (0 ppm) upon addition of the acid. A one-bond coupling ¹J(H₁-N₁) of 70 Hz could also be measured.

Examination of the imine nitrogen N₂₁ in the protonated species **80a** further revealed an upfield change in the ¹⁵N chemical shift from 333.8 ppm to 318.3 ppm with respect to NH₃ (0 ppm), which is typical for (partial) protonation of sp² nitrogen atoms.^[146] This upfield shift was not sufficient to justify a full protonation of the imine to iminium upon acid addition, since an upfield shift on the order of 100 ppm would be expected.^[147] There was also no indication of a ¹J_{HN} coupling constant for N₂₁ even at low temperature where several conformation of **80a** could be observed, supporting the absence of full protonation. The chemical shift of the quinoline nitrogen N₂₂ was determined to be essentially unchanged. Taken together, these results support a model in which the protonated quinuclidine (N₁-H₁) participates in a hydrogen bond with N₂₁, forming a pseudo-five-membered-ring (H₁-N₁-C₈-C₉-N₂₁) (Figure 4.12). This effectively rigidifies the iminium structure, discouraging rotation around the C₈-C₉ bond.

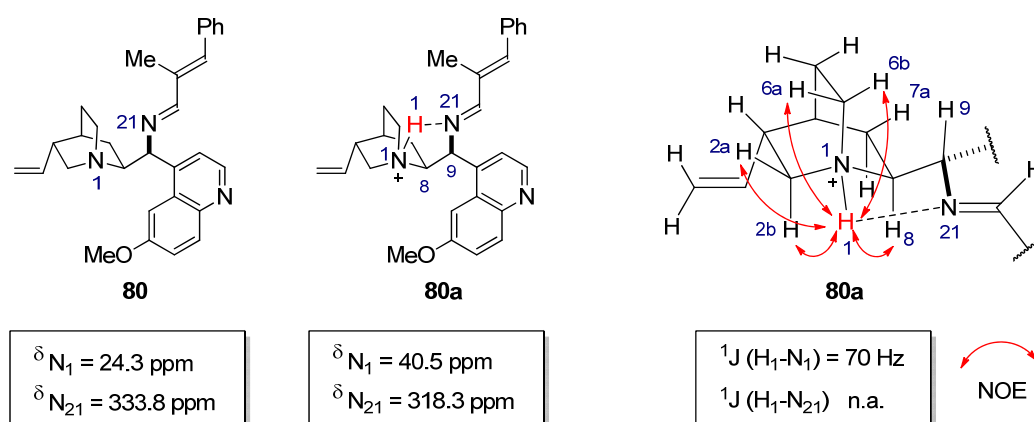


Figure 4.12 Structure of the monoprotinated salt **80a** as suggested by NMR data and key *NOE* signals indicating the site of full protonation.

The data obtained for the (*R*)-TRIP salt **80c** were in very close agreement with those of **80a**, suggesting that the counteranion does not affect the protonation behaviour of the iminium species (cf. Chapter 7 for full characterization).

4. Results and Discussion

Protonation sites with 2 equivalents of TFA (salt **80b**) or (*R*)-TRIP (salt **80d**)

The monoprotonated TFA salt **80a** and its bis-protonated analogue **80b** displayed essentially identical catalytic behaviour under unoptimized conditions (cf. Section 4.1.2, Table 4.4). However, because we employed 2 equivalents of the acid under the optimized conditions to improve the diastereoselectivity of the reaction (cf. Section 4.1.5.2, Table 4.15), we sought to determine how the second acid equivalent is involved in the structure and whether major conformational changes are caused by the additional protonation. Analysis of the doubly protonated salts **80b** and **80d**, however, did not show any significant changes in the iminium structure. Importantly, the pseudo-five-membered ring formed by hydrogen bonding between the protonated quinuclidine and the imine moiety was not disrupted (Figure 4.13). Instead, the second site of protonation was found to be on the quinoline nitrogen, which was again in accord with the relative pKa values of the three nitrogen atoms.^[145] This was supported by the disappearance of the quinoline nitrogen signal (N₂₂) in the NMR spectrum and an upfield shift of the surrounding carbon signals C_{2'}, C_{8a'}, C_{8'} and C_{7'} (Figure 4.13), which was not observed in the monoprotonated sample **80a**. In addition, the broad peak at approx. 12 ppm corresponding to both acidic protons displayed additional *NOE* cross-peaks to H_{2'} and H_{8'}.

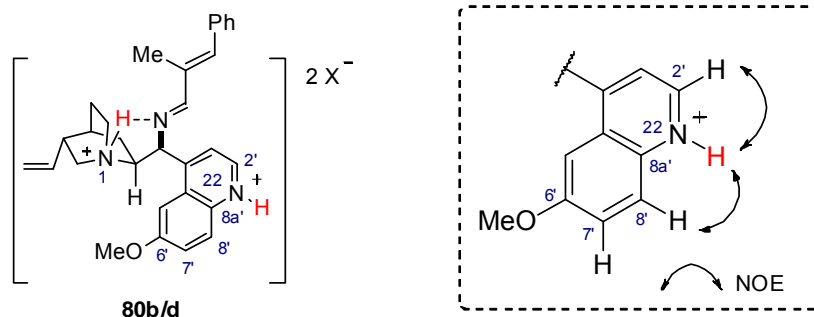


Figure 4.13 Protonation sites of the 2TFA salt **80b**.

Position of the counteranion with 1 equivalent of TFA (**80a**) and (*R*)-TRIP (**80c**)

In the epoxidation of enals **53**, the counteranion derived from the acid co-catalyst was found to exert a pronounced effect of the reaction (cf. Section 4.1.4, Table 4.4). Nevertheless, analysis of the different salts **80a-e** revealed an essentially unchanged conformation of the iminium cation. This suggested that the effect of the counteranion is not vicarious (i.e. in altering the iminium structure) but a direct one, i.e. as a **structural** or **directing element**. To investigate this hypothesis, we sought to determine the proximity of the ion association, and in the event of a close association, map the exact position of the counteranion relative to the iminium species. In

4. Results and Discussion

approaching this problem, we resorted to (hetero)nuclear *Overhauser* effect (*NOESY* and *HOESY*) measurements as well as diffusion ordered spectroscopy (*DOSY*) using the non-protic polar solvent chloroform, protic solvent methanol, or a mixture of both.

In the TFA salt **80a**, protons neighbouring the trifluoroacetate counteranion were identified by a 1-D $^1\text{H},^{19}\text{F}$ *HOESY* using several mixing times from the CF_3 frequency of TFA. The spectrum in chloroform (Figure 4.14) showed a large number of weak cross peaks with similar intensities, correlating to the proton signals of all three sub-components of **80** (quinuclidine, quinoline and aza-diene), indicating a *close but unspecific association* with the counteranion.

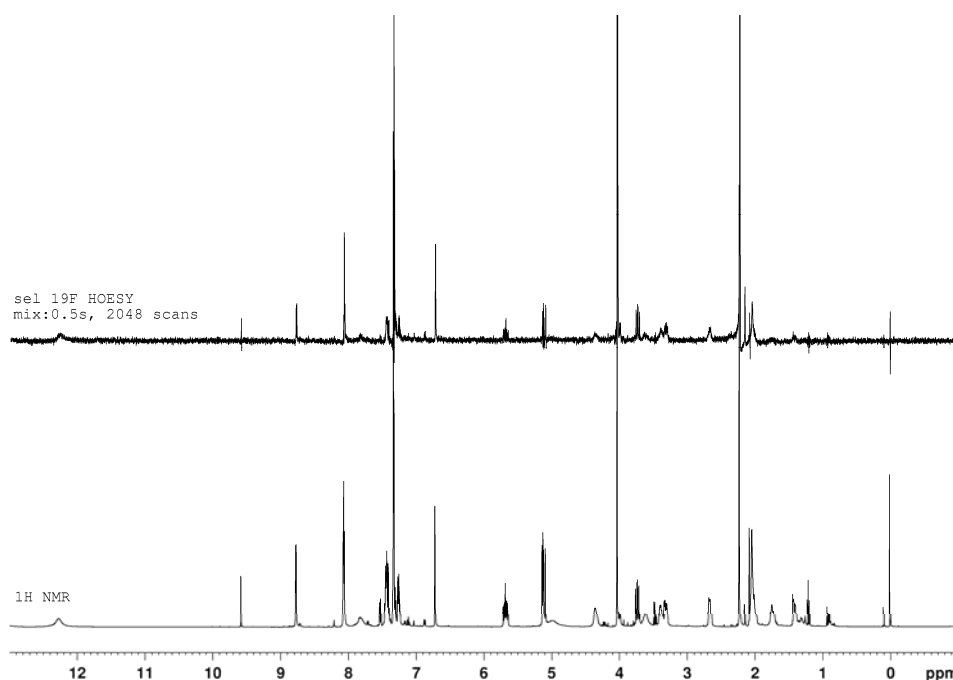


Figure 4.14 1-D $^1\text{H},^{19}\text{F}$ *HOESY* spectrum of the TFA salt **80a**.

Similar results were obtained from ^{31}P -*HOESY* and 2D-*NOESY* analyses on the (*R*)-TRIP salt **80c**, which also demonstrated unspecific ionic pairing between the positively charged iminium ion $[\mathbf{80}+\text{H}]^+$ and the negatively charged counteranion of TRIP. This was further supported by the observation that the NMR symmetry of the TRIP counteranion was not broken in the salt **80c**, as would be expected for ionic pairs that are rapidly associating and dissociating. Nevertheless, when we prepared a mixture of **80** with 0.5 equiv of (*R*)-TRIP (salt **80e**), ^1H NMR analysis clearly indicated the presence of two distinct species and not an average of partly protonated structures. *DOSY* spectroscopy further confirmed two sets of peaks with different diffusion coefficients, corresponding to unprotonated imine **80** ($7.3 \times 10^{-10} \text{ m}^2/\text{s}$) and the monoprotonated TRIP salt **80c** ($5.7 \times 10^{-10} \text{ m}^2/\text{s}$) in which $[\mathbf{80}+\text{H}]^+$ and the negatively charged

4. Results and Discussion

counteranion of TRIP diffused together (Figure 4.15 (a)). This implied that despite the lack of *geometrically specific* binding between **80** and (*R*)-TRIP, the ion pair association is *relatively strong* in neat CDCl₃.

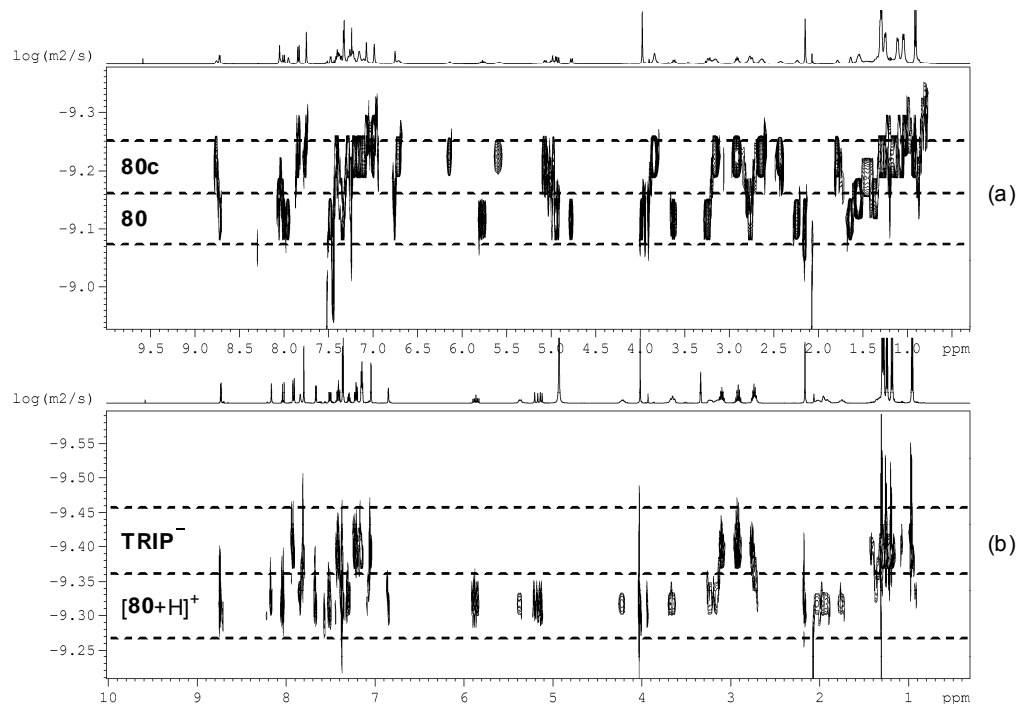


Figure 4.15 DOSY spectrum of salt **80e** ([**80**·0.5 (*R*)-TRIP]) showing the presence of unprotonated imine **80** and the monoprotonated (*R*)-TRIP salt **80c** in CDCl₃ (a), and ion-separated salt **80c** in protic solvent MeOD (b).

We next examined how the ion pairing was affected by the presence of a protic solvent or a protic additive, since an excess of aqueous hydrogen peroxide is employed in the epoxidation of enals **53**. In neat methanol, complete ion separation was observed for the salt **80c** as indicated by a DOSY experiment. Under these conditions, the [**80**+H]⁺ cation and the TRIP⁻ anion clearly diffused at different rates (Figure 4.15 (b)). However, since the environment of a standard epoxidation reaction is only slightly protic, we also examined the effect of a protic *additive* in chloroform. Under the optimized conditions of epoxidation (cf. Section 4.1.5.2), a combined 144 equivalents of H₂O₂ and H₂O with respect to the catalyst are present in ca. 987 equiv of solvent (THF), which corresponds to a 1:7 ratio of protic to aprotic media. Based on these calculations, we prepared a sample of **80a** in CDCl₃ containing 7 equiv of MeOH^{viii} with respect to **80a**, which corresponded to a similar 1:10 ratio of protic to aprotic solvent. A 1-D ¹H, ¹⁹F

^{viii} Since the presence of water or aqueous hydrogen peroxide would cause immediate and complete hydrolysis of salts **80a-e**, methanol was chosen to simulate the slightly protic environment of the epoxidation.

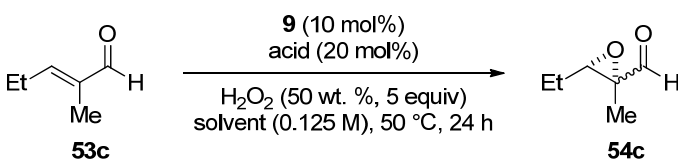
4. Results and Discussion

HOESY of this sample revealed weak non-specific cross-peaks, suggesting that the ion association remained largely undisrupted. Although direct observation of the diffusion coefficient of the counteranion by *DOSY* was not possible as a trifluoroacetate anion lacks protons, the diffusion coefficient of the iminium species was found to be between that of **80** alone and the heavier TRIP salt **80c**, further supporting the existence of ion pairing. Hence, we speculated that under the slightly protic reaction conditions, the counteranion remains in close association with the iminium cation $[\mathbf{80}+\text{H}]^+$, albeit this association lacks any obvious organization.

Structure-activity analysis of the effect of the counteranion

Drawing on the findings by NMR, we decided to perform additional experiments on the epoxidation of the model substrate **53c** with the aim of elucidating the role of the counteranion. The observation by NMR that methanol completely separates the ions of the salt **80c** (cf. Figure 4.15) suggested that carrying out the epoxidation reaction in this solvent should create a transition state which lacks the counteranion, and thus directly highlight the contribution of the counteranion to stereoselectivity. This hypothesis was further supported by the observation that solvation of the iminium cation $[\mathbf{80}+\text{H}]^+$ by methanol did not appear to cause any major conformational changes, as indicated by NMR analysis. Table 4.19 shows the results of the experiments using the amine catalyst **9** with TFA and (*R*)-TRIP acid co-catalysts in methanol (entries 1-2), together with control reactions in THF (entries 3-4).

Table 4.19 The effect of ion-separating solvent methanol on the stereoselectivity of epoxidation of the model α -branched enal **53c**.



Entry	Acid	Solvent	Conversion, % ^a	dr ^a	er (<i>trans</i>) ^b
1	(<i>R</i>)-TRIP	MeOH	37	51:49	43:57
2	TFA	MeOH	78	51:49	46:54
3	(<i>R</i>)-TRIP	THF	81	87:13	99:1
4	TFA	THF	73	65:35	75:25

^a Determined by GC. ^b Determined by chiral-phase GC.

4. Results and Discussion

The (*R*)-TRIP salt of the catalyst was found to be incompletely soluble in methanol, which likely explains the low conversion observed in this reaction (entry 1). Employing the readily soluble TFA salt in methanol (entry 2) resulted in a smooth reaction, with the conversion after 24 hours comparable to the control (entry 4). However, a dramatic effect was observed on the stereoselectivity of the reactions in methanol. In accordance with our predictions, the lack of counteranion contribution was clearly evident as both (*R*)-TRIP and TFA co-catalyst salts gave essentially the same diastereo- and enantioselectivity (entries 1-2), in stark contrast to the control reactions in THF (entries 3-4). Furthermore, the diastereoselectivity of both reactions in methanol was completely eroded, while the enantioselectivity was considerably lower and even reversed, compared to THF. These results strongly indicate that while the close association of the counteranion is irrelevant for conversion (entry 2 vs. 4) it is crucial for enantioselectivity (entries 1-2 vs. 3-4)

To approach the same hypothesis differently, we also screened various acid co-catalysts which, upon dissociation, form anions of different coordinating strength (strength of cation-anion association). A summary of these results is presented in Table 4.20. In the absence of acid (entry 1), weakly acidic H₂O₂ or H₂O is presumed to be the formal proton source.

Table 4.20 Analysis of acid co-catalysts with different coordinating strength of the conjugate base in the epoxidation of **53c**.

Reaction scheme showing the epoxidation of **53c** to **54c**. Reagents: **9** (10 mol%), acid (20 mol%), H₂O₂ (50 wt. %, 5 equiv), THF (0.125 M), 50 °C, 24 h.

Entry	Acid co-catalyst	Conversion,% ^a	dr ^a	er (<i>trans</i>) ^b
1	none	13	63:37	85:15
2	TFA	73	65:35	75:25
3	TCA	14	63:37	78:22
4	CF ₂ HCO ₂ H	34	68.5:31.5	82:18
5	CCl ₂ HCO ₂ H	36	69:31	80:20
6	MeCO ₂ H	18	60:40	84:16
7	HCl	69	65:35	89:11
8	HBr	1 ^c	n.d.	n.d.
9	HBF ₄	100	46:54	57:43

^a Determined by GC. ^b Determined by chiral-phase GC. ^c Discolouration (Br₂ evolution) and sample decomposition observed.

4. Results and Discussion

Plotting these results, as well as the earlier results of acid co-catalyst optimization (Section 4.1.2, Table 4.4), under a scale of anion coordinating strength^[148] revealed a clear pattern, whereby the enantioselectivity of the epoxidation was greatest with the most coordinating anions and decreased with diminishing coordinating strength (Figure 4.16). Once again, conversion appeared to be independent of the counteranion, and did not follow any easily observable trend.

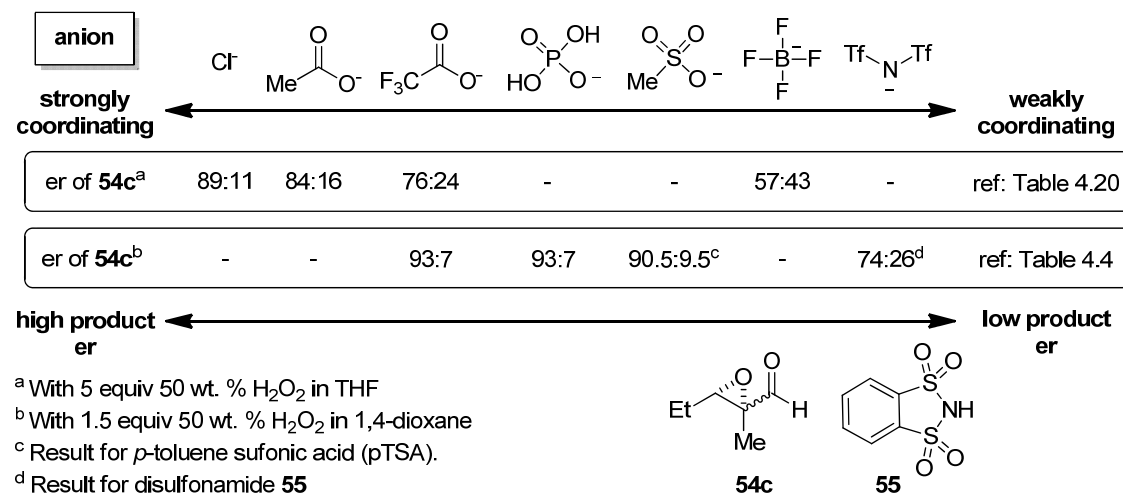


Figure 4.16 Dependence of enantioselectivity in the epoxidation of **53c** on the coordinating strength of the counteranion^[148] derived from the acid co-catalyst.

All of the results combined suggest that a tight association of the counteranion with the iminium ion is crucial for enantioselectivity, that is, *the counteranion plays a direct role in the observed sense and degree of enantioselectivity*. Since the counteranion does not appear to have a specific docking site in the putative pre-transition state assemblies **80a-e** as determined by NMR studies, it likely undergoes organization in the transition state, i.e. with the attack of hydrogen peroxide.

Calculated model of **[80+H]⁺** and proposed rationalization of the absolute stereochemistry

Using *NOE* integrals obtained from the NMR analysis of samples **80** and **80a-e** for distance restraints, an NMR-derived model for the iminium structure **[80+H]⁺** was calculated using XPLOR-NIH Ver. 2.9.7^[149] (cf. Chapter 7 for a detailed description of all the parameters used). Figure 4.17 (a) shows the energy-optimized structure of **[80+H]⁺** obtained with this method. To support the validity of this low-theory structure, DFT calculations (B3LYP, vacuum) with SVP or TZVPP basis set using the Turbomole program^{ix} were used in parallel to derive a model of **[80+H]⁺** (Figure 4.17 (b)). Gratifyingly, both NMR-derived (i.e. empirically supported) model

^{ix} For prescreening of initial structures, MNDO program and OM3 semi-empirical method were used.

4. Results and Discussion

and the DFT-calculated model using a much higher level of theory produced essentially the same structure.

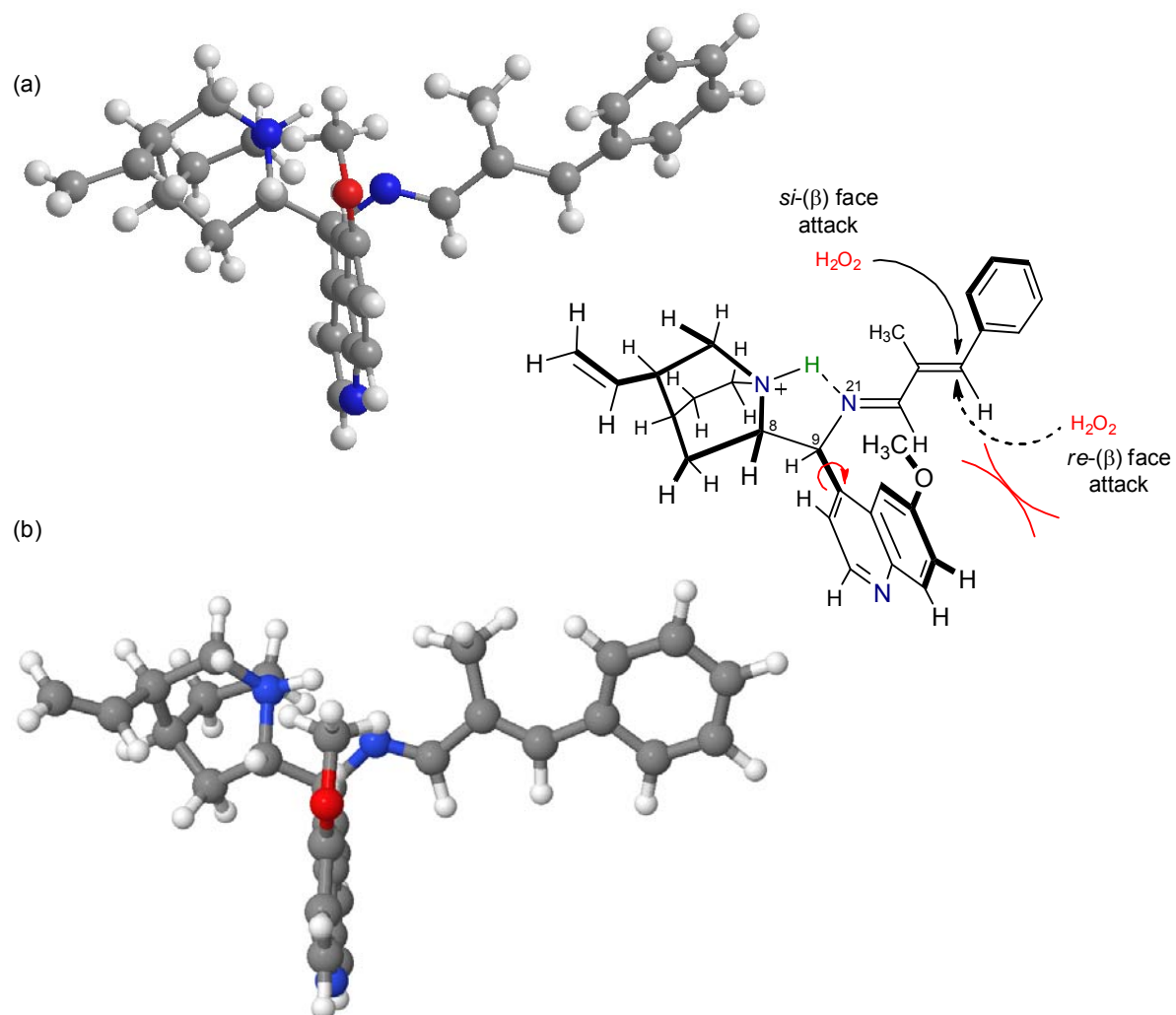


Figure 4.17 NMR-derived model for the iminium structure [80+H]⁺, calculated using XPLOR-NIH Ver. 2.9.7^[149] (a), and a model of the same structure derived by DFT (B3LYP, vacuum) calculations (b).

Significantly, both of the energy-optimized models are in perfect agreement with the results obtained by NMR analysis, including a proton bridge between the quinuclidine and imine nitrogens, (*E,E*)-*s-trans* geometry of the unsaturated iminium moiety and the preferred “*syn*” orientation of the quinoline group. As discussed previously, the pseudo-five-membered ring formed between the quinuclidine and imine nitrogens, together with the planar π -conjugated system of the unsaturated iminium moiety effectively rigidify the whole system (and in particular single bonds C₈-C₉ and C₉-N₂₁), and presumably allow for a very organized transition state. Indeed, the only dynamic moiety appears to be the quinoline group, which presumably

4. Results and Discussion

sweeps the area in front of the *re*-(β) face of the substrate and shields it. The resulting *si*-(β) face attack is in accord with the absolute configuration observed in the reaction. Furthermore, when we used the truncated catalyst **61** which lacks the quinoline moiety, a much lower and reversed enantioselectivity was observed compared to catalyst **9** (cf. Section 4.1.2, Table 4.5), supporting the direct role of the quinoline group in enantiodiscrimination.

Although entirely consistent with the empirical data, the model based on the iminium species alone cannot be used to fully rationalize the excellent enantioselectivity observed in the epoxidation of enals **53**. Indeed, as shown experimentally, a significant contribution to enantiodiscrimination is provided by the counteranion (cf. Table 4.19 and 4.20). Its exact role is more difficult to rationalize, however, since analysis of the ground-state conformation of salts **80a-e** does not indicate any specific association of the counteranion with the iminium cation. Presumably, the organization of the counteranion first occurs in the transition state, i.e. with the attack of hydrogen peroxide. In fact, an association of the weakly acidic hydrogen peroxide and the basic counteranion is possible. Such an association would increase the effective steric bulk of hydrogen peroxide, making an attack from the shielded *re*-(β) face even more difficult and thus contributing to enantioselectivity (Figure 4.18, (a)). In the case of chiral counteranions such as that of (*R*)-TRIP, the association with hydrogen peroxide would effectively create a “chiral” nucleophile ($\text{H}_2\text{O}_2 \cdot \text{X}^-$) attacking a chiral electrophile (iminium [**80+H**]⁺), thus explaining the often dramatic match/mismatch observed with different enantiomers of the same chiral acid co-catalysis. The counteranion in this association would also be perfectly positioned to accept the proton from the developing oxonium ion in the transition state (Figure 4.18, (b)).

Alternative mechanistic scenarios cannot be excluded, however. An existence of an iminium conformer in which the intramolecular proton bridge is disrupted in the transition state and the quinuclidine moiety acts as a free base to direct the attack of hydrogen peroxide is possible and has been frequently suggested in the literature, albeit without mechanistic support.^[52, 80, 82, 136] This scenario would involve a conformational reorganization of the iminium species [**80+H**]⁺ in the transition state from a stable and highly populated conformer to a higher-energy species in which the imine moiety is fully protonated and the quinuclidine moiety exists as a free base (Figure 4.18, (c)). However, since multiple protonation of the amine catalyst **9** with up to 3 equiv of TFA does not affect the enantioselectivity or the rate of the reaction (cf. Section 4.1.2, Table 4.4), the involvement of quinuclidine as a free base seems unlikely. In addition, the (*E,E*)-*s-trans* geometry of the unsaturated iminium moiety does not allow a close approach of the quinuclidine nitrogen to the reactive carbon center C-16, suggesting that a direct coordination of hydrogen peroxide with the quinuclidine nitrogen in the transition state is implausible.

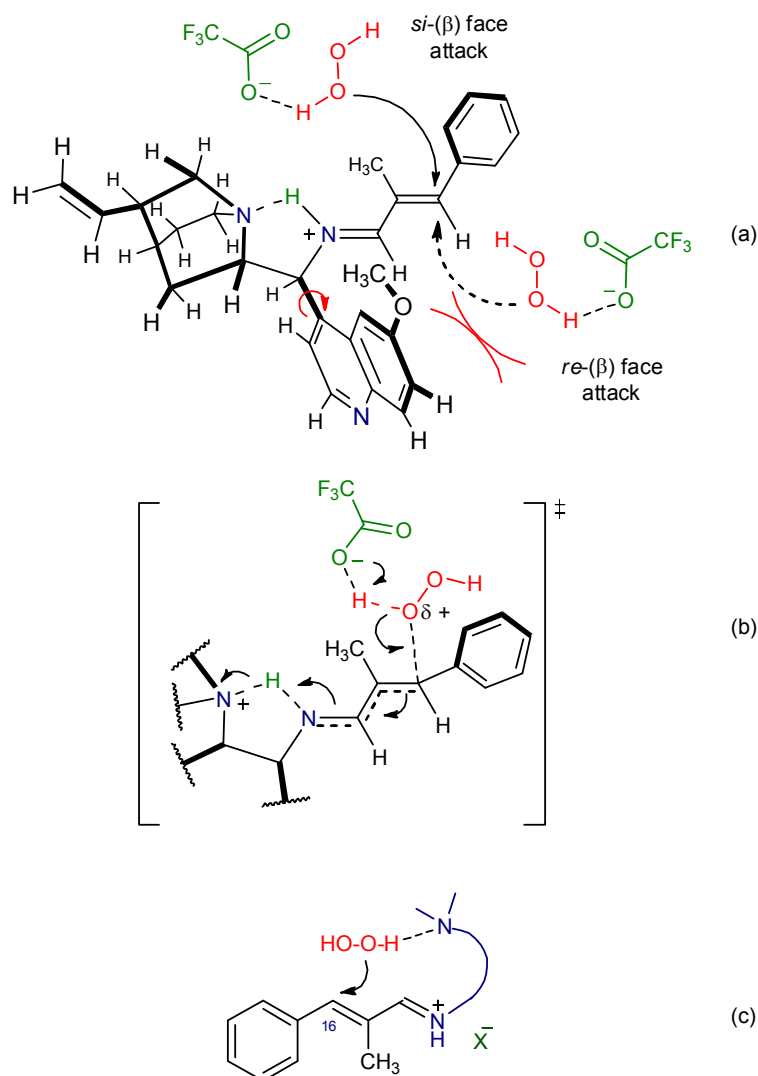
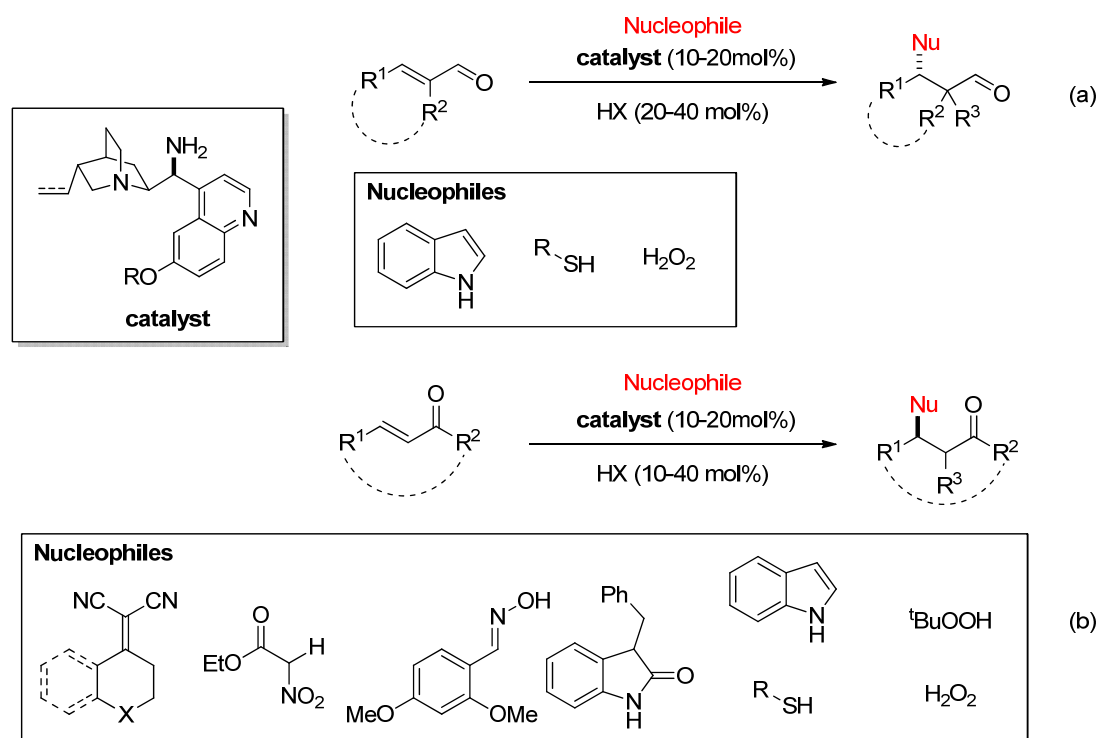


Figure 4.18 Proposed association of the counteranion with hydrogen peroxide, enhancing enantioselectivity (a), and acting as a proton acceptor in the putative transition state (b); an alternative mechanistic scenario in which the quinuclidine group directs the attack of hydrogen peroxide.

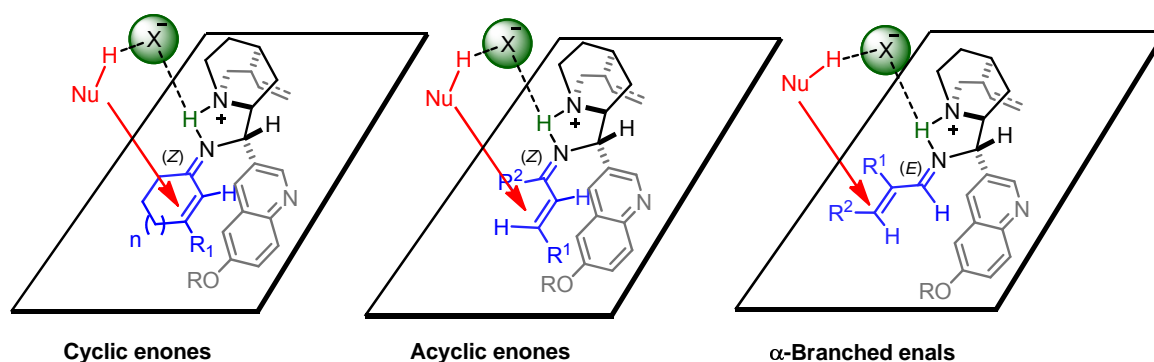
As previously mentioned, a survey of the literature revealed that the stereochemical outcome of *Michael* reactions between various nucleophiles and α -branched enals^[91, 150] and enones^[38-39, 41b, 41c] catalyzed by **9** and its closely related analogues is remarkably consistent (Scheme 4.18). Given the importance of the Brønsted acid co-catalyst in all of the reported reactions, and the fact that all of the nucleophiles must lose a proton in the transition state, a common mechanistic scenario responsible for the observed facial stereoselectivity is possible. The mechanism derived by our studies (Figure 4.18, (c)) could in principle be generalized to all reactions listed in Scheme 4.18 with one important consideration: the absolute stereochemistry is expected to

4. Results and Discussion

depend on the geometry of the iminium ion, which can presumably vary with the carbonyl substrate. Indeed, a simple mnemonic can be drawn for the iminium-catalyzed *Michael* additions of nucleophiles to α -branched enals and enones, which takes into consideration the most stable iminium configuration of each substrate^[52] together with the conformation of the cinchona-derived catalyst **9**, as derived from our studies (Scheme 4.19).



Scheme 4.18 Absolute facial selectivity observed in *Michael* reactions of various nucleophiles and α -branched enals^[91, 150] (a), and enones^[38-39, 41b, 41c] (b) catalyzed by **9** and its closely related analogues based on a literature survey. HX = Bronsted acid.



Scheme 4.19. A simplified mnemonic to explain the facial selectivity in the iminium-catalyzed *Michael* additions to α -branched enals and enones. HX = Bronsted acid co-catalyst.

4.2 Catalytic Asymmetric α -Benzoyloxylation of Carbonyl Compounds

The excellent reactivity and enantioselectivity of 9-amino(9-deoxy)*epi*quinine **9** in the epoxidation of sterically demanding substrates (cf. Section 4.1.6.1) prompted us to explore this catalyst in other oxidative transformations. As discussed in Section 2.3.2, α -oxidation of carbonyl compounds presented the ideal challenge. While α -aminoxylation with nitrosobenzene under secondary amine catalysis had established itself as a highly enantioselective procedure for aldehydes and ketones, it suffered from the major disadvantage of using a large excess of the carbonyl substrate, as well as being inapplicable to α -branched aldehydes and aromatic ketones (cf. Section 2.3.2). On the other hand, secondary amine-catalyzed methods using benzoyl peroxide as the oxidant, which are stoichiometric in the carbonyl compound, had not been extended to any substrate classes beyond unbranched aldehydes (cf. Section 2.3.2.1).^[151] We thus reasoned that catalytic asymmetric α -oxidation of sterically demanding substrates, which is stoichiometric in the carbonyl reagent, might be possible with the primary amine catalyst **9**.

The work described in this section was performed in collaboration with N. Demoulin.

4.2.1 α -Benzoyloxylation of Cyclic Ketones

4.2.1.1 Identification of a Model System

We began our investigations with ketone substrates and chose the commercially available cyclohexanone **83a** as the model substrate. In order to establish an oxidant compatible with a primary amine catalytic system, we first screened several common electrophilic oxygen sources with substrate **83a** and catalytic salt [**9**·TFA] at room temperature (Table 4.21). THF was used as a solvent based on our previous studies on epoxidation (Section 4.1), and radical inhibitor **85** (commonly used to stabilize ethereal solvents against radical chain reactions) was employed with benzoyl peroxide to avoid any possible side reactions of benzoyl radicals. Under the conditions tried, only benzoyl peroxide, which was used as the commercially available 30% hydrate, gave traces (4%) of the desired α -benzoyloxyated product **84a** (entry 5). The reaction with nitrosobenzene did not furnish any of the corresponding α -aminoxylated ketone, and only dimerized oxidant was observed in addition to the recovered starting material (entry 1). Di-*tert*-butyl peroxide (entry 2), cumene hydroperoxide **36** (entry 3) and *m*-CPBA (entry 4) similarly failed to provide any conversion after 15 hours, giving only recovered starting material. Repeating the reaction with benzoyl peroxide but in the presence of 30 mol% of the acid co-catalyst TFA failed to improve conversion (entry 6).

4. Results and Discussion

Table 4.21 Evaluation of common oxidants in the α -oxidation of **83a** with catalyst **9**.

83a $\xrightarrow[\text{THF (0.4 M), r.t., 15 h}]{\text{9} \cdot \text{TFA (10 mol\%)}, \text{oxidant (1.5 equiv)}}$ **84a**

BzOOBz (49)
CHP (36)
85

Entry	Oxidant	R	Yield,% ^a	Notes
1	PhN=O (45)	NH ₂ Ph	0	only dimerized PhNO + 83a
2	^t BuOO ^t Bu	^t Bu	0	83a only
3	CHP (36)	H	0	83a only
4	<i>m</i> -CPBA	H	0	83a only
5	BzOOBz (49) ^b	Bz	4	30% hydrate of 49 used
6	BzOOBz (49) ^{b,c}	Bz	4	30% hydrate of 49 used

^a Determined by ¹H NMR with an internal standard (Ph₃CH). ^b In the presence of 10 mol% radical inhibitor **85**. ^c Using 30 mol% TFA.

Since the amine catalyst **9** is known to activate ketones toward α -functionalization with various electrophiles (cf. Section 2.3.4), and since benzoyloxylation is known to be amenable to enamine catalysis,^[118-120] we wondered why the combination of these two principles resulted in only traces of the desired reaction (Table 4.21, entry 3). To address this question, we first examined if the catalyst **9** undergoes decomposition under the reaction conditions. After stirring the catalytic salt **9**·3TFA with excess of benzoyl peroxide (30% hydrate) at room temperature for 16 hours in deuterated THF, analysis of the crude mixture by ¹H NMR revealed no changes in the catalyst structure, ruling out catalyst decomposition (Figure 4.19).

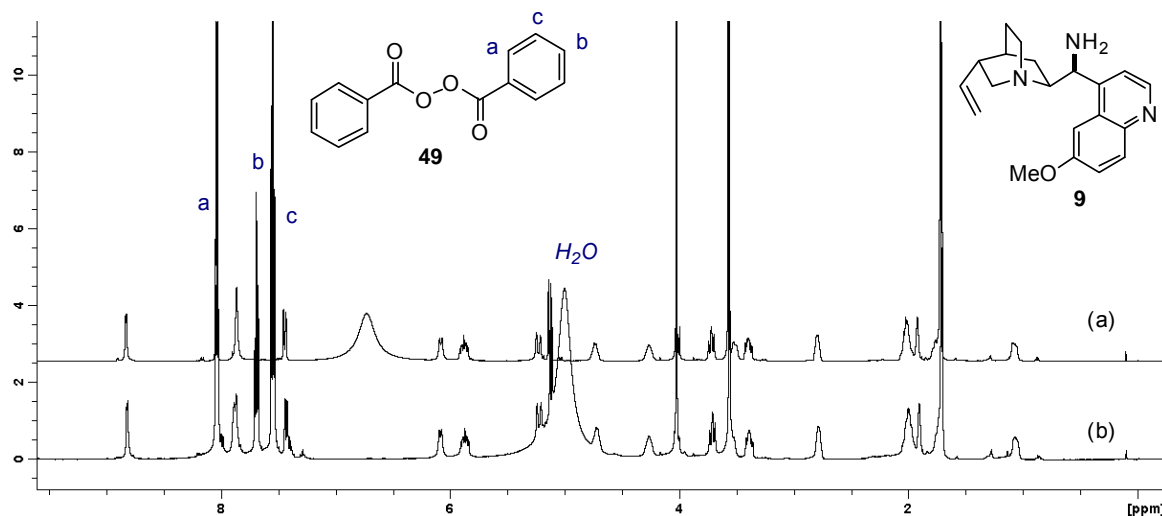
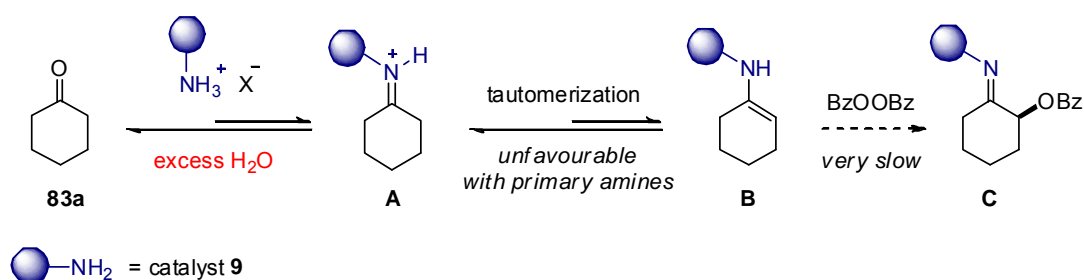


Figure 4.19 ¹H NMR spectrum of **9**·3TFA alone (a), and of **9**·3TFA after treatment with excess BzOOBz (**49**) for 16 h at r.t. (b) (in THF-*d*₈).

4. Results and Discussion

Having established that the catalytic salt **9**·3TFA is stable in the presence of benzoyl peroxide, we next considered the effect of water present in the reaction. Indeed, the commercially available 30% hydrate of benzoyl peroxide introduces a large excess of water into the reaction. Since the reversible formation of catalytically relevant enamine **B** proceeds *via* the iminium intermediate **A**, excess of water can hinder the overall reaction by shifting the first equilibrium toward the carbonyl substrate and lowering the effective concentration of **A** (Scheme 4.20). An unfavourable iminium-enamine equilibrium characteristic to primary amine catalysts (cf. Section 2.1.3.2) in the subsequent tautomerization might further suppress the formation of enamine **B**, resulting in a very slow catalytic cycle.



Scheme 4.20 The hypothesized effect of excess water on the α -benzoyloxylation of ketones with primary amine catalyst **9**.

In order to test this hypothesis, we prepared anhydrous benzoyl peroxide by a simple treatment with MgSO_4 , filtration and evaporation of the solvent (cf. Chapter 7 for experimental details). Table 4.22 shows the results of experiments in which water was excluded either with dried benzoyl peroxide **49** and/or with addition of 4Å molecular sieves.

Table 4.22 The effect of water exclusion on α -benzoyloxylation of **83a** with catalyst **9**.

Entry	Oxidant	Additive	Yield, % ^a	er ^b
1	49 (30% hydrate)	-	4	-
2	49 (anhydrous)	-	19	-
3	49 (anhydrous)	4Å MS	77	75:25

^a Determined by NMR with an internal standard (Ph_3CH). ^b Determined by chiral-phase HPLC.

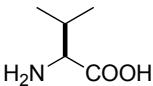
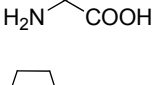
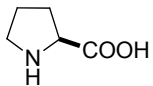
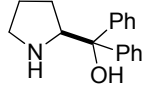
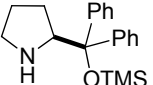
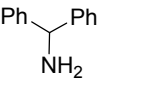
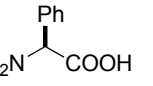
4. Results and Discussion

To our delight, excluding the excess of water by using anhydrous benzoyl peroxide (entry 2) resulted in an increase of yield from 4% to 19%. Using 4Å molecular sieves in combination with the dried reagent improved the yield even further, albeit the product **84a** was isolated with a modest enantioselectivity of 75:25 er (entry 3). The absolute (*S*) configuration of **84a** was established by comparing its optical rotation to the literature value.^[108]

The encouraging conversion obtained with the exclusion of water confirmed our expectations that asymmetric α -benzyloxylation of ketones was possible with primary amine catalysis employing the quinine derivative **9**. At this point, we wished to examine how other amine catalysts performed in the transformation, and screened various primary, as well as secondary amine scaffolds (Table 4.23). For reasons of solubility, DMSO was used as solvent with zwitterionic amino acid catalysts **1** and **86** instead of THF.

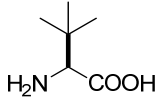
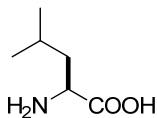
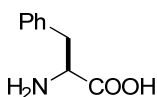
Table 4.23 Screen of amine catalysts in the α -benzyloxylation of **83a**.

Reaction scheme: **83a** (cyclohexanone) reacts with **BzOOBz** (anhyd., 1.5 equiv) in THF (0.4 M) at r.t. for 24 h, catalyzed by 10 mol% catalyst and 10 mol% BHT (**85**), to yield **84a** (α -benzyloxy cyclohexanone).

Entry	Amine catalyst	Acid co-catalyst ^a	Solvent	Conv., % ^b	er ^c
1	 86	none	DMSO	<5	-
2	 86	TCA	THF	<5	-
3	 1	none	DMSO	11 ^d	n.d.
4	 87	none	THF	0	-
5	 17	none	THF	0	-
6	 88	(<i>R</i>)-TRIP (3)	THF	29	57:43
7	 89	(PhO) ₂ PO ₂ H	THF	<5	-

^a 10 mol% loading. ^b Determined by ¹H NMR with an internal standard (Ph₃CH). ^c Determined by chiral-phase HPLC. ^d After 5 d.

4. Results and Discussion

Entry	Amine catalyst	Acid co-catalyst ^a	Solvent	Conv., % ^b	er ^c	
6		90	(PhO) ₂ PO ₂ H	THF	<5	-
7		91	(PhO) ₂ PO ₂ H	THF	<5	-
10		92	(PhO) ₂ PO ₂ H	THF	<5	-

^a 10 mol% loading. ^b Determined by ¹H NMR. ^c Determined by chiral-phase HPLC.

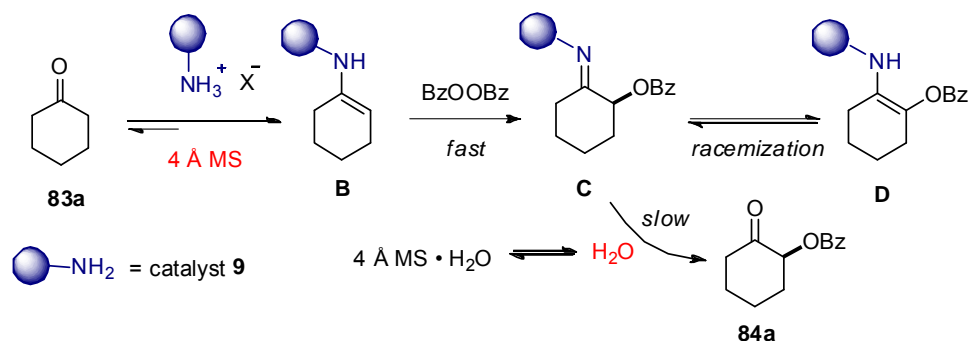
In general, none of the tested catalysts afforded the desired product **84a** with useful levels of conversion. As expected, secondary amine catalysts (entries 3-5) proved ineffective, presumably due to difficulties in condensing with a ketone substrate and concurrent decomposition by benzoyl peroxide.^[118, 121] Of these, only L-proline **1** (entry 3) gave some conversion (11%) after 24 hours, which was unchanged over the next 5 days, strongly suggesting catalyst deactivation. Amino acid-based primary amine catalysts **86** and **89-92** also furnished only traces of the desired product, when used as zwitterionic species in DMSO (entry 1) or as THF-soluble salts with inorganic acids (entries 2, 7-10). We also tested a combination of the achiral primary amine **88** together with the chiral Brønsted acid (*R*)-TRIP (entry 6). Intriguingly, while the conversion was low, some enantioselectivity (57:43 er) was observed, suggesting that the Brønsted acid was involved in the enantioselective step of the reaction. Presumably, the acid can activate benzoyl peroxide toward nucleophilic substitution by protonating the benzoate leaving group.

Having identified an unprecedented α -benzoyloxylation of ketones using anhydrous benzoyl peroxide and a catalytic salt of 9-amino(9-deoxy)*epi*quinine **9**, we set out to optimize the reaction parameters.

4.2.1.2 Optimization of the Reaction Parameters

Considering the high conversion and low enantioselectivity obtained when using molecular sieves (Table 4.22, entry 3), we wondered if the relatively labile product **84a** was undergoing racemization under the reaction conditions. In particular, we speculated that the (reversible) trapping of water by molecular sieves not only encouraged the formation of the catalytically active enamine intermediate **B**, thus speeding up the reaction, but also retarded hydrolysis of the intermediate **C** encouraging racemization *via* formation of enamine **D** (Scheme 4.21).

4. Results and Discussion



Scheme 4.21 The possible effect of water trapping by 4Å MS on the enantioselectivity of **84a**.

Another source of racemization could be the high loading (30 mol%) of the acid co-catalyst TFA. We thus varied several parameters of the reaction with the aim of identifying racemization-free conditions. Table 4.24 shows the results of changing the amount and identity of the Brønsted acid, and examining the effect of molecular sieves.

Table 4.24 Identifying racemization-free conditions in the α -benzoyloxylation of **83a**.

$\text{83a} \xrightarrow[\text{THF (0.4 M), r.t., 24 h}]{\text{9 (10 mol\% acid co-catalyst, BHT (85, 10 mol\%), BzOOBz (anhyd., 1.5 equiv)}} \text{84a}$

Entry	Acid co-catalyst	mol %	Additive	Yield,% ^a	er ^b
1	TFA	30	4Å MS	77	75:25
2	TFA	20	4Å MS	41	83:17
3	TFA	10	4Å MS	22	91:9
4 ^c	TFA	30	4Å MS	0	-
5	TCA	40	4Å MS	79	68:32
6	TCA	40	none	32	93.5:6.5
7	TCA	10	none	34	97:3

^a Determined by ¹H NMR with an internal standard (Ph₃CH). ^b Determined by chiral-phase HPLC. ^c Performed without amine **9**.

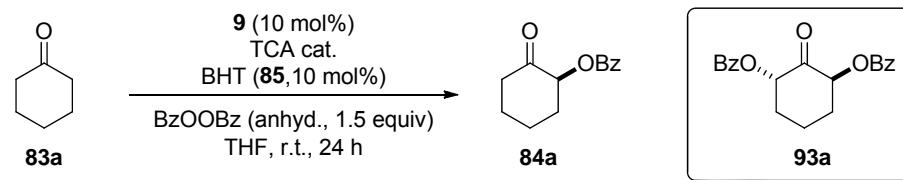
As seen from entries 1-3, and in accord with our expectations, lowering the amount of the acid co-catalyst TFA in the presence of molecular sieves resulted in improved enantioselectivity, albeit a diminished yield. At this point we also tested for a racemic background reaction which might be catalyzed by TFA and/or molecular sieves; however, no conversion was observed in the absence of the amine catalyst **9** (entry 4). Testing the less acidic co-catalyst TCA, we found

4. Results and Discussion

a similar yield compared to TFA in the presence of molecular sieves (cf. entry 1), but the product was obtained with poor enantioselectivity (entry 5). When we excluded the molecular sieves (entry 6), the yield of the product dropped but the enantioselectivity improved dramatically, supporting the hypothesis outlined in Scheme 4.22. Gratifyingly, combining lower catalyst loading (10 mol%) with the absence of molecular sieves resulted in an additive effect and the product was obtained with an excellent er of 97:3 (entry 7).

With the racemization-free conditions in hand, we set out to improve the conversion of the α -benzoyloxylation. A screen of different reaction concentrations in the presence of various amounts of the co-catalyst TCA was performed (Table 4.25).

Table 4.25 Evaluation of reaction concentration at different loadings of the acid-cocatalyst TFA in the α -benzoyloxylation of **83a**.



Entry	TCA, mol%	[THF], M	Yield, % ^a	er ^b
1	40	0.4	32	93.5:6.5
2	40	1	56	85:15
3	10	0.4	34	97:3
4	10	0.5	56	97:3
5	10	1	67	97:3
6 ^c	10	2	66 ^d	n.d
7	10	1	15	n.d
8	1	1	28	97:3
9	2	1	27	97:3

^a Determined by ¹H NMR with an internal standard (Ph₃CH).

^b Determined by chiral-phase HPLC. ^c BzOOBz (30 % hydrate) used.

^d 11% of bis-benzoylated product **93a** also observed.

At 40 mol% TCA loading, increasing the concentration from 0.4 M (entry 1) to 1 M (entry 2) improved the yield nearly twofold, but resulted in diminished enantioselectivity. Fortunately, at lower TCA loading (10 mol%), increasing the concentration improved the yield without affecting the enantioselectivity (entries 3-5), with the best result obtained at 1 M concentration (entry 5). Further increase in the concentration to 2 M (entry 6) led to an appreciable formation

4. Results and Discussion

(11%) of the bis-benzoyloxyated product **93a** together with the desired product which was formed in a similar 66% yield. Using hydrated benzoyl peroxide (30% hydrate) under the optimal concentration of 1 M still resulted in only 15% yield of the product **84a**, suggesting that the exclusion of excess water was crucial for the reaction rate (entry 6). Decreasing the loading of the acid co-catalyst TCA to 1 mol% (entry 8) and 2 mol% (entry 9) gave the product with the optimal enantioselectivity (97:3 er) but a compromised yield of only 27-28%.

With the optimal concentration and acid co-catalyst loading in hand, we next examined the reaction medium by testing a range of protic and aprotic solvents with different polarity (Table 4.26). Compared to the control reaction in THF (entry 1), toluene gave an improved conversion but a diminished enantioselectivity (entry 2). Chloroform proved to be inferior to THF (entry 3), while the use of methanol as solvent under weakly acidic reaction conditions resulted in complete acetalization of the starting material (ketal **94**) which shut down the benzoyloxylation reaction (entry 4). In acetonitrile, the product was obtained in a very low yield of 13% and a slightly reduced enantiomeric excess (entry 5). 1,4-Dioxane proved to be the optimal solvent, giving the product in 76% yield and an unchanged 97:3 er (entry 6).

Table 4.26 Screen of solvents in the α -benzoyloxylation of **83a**.

Entry	Solvent	Yield,% ^a	er ^b
1	THF	67	97:3
2	toluene	78	91:9
3	CHCl ₃	54	96:4
4	MeOH	0 ^c	-
5	MeCN	13	94:6
6	1,4-dioxane	76	97:3

^a Determined by ¹H NMR with an internal standard (Ph₃CH).

^b Determined by chiral-phase HPLC. ^c Complete conversion of SM to **94**

Since the different acid co-catalysts which were briefly screened up to this point (Tables 4.23, 4.24) were found to exert an observable effect on the reaction, we next systematically examined achiral Brønsted acids covering a range of pK_a values (Table 4.27).

4. Results and Discussion

Table 4.27 Screen of Brønsted acid co-catalysts in the α -benzyloxylation of **83a**.

83a $\xrightarrow[\text{1,4-dioxane (1 M), r.t., 24 h}]{\text{9 (10 mol\%), acid (10 mol\%), BHT (85, 10 mol\%), BzOOBz (anhyd., 1.5 equiv)}}$ **84a**

Entry	Acid co-catalyst	Yield, % ^a	er ^b
1	TCA	76	97:3
2	CCl ₂ HCO ₂ H	59	87:13
3	TFA	66	87:13
4	MeCO ₂ H	11	n.d.
5	pTSA	<5	-
6	(PhO) ₂ PO ₂ H	83	96:4
7 ^c	(PhO) ₂ PO ₂ H	56	96:4
8	56	28	96:4

9

56

^a Determined by ¹H NMR with an internal standard (Ph₃CH).

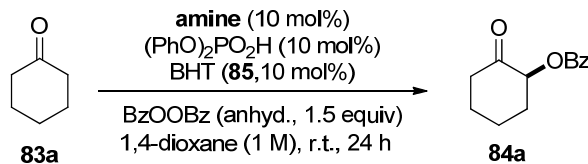
^b Determined by chiral-phase HPLC. ^c 20 mol% of acid used.

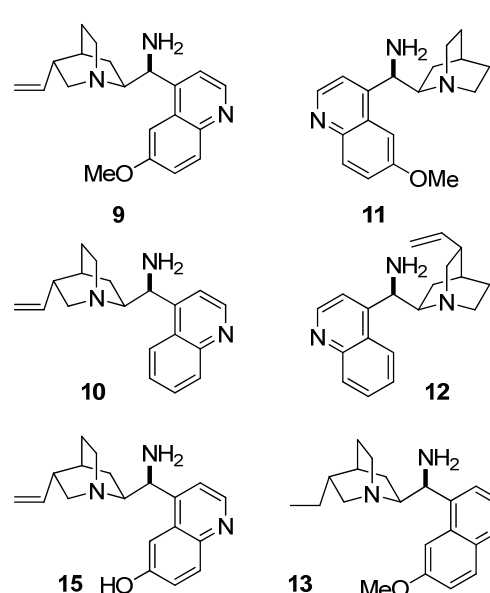
Compared to the control (TCA, entry 1), all other acetic acids proved to be inferior. Both weaker dichloroacetic acid (entry 2) and acetic acid (entry 4), and stronger acid TFA (entry 3) gave lower conversion and enantioselectivity. Very strong acid pTSA (entry 5) afforded only traces of the desired product. Phosphoric acid diphenyl ester (DPP), however, gave an improved conversion albeit a slightly lower enantioselectivity (entry 6). Increasing the catalyst loading of this acid to 20 mol% resulted in diminished conversion (entry 7). Applying the more acidic phosphoric acid **56** also resulted in a significantly decreased yield (entry 8).

Using 10 mol% DPP, we examined the related cinchona scaffolds as primary amine catalysts (Table 4.28). Within the same enantiomeric series (entries 1-4), the best catalyst remained to be **9**, affording the desired α -benzyloxylation product with the highest yield and enantioselectivity. As expected, the pseudoenantiomeric catalysts **11** and **12** gave the opposite (*R*)-configured product *ent*-**84a**, albeit with reduced enantioselectivity. Interestingly, the cinchonine derivative **12** gave the highest yield of the desired product among all the screened catalysts (entry 6).

4. Results and Discussion

Table 4.28 Evaluation of different cinchona derived primary amine catalysts in the α -benzoyloxylation of **83a**.

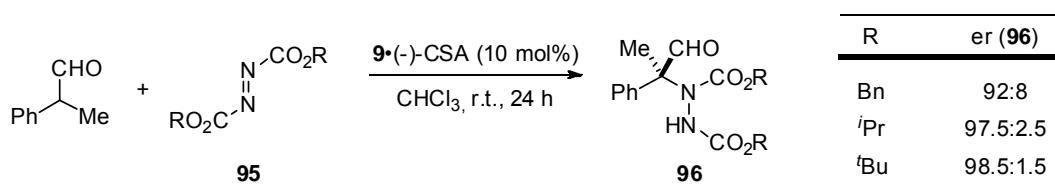




Entry	Amine	Yield, % ^a	er ^b
1	9	83	96:4
2	10	48	93:7
3	15	65	90:10
4	13	49	94:6
5	11	51	8:92
6	12	88	12:88

^a Determined by ¹H NMR with an internal standard (Ph₃CH).
^b Determined by chiral-phase HPLC.

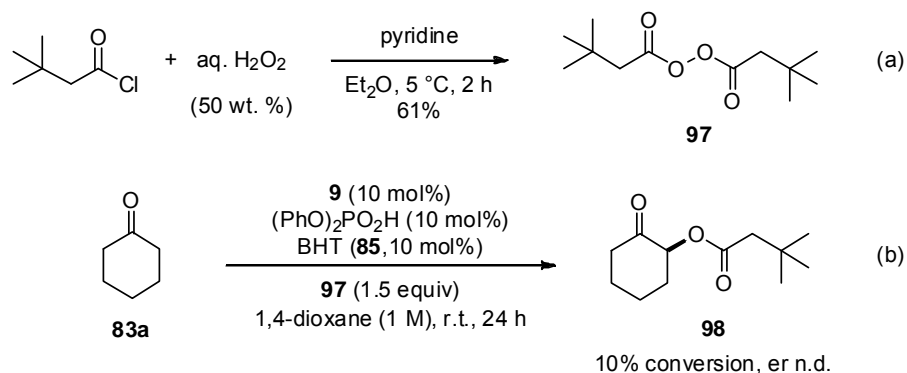
We next turned our attention to the structure of the electrophilic peroxide reagent. In particular, we considered conceptually related organocatalytic α -amination reactions with azocarboxylate reagents **95**, in which the enantioselectivity of the reaction is generally directly proportional to the steric bulk of the aminating reagent. Scheme 4.22 shows such an example from the recent report of *Lu* and colleagues.^[35b]



Scheme 4.22 The dependence of enantioselectivity in organocatalytic α -amination reactions on the bulk of the azocarboxylate reagent.^[35b]

To emulate this effect, we prepared the more sterically demanding neopentenoyl peroxide **97** from the corresponding acyl chloride and hydrogen peroxide,^[152] and tested it in the benzoyloxylation of cyclohexanone **83** (Scheme 4.23). Unfortunately, the desired product **98** was formed with only 10% conversion, presumably due to the lower reactivity of aliphatic acyl peroxides, which generate a less stabilized acetate as the leaving group compared to benzoyl peroxide. Synthesis of bulkier aromatic acyl peroxides which require multiple steps was not attempted for reasons of practicability.

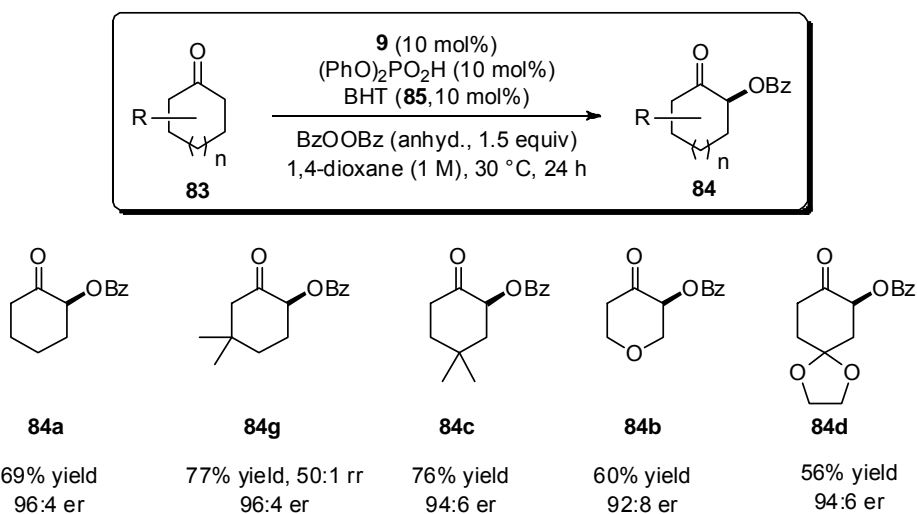
4. Results and Discussion



Scheme 4.23 Synthesis of neopentenoyl peroxide **97** (a), and its application in the benzoyloxylation of **83a** (b).

Finally, we briefly tested the reaction temperature and found that the slightly elevated temperature of 30 °C gave the most reproducible results. Higher temperature (40 °C) resulted in diminished and poorly reproducible enantioselectivity, possible due to a slow thermal decomposition of benzoyl peroxide.

With the optimal conditions in hand, we screened several commercially available cyclic ketones in the α -benzoyloxylation reaction. Disappointingly, we found generally unsatisfactory enantioselectivities, compared to the model substrate (Scheme 4.24).



Scheme 4.24 Preliminary scope of catalytic asymmetric α -benzoyloxylation of cyclic ketones (rr = regioisomeric ratio).

Using the substrate **83b** which afforded the product with the lowest enantioselectivity (92:8 er), we sought to re-optimize the reaction conditions. Toward this end, we evaluated the catalyst loading of the acid (PhO)₂PO₂H, and also screened other Brønsted acids, including chiral acid

4. Results and Discussion

TRIP and Mosher's acid **100**, in hopes of achieving a cooperative effect with the chiral amine catalyst **9** (Table 4.29).

Table 4.29 Re-evaluation of Brønsted acid co-catalysts in the α -benzyloxylation of **83b**.

83b $\xrightarrow[\text{BzOOBz (anhyd., 1.5 equiv), 1,4-dioxane (1 M), r.t., 24 h}]{\text{9 (10 mol%), acid cat., BHT (85, 10 mol%)}}$ **84b**

Entry	Acid co-catalyst	mol%	Yield, % ^b	er ^c
1	(PhO) ₂ PO ₂ H	5	31	95:5
2	(PhO) ₂ PO ₂ H	10	74	95:5
3	(PhO) ₂ PO ₂ H	20	37	95:5
4	(PhO) ₂ PO ₂ H	30	10	n.d.
5	56	10	40	94:6
6	99	10	76	94.5:5.5
7	(<i>R</i>)-TRIP	10	61	91:9
8	(<i>S</i>)-TRIP	10	85	93:7
9	100	10	46	94:6

56

99

100

^a Determined by ¹H NMR with an internal standard (Ph₃CH).
^b Determined by chiral-phase HPLC.

However, varying the loading of phosphoric acid diphenyl ester (entries 1-4) confirmed that the original 10 mol% loading was optimal, as both lower and higher loading resulted in diminished yield, although unchanged enantioselectivity. Achiral phosphoric acids **56** and **99** gave a similar enantioselectivity but failed to improve the yield. Unfortunately, neither enantiomer of the chiral phosphoric acid TRIP (entries 7-8) resulted in improved enantioselectivity, although (*S*)-TRIP appeared to be the more “matched” enantiomer, giving complete conversion and a high NMR yield of 85%. Mosher's acid **100** proved to be only moderately active and also failed to improve the enantioselectivity (entry 9).

Nevertheless, comparing the results of this optimization with those of the preliminary scope under the same reaction condition (Table 4.29, entry 2 vs. Scheme 4.24), we became cognizant of a disparity in the enantiomeric excess of the product **84b** (95:5 er during optimization vs. 92:8 er after isolation of the pure product). Given the identical reaction conditions, we realized that this difference in the enantiomeric excess must be attributable to product purification. In particular, preparative thin-layer chromatography was used to isolate the products for the

4. Results and Discussion

optimization study and flash column chromatography was employed in the study of the reaction scope. Consulting the literature, we found that products **84** are indeed known to be labile under the conditions of silica gel chromatography and typically require a rapid plug to preserve their enantiomeric excess.^[153] At this point, we decided to keep the optimal reaction conditions and focus on optimizing the purification of the product by flash column chromatography. Unfortunately, attempts at purifying the product with deactivated silica gel,^x preparative TLC-grade silica gel^{xi} and alumina failed to improve the enantiomeric excess of the pure isolated products. However, faster column chromatography (under 30 min elution time) was found to be more reproducible and afford the product with a better enantiomeric excess.

Re-screen of other substrates **83** revealed that the enantiomeric excess could also be improved by using the originally identified acid TCA as the co-catalyst. We thus decided to use either TCA or DPP as the co-catalyst under the optimized conditions, depending on the substrate.

4.2.1.3 Reaction Scope and Discussion

A range of cyclic ketones was tested in the α -benzoyloxylation reaction (Table 4.30). All of the substrates were obtained from commercial sources except for 4-isopropylidencyclohexanone **83e** which was prepared following a literature method.^[154] Various six-, seven-, and eight-membered carbocyclic and heterocyclic ketones cleanly underwent α -benzoyloxylation, affording the desired products **84** with good yields and excellent enantioselectivities. Using the pseudoenantiomeric catalyst **12**, the opposite enantiomer of the product **84a** could be obtained in a good yield, though with lower enantioselectivity (entry 2). However, using DPP as the acid co-catalyst and the pseudoenantiomeric cinchonine-derived amine **12**, both enantiomers of product **84b** could be generated with equal efficiency (entries 3 and 4). A range of functional groups were tolerated in the reaction, including an acetal, an olefin and a carbamate (entries 6-8). The β,β -disubstituted substrate **83g** afforded the product **84g** as a single regioisomer, with benzoyloxylation taking place at the less substituted side (entry 9). The enantiopure substrate **83h** (entry 10) was found to undergo a highly regioselective and *trans*-diastereoselective α -benzoyloxylation with the pseudoenantiomeric quinidine-derived amine **11**, which was identified as the optimal catalyst after a brief screen of several cinchona-derived amines. Highly *cis*-selective benzoyloxylation was also possible for this substrate under standard conditions with catalyst **9**, albeit with reduced regioselectivity (entry 11). In all cases, less than 5% of the

^x Deactivation of standard silica gel (Merck, 60, particle size 0.040-0.063 mm) was performed with concentrated ammonia (10 wt. %).

^{xi} Scratched from preparative TLC plates (Macherey-Nagel, SIL G-25 UV₂₅₄), pulverized and packed in a column.

4. Results and Discussion

bis-benzoyloxyated ketone was observed as the only by-product except for larger ring-sized cycloheptanone and cyclooctanone (entries 12 and 13), where oxygenation was a competitive process that could be effectively suppressed by using two equivalents of the starting material.

Table 4.30 Substrate scope of the catalytic asymmetric α -benzoyloxylation of cyclic ketones **83**.

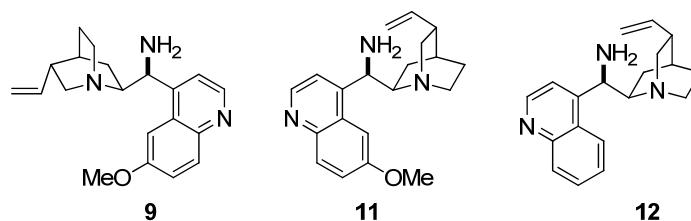
Entry ^a	Substrate	Product ^b	Yield, % ^c	er ^d
1	83a	84a	67 61 ^f	97:3 (>99:1) ^e 96.5:3.5 ^f
2 ^h	83a	<i>ent</i> - 84a	73	89:11
3 ^g	83b	84b	66	95:5
4 ^{g,h}	83b	<i>ent</i> - 84b	63	95:5
5	83c	84c	78	94.5:5.5
6	83d	84d	52 (89 brsm)	95.5:4.5
7	83e	84e	63	94:6
8	83f	84f	45	92:8

^a Reactions performed on 0.4 mmol scale. ^b The absolute configuration of **84** was assigned by comparison of the optical rotation with the literature values or by analogy (see Chapter 7 for details). ^c Isolated yield. ^d Determined by chiral-phase HPLC. ^e After a single recrystallization. ^f Using 2-methyltetrahydrofuran as solvent. ^g Using (PhO)₂PO₂H as the acid co-catalyst. ^h Using catalyst **12**.

4. Results and Discussion

Entry ^a	Substrate	Product	Yield,% ^b	er ^c
9	83g		84g 77 (> 20:1 rr) ^j	96:4
10 ^j	83h		84h 60 (18:1 dr) (12:1 rr) ^j	>99:1 ^k
11	83h		84i 57 (18.5:1 dr) (2:1 rr) ^j	>99:1 ^k
12 ^{g,l}	83j		84j 74	98:2
13 ^{g,l}	83k		84k 81 ^m	98:2

^a Reactions performed on 0.4 mmol scale. ^b The absolute configuration of **84** was assigned by comparison of the optical rotation with the literature values or by analogy (see Chapter 7 for details). ^c Isolated yield. ^d Determined by chiral-phase HPLC. ^g Using (PhO)₂PO₂H as the acid co-catalyst. ⁱ rr = regiomer ratio. ^j Using catalyst **11**. ^k Enantiomerically pure starting material **83h** was used. ^l Contains 11% of the dibenzoyloxylated product.



We also examined the compatibility of our reaction with the environmentally benign and industrially valuable solvent 2-methyltetrahydrofuran. Gratifyingly, the reaction with the model ketone **83a** afforded the product with a similar yield and enantioselectivity (entry 1).

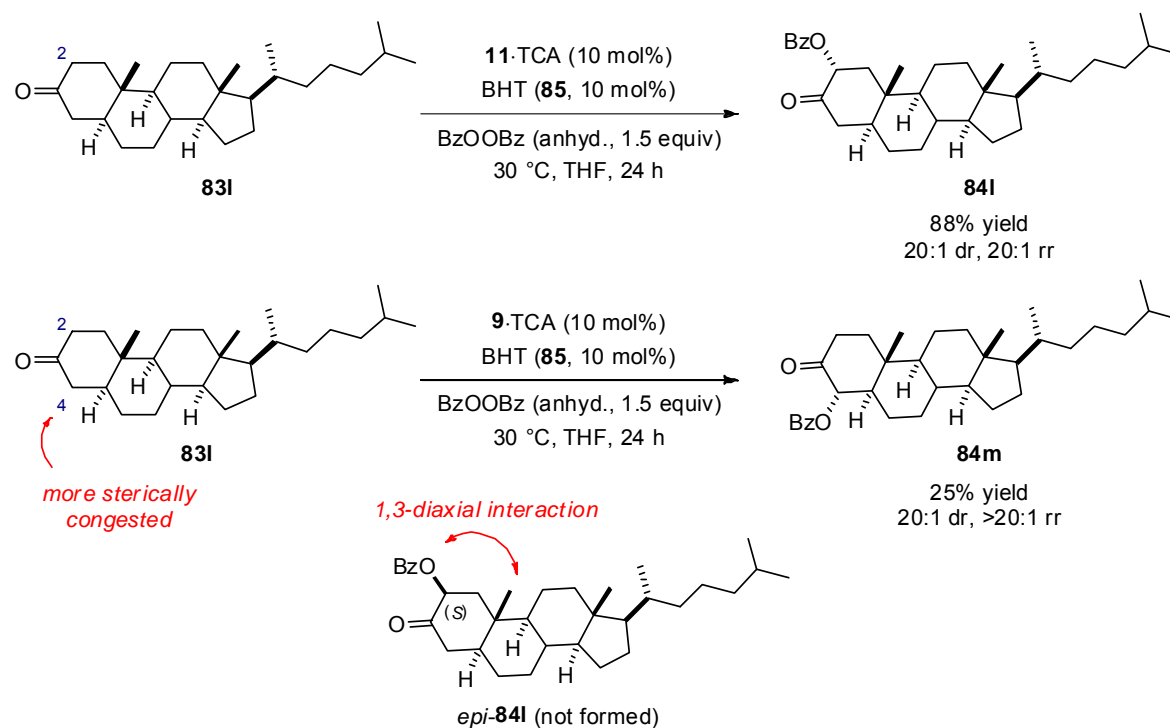
To probe the utility of our method in preparative synthesis, we also performed the reaction with ketone **83a** on a fivefold scale (2 mmol, 0.4 g) and were pleased to obtain the corresponding product **83a** with a good yield (76%) and essentially uncompromized enantioselectivity (95.5:4.5 er), which could be readily improved to 99.5:0.5 er by a single recrystallization.^{xii} Furthermore, we tested a substrate with a complex pre-existing architecture, where use of stoichiometric amounts of the ketone is particularly valuable. From cholestanone (**831**), we could successfully obtain the corresponding 2 α -benzoyloxylated product **831** with excellent regio- and diastereocontrol and a high yield of 88% using catalyst **11** (Scheme 4.25).

^{xii} See Chapter 7 for experimental details.

4. Results and Discussion

Notably, the corresponding 2 α -hydroxycholestanone has been synthesized using nitrosobenzene and 0.5 equiv of L-proline followed by *in situ* deprotection, which afforded the corresponding product in 63% yield.^[155]

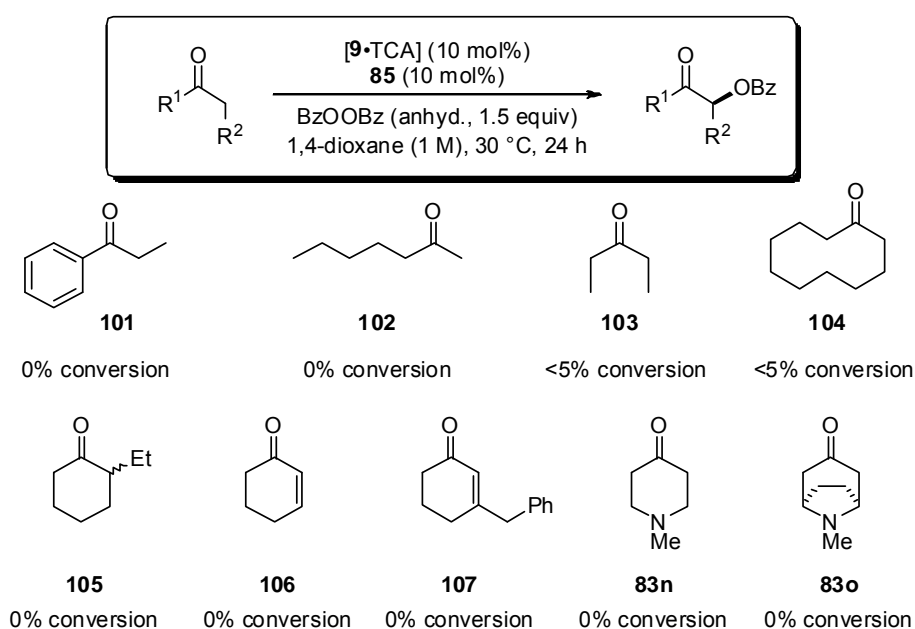
The highly sterically biased substrate **83i** also allowed us to test the extent of catalyst control in the benzoyloxylaton reaction. Applying the pseudoenantiomeric catalyst **9**, we obtained the C-4 regioisomer **83m** in a modest yield of 25% instead of the expected C-2 diastereomer *epi*-**84i**. Although the C-4 position of the starting material is more sterically hindered, this outcome is not surprising, since installing an (*S*)-configured benzoyloxy group at C-2 would create a highly unfavourable 1,3-diaxial strain (Scheme 4.23). Benzoyloxylation at C-4, on the other hand allows the catalyst to exercise its inherent sense of stereoselectivity while placing the benzoyloxy group in an equatorial position. The steric congestion of C-4 due to a neighbouring β -substituent, however, makes this process sluggish, explaining the low yield obtained for **83m**. Complete regioselectivity at the less substituted site observed for the β,β -disubstituted substrate **83g** (Table 4.30, entry 9) underscores the sensitivity of the catalyst to steric bulk near the reactive α -carbon. Overall, these results indicate that while substrate control was dominant in the *regioselectivity* of the reaction, the catalyst exercised excellent control of the *absolute stereochemical outcome*, as evidenced by high diastereoselectivities and the complete absence of the regioisomeric product **84i** with catalyst **9**.



Scheme 4.25 α -Benzoyloxylation of cholestanone **83i** using primary amine catalysts **11** and **9**.

4. Results and Discussion

Unfortunately, acyclic and medium or large ring-sized ($n > 8$) ketones proved to be a limitation of the method, as they underwent benzoyloxylation with none to very poor conversion (Scheme 4.26). This lack of reactivity presumably stems from the low nucleophilicity of the primary-amine derived enamine intermediates, which is further reduced by the lack of ring strain. α -Substituted cyclohexanone **105** and the aromatic ketone **101** were similarly unreactive even in the presence of molecular sieves (cf. Section 4.2.1.1), presumably due to steric hindrance around the ketone moiety. Highly basic amines **83n** and **83o** were also found to be incompatible with the reaction and gave no product. For reasons which are difficult to explain, cyclic enones **106** and **107** were found to be unreactive.



Scheme 4.26 Limitations in the α -benzoyloxylation of ketone using primary amine catalyst **9**.

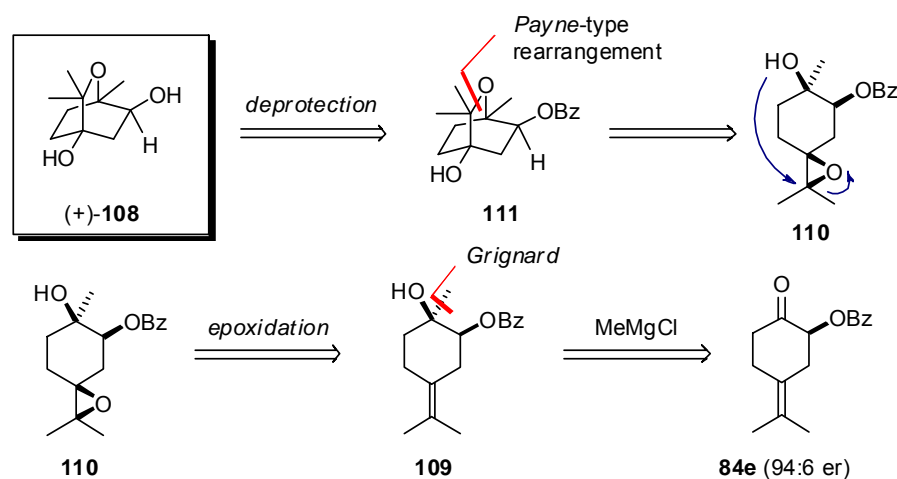
4.2.1.4 Asymmetric Total Synthesis of Cineole Monoterpenoids

To further demonstrate the utility of the novel α -benzoyloxylation methodology, we applied it in a concise asymmetric total synthesis of the monoterpene (+)-2 β ,4-dihydroxy-1,8-cineole (**108**), a predicted metabolite of the bio-oxidation of 1,8-cineole in mammals.^[156] Only the synthesis of *rac*-**108** had been reported previously by epimerization of synthetic racemic *epi*-**108** via a non-diastereoselective oxidation-reduction sequence.^[156] Cineoles and their oxidized derivatives are found in many plant and animal species, and have numerous applications as herbicides, medications and perfumes.^[157] Efficient and stereoselective approaches for creating libraries of

4. Results and Discussion

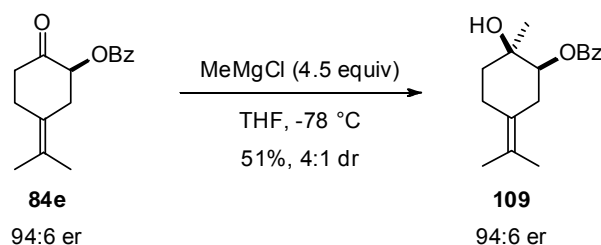
cineole derivatives thus represent an important pursuit not only for biosynthetic studies, but also for discovery of new potent bioactive compounds.

Our retrosynthetic strategy for (+)-**108** consisted of a *Payne*-type rearrangement of the epoxide **110** to construct the requisite bicyclic ether core **111** (Scheme 4.27). The epoxide **110** could be derived from the monoprotected diol **109**, which itself would come from a *Grignard* methylation of the already synthesized α -benzoyloxylated ketone **84e** (cf. Table 4.30, entry 7).



Scheme 4.27 Retrosynthetic analysis of (+)-2 β ,4-dihydroxy-1,8-cineole ((+)-**108**).

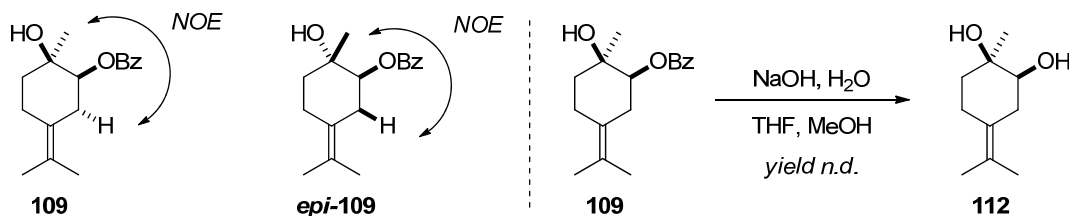
The forward synthesis of (+)-**108** began with the diastereoselective *Grignard* reaction of **84e** using methylmagnesium chloride, which afforded the desired monoprotected *cis*-diol **109** with an acceptable dr of 4:1 and 51% yield (Scheme 4.28). The low yield was attributable to partial deprotection of the benzoyl group by the excess of the *Grignard* reagent. Using only a slight excess of MeMgCl resulted in a very sluggish reactivity of at -78 °C; warming up the reaction to 0 °C resulted in competitive deprotection of the benzoyl group. A brief screen of various organometallic reagents, including MeMgBr, MeLi and MeMgBr with catalytic zinc (II) chloride failed to improve the yield and diastereoselectivity. Gratifyingly, no racemization of **84e** was observed during the reaction, and the desired monoprotected diol **109** was obtained with an unchanged er of 94:6, which was confirmed by chiral-phase HPLC analysis.



Scheme 4.28 *Grignard* reaction of **84e** to afford the monoprotected diol **109**.

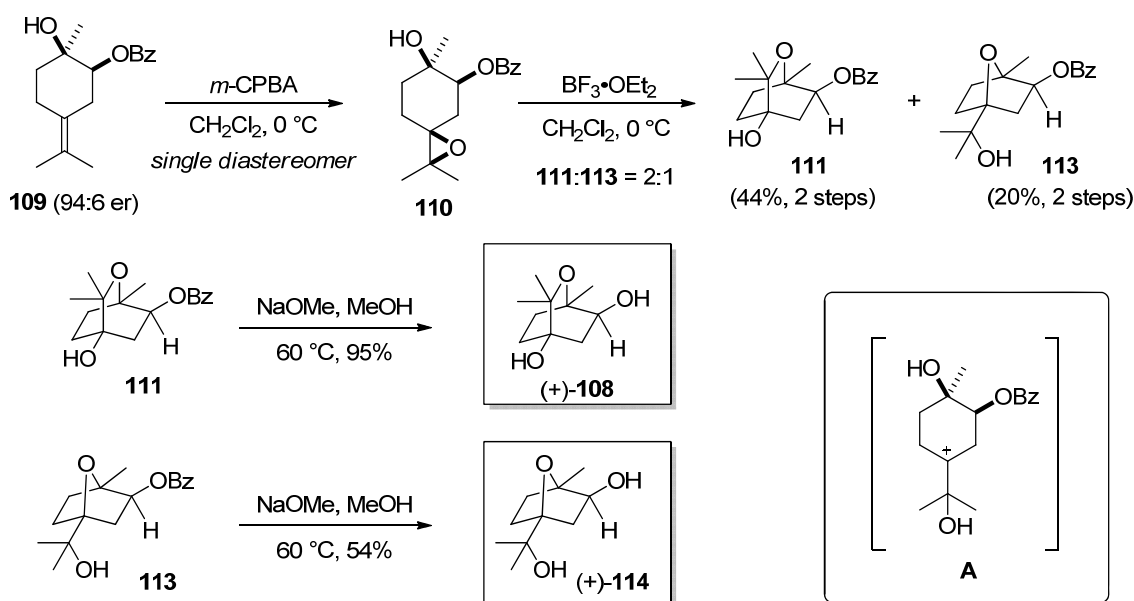
4. Results and Discussion

The relative configuration of **109** and its diastereomer *epi-109* was verified by *NOESY* correlation. In addition, **109** was derivatized to the literature-known diol **112**^[158] by basic hydrolysis, which confirmed the *cis*-configuration of the two hydroxy groups (Scheme 4.29).



Scheme 4.29 Determination of the relative stereochemistry of **109** and *epi-109* by *NOESY* correlation and derivatization to **112**.^[158]

Treatment of **109** with *m*-CPBA at 0 °C cleanly generated epoxide **110** as a single diastereomer, whose relative configuration was tentatively assigned as shown, based on the ability of oxygenated moieties to direct the approach of *m*-CPBA^[159] (Scheme 4.30). Submitting crude **110** to a Lewis acid-catalyzed *Payne*-type rearrangement afforded the desired 1,8-bicyclic ether **111** (6-*endo*-cyclization) together with the readily separable 1,4-cineole derivative **113** (5-*exo*-cyclization) in 2:1 ratio and a combined yield of 64% over 2 steps. Given the possibility of cationic intermediate **A** under Lewis acid catalysis (Scheme 4.30), we could not confirm the relative configuration of epoxide **110** from the configurational outcome in **111** and **113**. Deprotection of **111** by methanolysis cleanly afforded (+)-**108**. The related 2 β ,4-dihydroxy-1,4-cineole (+)-**114**^[156] could be similarly obtained by the deprotection of **113**.

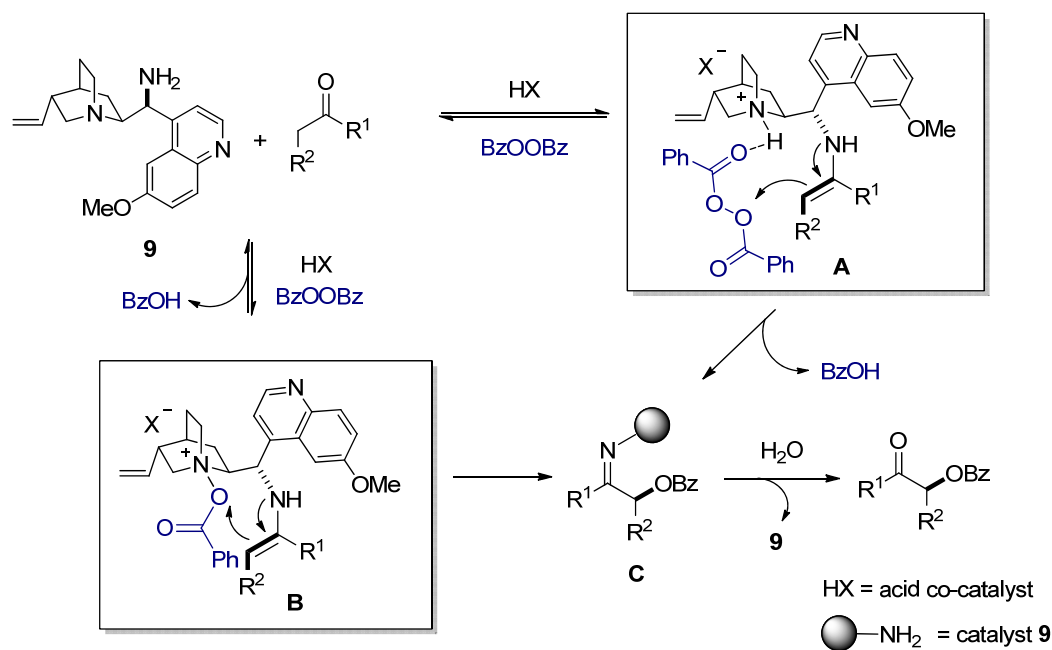


Scheme 4.30 Completion of the synthesis of (+)-**108** and a related monoterpene (+)-**114**.

4. Results and Discussion

4.2.1.5 Mechanistic Considerations

Mechanistically, we believe that the developed α -benzoyloxylaton of ketones catalyzed by the primary amine **9** proceeds *via* enamine activation of the carbonyl substrate toward an intermolecular attack on benzoyl peroxide. Furthermore, in the presence of an acid co-catalyst, the quinuclidine moiety of the catalyst is expected to be protonated. This internal Brønsted acidic sight might coordinate the basic carbonyl group of benzoyl peroxide, bringing it close to the nucleophile and simultaneously activating it toward fragmentation (Scheme 4.31, structure **A**). An alternative, *intramolecular* mechanistic scenario cannot be excluded, however. Given the high reactivity of the quinuclidine nitrogen in **9**, *N*-benzoyloxylation^[160] of the catalyst and/or the enamine intermediate shown in assembly **A** can be envisioned, giving species **B** which could rearrange to afford the common intermediate **C** (Scheme 4.31). Although nucleophiles normally attack *N*-benzoyloxylated amines at the carbonyl carbon to give stable *N*-oxides, the intramolecular nature of this putative process may change the inherent reactivity. The fact that *N*-fluorinated cinchona alkaloids are known to effect α -fluorination of silyl enol ethers and ketoesters^[48] further adds to the plausibility of an intermediate of type **B**.



Scheme 4.31 Possible mechanistic scenarios in α -benzoyloxylaton of ketones catalyzed by **9**.

In order to clarify the mechanism, we decided to investigate the fate of the catalyst **9** under the reaction conditions using NMR spectroscopy. At the outset of these investigations (cf. Section 4.2.1.1), we performed ^1H NMR studies on the triply protonated catalyst **9**·3TFA which was

4. Results and Discussion

treated with benzoyl peroxide for 16 hours at room temperature, and found no changes in the structure of the catalyst. Repeating this study with the monoprotonated catalyst **9**·TCA at 30 °C to simulate the *optimized* reaction conditions afforded different results, however. Figure 4.20 shows that stirring **9**·TCA with 1.5 equiv of benzoyl peroxide for 24 hours resulted in complete conversion of **9** to a new product (**115**). An aqueous workup to remove the acid components allowed us to isolate this derivative in a spectroscopically pure form in 92% isolated yield.

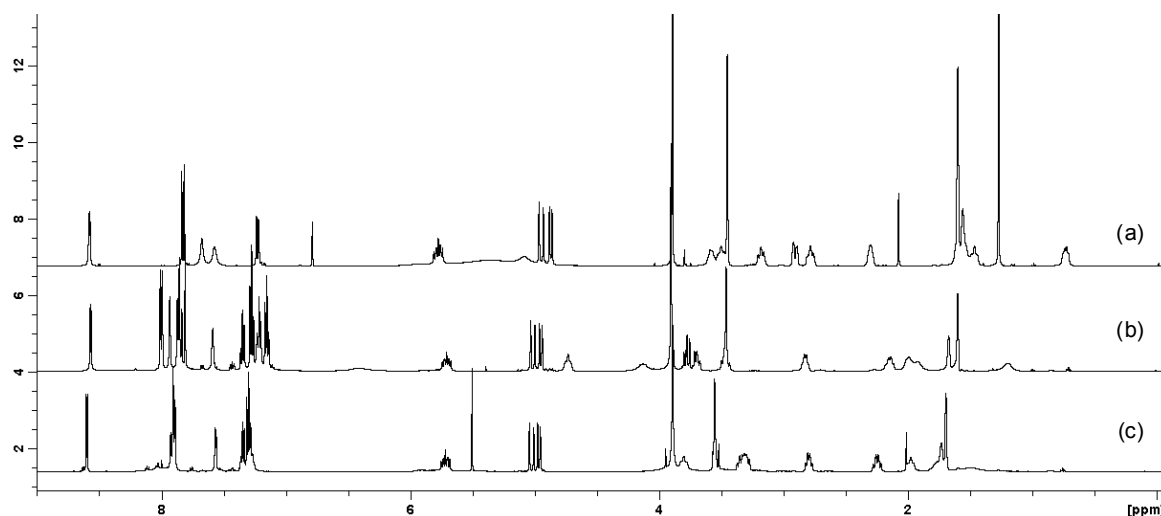


Figure 4.20 ¹H NMR spectrum of the catalyst salt **9**·TCA (a), the crude spectrum of a new compound (**115**) formed from the treatment of **9**·TCA with 1.5 equiv benzoyl peroxide for 24 h at 30 °C (b), compound **115** purified by an aqueous workup to remove acidic components.

Mass analysis of **115** indicated the incorporation of a benzoyloxy (PhCOO) group and NMR analysis showed significant deshielding of the quinuclidine nitrogen as well as the surrounding carbon and proton atoms, consistent with *N*-oxidation. A ¹⁵N-¹H HMBC spectrum further revealed an appearance of a second new nitrogen chemical shift. Particularly revealing was also IR analysis, which suggested that neither *N*-benzoyloxy ammonium^[160b] nor *N*-benzoyl ammonium^[161] stretching frequencies were present (both around 1770 cm⁻¹), but instead revealed two strong bands at 1650 and 1620 cm⁻¹. At room temperature, compound **115** displayed several broadened peaks in the ¹H and ¹³C NMR spectra, which could be sharpened at -20 °C. At this low temperature, all peaks also split into pairs in a 2.5:1 ratio, suggesting the existence of conformers which slowly interconvert at room temperature. Importantly, setting up **115** as a catalyst (10 mol%) or as a stoichiometric reagent in the absence of benzoyl peroxide (1.5 equiv) under optimized conditions with substrate **83a** gave no conversion.

In order to gain more insight into this transformation, we also followed the reaction of **9**·TCA with benzoyl peroxide over time (Figure 4.21). This study revealed that conversion of **9** to the

4. Results and Discussion

new derivative **115** proceeded through a single detectable intermediate **116**. This intermediate appeared to be present at a constant concentration until the full consumption of the starting material **9** between 6 and 9 hours, after which the intermediate was completely converted to **115** ($t = 22 \text{ h } 5 \text{ min}$).

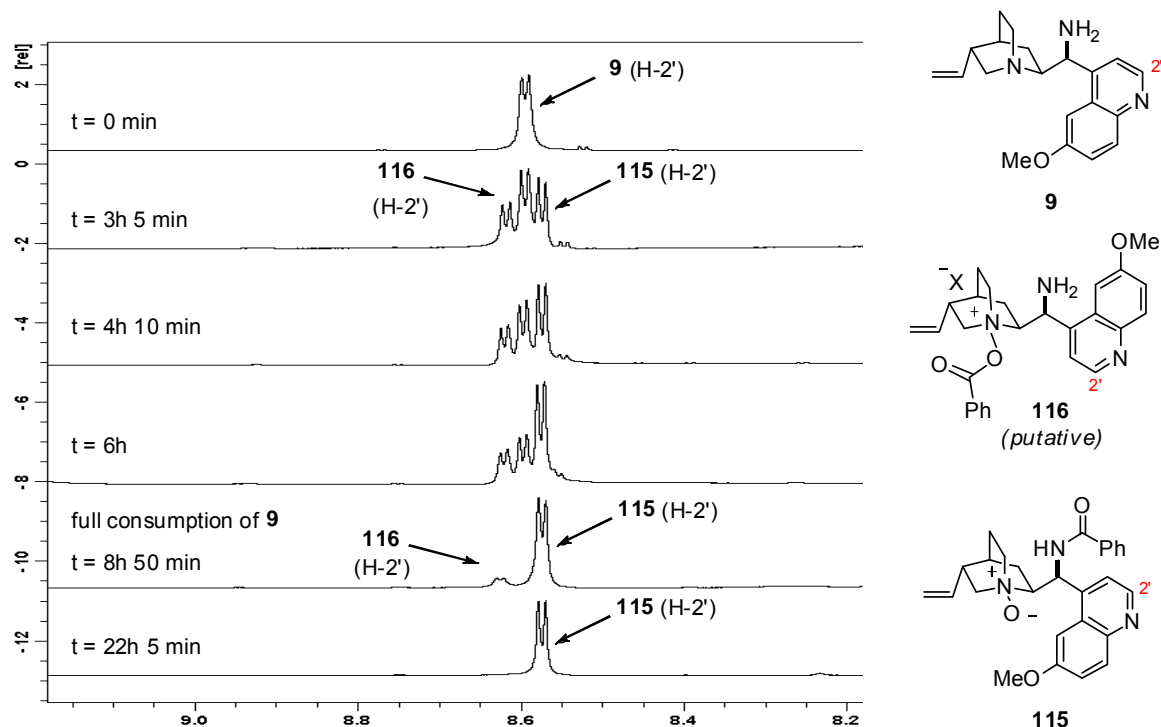
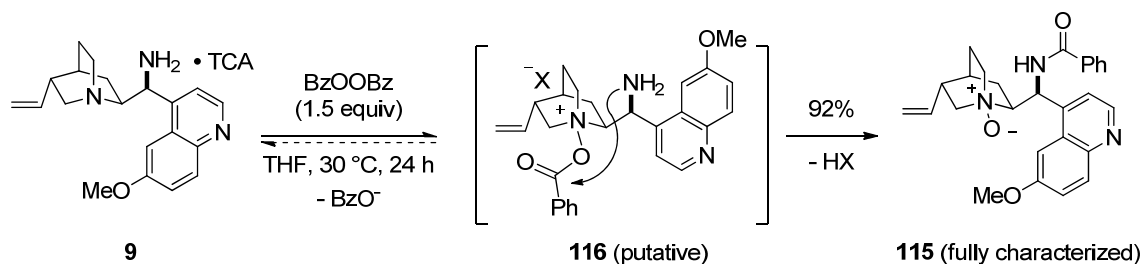


Figure 4.21 ^1H NMR analysis of the reaction between **9** and 1.5 equiv benzoyl peroxide over 24 hours at 30°C (selected region showing H-2', spectra recorded in THF-d_8).

Taking all of these results together, we hypothesized that catalyst **9** indeed undergoes *N*-benzoyloxylation (putative intermediate **116**) under the conditions tested, but this intermediate is unstable^[160a] and slowly rearranges to the *N*-oxide derivative **115** via an intramolecular process (Scheme 4.32). The initial *N*-benzoyloxylation $\mathbf{9} \rightarrow \mathbf{116}$ may be reversible.^[162]



Scheme 4.32 Decomposition of **9** into **115** via the putative intermediate **116** by benzoyl peroxide in the absence of a ketone substrate.

4. Results and Discussion

The extensive characterization of the stable isolated product **115** discussed above was found to be fully consistent with the proposed structure shown in Scheme 4.32, including quinuclidine *N*-oxidation, the IR stretching frequencies of 1650 and 1620 cm^{-1} which are typical for the *N*-benzoyl amide bands I and II,^[163] and the observation of amide rotamers by NMR which could be “frozen out” at $-20\text{ }^{\circ}\text{C}$. A single intermediate observed in the NMR (Figure 4.21) tentatively suggests that quinuclidine *N*-oxidation and primary amine benzylation do not occur as two separate processes but share a common precursor (i.e. compound **116**). The inability of **115** to mediate benzoyloxylation is also explained by the amidation of the primary amine group. Unfortunately, we could not confirm the identity of **116** by mass spectroscopy because the ion $[\mathbf{116}]^+$ has an identical m/z value as $[\mathbf{115}+\text{H}]^+$ and a very similar fragmentation pattern, making results ambiguous.

Since we observed no reaction of benzoyl peroxide with the *triply protonated* catalyst **9**·3TFA (Figure 4.19), but complete conversion of the *monoprotonated* catalyst **9**·TCA to product **115** (Figure 4.20) in the absence of a ketone substrate, we decided to test if full protonation of the catalyst with TCA would similarly suppress the reaction **9**→**115**. Indeed, forming the salt **9**·3TCA and subjecting it to benzoyl peroxide, we observed only traces of product **115** after 24 hours (Figure 4.22).

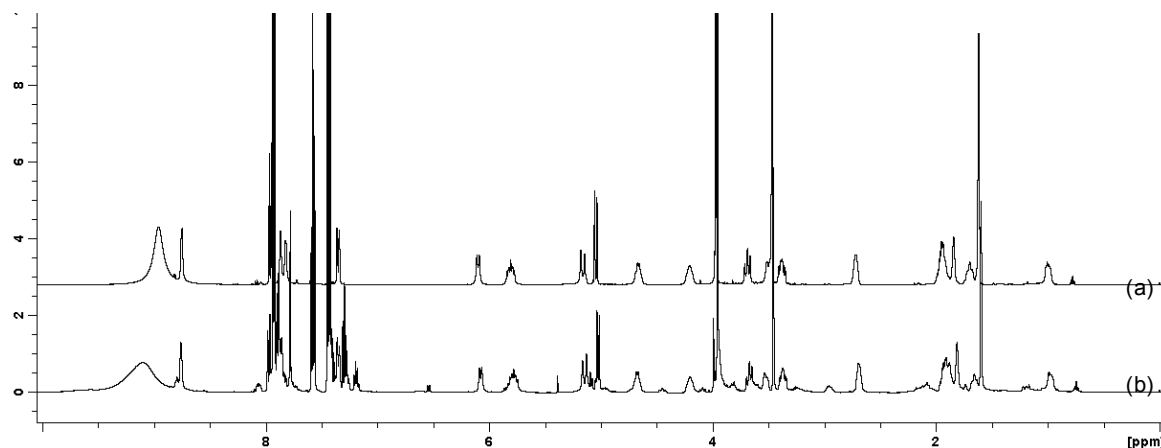


Figure 4.22 ^1H NMR spectrum of **9**·3TCA (a), and the crude spectrum of **9**·3TCA treated with 1.5 equiv BzOOBz for 24 h at $30\text{ }^{\circ}\text{C}$ showing only traces of **115** (b) in THF-d_8 .

Because benzoic acid (BzOH) is generated during the α -benzoyloxylation reaction from benzoyl peroxide, we further speculated that the triply protonated species **9**·TCA·2BzOH could also be resistant to the formation of **115**. Toward this end, we prepared salt **9**·TCA·2BzOH by stirring **9** with 1 equiv of TCA and 2 equiv of benzoic acid. However, subjecting the resulting salt to benzoyl peroxide for 24 h at $30\text{ }^{\circ}\text{C}$ resulted in complete conversion of **9** to **115** (Figure 4.23).

4. Results and Discussion

This suggested that a simple excess of an acidic component (i.e. 3 equiv of acid with respect to **9**) is not enough to prevent catalyst decomposition **9**→**115**; the pKa of the acid co-catalyst plays a decisive role in the process as well.

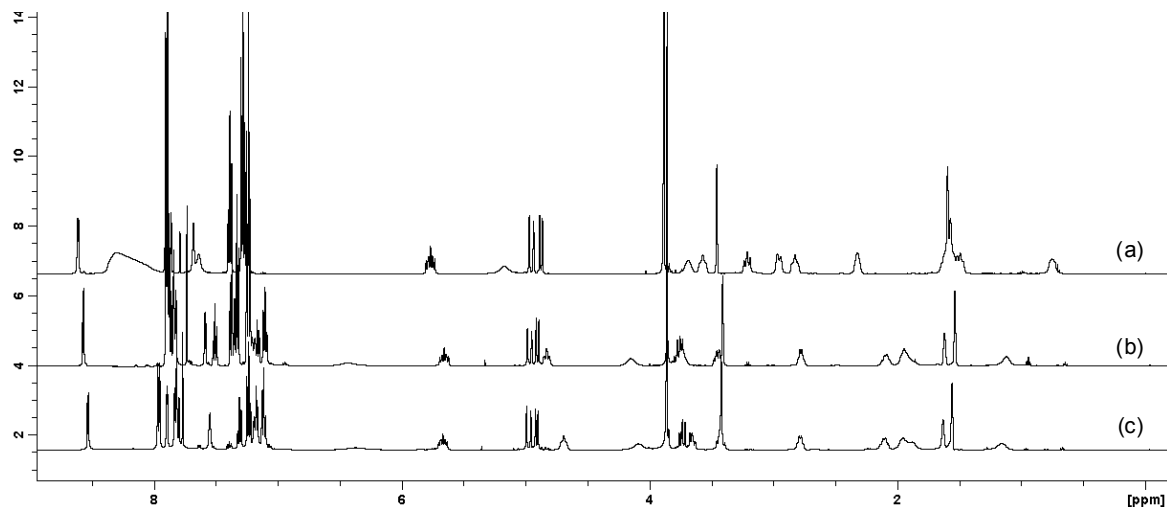


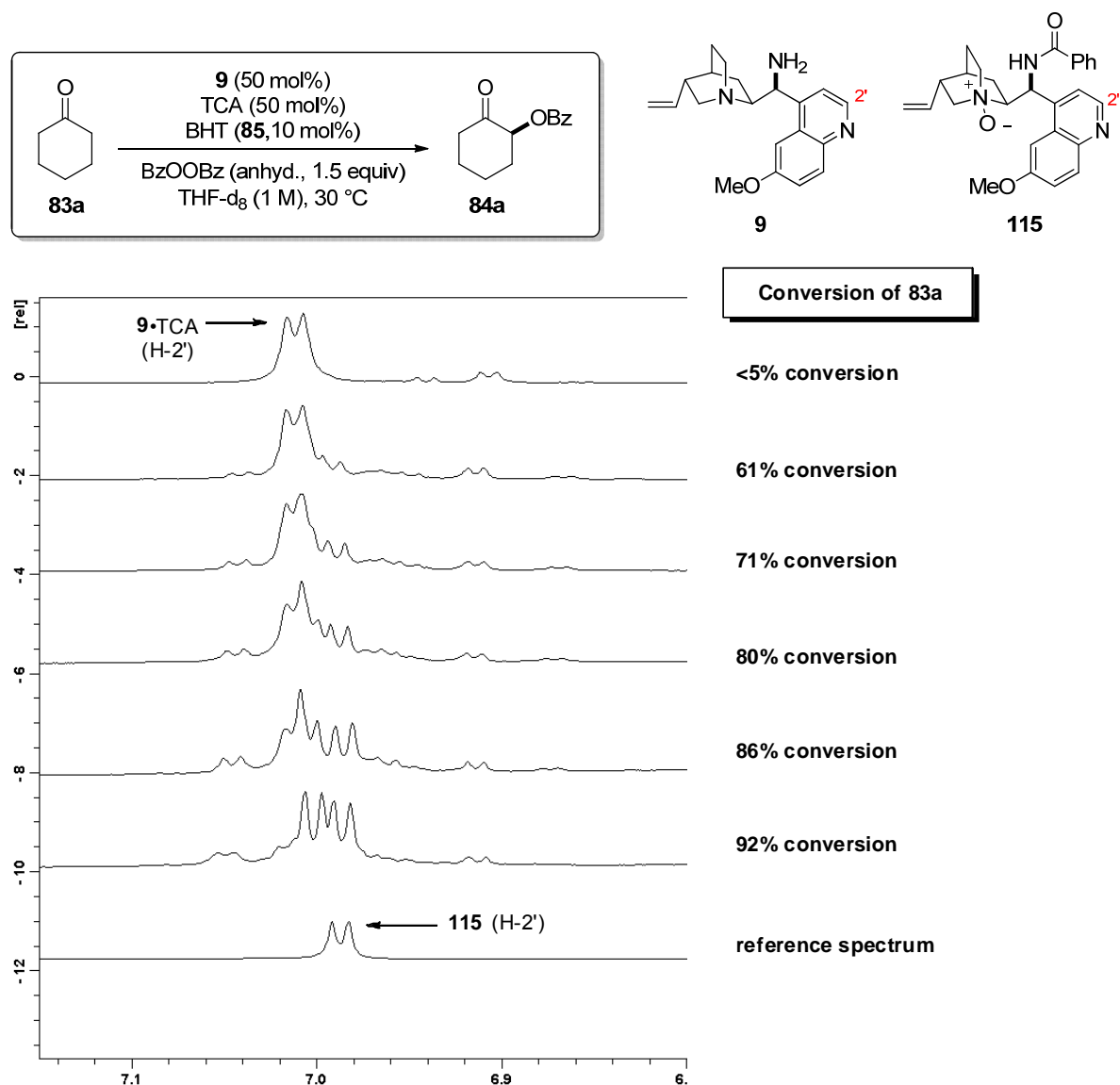
Figure 4.23 ^1H NMR spectrum of the catalyst salt **9**·TCA·2BzOH (a), the crude spectrum of **115** formed from the treatment of **9**·TCA·2BzOH with 1.5 equiv benzoyl peroxide for 24 h at 30 °C (b), purified compound **115** shown for reference (c). All spectra in THF- d_8 .

Thus, we established that in the presence of benzoyl peroxide, the optimal salt **9**·TCA undergoes the decomposition pathway **9**→**115** in the absence of a ketone substrate, presumably *via* *N*-benzoyloxylation of the quinuclidine moiety. This process occurs even in the presence of excess benzoic acid, which is normally generated during the benzoyloxylation reaction. With these results in hand, we next followed the fate of the catalyst salt **9**·TCA *in the presence* of the ketone substrate **83a** (Scheme 4.33). Optimized reaction conditions were used, except for the solvent THF- d_8 instead of dioxane and a higher catalyst loading of 50 mol%, employed for better resolution of the catalyst NMR signals. Although higher catalyst loading resulted in an increased reaction rate (>95% conversion after 8 h instead of 24 h with 10 mol% catalyst loading), product **84a** was obtained with the same enantioselectivity and a comparable yield.^{xiii} We monitored the reaction by taking samples at approximately 15 min intervals and measured the conversion of ketone **83a**, as well as examined the structure of the catalyst. As expected, the NMR spectra contained more signals related to the catalyst **9** in the presence of the ketone substrate, which can be attributed to the formation of iminium and enamine catalytic intermediates. However, the catalyst salt **9**·TCA represented the major species and could be followed over time. As can be seen from Scheme 4.33, up to 71% conversion of **83a**, catalyst

^{xiii} However, bis-benzoyloxyated product **93a** was observed as a side product.

4. Results and Discussion

salt **9**·TCA appears to be largely unchanged, but above 80% conversion of **83a**, new species related to the catalyst begin to predominate.

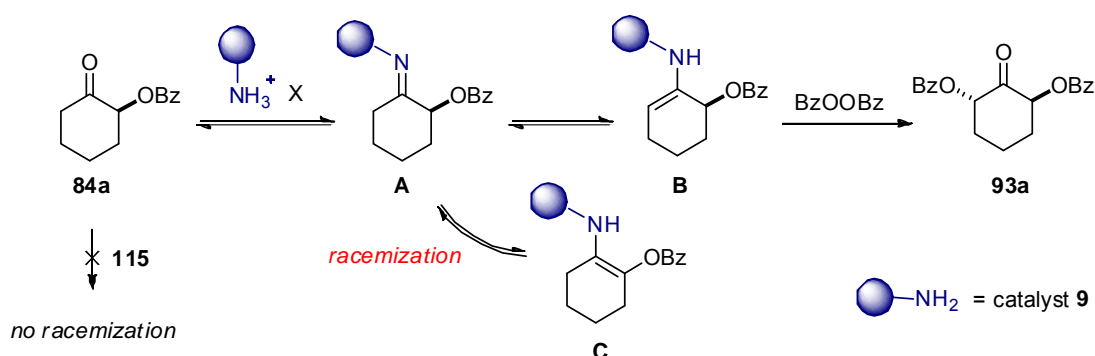


Scheme 4.33 Following the fate of catalyst **9** under the conditions of α -benzoyloxylation with the model substrate **83a** by ^1H NMR analysis in THF- d_8 (selected region shows H-2').

These results suggest that at low concentration of the ketone substrate, catalyst decomposition pathways begin to be operative. The formation of **115** was confirmed by ^1H NMR analysis at the end of the reaction. Presumably, when the primary amine moiety in **9** is covalently bound to the ketone substrate, it cannot participate in the irreversible rearrangement to **115** even if the quinuclidine moiety is (reversibly) *N*-benzoyloxylation. Although detailed interpretation of this NMR study was not possible due to concurrent formation of various catalytic intermediates as well as the generation of benzoic acid which formed new salts thus slightly shifting the NMR

4. Results and Discussion

signals, it raises interesting questions about catalyst stability under the reaction conditions. In particular, the study suggests that the singly protonated catalyst **9**·TCA undergoes decomposition when none or little of the ketone substrate is left. Recalling the effect of acid co-catalyst stoichiometry on suppressing the decomposition pathway **9**→**115**, the study furthermore implies that in reactions mediated by the triply protonated catalytic species (e.g. **9**·3TCA), the catalyst should be active even after complete consumption of the ketone substrate. This, in turn, should have direct consequences on the configurational stability of the products **84**, which are sensitive to racemization. The observation of bis-benzoyloxyated products such as **93a** under standard reaction conditions suggests that catalyst **9** can form a new enamine species **B** with the product **84** *via* the imine intermediate **A** (Scheme 4.34). Imine **A** can also isomerize to enamine **C** causing racemization of the stereocenter in **84**. In contrast, the inactivated catalyst derivative **115** should not result in any racemization of the product **84** since it lacks a primary amine moiety to form covalent intermediates **A**-**C** and/or the quinuclidine group to act as a Brønsted base.



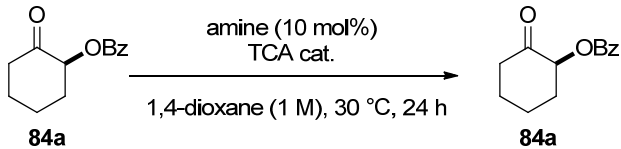
Scheme 4.34 Possible racemization and bis-benzoyloxylation of **84a** by intact catalyst **9**.

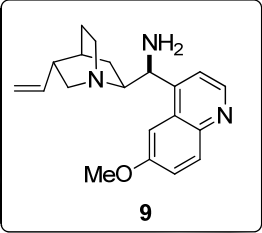
Indeed, we had found a direct effect of acid co-catalyst stoichiometry on the enantiomeric excess of the product **84a** in the model reaction of cyclohexanone **83a** during optimization (cf. Section 4.2.1.2), where the best er was consistently obtained with the lower acid co-catalyst loading of 10 mol% compared to 30-40 mol% (cf. Tables 4.24-4.25). We wondered if this effect was directly related to catalyst stability which was maintained at high acid co-catalyst loading, allowing the active catalyst to racemize the newly created stereocenter in the product **84** at the end of the reaction

In order to test this hypothesis, we stirred the enantioenriched product **84a** with the catalytic salts **9**·TCA, **9**·3TCA and the inactivated catalyst salt **115**·TCA in dioxane at 30 °C in the absence of benzoyl peroxide. The initial and final enantiomeric excess of the product **84a** is summarized in Table 4.31 for each set of conditions.

4. Results and Discussion

Table 4.31 Testing for racemization of **84a** with salts of **9** and **115**.

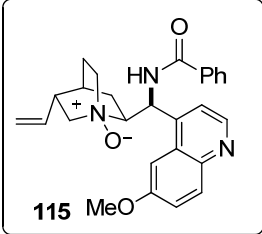




9

Entry	Amine	TCA, mol%	er, t = 0 h ^a	er, t = 24 h ^a
1	9	10	96:4	84:16
2	9	30	96:4	76:24
3	115	10	96:4	95.5:4.5
4	none	10	96:4	95.6:4.6

^a Determined by chiral-phase HPLC.



115

In accord with our expectations, both salts **9**·TCA and **9**·3TCA caused racemization of the product **84a**, while the inactivated salt **115**·TCA or TCA alone did not change the enantiomeric excess of **84a** after 24 h. Since no erosion of the enantiomeric excess is observed in the α -benzoyloxylation of ketones **83** under optimized conditions even after 48 h, these results strongly support a mechanistic scenario in which the salt **9**·TCA catalyzes the α -benzoyloxylation of ketones **83** until nearly complete conversion, after which the decomposition pathway **9**→**115** becomes operative. Although irreversibly destroying the catalyst, this decomposition appears to suppress bis-benzoyloxylation and maintain a high enantiomeric excess of product **84** by preventing its racemization.

Finally, we wished to determine if the putative *N*-benzoyloxylation of the quinuclidine moiety of amine **9** only participates in the decomposition **9**→**115** or if it also serves as the source of the benzoyloxy group in the transition state (cf. Scheme 4.31, structure **B**). Although the unstable intermediate **116** could not be isolated, kinetic NMR studies shown in Figure 4.21 demonstrated that in the reaction of **9**·TCA with benzoyl peroxide, **116** can be intercepted at a time point between 6 and 9 hours of reaction time. At this time point, all of **9** is consumed and only the desired compound **116** along with inactive **115** are present. Careful NMR control of this reaction allowed us to intercept this time point and inject cyclohexanone **83a**. Formation of the product **84a** would strongly suggest that the intermediate **116** is catalytically competent, supporting *N*-benzoyloxylation of the catalyst in the transition state. However, only traces of **84a** could be observed, rendering the results ambiguous. At this point, differentiation of the two mechanistic scenarios shown in Scheme 4.31 awaits further experimental work (cf. Outlook, Section 6).

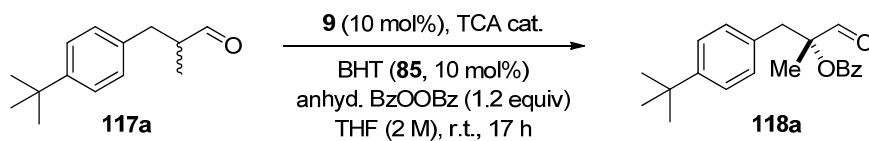
4.2.2 α -Benzoyloxylation of α -Branched Aldehydes

As discussed in Section 2.3.2, no direct asymmetric α -oxidation methodologies, whether organocatalytic or metal-based, exist for α -branched aldehydes to date.^[97] Nevertheless, activation of α -branched aldehydes has been successfully developed by using primary amine catalysts in our laboratories^[164] and by others.^[38-39, 41] In addition, the groups of *Maruoka*, *Hayashi* and *Tomkinson* have shown that simple unbranched aldehydes serve as suitable substrates for α -benzoyloxylation.^[118-120] Inspired by these considerations and by the excellent performance of the amine catalyst **9** in the α -benzoyloxylation of cyclic ketones, we sought to expand the reaction to α -branched aldehydes.

4.2.2.1 Development and Optimization of the Catalytic System

As a model substrate, we chose the commercially available racemic aldehyde **117a** and carried out the benzoyloxylation reaction using the previously established catalytic salt **9**·TCA. A slight excess of anhydrous benzoyl peroxide (1.2 equiv) in THF at room temperature was employed, and radical inhibitor BHT (**85**) was added as before to avoid any possible side reactions of benzoyl radicals. We were pleased to obtain the desired product **118a** with an excellent NMR yield of 90% and full conversion of the starting material after 17 h, albeit in nearly racemic form (Table 4.32, entry 1). Interestingly, when we excluded the acid co-catalyst, the reaction still proceeded with complete conversion and the same yield, but a significantly higher enantioselectivity. It is noteworthy that, in contrast to the ketones **84**, products **118** are configurationally stable, and their enantiomeric excess thus reliably reflects the enantioselectivity of the catalyst.

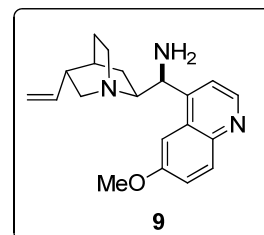
Table 4.32 Preliminary results for α -benzoyloxylation of **117a** with catalyst **9**.



Entry	TCA, mol%	Yield ^a	er ^b
1	10	90	51.5:48.5
2	0	90	66.5:33.5

^a Determined by ¹H NMR with an internal standard (Ph₃CH).

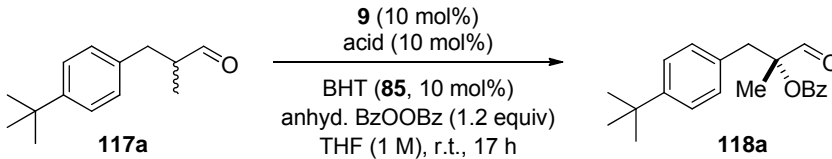
^b Determined by chiral-phase HPLC after reduction with NaBH₄; **118a** was found to be unstable under conditions of HPLC.



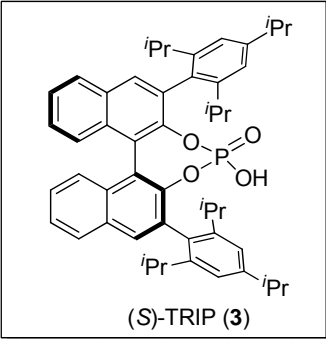
4. Results and Discussion

Although the results in Table 4.32 suggested that an external acid additive was unnecessary, we hypothesized that the primary amine-catalyzed benzoyloxylation of α -branched aldehydes still involves a Brønsted acid in the catalytic cycle, and that this role is fulfilled by the *in situ* generated benzoic acid after the first catalytic turnover. Based on these considerations, we screened several Brønsted acid co-catalysts, including both enantiomers of the chiral phosphoric acid TRIP in hopes of influencing the enantioselectivity of the reaction (Table 4.33). Although both the achiral phosphoric acid diphenyl ester (entry 2) and (*R*)-TRIP (entry 3) resulted in reduced enantioselectivity of the product **118a**, (*S*)-TRIP appeared to be a “matched” combination with the catalyst **9** and increased the enantiomeric excess of the product to 70:30 er (entry 4).

Table 4.33 Effect of the acid co-catalyst in the α -benzoyloxylation of **117a** with catalyst **9**.



Entry	Acid	Yield ^a	er ^b
1	none	90	66.5:33.5
2	(PhO) ₂ PO ₂ H	93	56:44
3	(<i>R</i>)-TRIP	83	52:48
4	(<i>S</i>)-TRIP	78	70:30

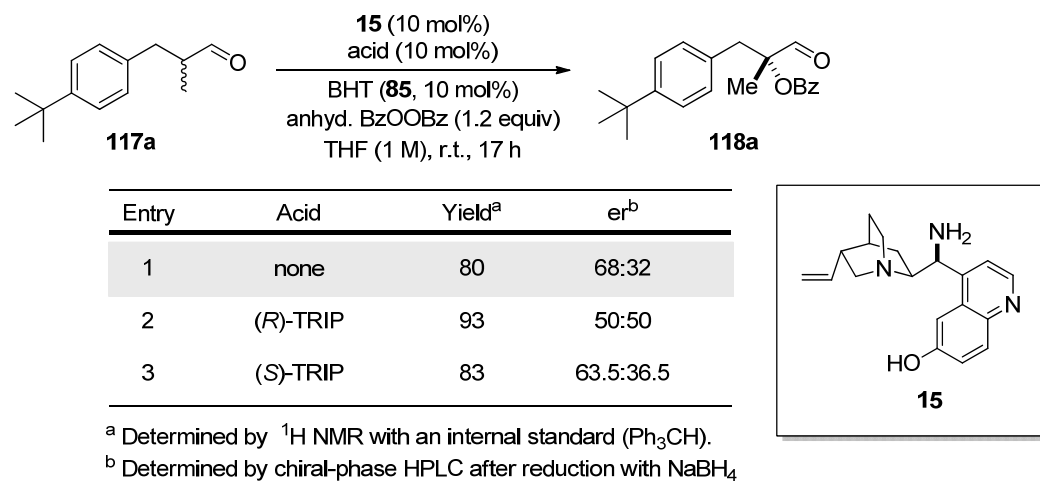


^a Determined by ¹H NMR with an internal standard (Ph₃CH).
^b Determined by chiral-phase HPLC after reduction with NaBH₄.

Inspired by the recent report of *Melchiorre et al.* who had shown that the cupreine-derived catalyst **15** was particularly effective in the γ -functionalization of α -branched aldehydes,^[25a] we also tested this catalyst alone and in combination with both enantiomers of TRIP (Table 4.34). In the absence of an acid co-catalyst, catalyst **15** proved to be slightly more enantioselective than **9** under the same reaction conditions (cf. Table 4.33, entry 1). However, unlike with the catalyst **9**, even the “matched” (*S*)-enantiomer of TRIP failed to improve the enantioselectivity (entry 2). Employing (*R*)-TRIP as catalyst resulted in racemic product **118a**, in accord with our earlier observations (entry 3).

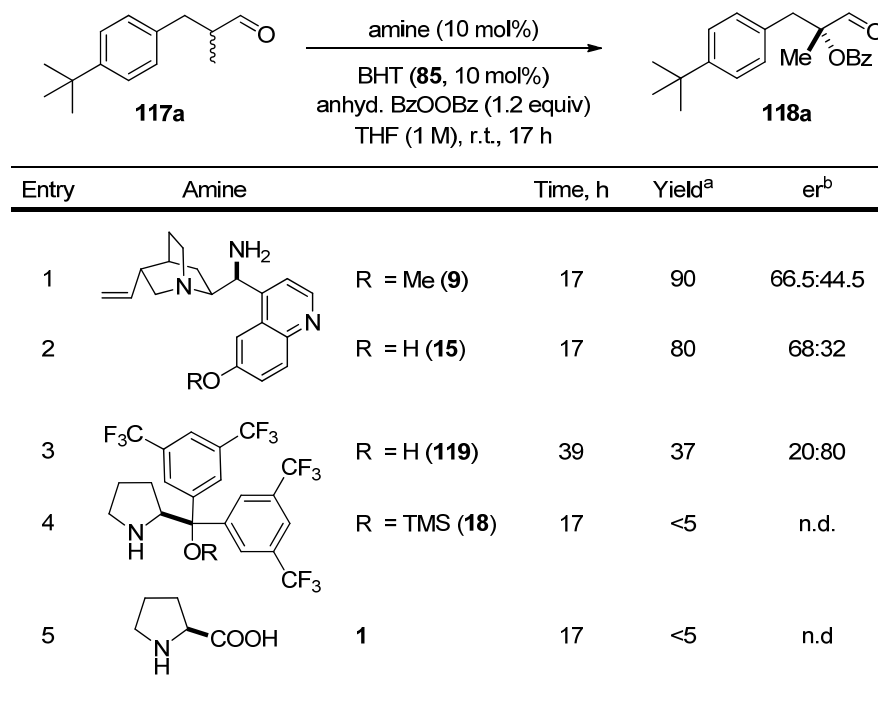
4. Results and Discussion

Table 4.34 Evaluation of cupreine-derived catalyst **15** in the α -benzyloxylation of **117a**.



At this point we decided to evaluate other amine catalysts. In particular, we were intrigued if secondary amines could promote the α -benzyloxylation of α -branched aldehydes, even though this catalyst class has failed in reactions employing nitrosobenzene as the oxidant.^[97] Table 4.35 summarizes the screen of various common secondary amine catalysts, together with the results obtained for primary cinchona-derived amines **9** and **15** for comparison.

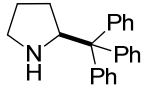
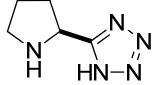
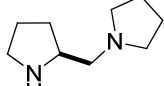
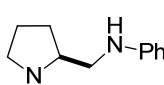
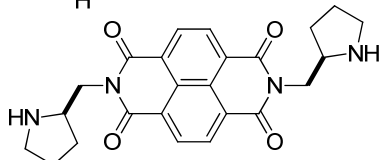
Table 4.35 Evaluation secondary amine catalysts in the α -benzyloxylation of **117a**.



^a Determined by ¹H NMR with an internal standard (Ph₃CH).

^b Determined by chiral-phase HPLC after reduction with NaBH₄.

4. Results and Discussion

Entry	Amine		Time, h	Yield ^a	er ^b
6		50	41	49	39:61
7		47	17	33	39:61
8		120	17	44	43:57
9		121	17	<5	n.d.
10		122	40	80	61:39

^a Determined by ¹H NMR with an internal standard (Ph₃CH).

^b Determined by chiral-phase HPLC after reduction with NaBH₄.

Compared to the primary amines **9** and **15**, most secondary amines mediated benzoyloxylation of **117a** with a similar enantioselectivity of approximately 60:40 er, except for prolinol **119** which gave an improved enantiomeric ratio of 80:20 (entry 3). However, the conversion of the starting material was only modest with all secondary amine catalysts tried (entries 3-9), with a single exception of the dimeric catalyst **122**^{xiv} (entry 10). The success of **122** which possesses two secondary amine groups may be attributable to a higher effective catalyst loading (20 mol%), however.

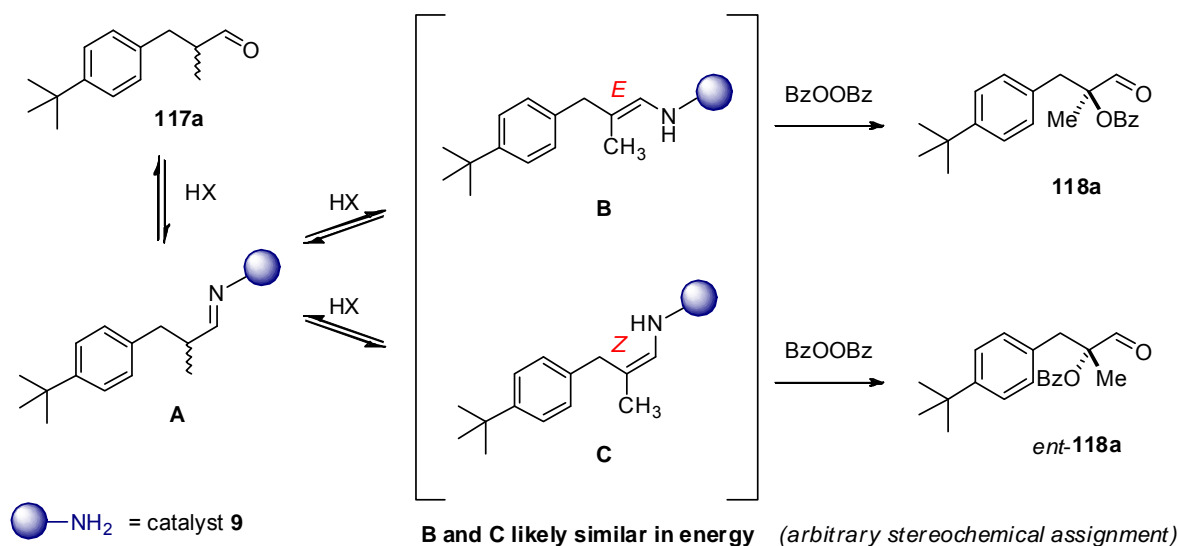
The low yields observed with secondary amine catalysts likely resulted from their difficulty in forming covalent enamine intermediates with the sterically hindered α -branched aldehydes. In addition, as suggested by *Maruoka* and co-workers, nucleophilic secondary amines can react with benzoyl peroxide leading to catalyst decomposition, unless flanked by sterically demanding groups.^[118] In view of this, we decided to pursue α -benzoyloxylation of α -branched aldehydes further using primary amine catalysis which furnished the desired products with the best yields.

Given the modest enantioselectivity observed in the α -benzoyloxylation of aldehyde **117a** under various conditions, we turned our attention to the mechanism of the reaction. It is well known that in reactions operating under enamine catalysis, effective control of enamine geometry is crucial for enantioselectivity,^[27a, 165] since (*E*) and (*Z*) enamine isomers typically

^{xiv} This catalyst was prepared by *G. Bordeau* in our group.

4. Results and Discussion

furnish opposite enantiomers of the product. Under thermodynamic conditions of organocatalysis, substrates with a low steric and/or electronic bias might form equilibrium mixtures of (*E*) and (*Z*) enamine intermediates which are similar in energy. In such situations, unless one of the enamine isomers reacts at a significantly higher rate, even the most facially selective catalysts will produce racemic or nearly racemic products. For this reason, nearly all highly enantioselective methodologies employing enamine catalysis with α -branched aldehydes rely on sterically biased substrates, such as aliphatic aldehydes bearing α -aryl substituents.^[27a] In this respect, substrate **117a** represents a less biased substrate, as the electronically and sterically similar α -methyl substituent and the methylene group of the main chain likely result in *E* and *Z* enamine intermediates **B** and **C** having very similar energies (Scheme 4.35).

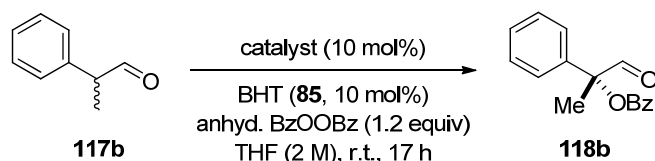


Scheme 4.35 Mechanistic considerations with the sterically unbiased substrate **117a**.

Thus, in order to test the true enantioselectivity of cinchona-derived primary amine catalysts in the α -benzyloxylation of α -branched aldehydes, we decided to evaluate a more sterically biased 2-phenyl acetaldehyde **117b** (Table 4.36). Gratifyingly, in the absence of an acid co-catalyst both quinine-derived catalyst **9** (entry 1) and cupreine-derived catalyst **15** (entry 2) catalyzed the formation of the corresponding product **118b** with complete conversion and an excellent NMR yield. In accordance with our expectations, the product **118b** was also obtained with higher enantioselectivity compared to **118a** using either catalyst, whereby amines **9** and **15** gave very similar results. The absolute (*R*)-configuration of the product **118b** was established by comparison of the optical rotation with the literature value^[166] after global reduction to 2-phenylpropane-1,2-diol with LiAlH_4 .

4. Results and Discussion

Table 4.36 α -Benzoyloxylation of sterically biased substrate **117b** with catalysts **9** and **15**.



Entry	Catalyst	Yield ^a	er ^b
1	9	95	74:26
2	15	95	76:24

^a Determined by ¹H NMR with an internal standard (Ph₃CH).

^b Determined by chiral-phase HPLC after reduction with NaBH₄.

We also followed the conversion of the aldehyde **117b** over time with the catalyst **9** using ¹H NMR spectroscopy. Plotting the results, we obtained a sigmoidal curve characteristic to autocatalytic reactions, which contained an initial lag period until approximately 20% conversion of the starting material (Figure 4.24).

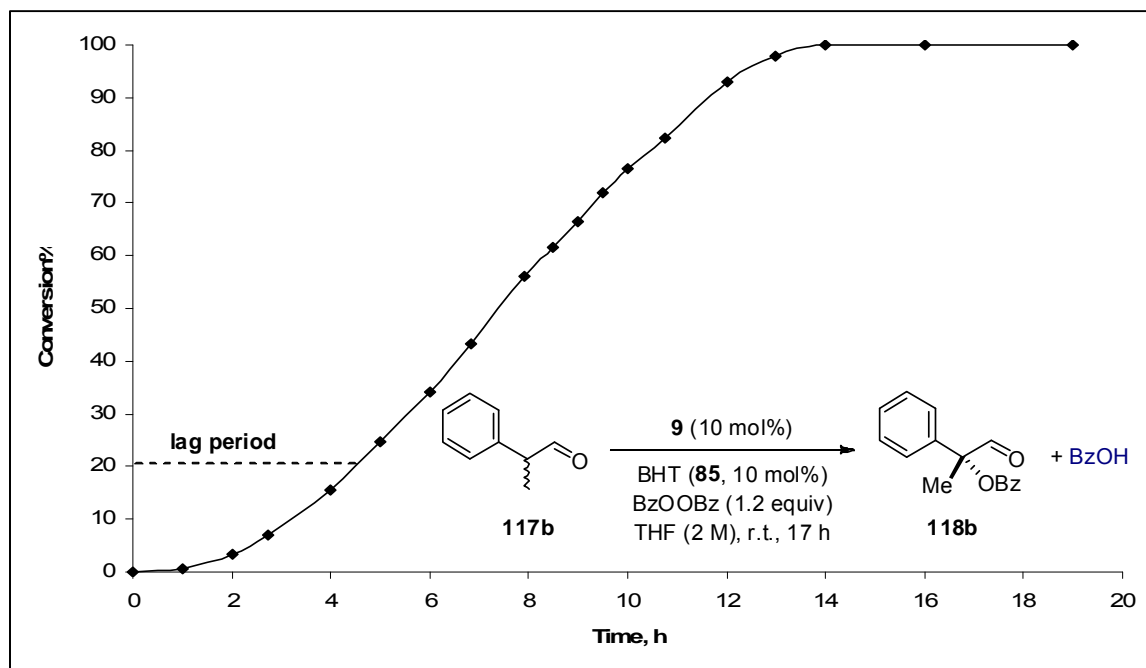


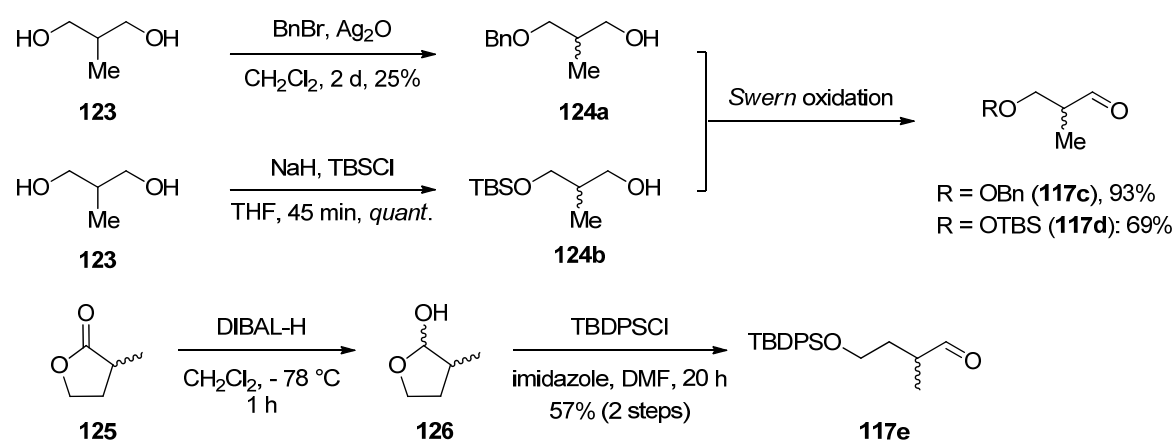
Figure 4.24 α -Benzoyloxylation of **117b** with catalyst **9**: a plot of conversion over time showing a sigmoidal graph with a lag period, typical for autocatalytic reactions.

This autocatalytic behaviour strongly supports our hypothesis on the role of benzoic acid which builds up in the reaction and participates in catalysis. In particular, at 20% conversion, 20 mol% of benzoic acid are generated, which might form a more active catalyst salt **9**·2BzOH.

4. Results and Discussion

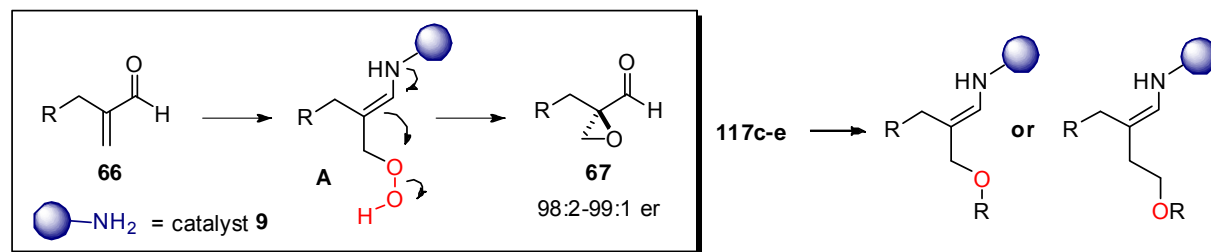
4.2.2.2 Preliminary Reaction Scope and Discussion

Since this kinetic study shown in Figure 4.24 confirmed that one or several molecules of acid participate in the catalytic cycle of the reaction, we were encouraged to further test chiral Brønsted acid additives to improve the enantioselectivity of the process. In addition, the results obtained with **117b** pointed out the influence of the substrate's steric bias on the enantioselectivity of the reaction. To understand the relative influence of these factors, we decided to perform a comprehensive analysis of various substrates, screening them against different acid co-catalysts and amine catalysts **9** and **15**. The required starting materials **117c-e** were prepared using standard chemical transformations (Scheme 4.36).



Scheme 4.36 Synthesis of the starting materials **117c-e**.

We chose to synthesize aldehydes containing a protected alcohol functionality in the main chain to create an electronic bias in the substrate, as well as a basic site, which might serve as a coordination point in the catalytic assembly. Effectively, we wished to mimic the epoxidation intermediates **A** derived from α -substituted acroleins **66** (Scheme 4.37) which contain two oxygen molecules in the β - and γ -positions, and which were found to undergo enamine-catalyzed ring-closure with remarkable enantioselectivity (cf. Section 4.1.5.3).



Scheme 4.37 Mechanistic rationale for the design of substrates **117c-e**.

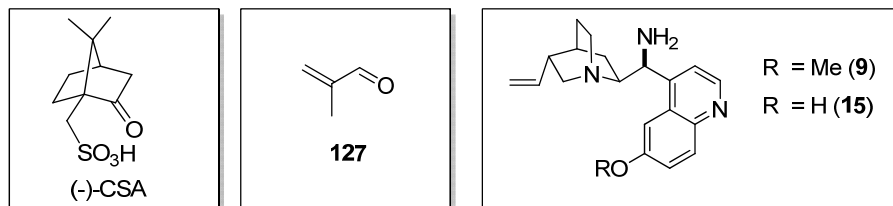
4. Results and Discussion

A screening matrix using substrates **117a-e**, amine catalysts **9** and **15** and different chiral is summarized in Table 4.37.

Table 4.37 Evaluation of various substrates **117** in the α -benzoyloxylation with catalysts **9** and **15** and various acid co-catalysts.

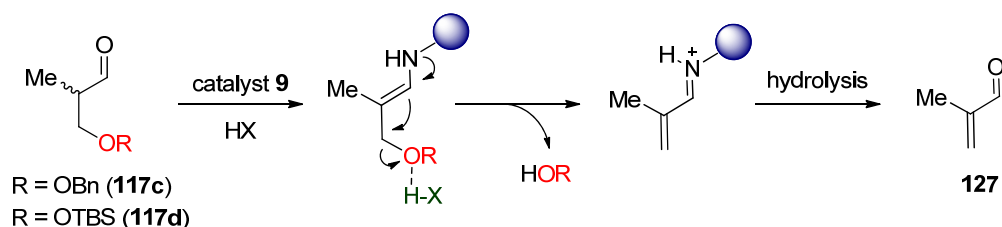
Entry ^a	Substrate	Amine catalyst	Acid co-catalyst			
			none	(<i>R</i>)-TRIP	(<i>S</i>)-TRIP	(-)-CSA
1		9	66.5:33.5 er 90% yield	52:48 er 83% yield	70:30 er 78% yield	-
		15	68:32 er 80% yield	50:50 er 59% yield	63.5:36.5 er 30% yield	-
2		9	74:26 er 95% yield	42:58 er 95% yield	84:16 er 95% yield	80:20 er 95% yield
		15	76:24 er 95% yield	15:85 er 95% yield	82:18 er 95% yield	-
3		9	78:22 er 76% + 9% 127	70:30 er 50% + 46% 127	92% 127	-
4		9	82:18 er 88% + 12% 127	57.5:42.5 er 43% + 57% 127	90:10 er 72% + 28% 127	-
5		9	72:28 er 63% yield	39.5:60.5 er 75% yield	88:12 er 90% yield	67.5:32.5 er 95% yield
		15	76:24 er 95% yield	23:77 er 85% yield	84:16 er 90% yield	-

^a Yields of products **118** were determined by ¹H NMR with an internal standard (Ph₃CH), and er values were determined by chiral-phase HPLC after reduction with NaBH₄.



4. Results and Discussion

In accord with our expectations, all sterically and/or electronically biased substrates **117b-e** afforded the corresponding products with a higher enantioselectivity than the model substrate **117a** in the absence of an acid co-catalyst (entries 1-5, column 1). Unfortunately, both substrates **117c** (entry 3) and **117d** (entry 4) proved to be liable to elimination of the protected β -hydroxy substituent, leading to the formation of methacrylic aldehyde **127** in various amounts. Presumably, this formal retro-oxa-*Michael* reaction was promoted by enamine catalysis with further activation of the leaving group by the acid co-catalyst (Scheme 4.38).



Scheme 4.38 A likely mechanism for the formation of methacrylic aldehyde **127** from **117c-d**.

Brønsted acid co-catalyst (*R*)-TRIP in combination with amine **9** proved to be a “mismatch” for all substrates, resulting in erosion of the product’s enantiomeric excess, presumably due to the conflicting sense of selectivity of the two chiral catalysts (column 2). Surprisingly, however, (*R*)-TRIP used in combination with **15** was quite enantioselective with the substrate **117b** (entry 2), furnishing the opposite enantiomer of the product **118b** with an er of 85:15. Gratifyingly, employing (*S*)-TRIP as the acid co-catalyst improved the enantioselectivity of all reactions. Interestingly, the amount of the elimination product **127** observed with substrate **117c** (entry 3) strongly depended on which *enantiomer* of the acid co-catalyst TRIP was employed. In the “mismatched” case with (*R*)-TRIP, the elimination side product **127** amounted to 46% of the total yield, whereas with (*S*)-TRIP, **127** was the only product of the reaction (92% yield). These results are in agreement with our hypothesis that the oxygen moiety in the substrate serves as a coordination site in the catalyst assembly, which leads to both the desired reaction pathway forming α -benzyloxylation product **118** and the undesired elimination leading to side product **127**.

Using the best catalyst salt **9**·(*S*)-TRIP, we performed the α -benzyloxylation reaction on selected substrates on a preparative scale (0.4 mmol). Table 4.38 shows the isolated yields and enantioselectivities of the products **118b,d-e**. Although still preliminary, these results suggest that the primary amine catalysis holds significant promise for α -benzyloxylation of α -branched aldehydes. Both aromatic (entries 1-2) and aliphatic (entries 3-4) substrates could be converted to the corresponding products with good yields and useful enantioselectivities at the newly

4. Results and Discussion

created quaternary stereocenter. Importantly, the opposite enantiomer of **117b** could be accessed using the cupreine derivative **15** and (*R*)-TRIP, although the generality of this system has yet to be tested on other substrates.

Table 4.38 Preliminary scope of α -benzoyloxylation of α -branched aldehydes **117** with the catalyst salt **9**·(*S*)-TRIP.

117 $\xrightarrow[\text{anhyd. BzOOBz (1.2 equiv), THF (1 M), r.t., 17 h}]{\text{9 (10 mol%), (S)-TRIP (10 mol%), BHT (85, 10 mol%)}}$ **118**

Entry ^a	Substrate	Product ^b	Yield, % ^c	er ^d
1	117b		83	85.5:14.5
2 ^e	117b		76	88:12
3	117d		57 ^f	91.5:8.5
4	117e		90	88:12

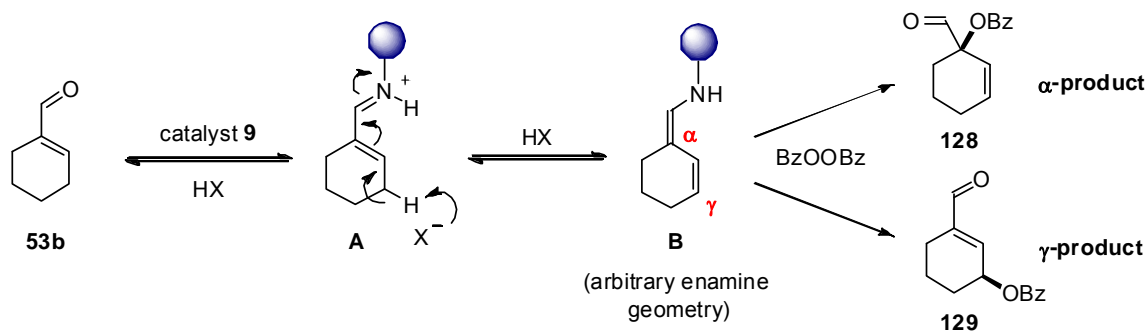
^a Reactions performed on 0.4 mmol scale. ^b The absolute configuration of **118** was assigned by comparison of the optical rotation with the literature values or by analogy (see Chapter 7 for details). ^c Isolated yield. ^d Determined by chiral-phase HPLC after reduction with NaBH₄. ^e Using catalyst **15** and (*R*)-TRIP as co-catalyst. ^f Side product **127** observed.

4.2.3 α -Benzoyloxylation of α -Branched Enals

In parallel with our investigations on the α -benzoyloxylation of α -branched aldehydes *via* enamine catalysis, we also explored a related transformation of α,β -unsaturated α -branched aldehydes *via* dienamine catalysis. We have already shown that enals **53** and **66** readily condense with the catalyst **9** to form iminium species **A** (Scheme 4.39) which act as substrates for *Weitz-Scheffer* epoxidation with nucleophilic hydrogen peroxide (cf. Section 4.1). In the presence of *electrophilic* benzoyl peroxide, such an iminium species cannot participate in any productive reaction pathways; however, it can isomerize to a dienamine **B** and as such react with benzoyl peroxide as a nucleophile. Since dienamines have two potential sites of reactivity, the

4. Results and Discussion

benzoyloxylation could occur at either α - or γ -position of the nucleophile, or give a mixture of both. Although dienamine catalysis has been increasingly explored in recent years, analysis of the literature gives no hints at the precise factors which govern α/γ selectivity, making predictions difficult (cf. Section 2.1.3.4).



Scheme 4.39 Benzoyloxylation of enal **53b** via dienamine catalysis.

4.2.3.1 Development and Optimization of the Catalytic System

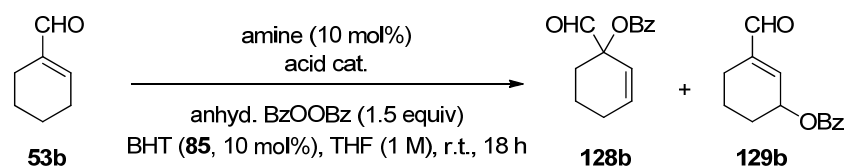
As a model substrate, we chose the cyclic enal **53b**, which was reported by *Melchiorre et al.*^[25e] to undergo selective γ -amination *via* dienamine catalysis.^{xv} In order to identify a suitable catalytic system, we screened various amine catalysts at 10 mol% loading together with different acid co-catalysts (Table 4.39). The model substrate **53b** was used with a slight excess of anhydrous benzoyl peroxide (1.5 equiv) in THF at 1 M concentration and room temperature, in the presence of the radical inhibitor BHT (**85**). Carrying out the reaction with the achiral amine catalyst *meso*-**8** and an equal amount (10 mol%) of Brønsted acid TCA (entry 1) afforded a mixture α and γ products in a modest yield, favouring the α -product with a 84:16 ratio. Excluding the acid co-catalyst (entry 2) shut down the reaction, presumably because the acid is required to catalyze iminium-dienamine isomerization shown in Scheme 4.40 (*vide supra*). Employing the chiral version of the catalyst (*R,R*)-**8** with TCA gave the product in a similar yield and a slightly lower α/γ ratio, and only very low enantioselectivity (entry 3). Pairing this catalyst with the chiral phosphoric acid TRIP failed to improve the enantioselectivity, although opposite enantiomers of the major product **128b** were observed with (*R*)- and (*S*)-TRIP (entries 4-5). When we used the cupreine-derived catalyst **15** together with 30 mol% TCA, both the α/γ ratio and the enantiomer excess of the product **128b** were improved (entry 6). Unfortunately, pairing the catalyst with either enantiomer of the BINOL-derived chiral phosphoric acid **63a**

^{xv} Our subsequent characterization of the product revealed it to be misassigned, and showed that α -aminated compound is actually formed (cf. Section 2.1.2.4, Scheme 2.15 and Section 7.4).

4. Results and Discussion

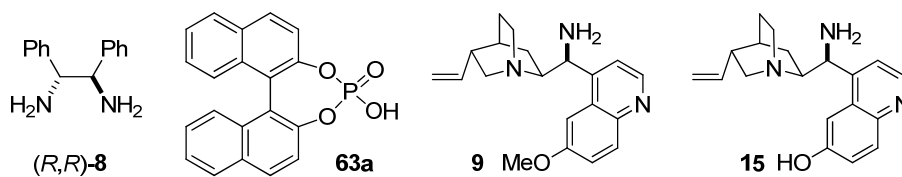
resulted in decreased enantioselectivity and α/γ ratios (entries 7-8). The highest α/γ selectivity and enantioselectivity were once again obtained with the quinine-derived catalyst **9** and TCA as the acid co-catalyst (entry 9). Excluding the acid from this reaction resulted in no conversion of the starting material (entry 10).

Table 4.39 Identification of a suitable catalytic system for the benzoyloxylation of **53b**.



Entry	Amine	Acid	mol%	128:129	yield (128), % ^a	er (128) ^b
1	<i>meso</i> - 8	TCA	10	86:14	54	-
2	<i>meso</i> - 8	none	0	-	0	-
3	(<i>R,R</i>)- 8	TCA	10	80:20	45	54:46
4	(<i>R,R</i>)- 8	(<i>R</i>)-TRIP	10	80:20	37	43:57
5	(<i>R,R</i>)- 8	(<i>S</i>)-TRIP	10	76:24	33	54:46
6	15	TCA	30	89:11	68	63:37
7	15	(<i>R</i>)- 63a	20	85:15	60	56:44
8	15	(<i>S</i>)- 63a	20	85:15	57	50:50
9	9	TCA	30	89:11	74	76:24
10	9	none	0	-	0	-

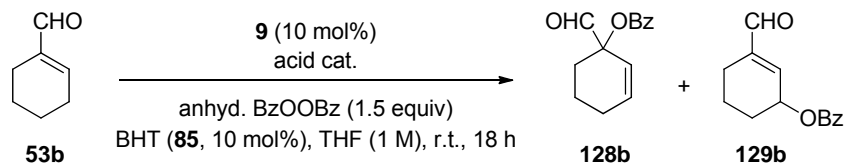
^a Determined by ¹H NMR with an internal standard (Ph₃CH). ^b Determined by chiral-phase HPLC.



Encouraged by the result with the catalyst **9**, we tested it with various achiral and chiral Brønsted acid co-catalysts of different strengths. Table 4.40 shows the results which are arranged from the highest to the lowest pK_a value of the tested acid. Weak acids (entries 1-3) gave only traces of the desired product, and a very strong acid pTSA (entry 12) afforded the product as a racemate with only a modest yield. Better results could be observed with acids of medium strength (entries 4-11). Although chiral Brønsted acids including Mosher's acid **100** (entry 5) and (*R*)-TRIP (entry 8) catalyzed the reaction with an improved enantioselectivity for the major product **128b**, the yield and α/γ selectivity were only moderate. The original catalyst salt **9**·TCA remained to be optimal in terms of activity and regioselectivity.

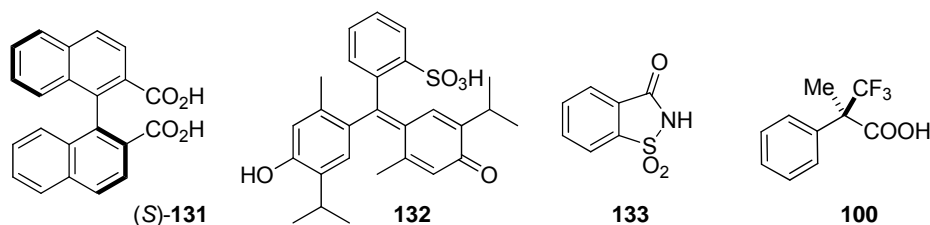
4. Results and Discussion

Table 4.40 Evaluation of various Brønsted acid co-catalysts with amine catalyst **9** in the benzoyloxylation of **53b**.



Entry	Acid	mol%	128:129	yield (128), % ^a	er (128) ^b
1	PhCO ₂ H	30	-	0	-
2	(<i>S</i>)- 131	30	-	<10	64.5:35.5
3	132	10	-	<10	-
4	133	30	89:11	39	62:38
5	100	20	85:15	21	80.5:19.5
6	(PhO) ₂ PO ₂ H	30	86:14	76	50:50
7	(<i>S</i>)-TRIP	20	79:21	41	62:38
8	(<i>R</i>)-TRIP	20	71:29	31	17:83
9	(+)-CSA	20	87:13	58	65.5:34.5
10	TCA	30	89:11	74	76:24
11	TFA	30	88:12	59	63:37
12	pTSA	30	86:14	33	50:50

^a Determined by ¹H NMR with an internal standard (Ph₃CH). ^b Determined by chiral-phase HPLC.



Recognizing an effect of the acid pK_a,^[126] we decided to evaluate it more thoroughly using a range of achiral carboxylic acids as co-catalysts (Table 4.41). Indeed, a clear trend could be observed with respect to the enantioselectivity of the major product **128b**, which peaked at pK_a = 1.2-1.6, albeit the yields were generally only modest (entries 3-6). The highest enantioselectivity and regioselectivity was obtained when using dibromoacetic acid (pK_a = 1.47, entry 4). Interestingly, tribromoacetic acid gave no conversion of the product and discolouration of the reaction medium, suggesting its decomposition into Br₂ under the reaction conditions (entry 8).

4. Results and Discussion

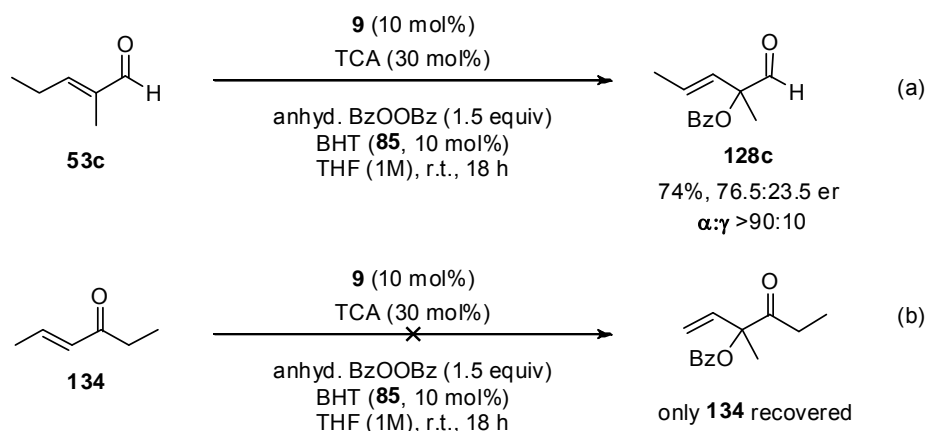
Table 4.41 Examining the effect of Brønsted acid pKa^[126] in the benzoyloxylation of **53b** with amine catalyst **9**.

Entry	Acid	pKa ^a	128:129	yield (128), % ^b	er (128) ^c
1	PhCO ₂ H	4.19	-	0	-
2	Ph ₃ CCO ₂ H	4.07	-	2	-
3	C ₆ F ₅ CO ₂ H	1.60	90:10	28	78:22
4	CHBr ₂ CO ₂ H	1.47	90:10	37	84:16
5	CHCl ₂ CO ₂ H	1.29	88:12	42	79:21
6	CHF ₂ CO ₂ H	1.24	88:12	22	78.5:21.5
7	HO ₂ C-CO ₂ H	1.23	82:18	29	65.5:34.5
8 ^d	CBr ₃ CO ₂ H	0.66	-	0	-
9	CCl ₃ CO ₂ H	0.65	89:11	74	76:24
10	CF ₃ CO ₂ H	-0.25	88:12	59	63:37

pKa = 1.2 - 1.6

^a See reference in text. ^b Determined by ¹H NMR with an internal standard (Ph₃CH). ^c Determined by chiral-phase HPLC. ^d Discolouration of reaction medium (evolution of Br₂) observed.

At this point we also tested the acyclic enal **53c** and enone **134** for reactivity using the most reactive catalyst salt **9**·TCA (Scheme 4.40). While the enal **53c** underwent the desired reaction with a good yield and a very similar enantio- and regioselectivity as its cyclic counterpart **53b**, enone **134** proved to be inert to the reaction conditions, and only starting material was recovered after 18 hours of reaction time.

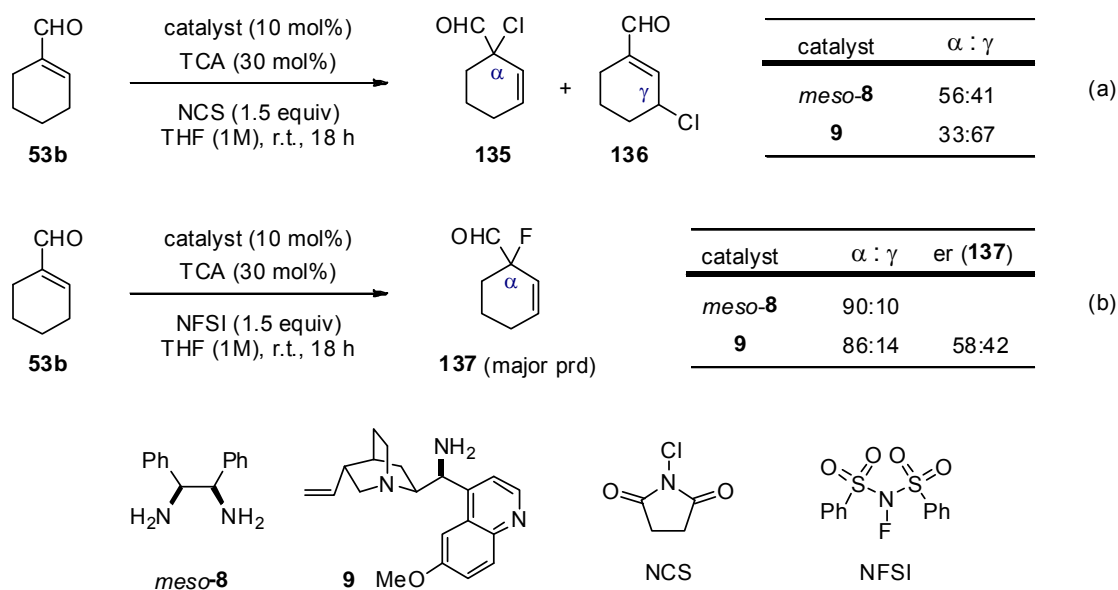


Scheme 4.40 Benzoyloxylation of linear enal **53c** (a) and enone **134** (b) with amine catalyst **9**.

4. Results and Discussion

4.2.3.2 Investigations on α/γ Selectivity

Since the majority of the reported dienamine-catalyzed reactions do not form a quaternary stereocenter if a choice between α and γ -substitution allows it (cf. Section 2.1.3.4), we were intrigued by the unusually high α -selectivity observed in the benzoyloxylation of α -branched enals which leads to the formation of a quaternary stereocenter. Wishing to rationalize this behaviour, we briefly tested other electrophiles with the cyclic substrate **53b** using quinine-derived primary amine catalyst **9** and achiral primary diamine catalyst *meso*-**8**. Electrophilic chlorination with NCS (Scheme 4.41 (a)) and fluorination with NFSI (Scheme 4.41 (b)) were tried.



Scheme 4.41 Electrophilic chlorination (a) and fluorination (b) of enal **53c** with amine catalysts *meso*-**8** and **9**.

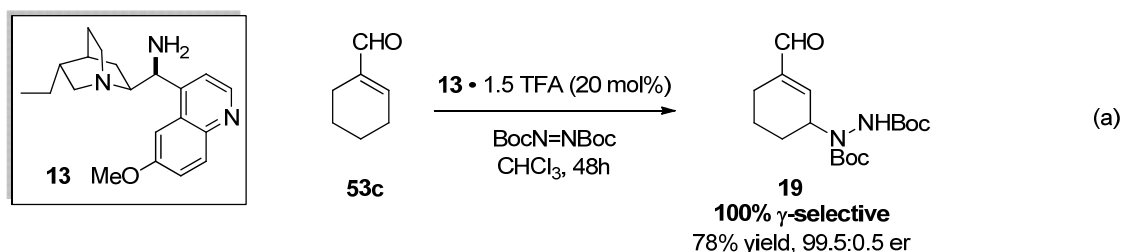
Interestingly, opposite results were obtained in the chlorination reaction of **53b** using the cinchona amine **9** which exceptionally favoured γ -substitution (product **136**), and diamine *meso*-**8** which slightly favoured α -substitution^{xvi} (product **135**). More consistent results were obtained with the fluorination of **53b** where both catalysts preferred α -substitution forming a quaternary stereocenter (product **137**). Chiral catalyst **9** promoted the formation of **137** with low enantioselectivity. These results imply that α/γ selectivity of dienamine-catalyzed reactions is not inherent to the catalyst structure, but strongly depends on the reaction and the electrophile used.

^{xvi} Although γ -substituted products of chlorination and fluorination were stable to chromatography, attempts at purifying the α -products **135** and **137** by silica gel chromatography consistently resulted in product decomposition.

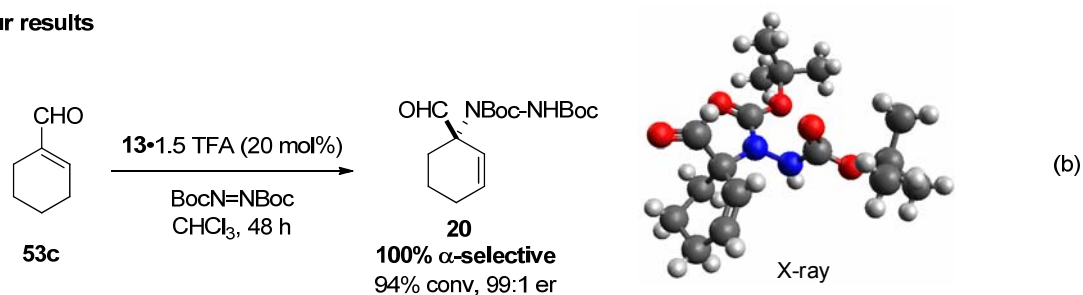
4. Results and Discussion

We also wished to revisit the γ -amination of **53b** reported by *Melchiorre* and colleagues,^[25e] in which the γ -selectivity was in stark contrast to our results with benzoyloxylation, despite very similar catalyst systems and electrophiles employed (Scheme 4.42, (a)). When we repeated the reaction, we could reproduce the yield and enantiomeric ratio of the product which was formed with very high selectivity. However, the reported structure of the product was found to be erroneous. Indeed, 2D-NMR spectroscopy and X-ray analysis allowed us to unambiguously establish that the product of α -amination was formed in the reaction (structure **20**, Scheme 4.42, (b), cf. Chapter 7 for experimental details). Interestingly, although the α -selectivity was confirmed to be consistent in both amination and benzoyloxylation of enals **53b**, the former reaction furnished the product with a much higher enantioselectivity. Presumably, the greater steric bulk of the aminating reagent compared to benzoyl peroxide is responsible to higher enantiocontrol.

Reported results



Our results



Scheme 4.42 Selectivity in the amination of enal **53b** as reported^[25e] (a), and after reassignment by us (b). X-ray: red = oxygen, blue = nitrogen, grey = carbon, white = hydrogen.

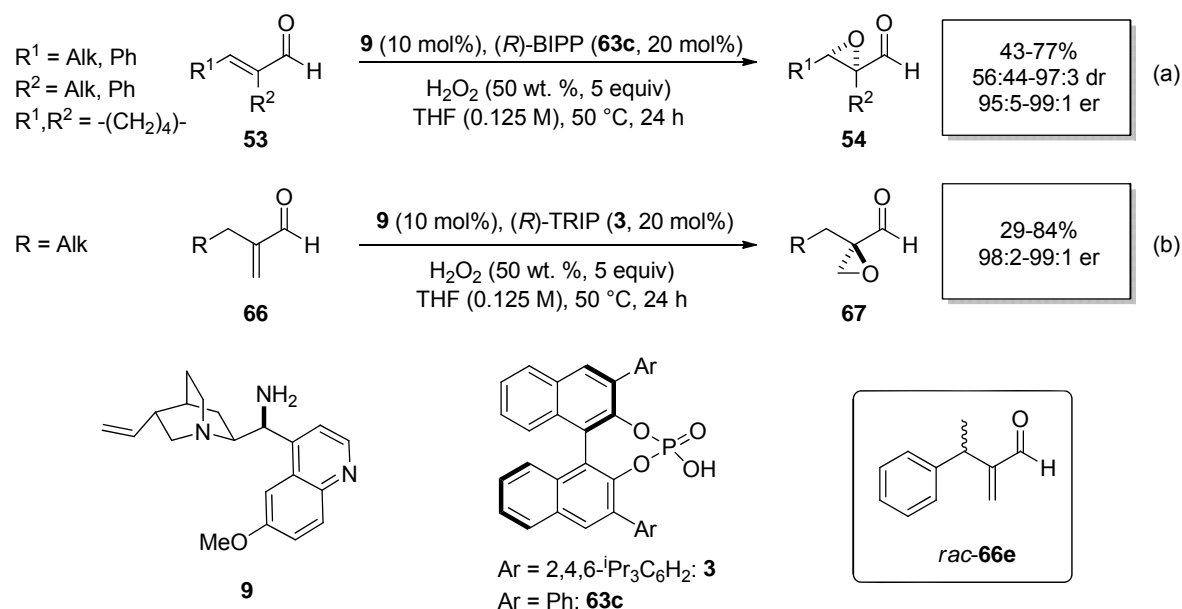
5. SUMMARY

Given the enormous importance of oxidative transformations in organic synthesis, an active research program in our laboratory is aimed at the development of organocatalytic approaches to asymmetric oxidation reactions. This Ph.D. thesis describes the development of highly enantioselective procedures for catalytic epoxidation of α -branched α,β -unsaturated aldehydes and α -benzoyloxylation of cyclic ketones. Both methodologies employ catalytic salts of 9-amino(9-deoxy)*epi*quinine **9** derived in a single-pot operation from the abundant cinchona alkaloid quinine, and inexpensive and environmentally benign oxidants.

Prior to this work, no general asymmetric methodologies existed for the epoxidation α -branched enals, whether organocatalytic or metal-based (cf. Section 2.2.4). The difficulties in the activation of the aldehyde moiety by metals, and the general inability of classically used secondary aminocatalysts to activate hindered α -branched unsaturated aldehydes resulted in this substrate being virtually unexplored for enantioselective epoxidation. Indeed, multistep approaches with reduced step, atom and redox economy had to be employed to access the corresponding α -branched α,β -epoxyaldehydes. Yet these structures serve as some of the most frequently employed synthons in total synthesis and other transformations (cf. Section 2.2.5). A growing body literature from our and other laboratories indicated that primary amine catalysts can often overcome the challenges of activating sterically hindered substrates (cf. Section 2.1.3.2). With these considerations in mind, and drawing on the results from our laboratory on the epoxidation of various α,β -unsaturated ketones^[80, 82] we hypothesized that the primary amine **9** could serve as a suitable catalytic platform for the epoxidation of α -branched enals.

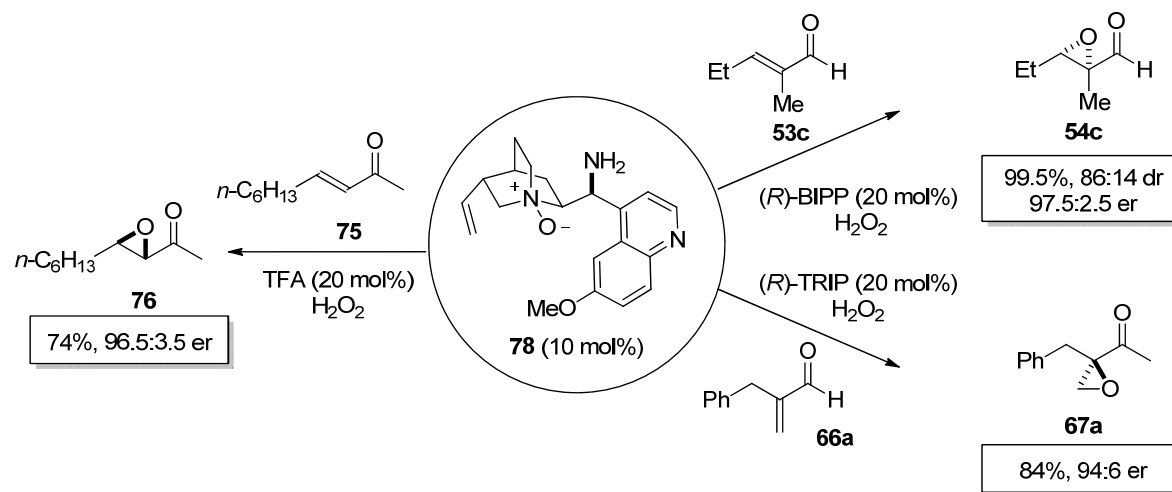
Focusing on the epoxidation of α,β -disubstituted enals **53** first, we discovered that catalytic salts of the primary amine **9** with the axially chiral BINOL-derived phosphoric acid (*R*)-BIPP (**63a**) promoted the epoxidation with outstanding enantioselectivity, and good to excellent diastereoselectivity and yields for a variety of linear and cyclic enals **53** (Scheme 5.1, (a)). *Z*-configured enals were found to undergo the epoxidation with partial diastereoconvergence, giving the same major product as the *E*-configured enals albeit with reduced stereoselectivity and yield (cf. Section 4.1.5.2). Expanding the reaction scope to α -branched acroleins **66** in which the enantiodiscriminating step operates under a different mechanistic regime (cf. Section 4.1.4), we found that a slightly different catalytic salt consisting of **9** and the bulkier phosphoric acid (*R*)-TRIP (**3**) mediated the reaction with excellent enantioselectivity and good yields (Scheme 5.1, (b)). In addition, a highly efficient kinetic resolution could be applied to the β' -substituted substrate *rac*-**66e** (cf. Section 4.1.5.3).

5. Summary



Scheme 5.1 Catalytic asymmetric epoxidation of α -branched α,β -unsaturated aldehydes achieved in this work.

Mechanistic studies aimed at elucidation of the catalytic intermediates and the rationalization of the absolute stereochemistry (in the epoxidation of enals **53**) were also carried out. During the course of these investigations, an *in situ* catalyst oxidation pathway, first identified by *C. Reisinger* in our group, was clarified. This pathway, which is common to all reactions catalyzed by **9** in the presence of hydrogen peroxide, was found to selectively generate *N*-oxide **78** under the reaction conditions. Compound **78** was found to be inactive as an oxygen transfer reagent (cf. Section 4.1.6.1), but a very powerful catalyst in the epoxidation of three different substrate classes, comparable to the unmodified amine **9** (Scheme 5.2).



Scheme 5.2 Product of *in situ* catalyst oxidation **78** and its catalytic competence.

5. Summary

The fact that *N*-oxidation of the catalyst's quinuclidine moiety does not appear to disrupt the formation of a highly organized transition state in all of the epoxidation reactions raises interesting mechanistic questions and encourages further studies.

Preliminary investigations aimed at catalyst recycling indicate that *N*-oxide **78** can be cleanly reduced back to **9**, albeit in a modest yield (56%). Although this reaction was not yet optimized, we anticipate that an efficient process can be developed through minor adjustment of the reaction conditions.

Finally, we performed extensive NMR studies on the catalytically relevant imine salts $[\mathbf{80}+\text{H}]^+\text{X}^-$ to rationalize the absolute configuration imparted to products **54** by the salts of catalyst **9**. These investigations clearly identified the ground state conformation of the iminium $[\mathbf{80}+\text{H}]^+$, which was found to be rigidified by an intramolecular hydrogen bridge (Figure 5.1). The counteranion was also found to be of critical importance for stereoselectivity but not yield, and determined to exist in a close albeit non-specific association with the iminium cation. Computational studies generated a model of the iminium cation with excellent agreement to the NMR data. Based on these ground-state conformational studies and experimental data, we propose an enantioselectivity model where the dynamic quinoline moiety of the amine catalyst **9** acts to shield the *re*-(β) face of the substrate, while the large and/or chiral counteranion from the Brønsted acid co-catalyst reinforces this facial selectivity by coordinating to the small hydrogen peroxide nucleophile, and by acting as a proton acceptor in the transition state (Figure 5.1).

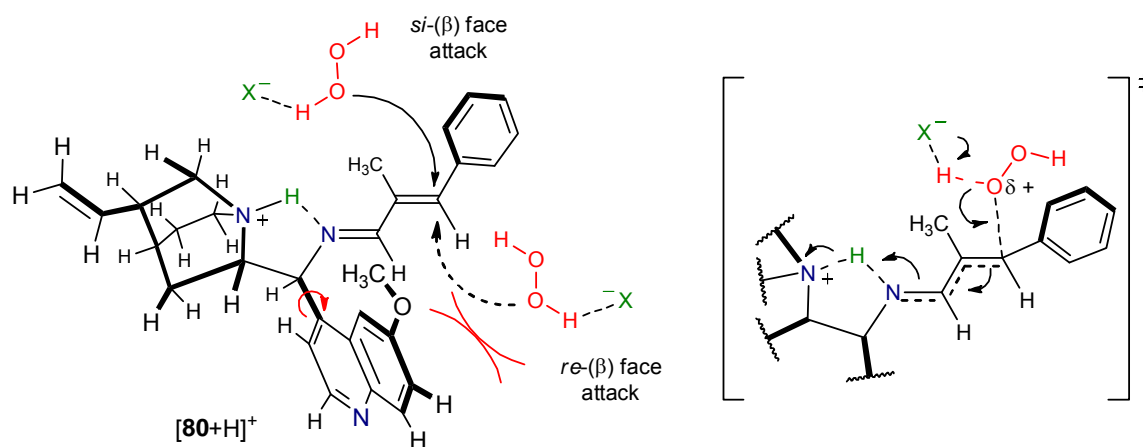


Figure 5.1 Proposed origin of facial selectivity and transition state in the epoxidation of enals **53**.

Similar studies on the epoxidation of acroleins **66** were not performed since the enantiodiscriminating step of the reaction presumably involves a very short-lived hydroperoxy enamine adduct **82** (Figure 5.2, *E/Z* geometry not determined). The leaving group is likely

5. Summary

activated by the Brønsted acid co-catalyst in the transition state,^[93] as shown in the two possible structures **82**.

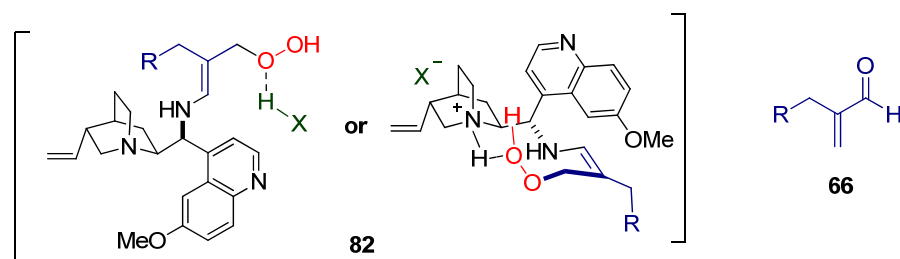


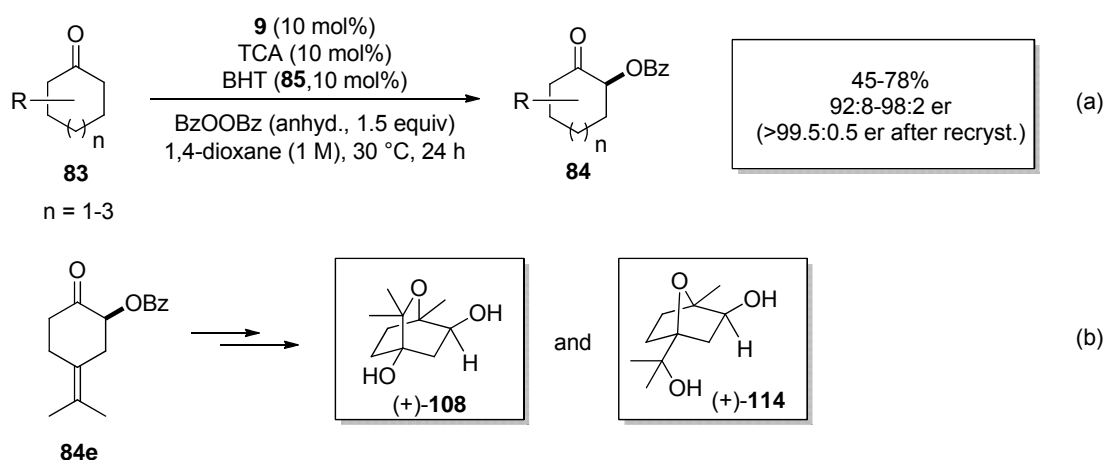
Figure 5.2 Putative catalytic intermediate involved in the enantiodiscriminating step of epoxidation of α -branched acroleins **66** (enamine geometry undetermined).

Encouraged by the excellent reactivity and enantioselectivity of 9-amino(9-deoxy)*epi*quinine **9** in the epoxidation of sterically demanding substrates, we decided to explore this catalyst in other oxidative transformations. As a consequence, we have developed an efficient, operationally simple and highly enantioselective methodology for the α -benzoyloxylation of cyclic ketones using a trichloroacetic acid salt of **9** as the catalyst, and anhydrous benzoyl peroxide as the inexpensive and easy-to-handle oxidant. Our approach took inspiration from the catalytic asymmetric α -benzoyloxylation methodologies for simple unbranched aldehydes using secondary amine catalysts (cf. Section 2.3.2.1)^[118-120] The high reactivity of benzoyl peroxide with secondary amines posed a unique challenge in catalyst design, and in all of the reports bulky groups were included around the reactive nitrogen centre to prevent catalyst decomposition. Although ensuring catalyst stability, this steric bulk inadvertently limited the substrate scope to unencumbered and highly reactive substrates. Indeed, ketones and α -branched aldehydes were not amenable to the developed α -benzoyloxylation methodologies, presumably due to difficulties of the catalysts in forming congested covalent intermediates. Alternative oxidation strategies using nitrosobenzene suffered from poor *O/N* chemoselectivity, and/or the need for a large excess of the carbonyl substrate.^[97] Our studies on the cinchona alkaloid-derived primary amine catalysts for organocatalytic epoxidation reactions^[82, 91, 136] identified this catalyst class as not only active with hindered substrates but also stable to oxidation, and encouraged us to test it in the α -benzoyloxylation reactions.

Over the course of our investigations, we discovered that the catalyst salt **9**·TCA promotes the α -benzoyloxylation of cyclic ketones **83** with excellent enantioselectivity and good yields (Scheme 5.3, (a)). An excess of water in the reaction was determined to be deleterious to conversion, and anhydrous benzoyl peroxide was identified as the optimal oxidant. A range of functional groups, pre-existing stereocenters and ring sizes in ketones **83** could be tolerated. In

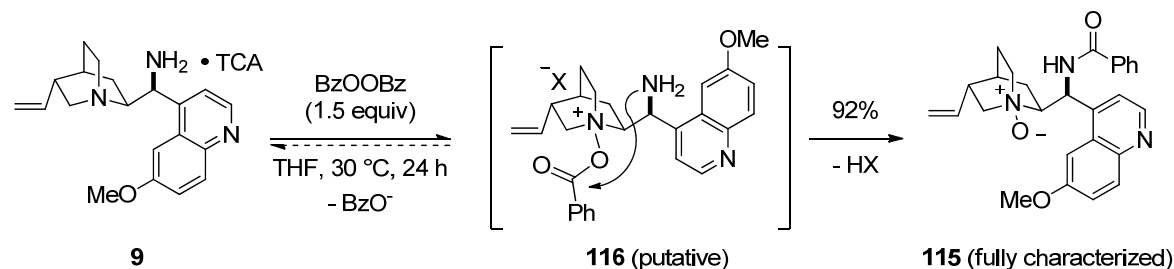
5. Summary

addition, the reaction was found to be amenable to large-scale synthesis without any loss in yield or enantioselectivity, and could be carried out in the industrially valuable solvent 2-methyltetrahydrofuran. A concise, enantioselective synthesis of putative natural products (+)-2 β ,4-dihydroxy-1,8-cineole **108** and 2 β ,4-dihydroxy-1,4-cineole **114**^[156] could be carried out by using the developed α -benzoyloxylation as the key enantioselective step (Scheme 5.3, (b)).



Scheme 5.3 Scope of the α -benzoyloxylation of cyclic ketones **83** (a), and synthesis of putative natural products **108** and **114** using α -benzoyloxylation as the key step (b).

Mechanistic studies revealed that the optimal catalyst salt **9**·TCA undergoes decomposition in the absence of a ketone substrate by a reaction with benzoyl peroxide. Observation of an unstable intermediate by NMR suggested that this decomposition occurs by an initial *N*-benzoyloxylation of the quinuclidine moiety (putative intermediate **116**) followed by an intramolecular rearrangement (Scheme 5.4). Triply protonated species [**9**·3TCA] was found to be resistant to this process.



Scheme 5.4 Decomposition of catalyst salt **9**·TCA by benzoyl peroxide in the absence of the ketone substrate.

Based on these observations, similar *N*-benzoyloxylation of the catalytically relevant enamine intermediate cannot be excluded as a mechanistic scenario, which promotes α -benzoyloxylation

5. Summary

of ketones by an intramolecular rearrangement (Figure 5.3, (a)). Indeed, extensive catalyst decomposition $9 \cdot \text{TCA} \rightarrow 115$ was found to occur either in the absence of a ketone substrate or *at the end* of the benzoyloxylation reaction with ketone **83a**, i.e. when the concentration of ketone **83a** is low. At high ketone concentration, the desired α -benzoyloxylation was the only productive pathway, even though facile quinuclidine *N*-benzoyloxylation would still be expected. No conclusive experimental support could be obtained for this hypothesis, however, making further mechanistic studies necessary. An alternative, intermolecular mechanistic scenario is equally likely (Figure 5.3, (b)).

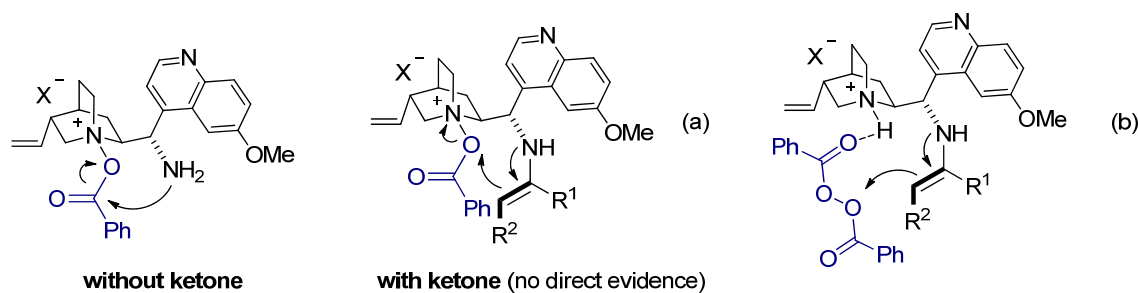
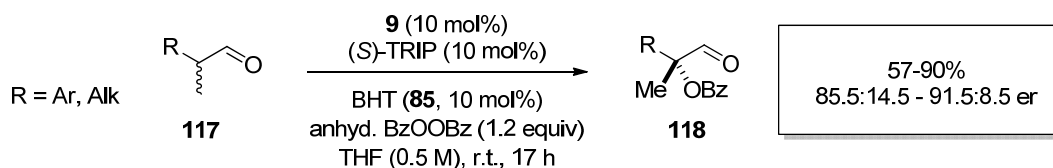


Figure 5.3 Possible mechanistic scenarios of the α -benzoyloxylation of ketones *via* an intramolecular rearrangement (a), and an intermolecular substitution reaction (b).

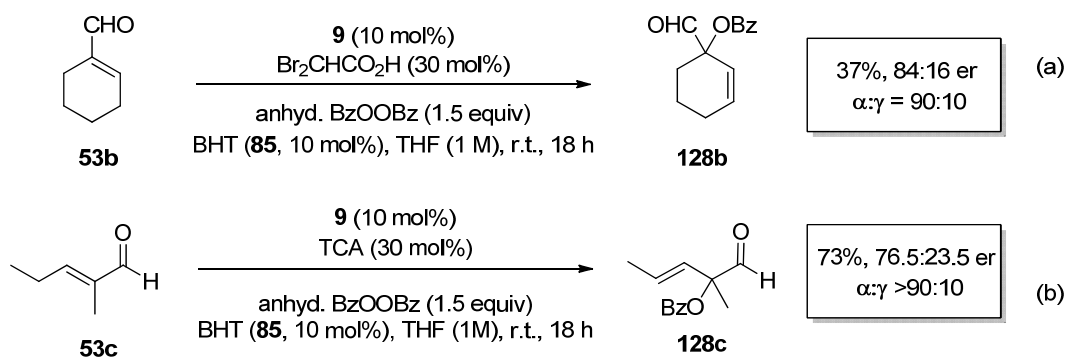
Preliminary studies aimed at expanding the α -benzoyloxylation protocol to α -branched aldehydes revealed that the catalyst **9** paired with the chiral phosphoric acid (*S*)-TRIP could mediate the reaction with excellent yields and useful enantioselectivities up to 91.5:8.5 er for a range of aromatic and aliphatic aldehydes **117** (Scheme 5.5).



Scheme 5.5 Preliminary scope of the α -benzoyloxylation of α -branched aldehydes **117**.

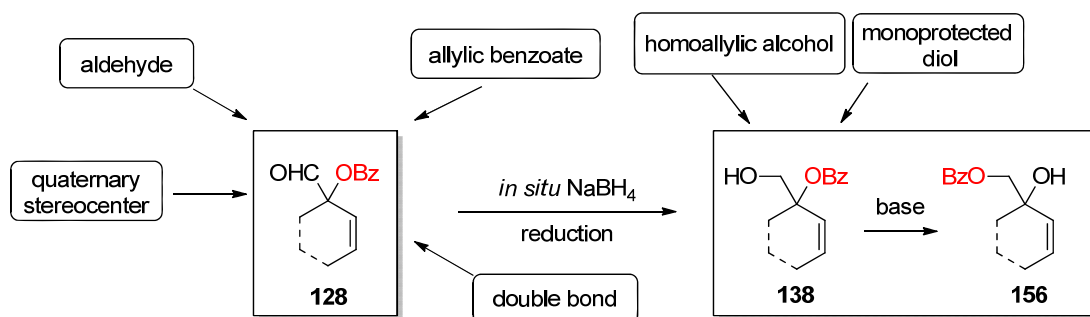
Finally, the α -benzoyloxylation method was also extended to α -branched enals **53** by invoking dienamine catalysis. The desired transformation was shown to occur with good yields and promising enantioselectivity for both cyclic and linear substrates (Scheme 5.6). High α -regioselectivity favouring the formation of quaternary stereocenters was observed, which represents an unusual case of reactivity in dienamine catalysis (cf. Section 2.1.3.4).

5. Summary



Scheme 5.6 Preliminary results for the α -benzoyloxylation of the cyclic α -branched enal **53b** (a), and linear α -branched enal **53c**.

Importantly, the resulting products **128** represent extremely useful building blocks, possessing a quaternary stereocenter and three different handles for further functionalization, including a reactive aldehyde moiety, an allylic benzoate, and a double bond. In addition, simple reduction of the aldehyde moiety with NaBH₄ in the same pot at the end of the reaction affords a monoprotected diol **138**,^{xvii} which contains an allylic and a homoallylic alcohol (Scheme 5.7). Simple equilibration under basic conditions furthermore quantitatively transforms **138** into the allylic alcohol **156**.

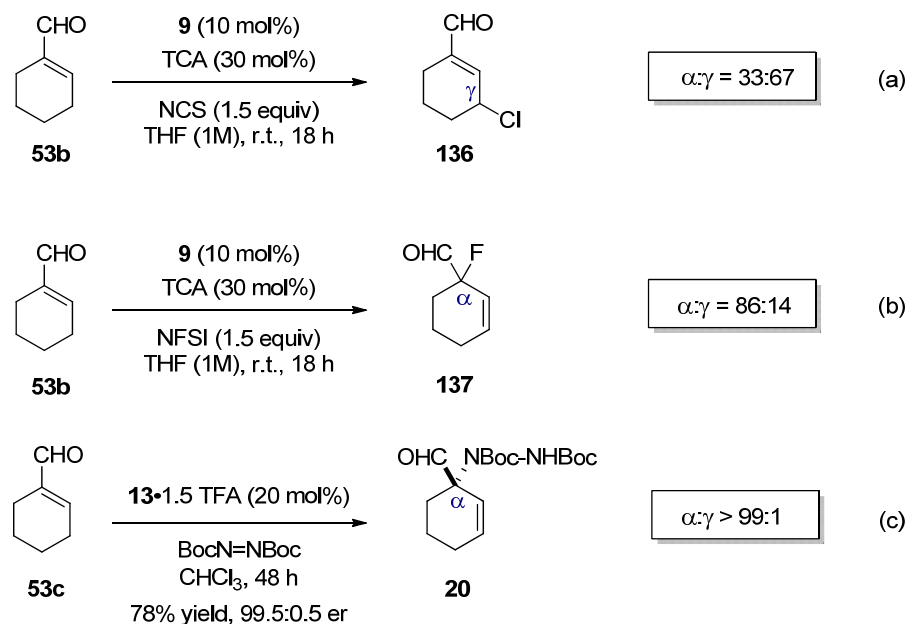


Scheme 5.7 Synthetic versatility of products **128**.

A brief examination of other electrophiles with the enal **53b** revealed that α/γ selectivity in reactions catalyzed by **9** is reaction- and not catalyst-specific. In particular, chlorination with NCS using catalyst **9** favoured the γ -product **136**, while fluorination with NFSI using catalyst **9** and amination with BocN=NBoc using the closely related catalyst **13** favoured the α -products **137** and **20**, respectively (Scheme 5.8).

^{xvii} Short reaction times (10 min) or low temperatures (-78 °C) are necessary to isolate **138** which isomerizes to **156** under the conditions of NaBH₄ reductions with prolonged stirring at room temperature (cf. Chapter 7 for details).

5. Summary



Scheme 5.8 α/γ Selectivity of catalyst **9** and its saturated congener **13** in the dienamine-catalyzed chlorination (a), fluorination (b), and amination (c) of α -branched enal **53b**.

This work has been disclosed in part in the following publications:

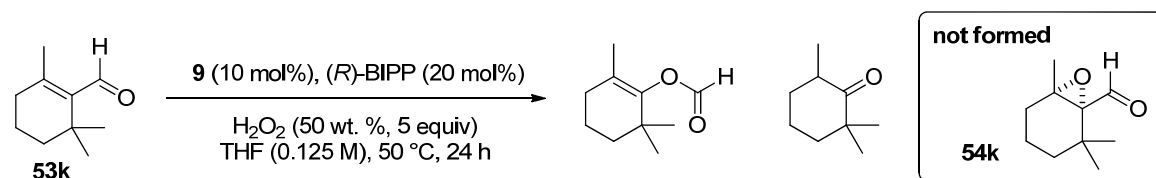
“Catalytic Asymmetric Epoxidation of α -Branched Enals”: O. Lifchits, C. M. Reisinger, B. List, *J. Am. Chem. Soc.* **2010**, *132*, 10227.

“Direct Asymmetric α Benzoyloxylation of Cyclic Ketones”: O. Lifchits, N. Demoulin, B. List, *Angew. Chem.* **2011**, *123*, 9854; *Angew. Chem. Int. Ed.* **2011**, *50*, 9680.

6. OUTLOOK

6.1 Epoxidation of Sterically Hindered Electron-Deficient Olefins

As described in Section 4.1, we have identified catalyst salts **9**·(*R*)-BIPP and **9**·(*R*)-TRIP which promote the epoxidation of α -branched enals **53** and **66**, respectively, with good yields and outstanding enantioselectivities. While the protocol appears to be very general for a variety α,β -disubstituted enals and α -substituted acroleins, more dense enals represent a limitation of the method. In particular, substrates containing a tetrasubstituted double bond are inert to the reaction conditions. β -Cyclocitral **53k**, for example, was found to undergo *Baeyer-Villiger* type decomposition under the optimized reaction conditions, instead of the desired epoxidation (Scheme 6.1). This strongly suggests the absence of iminium activation of the double bond *via* covalent catalysis. Presumably, the high steric hindrance around the aldehyde group in **53k** prevents its condensation with the catalyst **9**. In the absence of this catalytic pathway, non-catalyzed addition of hydrogen peroxide (present in excess and at 50 °C) to the substrate's aldehyde group leads to the formation of the observed decomposition products.



Scheme 6.1 Limitation of the epoxidation methodology with trisubstituted enals.

Two possible approaches can be pursued to solve this problem. Firstly, non-covalent catalysis may be employed to activate hindered enals. Although the aldehyde group is notoriously difficult for such activation, recent progress in so-called “super Brønsted acid catalysis” has made a variety of reactions relying on electrophilic activation of aldehydes possible.^[167] Secondly, covalent catalysis using smaller and more reactive Lewis bases might prove successful, since reducing the steric bulk of the catalyst has been proven effective in tackling sterically demanding substrates. Preliminary investigations revealed that small amines such as ammonia, methylamine and longer-chain primary aliphatic amines are unreactive with tetrasubstituted enals such as **53k** at atmospheric pressure, presumably due to their low nucleophilicity. An intriguing approach based on α -heteroatom effect^[168] has recently been introduced to create powerful Lewis base catalysts **138** containing a cyclic hydrazine core (Scheme 6.1).^[169] These catalysts mimic secondary and primary amines, but are more nucleophilic due to the electronic contribution of the α -nitrogen. Just like their amine

6. Outlook

counterparts, secondary hydrazines **138a** proved to be best for the iminium-like activation of unsaturated aldehydes, while the primary hydrazine **138b** was found to be optimal for less reactive enones.^[169]

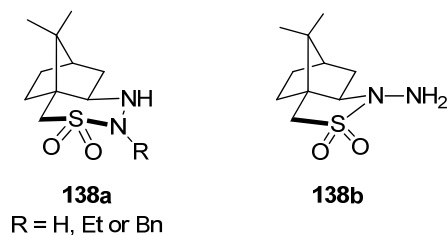
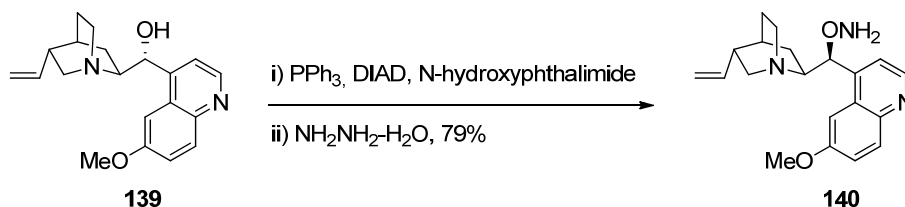


Figure 6.1 Examples of cyclic hydrazines used as more nucleophilic mimics of secondary and primary amine catalysts.^[168]

Catalysts of type **138b** might prove to be more reactive with hindered enals **53**. Another, yet unexplored, scaffold for more nucleophilic yet less sterically demanding Lewis bases could be based on hydroxylamines. These structures are expected to not only possess increased nucleophilicity due to the α -heteroatom effect, but also a particularly unencumbered primary amine functionality due to a small oxygen linker. In our investigations toward this end, we successfully synthesized hydroxylamine **140** from natural quinine **139** (Scheme 6.2).



Scheme 6.2 Synthesis of the hydroxylamine derivative **140** from quinine **139**.

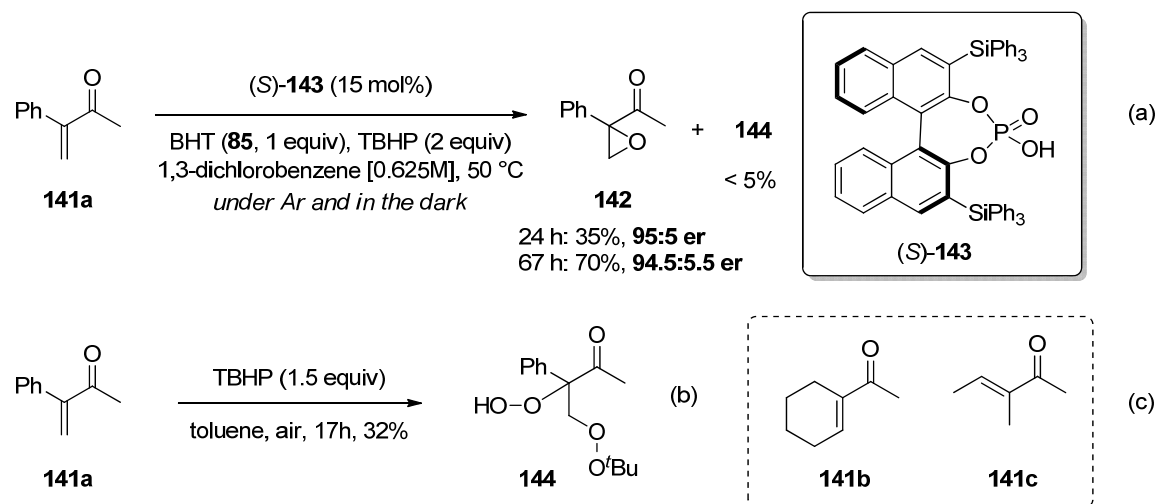
Unfortunately, **140** failed to catalyze epoxidation of sterically hindered enals **53**, when used with a phosphoric or trifluoroacetic acid co-catalyst. However, we suspect that this lack of reactivity is attributable to the weak basicity of the hydroxylamine nitrogen leading to sluggish protonation of the imine intermediates, necessary for the LUMO-lowering activation of the substrate. A solution to this problem could be highly acidic “super-Brønsted acids” used in combination with **140** or similar structures, which have not been attempted yet.

A very similar problem of substrate activation exists for α -branched enones, for which no general and enantioselective epoxidation method exists to date. *Julia-Colonna*^[170] and PTC^[171] catalysis cover a very narrow substrate scope and generally offer moderate enantioselectivity; isolated examples of Brønsted acid/Brønsted base activation with chiral secondary amines^[42b],

6. Outlook

^{172]} are also poorly enantioselective with this substrate class. Although *Melchiorre* and colleagues have recently disclosed a relatively efficient catalytic asymmetric sulfa-*Michael* reaction of α -branched enones using the cinchona-derived primary amine catalyst **15** and various Brønsted acid co-catalysts,^[173] the method is limited to highly nucleophilic thiols as nucleophiles. This limitation, together with the strong dependence of the reaction on solvent cast doubt on the covalent nature of the catalysis, proposed by the authors. Indeed, we found that α -branched enones are quite resistant to forming iminium intermediates, even with less hindered primary amine catalysts such as **15**.

Our own efforts on the epoxidation of α -branched enones have revealed that substrate **141a** can react with nucleophilic *tert*-butyl peroxide to form epoxide **142** in the absence of iminium activation, although long reaction times are necessary for useful yields (Scheme 6.3, (a)). Brønsted acid (*S*)-**143**^[174] alone, which presumably catalyzes the enantioselective epoxide ring-closure step after initial (uncatalyzed) oxa-*Michael* addition is sufficient to effect up to 95:5 er for product **142**. Importantly, the high reactivity of enone **141** leads to an uncatalyzed and presumably radical side reaction under ambient atmosphere in the presence of *tert*-butyl peroxide forming the tetraoxygenated compound **144** (Scheme 6.3, (b)). This side reaction can be effectively suppressed by the addition of radical inhibitor BHT (**85**), whereby the best results were obtained with 1 equiv of BHT and by carrying out the reaction under argon (i.e. with the exclusion of ambient oxygen) and in the dark.



Scheme 6.3 Epoxidation of α -branched enone **141a** with Brønsted acid catalyst (*S*)-**143** in the absence of iminium catalysis (a), radical side reaction of **141a** with *tert*-butyl peroxide under ambient atmosphere (b), and substrates which are unreactive under the optimized conditions (c).

Despite these promising results, we found that the less reactive aliphatic substrates **141b** and **141c** were inert to the reaction conditions, suggesting that activation of the substrate toward the

6. Outlook

initial oxa-*Michael* addition by the peroxide reagent is crucial. Although a screen of numerous small amines and hydroxylamines was not successful in effecting iminium catalysis, approaches discussed above for hindered enals **53** had not been tried and represent a possible solution to this long-standing problem.

Our mechanistic studies of the catalytic intermediates in the epoxidation of enals **53** also raise interesting questions. As discussed in Section 4.1.6.1, catalyst **9** was found to undergo *N*-oxidation of the quinuclidine moiety during all epoxidation reactions to form compound **78**. Employing isolated **78** as a catalyst in the epoxidation of enals **53**, **66** and enone **75**, we found essentially unchanged yields and enantioselectivities compared to the standard reaction with catalyst **9**. This implies that *N*-oxidation of the quinuclidine moiety of **9** might not change the active conformation of the catalyst in the transition state. Detailed structural investigations of the corresponding imine adduct **145** (Figure 6.2) would therefore be of immense value. In particular, we expect that the pseudo-five-membered ring formed by a hydrogen bond between the iminium and the quinuclidine moiety of the protonated adduct $[\mathbf{80}+\text{H}]^+$ observed by NMR (cf. Section 4.1.6.2), must be preserved in the analogous *N*-oxidized imine adduct $[\mathbf{145}+\text{H}]^+$ as an extended pseudo-six-membered ring (Figure 6.2). A similar type of hydrogen bonding between tertiary amine *N*-oxides and amide hydrogens is well documented, and serves as the basis of dimeric organocatalysts **146**^[175] (Figure 6.2).

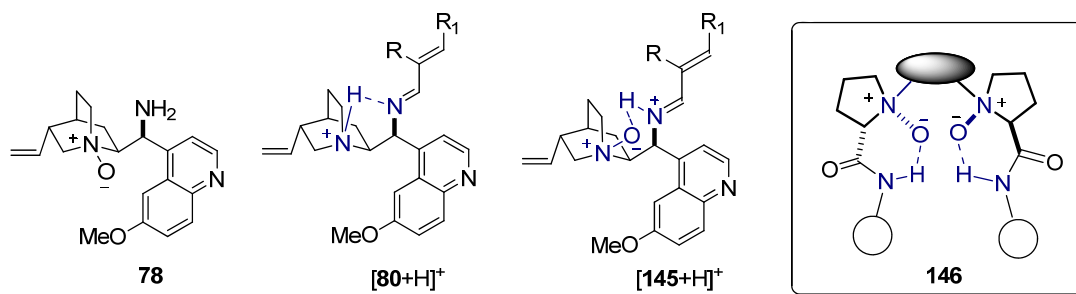


Figure 6.2 Predicted conformation of the protonated imine adduct $[\mathbf{145}+\text{H}]^+$ formed between *N*-oxidized catalyst **78** and an α -branched enal, in analogy to $[\mathbf{80}+\text{H}]^+$ observed by NMR (cf. Section 4.1.6.2) and catalysts of type **146**.^[175]

Our initial attempts at synthesizing **145** proved unsuccessful, as neither condensation of **78** with α -methyl cinnamaldehyde **53a** under optimized conditions (cf. Section 4.1.6.2), nor *N*-oxidation of **80** with *m*-CPBA provided the desired product. However, condensation of **78** with **53a** in the presence of 1 equiv TFA and 3 Å mol. sieves afforded **145**·TFA with 76% conversion after 17 hours. We expect that a longer reaction time would afford **145**·TFA with full conversion, allowing facile characterization of this salt by various NMR techniques.

6.2 Benzoyloxylation of Carbonyl Compounds

Mechanistic investigations of the catalytic asymmetric α -benzoyloxylation of cyclic ketones with amine **9** is another highly interesting area for further research. In particular, we have shown a catalyst degradation pathway which produces the derivative **115** from **9** and presumably proceeds *via* the unstable *N*-benzoyloxyated intermediate **116** (cf. Section 4.2.1.5). This observation raises the possibility of *N*-benzoyloxyated catalytic intermediate **A** which acts as an intramolecular benzoyl transfer reagent (Figure 6.3). On the other hand, a simple intermolecular mechanism shown in assembly **B** is also possible, necessitating a study to distinguish the two potential mechanisms.

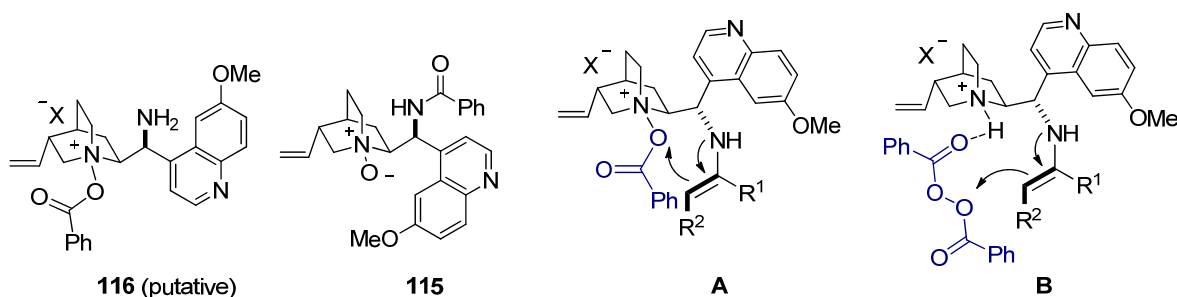
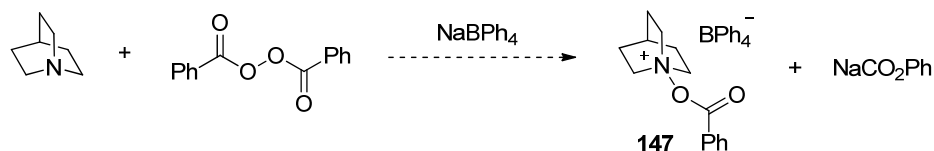


Figure 6.3 Observed catalyst decomposition product **115** formed from the rearrangement of the putative intermediate **116** and the possible mechanisms of ketone α -benzoyloxylation promoted by catalyst **9**.

Reacting the intermediate **116** with a ketone substrate in the absence of benzoyl peroxide could clarify if an intramolecular benzoyl transfer is possible. However, isolation of **116** is impossible since it only exists as an unstable intermediate and completely decomposes into **115** during the course of its synthesis. One way to approach this problem could involve the synthesis of *N*-benzoyloxyated quinuclidine salt **147**, which can be stabilized as a tetraphenyl borate salt^[176] (Scheme 6.4)

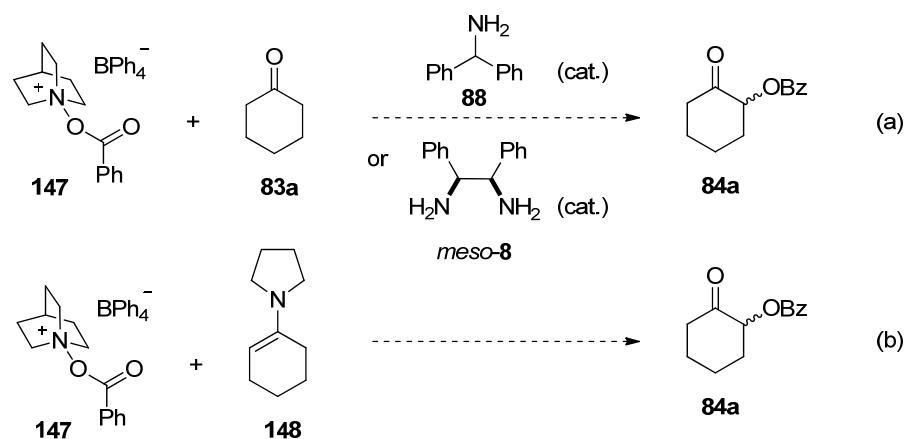


Scheme 6.4 Proposed synthesis of *N*-benzoyloxyated quinuclidine salt **147** to be used as a mechanistic probe.

The isolated salt **147** could then be used as a potential benzoyl transfer reagent in a reaction with the ketone substrate **83a** and a primary amine catalyst **88** or *meso*-**8** for the activation of ketone

6. Outlook

as an enamine (Scheme 6.5, (a)). Since there exists a possibility of the amine catalyst reacting with **147** instead of forming an enamine intermediate with the ketone **83a**, a preformed enamine **148** which is stable under anhydrous conditions could be used instead (Scheme 6.5, (b)). Formation of the α -benzyloxyated product **84a** in either reaction shown in Scheme 6.5 would be a strong indication for a mechanistic scenario involving an intramolecular benzoyl transfer.



Scheme 6.5 Proposed mechanistic studies to test the possibility of intramolecular benzoyl transfer in the α -benzyloxylation of ketones **83**.

Preliminary studies on the catalytic asymmetric α -benzyloxylation of α -branched aldehydes **117** and enals **53** revealed that primary amine catalysis holds significant promise. The high yields and useful enantioselectivities obtained with both substrate classes indicate that a highly enantioselective method is possible through suitable catalyst optimization. The corresponding products **118** and **128** bearing quaternary stereocenters represent extremely useful synthetic building blocks, for which no direct, general and enantioselective approaches exist yet.

7. EXPERIMENTAL SECTION

7.1 General Experimental Conditions

Solvents and reagents

All solvents used in the standard procedures were purified by distillation. Absolute diethyl ether, tetrahydrofuran and toluene were obtained by distillation over sodium with benzophenone as indicator; absolute chloroform and dichloromethane were obtained by distillation over calcium hydride, and ethanol, isopropanol and methanol were dried by distillation over magnesium. Absolute 1,4-dioxane, MTBE, DME, acetonitrile and DMSO were purchased from Sigma-Aldrich and used as received. Unsaturated aldehydes **53** were obtained from commercial sources (Sigma-Aldrich, TCI Europe) and used without purification if freshly purchased or distilled prior to use. All other commercial reagents were obtained from various sources and used without further purification.

Catalysts

Chiral binaphthol derived phosphoric acids **3** and **63** were prepared according to, or in analogy with the reported procedures of *Akiyama, Terada* and colleagues.^[177] Chiral binaphthol derived phosphoric acid **143** was prepared according to the procedure of *MacMillan et al.*^[174] Chiral binaphthol derived disulfonamide **57** and bis-sulfonic acid **62** were prepared according to the procedure of *List* and co-workers.^[178] Primary amine catalysts 9-amino(9-deoxy)*epi*quinine **9**, 9-amino(9-deoxy)*epi*cinchonidine **10**, 9-amino(9-deoxy)*epi*quinidine **11**, 9-amino(9-deoxy)*epi*cinchonine **12**, 9-amino(9-deoxy)*epi*hydroquinine **13** and 9-amino(9-deoxy)*epi*cupreine **15** were prepared according to the procedure of *Soós et al.*^[177i] with modifications by *Reisinger*.^[136] The secondary catalyst **4** was prepared by *X. Wang* according to the reported procedure.^[36]

Inert gas atmosphere

Air and moisture sensitive reactions were conducted under an atmosphere of argon (*Air Liquide*, >99.5% purity). Unless otherwise stated, all organocatalytic reactions were performed under an ambient atmosphere without the exclusion of moisture or air.

7. Experimental Section

Chromatographic analysis and purification

Reactions were monitored by **thin layer chromatography (TLC)** on silica gel pre-coated plastic sheets (0.2 mm, Machery-Nagel). Visualization was accomplished by irradiation with UV light at 254 nm and/or *p*-anisaldehyde stain (0.7 mL *p*-anisaldehyde, 250 mL EtOH, 9.5 mL conc. H₂SO₄, 2.7 mL glacial AcOH) or potassium permanganate stain (1.5 g KMnO₄, 10 g K₂CO₃, 1.25 mL 10% NaOH, 200 mL H₂O). Preparative scale TLC was performed on Macherey-Nagel glass plates (SIL G-25 UV₂₅₄).

Flash column chromatography was performed using Merck silica gel (60, particle size 0.040-0.063 mm) using a specified solvent mixture and elevated pressure.

Gas chromatography (GC) was performed on HP 6890 and 5890 Series instruments equipped with a split-mode capillary injection system and a flame ionization detector (FID) using hydrogen as carrier gas. The following stationary phase columns were used in this work:

Hydrodex-β TBDAc (25 m x 0.25 mm): heptakis-(2,3-di-*O*-acetyl-6-*O*-*t*-butyldimethylsilyl)-β-cyclodextrin

BGB-176SE/ SE-52 (30 m x 0.25 mm): 2,3-dimethyl-6-*tert*-butyldimethylsilyl-β-cyclodextrin

Lipodex G (25 m x 0.25 mm): octakis-(2,3-di-*O*-pentyl-6-*O*-methyl)-γ-cyclodextrin

BGB-177/BGB-15 (30 m x 0.25 mm): 2,6-dimethyl-3-pentyl-β-cyclodextrin

BGB-174/BGB-1701 (25 m x 0.25 mm): 2,3-dimethyl-6-*tert*-butyldimethylsilyl-β-cyclodextrin

BGB-178/BGB-15 (30 m x 0.25 mm): 2,3-diethyl-6-*tert*-butyldimethylsilyl-β-cyclodextrin

High pressure liquid chromatography (HPLC) was performed on a Shimadzu LC-2010C system equipped with a spectrophotometric detector or a diode array. Commercial HPLC-grade solvents were used, and measurements were conducted at 25 °C. The chiral stationary phase of the columns is specified in each experiment.

Nuclear magnetic resonance (NMR)

Spectra were recorded on Bruker DPX (¹H: 300 MHz, ¹³C: 75.5 MHz), Bruker AV 400 (¹H: 400 MHz, ¹³C: 100.8 MHz), Bruker AV 500 (¹H: 500 MHz, ¹³C: 125 MHz) and Bruker AV 600 (¹H: 600 MHz, ¹³C: 150 MHz, ¹⁵N: 60 MHz, ¹⁹F: 376 MHz, ³¹P: 240 MHz) spectrometers. The

7. Experimental Section

spectra were recorded at room temperature (298 K) unless otherwise stated. Proton chemical shifts are reported in ppm (δ) relative to tetramethylsilane (TMS, 0 ppm) with the solvent resonance employed as the internal standard (CDCl_3 δ 7.26). ^{13}C chemical shifts are reported in ppm from tetramethylsilane (TMS) with the solvent resonance as the internal standard (CDCl_3 , δ 77.0). ^{31}P chemical shifts are reported in ppm relative to H_3PO_4 (0 ppm), ^{15}N shifts are reported in ppm relative to NH_3 (0 ppm), and ^{19}F are reported in ppm relative to CFCl_3 (0 ppm). Data are reported as follows: chemical shift, multiplicity (s = singlet, d = doublet, q = quartet, Q = quintuplet, h = heptuplet, m = multiplet, br = broad, c.m = centered multiplet), coupling constants J (Hz) and integration.

Mass spectrometry (MS)

Mass spectra were measured on a Finnigan MAT 8200 (70 eV) or MAT 8400 (70 eV) by electron ionization, chemical ionization or fast atom/ion bombardment techniques. High resolution mass spectra were obtained on a Bruker APEX III FT-MS (7 T magnet). All masses are given in atomic units/elementary charge (m/z) and reported in percentage relative to the basic peak.

Specific rotation

Optical rotations were determined with Autopol IV polarimeter (Rudolph Research Analytical) using a 0.5 mL cell with a path length of 1 dm at 589 nm (sodium D-line) and 25 °C. Data are reported as follows: $[\alpha]_{\lambda}^{\text{temp}}$, concentration (c in g/100 mL), and solvent.

Determination of enantiomeric ratios (er)

Enantiomeric ratios (er) were determined by chiral GC or chiral HPLC analysis by comparing samples with the appropriate racemic mixtures. All racemates of the epoxyaldehydes **54** and **67** and the corresponding alcohol products were prepared according to the procedure described by *Pihko et al.*^[88] All racemates of the α -benzoyloxyketones **84** and α -benzoyloxyaldehydes **118** were prepared according to the procedure of *Tomkinson et al.*^[179] Racemic compounds **128** were prepared analogously to the standard benzoyloxylation procedure for enals except using 10 mol% of *meso*-**8** and 10 mol% of TCA. Racemic **137** were prepared analogously to the standard fluorination procedure for enals except using 10 mol% of *meso*-**8** and 10 mol% of TCA. The absolute configuration was established by comparison of the optical rotation with the

7. Experimental Section

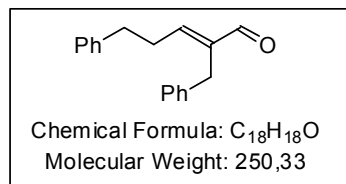
literature value as specified in individual experiments or X-ray crystallography (for compound **20**). All other absolute configurations were assigned by analogy.

Melting point (mp)

All melting points were measured on a *Büchi* 540 Melting Point apparatus in open glass capillaries. The values are given in °C and are uncorrected.

7.2 Catalytic Asymmetric Epoxidation of α -Branched Enals

7.2.1 Preparation of the Starting Materials



(E)-2-benzyl-5-phenylpent-2-enal (53e) Following the procedure of *Zumbansen et al.*,^[131] to a solution of 3-phenylpropanal (1 g, 7.45 mmol, 1 equiv) in dichloromethane (7.45 mL) was added morpholinium trifluoroacetate (300 mg, 1.49 mmol, 0.2 equiv) and the mixture was stirred at reflux for 19 h. Removal of the solvent under reduced pressure and flash chromatography (10% Et₂O in pentane) afforded **53e** as a colourless oil (800 mg, 3.2 mmol, 86%, E/Z = 97:3).

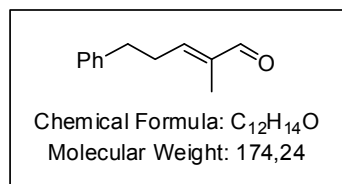
¹H NMR (500 MHz, CDCl₃) δ 9.43 (s, 1H, CHO), 7.30-7.27 (m, 2H, CH_{Ar}), 7.24-7.20 (m, 3H, CH_{Ar}), 7.17-7.09 (m, 5H, CH_{Ar}), 6.61 (apparent t, $J = 6.9$ Hz, 1H, C=CH), 3.57 (s, 2H, PhCH₂), 2.77-2.70 (m, 4H, PhCH₂CH₂).

¹³C NMR (125 MHz, CDCl₃): δ 194.6, 154.8, 142.8, 140.5, 139.1, 128.6, 128.5, 128.4, 128.3, 126.4, 126.1, 34.5, 31.1, 29.7.

FTIR (thin film) 3085, 3062, 3027, 2924, 2821, 2716, 1680, 1639, 1601, 1495, 1453, 1137, 1076, 1030, 1002, 883, 733, 697 cm⁻¹

HRMS (m/z) calcd for C₁₈H₁₈O [M]⁺: 250.1358, found: 250.1357.

The spectroscopic data are identical in all respects to those previously reported.^[129]



(E)-2-methyl-5-phenylpent-2-enal (53g) Following the procedure of *Chatterjee et al.*,^[132] to a stirring solution of *Grubbs* second generation catalyst **69** (53 mg, 0.063 mmol, 6.3 mol%) and 4-phenyl-1-butene (150.2 μ L, 1.0 mmol, 1 equiv) in dry dichloromethane (2.5 mL) under argon was added methacrylaldehyde (82.6 μ L, 1.0 mmol, 1 equiv) dropwise *via* a syringe. The mixture was stirred at reflux for 12 h and the solvent was removed under reduced pressure. Purification by flash chromatography (4% Et₂O in pentane) afforded **3e** as a yellow oil (226 mg, 1.3 mmol, 65%, E/Z > 20:1).

¹H NMR (500 MHz, CDCl₃) δ 9.38 (s, 1H, CHO), 7.33-7.19 (m, 5H, CH_{Ar}), 6.50 (tq, $J = 7.3$ Hz, $J = 1.3$ Hz, 1H, C=CH), 2.82 (apparent t, $J = 7.5$ Hz, 2H, PhCH₂), 2.68 (apparent q, $J = 7.5$ Hz, 2H, PhCH₂CH₂), 1.69 (br. s, 3H, CH₃).

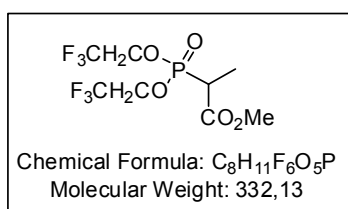
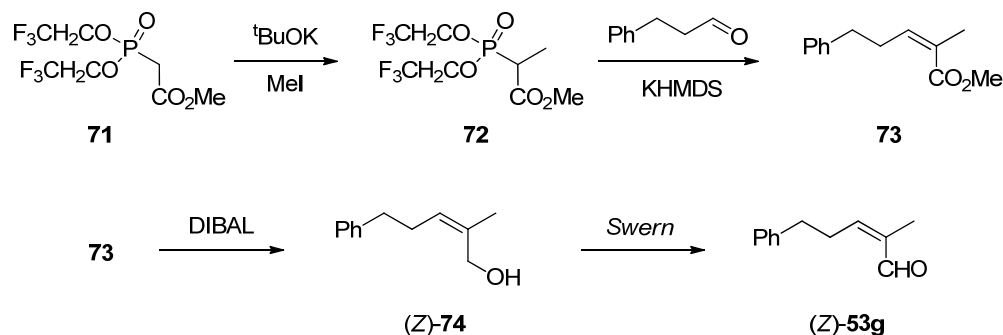
¹³C NMR (125 MHz, CDCl₃): δ 195.3, 153.3, 140.6, 139.9, 128.6, 128.4, 126.3, 34.4, 30.7, 9.2.

7. Experimental Section

FTIR (thin film) 3062, 3028, 2926, 2821, 2713, 1684, 1644, 1454, 1360, 1240, 1015, 700 cm^{-1}

HRMS (m/z) calcd for $\text{C}_{12}\text{H}_{14}\text{O}$ $[\text{M}]^+$: 174.1045, found: 174.1046.

The physical data are identical in all respects to those previously reported.^[180]



Methyl 2-(bis(2,2,2-trifluoroethoxy)phosphoryl)propanoate

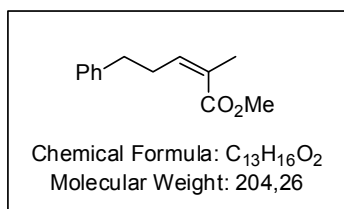
(72): Following the procedure of Sano *et al.*,^[134b] to a solution of $t\text{BuOK}$ (1.27g, 11.3 mmol, 1.2 equiv) in THF (13 mL) was slowly added methyl bis(2,2,2-trifluoroethyl)phosphonoacetate 71 (2 mL, 9.46 mmol, 1 equiv) at 0 °C under argon. The

mixture was stirred at 0 °C for 30 min under argon, and methyl iodide (2.96 mL, 47.3 mmol, 5 equiv) was slowly added at 0 °C. The solution was warmed up to room temperature, stirred for 23 h and treated with a saturated aqueous solution of NH_4Cl . The reaction mixture was extracted with EtOAc three times, dried over Na_2SO_4 , filtered and concentrated. Flash column chromatography eluting with 30% EtOAc in hexanes afforded 72 as a colourless oil (2.30 g, 6.93 mmol, 73%).

$^1\text{H NMR}$ (500 MHz, CDCl_3) δ : 4.49-4.38 (m, 4H, F_3CCH_2), 3.78 (s, 3H, CO_2CH_3), 3.20 (dq, $J_{\text{H,P}} = 22.8$ Hz, $J = 7.4$ Hz, 1H, $\text{P}(\text{O})\text{CHCH}_3$), 1.52 (dd, $J_{\text{H,P}} = 19.3$ Hz, $J = 7.4$ Hz, 3H, CH_3).

The physical data are identical in all respects to those previously reported.^[134b]

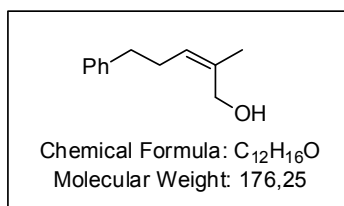
7. Experimental Section



(Z)-methyl 2-methyl-5-phenylpent-2-enoate (73): Following the procedure of *Still* and Gennari,^[133] a solution of **72** (332 mg, 1 mmol, 1 equiv) and 18-crown-6 (1.32 g, 5 mmol, 5 equiv) in THF (20 mL) was cooled to -78 °C under argon and treated with KHMDS (199.5 mg, 1 mmol, 1 equiv). 3-Phenylpropanal (133 μL, 1 mmol, 1 equiv) was added and the resulting mixture was stirred at -78 °C for 1h. Saturated aqueous solution of NH₄Cl was added and the product was extracted with diethyl ether three times, dried over Na₂SO₄, filtered and concentrated. The unsaturated ester **73** (Z/E > 20:1 by ¹HNMR) was used without purification.

¹HNMR (500 MHz, CDCl₃) δ: 7.30-7.17 (m, 5H, CH_{Ar}), 5.98 (td, *J* = 6.9 Hz, *J* = 1.2 Hz, 1H, C=CH), 3.72 (s, 3H, CO₂CH₃), 2.81-2.70 (m, 4H, PhCH₂CH₂), 1.89 (d, *J* = 1.2 Hz, 3H, CH₃).

The physical data are identical in all respects to those previously reported.^[133]

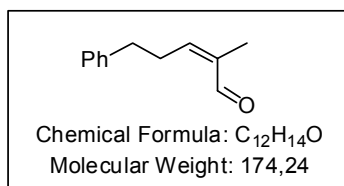


(Z)-2-methyl-5-phenylpent-2-en-1-ol ((Z)-74): Crude **73** (1 mmol) was dissolved in dichloromethane (3 mL) under argon and cooled to -78 °C. DIBAL (4.8 mL, 1M in hexanes, 4.8 mmol, 4.8 equiv) was added dropwise and the solution was stirred for 1 h at -78 °C. The reaction was quenched with aqueous Rochelle's salt and stirred vigorously for 2 h. The crude reaction mixture was extracted with dichloromethane three times, dried over Na₂SO₄, filtered and concentrated. Flash column chromatography eluting with 15% diethyl ether in pentane afforded (Z)-**74** as a colourless oil (93.2 mg, 0.53 mmol, 53% over two steps).

¹HNMR (500 MHz, CDCl₃) δ: 7.30-7.16 (m, 5H, CH_{Ar}), 5.33 (t, *J* = 7.6 Hz, 1H, C=CH), 3.92 (s, 2H, CH₂OH), 2.66 (apparent t, *J* = 7.2 Hz, 2H, PhCH₂CH₂), 2.37 (c. m, 2H, PhCH₂CH₂), 1.76 (d, *J* = 1.1 Hz, 3H, CH₃).

The physical data are identical in all respects to those previously reported.^[134a]

7. Experimental Section



(Z)-2-methyl-5-phenylpent-2-enal ((Z)-53g): Oxalyl chloride (50.3 μ L, 0.59 mmol, 2 equiv) was dissolved in dichloromethane (9 mL) and the solution was cooled to -78 $^{\circ}$ C. DMSO (83.2 μ L, 1.17 mmol, 4 equiv) was added dropwise

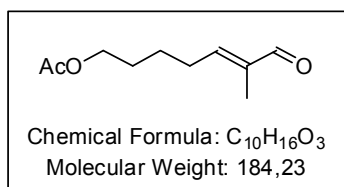
at -78 $^{\circ}$ C and the solution was stirred for 30 min. A solution of (Z)-74 in dichloromethane (2 mL) was added dropwise and the reaction was stirred for 30 min. Et₃N (244 μ L, 1.76 mmol 6 equiv) was added dropwise and the solution was stirred for 1 h at -78 $^{\circ}$ C. The reaction was warmed up to room temperature, treated with a saturated aqueous solution of NH₄Cl and extracted with dichloromethane three times, dried over Na₂SO₄, filtered and concentrated. ¹H NMR analysis of the crude reaction mixture indicated Z/E ratio of 97:3. Flash column chromatography eluting with 15% diethyl ether in pentane afforded (Z)-53g as a colourless oil (38.2 mg, 0.22 mmol, 75%, Z:E = 95:5).

¹H NMR (500 MHz, CDCl₃) δ : 10.0 (s, 1H, CHO), 9.38 (s, 0.05 H, *E*-isomer, CHO), 7.31-7.17 (m, 5H, CH_{Ar}), 6.53 (td, *J* = 8.0 Hz, 1H, C=CH), 2.91-2.78 (m, 4H, PhCH₂CH₂), 1.76 (d, *J* = 1.1 Hz, 3H, CH₃).

¹³C NMR (125 MHz, CDCl₃): δ 191.0, 147.9, 140.3, 136.6, 128.6, 128.5, 126.4, 35.7, 28.5, 16.4.

FTIR (thin film) 3063, 3028, 2925, 2859, 1678, 1645, 1496, 1355, 1242, 1016, 907, 730, 700 cm⁻¹.

The physical data are identical in all respects to those previously reported.^[181]



(E)-6-methyl-7-oxohept-5-en-1-yl acetate (53f) Prepared by Grubbs metathesis from hex-5-en-1-yl acetate and methacrylaldehyde according to the reported procedure.^[132]

¹H NMR (500 MHz, CDCl₃) δ 9.41 (s, 1H, CHO), 6.47 (tq, *J* = 7.3 Hz, *J* = 1.3 Hz, 1H, C=CH), 4.10 (t, *J* = 6.4 Hz, 2H, AcOCH₂), 2.40 (q, *J* = 7.5 Hz, 2H, CH₂C=CH), 2.06 (s, 3H, CO₂CH₃), 1.76-1.56 (m, 7H, CH₃, CH₂).

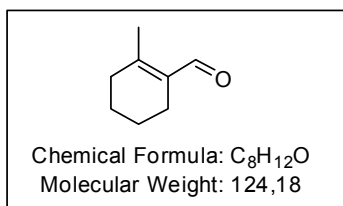
¹³C NMR (125 MHz, CDCl₃): 195.2, 171.1, 153.7, 139.8, 64.0, 28.5, 28.3, 24.9, 21.0, 9.3 δ ;

FTIR (thin film) 2949, 2867, 2715, 2256, 1736, 1684, 1645, 1457, 1388, 1366, 1236, 1047, 908, 729 cm⁻¹

HRMS (*m/z*) calcd for C₁₀H₁₆O₃ [M]⁺: 184.1099, found: 184.1099.

The physical data are identical in all respects to those previously reported.^[132]

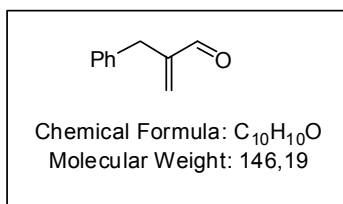
7. Experimental Section



2-methylcyclohex-1-enecarbaldehyde (53j): Following the procedure of *Piers et al.*,^[182] to a solution of 1-methylcyclohept-1-ene (200 mg, 1.81 mmol, 1 equiv) in MeCN (9 mL), CCl₄ (9 mL) and water (13 mL) was added NaIO₄ (1.6 g, 7.60 mmol, 4.2 equiv) followed by RuO₂·xH₂O (4.8 mg, 0.036 mmol, 0.02 equiv), and the mixture was stirred vigorously for 1h at room temperature. The mixture was diluted with water and extracted with CH₂Cl₂ three times. The combined organic layers were washed with brine, dried over Na₂SO₄ and the solvent was carefully evaporated. The crude reaction mixture was diluted with CH₂Cl₂ (18 mL) and L-proline (20.7 mg, 0.18 mmol, 0.1 equiv) was added. After 14h, AcOH (104 uL, 1.81 mmol, 1 equiv) was added, and the reaction mixture was stirred at room temperature for 34h after which all of the starting material was consumed. The crude reaction mixture was diluted with ether, washed with sat. aq. NaHCO₃ and extracted with ether three times. The combined organic layers were washed with brine, dried over Na₂SO₄ and evaporated under reduced pressure. Flash chromatography (30% Et₂O in pentane) afforded **53j** as a colourless oil (76.3 mg, 0.61 mmol, 34%).

¹H NMR (500 MHz, CDCl₃) δ 10.15 (s, 1H, CHO), 2.23-2.16 (m, 4H, CH₂C=CCH₂), 2.14 (br s, 3H, CH₃), 1.66-1.57 (m, 4H, CH₂).

The spectroscopic data are identical in all respects to those previously reported.^[183]



2-benzylacrylaldehyde (66a): Prepared from 3-phenylpropanal and formaldehyde according to the reported procedure.^[129]

¹H NMR (500 MHz, CDCl₃) δ 9.60 (s, 1H, CHO), 7.31-7.17 (m, 5H, CH_{Ar}), 6.10 (s, 1H, C=CH₂), 6.07 (s, 1H, C=CH₂), 3.57 (s, 2H, PhCH₂).

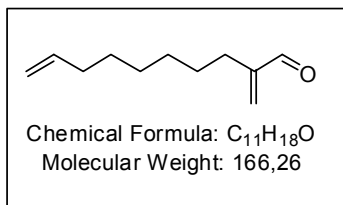
¹³C NMR (125 MHz, CDCl₃): δ 194.0, 149.8, 138.1, 135.3, 129.2, 128.6, 126.5, 34.2.

FTIR (thin film) 3087, 3063, 3029, 2919, 2824, 2701, 1686, 1602, 1496, 1453, 1434, 1245, 1075, 950, 737, 699 cm⁻¹

HRMS (*m/z*) calcd for C₁₀H₁₀O [M]⁺: 146.0732, found: 146.0733.

The physical data are identical in all respects to those previously reported.^[129]

7. Experimental Section



2-methylenedec-9-enal (66b): Following the procedure of *Erkkilä et al.*,^[129] pyrrolidine (17 μ L, 0.2 mmol, 0.1 equiv) and acid **70** (66 mg, 0.4 mmol, 0.2 equiv) were dissolved in dichloromethane (2 mL) and 36.5% aq. formaldehyde (160 μ L, 2 mmol, 1 equiv) was added followed by dec-9-enal (365 μ L, 2 mmol, 1 equiv). The reaction was stirred at 45 °C for 45 min and cooled to r.t. The crude mixture was washed with 10% aq. NaHCO₃, extracted with dichloromethane three times, and the combined organic layers were washed with brine, dried over Na₂SO₄ and evaporated under reduced pressure. Flash column chromatography eluting with 5% Et₂O in pentane afforded **66b** as a colourless oil (128.6 mg, 0.77 mmol, 39%).

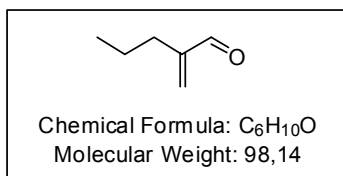
¹H NMR (500 MHz, CDCl₃) δ 9.54 (s, 1H, CHO), 6.24 (c. m, 1H, HC(O)C=CH₂), 5.98 (br d, J = 0.7 Hz, 1H, HC(O)C=CH₂), 5.80 (ddt, J = 17.1 Hz, J = 10.1 Hz, J = 6.7 Hz, CH=CH₂), 5.02-4.91 (m, 2H, CH=CH₂), 2.23 (t, J = 7.5 Hz, 2H, H₂C=CCH₂), 2.06-2.00 (m, 2H, H₂C=CHCH₂), 1.49-1.29 (m, 8H).

¹³C NMR (125 MHz, CDCl₃): δ 194.8, 150.5, 139.1, 133.9, 114.2, 33.7, 29.1, 28.9, 28.8, 27.8, 27.7.

FTIR (thin film) 3078, 2978, 2928, 2857, 1695, 1641, 1464, 1440, 1329, 995, 942, 910, 850 cm⁻¹

HRMS (m/z) calcd for C₁₁H₁₈O [M]⁺: 166.1358, found: 166.1359.

The physical data are identical in all respects to those previously reported.^[184]



2-methylenepentanal (67c): Prepared from pentanal and formaldehyde according to the reported procedure.^[129]

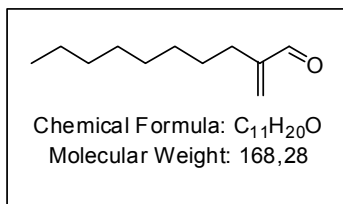
¹H NMR (500 MHz, CDCl₃) δ 9.55 (s, 1H, CHO), 6.26 (s, 1H, C=CH₂), 6.00 (s, 1H, C=CH₂), 2.21 (t, J = 7.6 Hz, 2H, H₂C=CCH₂), 1.49 (apparent sext, 2H, CH₃CH₂), 0.93 (t, J = 7.4 Hz, 3H, CH₃).

¹³C NMR (125 MHz, CDCl₃): δ 194.9, 150.2, 134.1, 29.8, 20.95, 14.1.

FTIR (thin film) 2961, 2932, 2874, 2704, 1686, 1640, 1464, 1379, 1087, 944, 876, 744 cm⁻¹

HRMS (m/z) calcd for C₆H₁₀O [M]⁺: 98.0732, found: 98.0731

7. Experimental Section



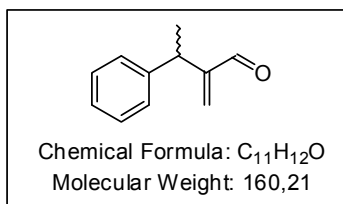
2-methylenedecanal (67d): Prepared from decanal and formaldehyde according to the reported procedure.^[129]

¹H NMR (500 MHz, CDCl₃) δ 9.71 (s, 1H, CHO), 6.25 (br s, 1H, C=CH₂), 5.99 (br s, 1H, C=CH₂), 2.23 (t, *J* = 7.6 Hz, 2H, H₂C=CCH₂), 1.44 (c. m, 2H, CH₂), 1.33-1.23 (m, 10H, CH₂), 0.88 (t, *J* = 6.7 Hz, 3H, CH₃).

¹³C NMR (125 MHz, CDCl₃): δ 194.9, 150.5, 134.0, 31.9, 29.4, 29.3, 29.2, 27.77, 27.75, 22.7, 14.1.

FTIR (thin film) 2926, 2856, 2256, 1694, 1628, 1466, 1330, 1106, 942, 907, 729 cm⁻¹

HRMS (*m/z*) calcd for C₁₁H₂₀O [M]⁺: 168.1514, found: 168.1514.



2-methylene-3-phenylbutanal (*rac*-66e): Prepared from 3-phenylbutanal and formaldehyde according to the reported procedure.^[129]

¹H NMR (500 MHz, CDCl₃) δ 9.54 (s, 1H, CHO), 7.30-7.18 (m, 5H, CH_{Ar}), 6.24 (br d, *J* = 1.1 Hz, 1H, C=CH₂), 6.08 (br s, 1H, C=CH₂), 4.03 (q, *J* = 7.2 Hz, 1H, CH₃CH), 1.43 (d, 7.1 Hz, 3H, CH₃).

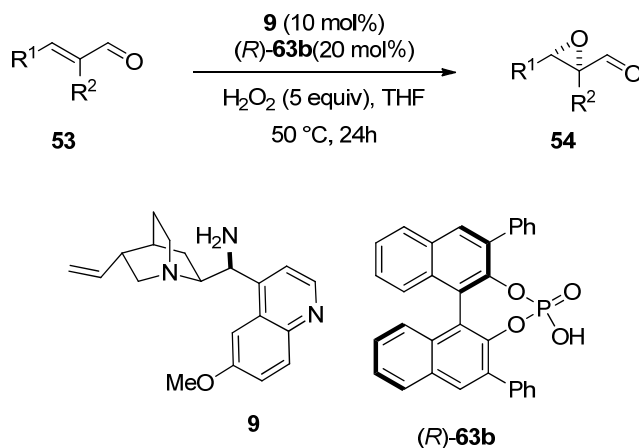
¹³C NMR (125 MHz, CDCl₃): δ 193.9, 154.3, 143.6, 133.7, 128.4, 127.5, 126.4, 37.2, 20.0.

FTIR (thin film) 3062, 3029, 2972, 2937, 2878, 2817, 2670, 2256, 1693, 1493, 1453, 1245, 948, 907, 730, 699 cm⁻¹

HRMS (*m/z*) calcd for C₁₁H₁₂O [M]⁺: 160.0888, found: 160.0886.

The spectroscopic data are identical in all respects to those previously reported.^[129]

7.2.2 General Epoxidation Procedures

7.2.2.1 Epoxidation of α,β -Disubstituted Enals **53**

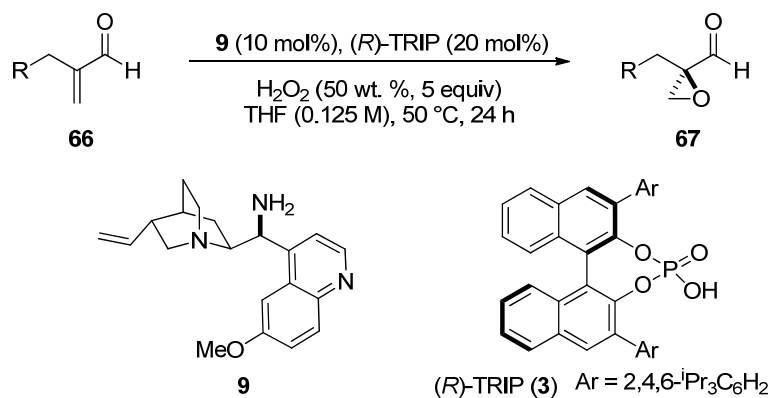
Procedure A: Phosphoric acid (*R*)-**63b** (25.0 mg, 0.05 mmol, 0.2 equiv) and amine **9** (8.08 mg, 0.025 mmol, 0.1 equiv) were dissolved in dry THF (2 mL, 0.125 M) and stirred for 5 min under ambient atmosphere at room temperature. The α -branched enal **53** (0.25 mmol, 1 equiv) was added and the mixture was stirred for an additional 5 min at room temperature. Aqueous hydrogen peroxide (77 μL , 50% w/w, 1.25 mmol, 5 equiv) was added, the reaction vessel was sealed and the reaction mixture was stirred for 24 h at 50 °C under an atmosphere of air. The reaction can be monitored by the disappearance of the starting material; the formed product is masked as a very polar species that appears as a poorly stainable spot on the TLC ($R_f \sim 0.1$) and is presumably a hydroperoxide adduct of the aldehyde **64** (cf. Section 4.1.3). The product **54** is liberated as the free aldehyde when the excess peroxide is quenched. This was performed by stirring the crude reaction mixture with 10% aqueous $\text{Na}_2\text{S}_2\text{O}_3$ (1 mL) for 10 min. The mixture was then diluted with water (5 mL) and diethyl ether (5 mL) and partitioned. The aqueous layer was washed with diethyl ether (5 mL x 3), and the combined organic layers were washed with brine and dried over Na_2SO_4 . Evaporation of the solvent and flash column chromatography with the specified solvent system afforded the desired product.

Procedure B: In cases when the epoxyaldehyde products were very volatile or unstable for GC/HPLC analysis, a modified workup procedure was used and the product was reduced to the corresponding alcohol. The crude reaction mixture was quenched by adding solid $\text{Na}_2\text{S}_2\text{O}_3$ (250 mg) and the suspension was stirred for 1 h. It was then filtered through a pad of Celite, washing with 2-5 mL diethyl ether and 2 mL EtOH. To this filtrate was added solid NaBH_4 (14.1 mg,

7. Experimental Section

0.375 mmol, 1.5 equiv) and the reaction mixture was stirred for 10 min. Saturated aqueous Na,K-tartrate (Rochelle's salt) was added and the reaction mixture was stirred for 1 h. The resulting biphasic solution was diluted with diethyl ether (5 mL) and water (10 mL) and partitioned. The aqueous layer was washed extracted with EtOAc (5 mL x 2), and the combined organic layers were washed with brine and dried over Na₂SO₄. Evaporation of the solvent and flash column chromatography with the specified solvent system afforded the desired product.

7.2.2.2 Epoxidation of α -Substituted Acroleins **66**

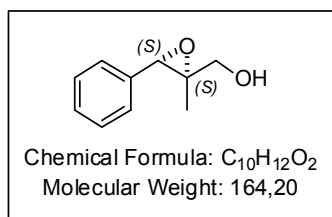


Procedure C: Epoxidation of disubstituted enals **66** was performed exactly as in **Procedure A** for non-volatile products and **Procedure B** for volatile products, except that phosphoric acid (*R*)-**3** ((*R*)-TRIP) was used (37.6 mg, 0.05 mmol, 0.2 equiv) instead of (*R*)-**63b**.

7. Experimental Section

7.2.3 Scope of Enantioenriched α,β -Epoxyaldehydes

7.2.3.1 α,β -Disubstituted Epoxyaldehydes 54



((2S,3S)-2-methyl-3-phenyloxiran-2-yl)methanol (149a):

Prepared according to the general **Procedure B** using commercial (*E*)-2-methyl-3-phenylacrylaldehyde followed by reduction with NaBH₄. Purification by flash chromatography (30% Et₂O in pentane) afforded **149a** as a colourless oil (20.1 mg, 0.12 mmol,

49%, 97:3 dr, 97.5:3.5 er).

¹H NMR (500 MHz, CDCl₃) δ 7.41-7.34 (m, 2H, CH_{Ar}), 7.34-7.28 (m, 3H, CH_{Ar}), 4.23 (s, 1H, PhCH), 3.87 (d, *J* = 12.4 Hz, 1H, CH₂OH), 3.77 (d, *J* = 12.4 Hz, 1H, CH₂OH), 1.99 (br s, 1H, OH), 1.10 (s, 3H, CH₃).

¹³C NMR (125 MHz, CDCl₃): δ 135.6, 128.1, 127.6, 126.4, 64.9, 63.6, 60.1, 13.5.

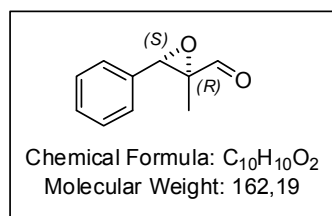
FTIR (thin film) 3412, 3064, 2932, 2870, 1605, 1495, 1451, 1385, 1249, 1070, 1040, 956, 601, 852 cm⁻¹

HRMS (*m/z*) calcd for C₁₀H₁₂O₂Na [M]: 164.0837. Found 164.0836.

m.p.: 52.2 – 53.2 °C.

$[\alpha]_D^{25}$: – 14.5 (*c* 0.815, CHCl₃), Lit^[185]: $[\alpha]_D^{25}$: – 16.9 (*c* 2, CHCl₃, >98% ee)

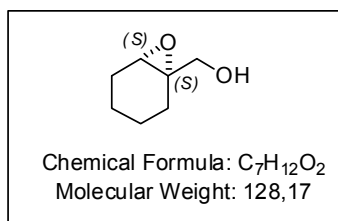
Chiral GC (Hydrodex – β -TBDAC, 60 min at 110 °C, 15 °C/min until 220 °C, 5 min at 220 °C, 0.6 bar H₂): *t_r* 42.6 min (major enantiomer, major diastereomer), *t_r* 46.3 min (major enantiomer, minor diastereomer), *t_r* 40.1 min (minor enantiomer, major diastereomer), *t_r* 51.6 min (minor enantiomer, minor diastereomer).



(2R,3S)-2-methyl-3-phenyloxirane-2-carbaldehyde (54a):

Chiral GC (BGB-177, 60 min at 120 °C, 15 °C/min until 220 °C, 5 min at 220 °C, 0.6 bar N₂): *t_r* 30.6 min (minor enantiomer), *t_r* 31.0 min (major enantiomer).

7. Experimental Section



(1S,6S)-7-oxabicyclo[4.1.0]heptan-1-ylmethanol (149b):

Prepared according to the general **Procedure B** using commercial cyclohex-1-enecarbaldehyde (0.36 mmol) followed by reduction with NaBH₄. Purification by flash chromatography (50% Et₂O in pentane) afforded **149b** as a colourless oil (32.2

mg, 0.25 mmol, 70%, 98.5:1.5 er).

¹H NMR (400 MHz, CDCl₃) δ 3.68 (dd, *J* = 12.2 Hz, *J* = 3.0 Hz, 1H, CH₂OH), 3.59 (dd, *J* = 12.1 Hz, *J* = 8.4 Hz, 1H, CH₂OH), 3.26 (d, *J* = 3.4 Hz, 1H, CHO_{epox}), 2.01-1.95 (m, 1H, OH), 1.90-1.64 (m, 4H, CH₂), 1.54-1.41 (m, 2H, CH₂), 1.34-1.23 (m, 2H, CH₂).

¹³C NMR (100 MHz, CDCl₃): δ 64.5, 60.1, 55.8, 25.3, 24.4, 19.9 19.7.

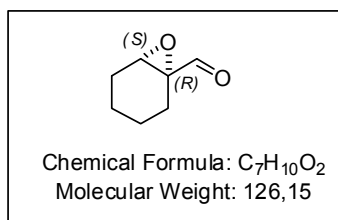
FTIR (thin film) 3417, 2938, 2872, 1435, 1032, 916, 731 cm⁻¹

HRMS (*m/z*) calcd for C₇H₁₃O₂ [M+H]⁺: 129.0916. Found 129.0916.

[α]_D²⁵: -22.6 (*c* 0.504, CHCl₃); Lit^[185]: [α]_D²⁵: -22.8 (*c* 2.6, CHCl₃, 93% ee).

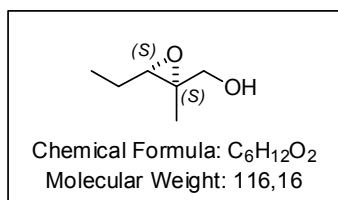
Chiral GC (BGB-177/BGB-15, 90 °C isocratic, 0.6 bar H₂) t_r 32.2 min (minor enantiomer), t_r 32.6 min (major enantiomer).

The physical data are identical in all respects to those previously reported.^[185]



(1R,6S)-7-oxabicyclo[4.1.0]heptane-1-carbaldehyde (54b):

Chiral GC (BGB-177/BGB-15, 65 °C isocratic, 0.7 bar H₂) t_r 31.7 min (minor enantiomer), t_r 34.2 min (major enantiomer).



((2S,3S)-3-ethyl-2-methyloxiran-2-yl)methanol (149c):

Prepared according to the general **Procedure A** using commercial (*E*)-2-methylpent-2-enal (*E/Z* >20:1, 0.4 mmol) followed by reduction with NaBH₄. Purification by flash chromatography (50% Et₂O in pentane) afforded **149c** as a

colourless oil (19.9 mg, 0.17 mmol, 43%, 92:8 dr, 98.5:1.5 er)

¹H NMR (400 MHz, CDCl₃) δ 3.69 (dd, *J* = 12.2 Hz, *J* = 4.3 Hz, 1H, CH₂OH), 3.58 (dd, *J* = 12.2 Hz, *J* = 8.2 Hz, 1H, CH₂OH), 3.00 (t, *J* = 6.4 Hz, 1H, CHO_{epox}), 2.82 (minor diastereomer, t, *J* = 6.4 Hz, 1H, CHO_{epox}), 1.72 (br dd, 1H, OH), 1.68-1.50 (m, 2H, CH₃CH₂), 1.29 (s, 3H, CH₃), 1.04 (t, *J* = 7.5 Hz, 3H, CH₃CH₂).

7. Experimental Section

^{13}C NMR (100 MHz, CDCl_3) only major diastereomer peaks detected: δ 65.4, 61.3, 60.9, 21.5, 14.1, 10.5.

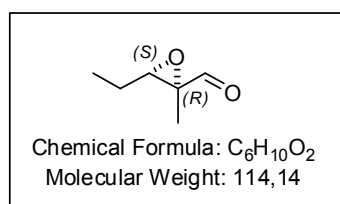
FTIR (thin film) 3427, 2972, 2937, 2878, 1460, 1348, 1040, 909, 732 cm^{-1}

HRMS (m/z) calcd for $\text{C}_6\text{H}_{13}\text{O}_2$ $[\text{M}+\text{H}]^+$: 117.0916, found 117.0915.

$[\alpha]_{\text{D}}^{25} - 14.1$ (c 0.170, CHCl_3); Lit^[125]: $[\alpha]_{\text{D}}^{22} = -13.5$ (c = 0.84, CHCl_3).

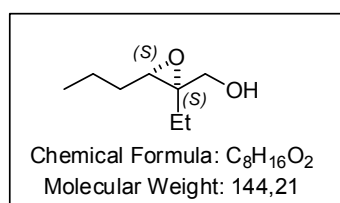
Chiral GC (Hydrodex- β TBDAC, 20 min at 100 °C, 8 °C/min until 220 °C, 5 min at 220 °C, 0.5 bar H_2) t_{r} 9.1 min (major enantiomer, major diastereomer), t_{r} 11.0 min (major enantiomer, minor diastereomer), t_{r} 12.0 min (minor enantiomer, major diastereomer), t_{r} 13.2 min (minor enantiomer, minor diastereomer).

The physical data are identical in all respects to those previously reported.^[125]



(2R,3S)-3-ethyl-2-methyloxirane-2-carbaldehyde (54c): Chiral GC (BGB-176SE/ SE-52, 45 min at 40 °C, 8 °C/min until 220 °C, 5 min at 220 °C, 0.5 bar H_2) t_{r} 29.9 min (minor enantiomer, minor diastereomer), t_{r} 32.2 min (major enantiomer, minor diastereomer), t_{r} 35.6 min (minor enantiomer, major diastereomer), t_{r} 35.9 min (major enantiomer, major diastereomer).

Conditions for efficient separation of (2S,3R)-enriched mixture: Lipodex G (40 °C, 1 °C/min until 60 °C, 12 °C/min until 220 °C, 5 min at 220 °C, 0.5 bar H_2) t_{r} 8.0 min (major enantiomer, minor diastereomer), t_{r} 8.9 min (minor enantiomer, minor diastereomer), t_{r} 9.1 min (major enantiomer, major diastereomer), t_{r} 10.9 min (minor enantiomer, major diastereomer).



((2S,3S)-2-ethyl-3-propyloxiran-2-yl)methanol (149d): Prepared according to the general **Procedure A** using commercial (*E*)-2-ethylhex-2-enal (*E/Z* = 94:6, 0.36 mmol) followed by reduction with NaBH_4 . Purification by flash chromatography (50% Et_2O in pentane) afforded **149** as a

colourless oil (33.1 mg, 0.23 mmol, 64%, 83:17 dr, 99:1 er).

^1H NMR (400 MHz, CDCl_3) δ 3.76 (dd, J = 12.1 Hz, J = 4.5 Hz, 1H, CH_2OH), 3.61 (dd, J = 12.1 Hz, J = 8.2 Hz, 1H, CH_2OH), 3.67 (minor diastereomer, dd, J = 11.8 Hz, J = 5.2 Hz, 1H, CH_2OH), 3.05 (apparent t, J = 5.6 Hz, 1H, CHO_{epox}), 2.87 (minor diastereomer, dd, J = 6.6 Hz, J = 5.7 Hz, 1H, CHO_{epox}), 1.95-1.84 (minor diastereomer, 2H, CH_2CH_3), 1.81-1.71 (m, 2H, CH_2CH_3), 1.62-1.44 (m, 4H, $\text{CH}_3\text{CH}_2\text{CH}_2$), 1.02-0.95 (m, 6H, CH_3 , CH_3).

7. Experimental Section

^{13}C NMR (100 MHz, CDCl_3) major diastereomer: δ 63.96, 62.9, 60.4, 29.9, 21.8, 20.1, 14.0, 9.3; minor diastereomer: δ 63.94, 63.3, 61.6, 30.0, 26.5, 20.0, 13.9, 8.9.

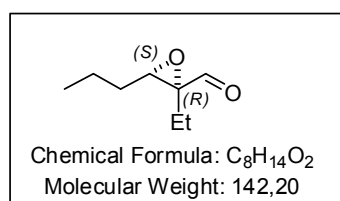
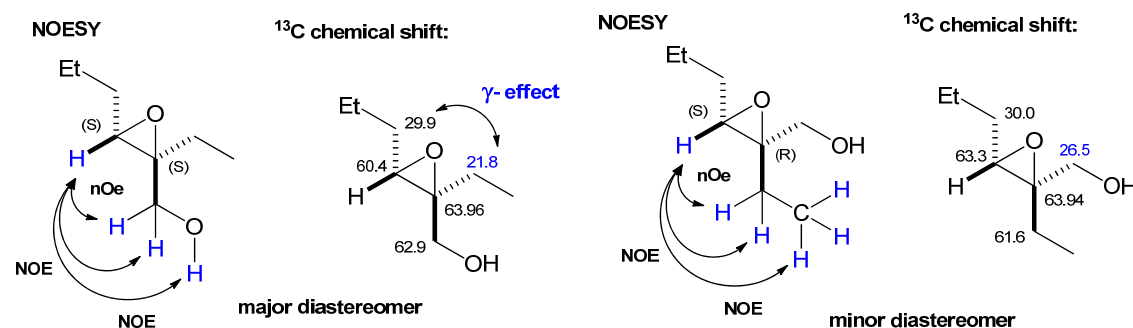
FTIR (thin film) 3431, 2963, 2937, 2876, 1465, 1381, 1048, 908, 733 cm^{-1}

HRMS (m/z) calcd for $\text{C}_8\text{H}_{17}\text{O}_2$ $[\text{M}+\text{H}]^+$: 145.1229. Found 145.1227.

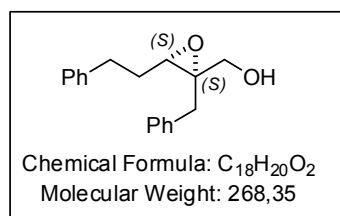
$[\alpha]_D^{25}$: -39.4 (c 0.508, CHCl_3).

Chiral GC (Lipodex G, 70 °C isocratic, 0.5 bar H_2) t_r 29.3 min (minor enantiomer, major diastereomer), t_r 32.0 min (major enantiomer, major diastereomer), t_r 36.1 min (major enantiomer, minor diastereomer), t_r 37.4 min (minor enantiomer, minor diastereomer).

The absolute stereochemistry was assigned by analogy and the relative stereochemistry was confirmed by NOESY and ^{13}C NMR experiments:



(2R,3S)-2-ethyl-3-propyloxirane-2-carbaldehyde (54d): Chiral GC (BGB-177/BGB-15, 35 min at 70 °C, 8 °C/min until 220 °C, 5 min at 220 °C, 0.6 bar H_2) t_r 19.6 min (minor enantiomer, minor diastereomer), t_r 21.4 min (major enantiomer, minor diastereomer), t_r 22.6 min (major enantiomer, major diastereomer), t_r 25.1 min (minor enantiomer, major diastereomer).



((2S,3S)-2-benzyl-3-phenethyloxiran-2-yl)methanol (149e): Prepared according to the general **Procedure B** using (*E*)-2-benzyl-5-phenylpent-2-enal (*E/Z* >20:1, 0.25 mmol) followed by reduction with NaBH_4 . Purification by flash chromatography (20% Et_2O in pentane) afforded **149e** as a colourless oil (51.6

mg, 0.19 mmol, 77%, 90:10 dr, 99:1 er).

7. Experimental Section

¹H NMR (500 MHz, CDCl₃) δ 7.33-7.15 (m, 10H, CH_{Ar}), 3.59 (dd, *J* = 12.3 Hz, *J* = 4.2 Hz, 1H, CH₂OH), 3.48 (dd, *J* = 12.3 Hz, *J* = 8.5 Hz, 1H, CH₂OH), 3.19 (dd, *J* = 7.5 Hz, *J* = 5.2 Hz, 1H, CHO_{epox}), 3.05 (minor diastereomer, d, *J* = 14.1 Hz, 1H, CHO_{epox}), 2.98 (d, *J* = 14.8 Hz, 1H, PhCH₂), 2.96-2.89 (m, 1H, PhCH₂), 2.86-2.77 (m, 1H, PhCH₂), 2.70 (d, *J* = 14.8 Hz, 1H, PhCH₂), 2.68-2.64 (minor diastereomer, m, 1H), 2.13-1.99 (m, 2H, PhCH₂CH₂), 1.92-1.80 (minor diastereomer, m, 1H), 1.52 (dd, *J* = 8.5 Hz, *J* = 4.2 Hz, 1H, OH).

¹³C NMR (125 MHz, CDCl₃) major diastereomer: δ 141.1, 136.5, 129.3, 128.6, 128.54, 128.48, 126.7, 126.2, 63.7, 63.1, 60.0, 35.0, 33.0; minor diastereomer (not all peaks detected): 136.3, 129.8, 128.44, 128.41, 126.3, 62.5, 61.6, 34.9, 32.7, 29.9.

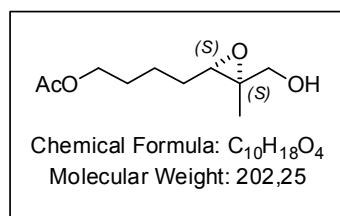
FTIR (thin film) 3437, 3063, 3028, 2928, 1603, 1496, 1454, 1068, 1031, 908, 732, 700 cm⁻¹

HRMS (*m/z*) calcd for C₁₈H₂₀O₂Na [M+Na]⁺: 291.1356. Found 291.1353.

α]_D²⁵: -38.0 (*c* 0.548, CHCl₃).

Chiral HPLC: Diastereomer separation: Zorbax XDB/C18, methanol/water = 70:30, flow rate 1.0 mL/min, 29.2 MPa, 210 nm. Upon separation, the major diastereomer was switched to a chiral column at 3.32 min till 3.42 min: Kromasil - AmyCoat, methanol/water = 98:2, flow rate 1.0 mL/min, 12.6 MPa, 220 nm). Major diastereomer: *t_r* 6.8 min (major enantiomer), *t_r* 8.4 min (minor enantiomer).

The absolute configuration was assigned by analogy.



4-((2*S*,3*S*)-3-(hydroxymethyl)-3-methyloxiran-2-yl)butyl acetate (149f): Prepared according to the general **Procedure B** using (*E*)-6-methyl-7-oxohept-5-enyl acetate **53f** (*E/Z* >20:1, 0.25 mmol) followed by reduction with NaBH₄. Purification by flash chromatography (50% Et₂O in pentane) afforded **149f** as a colourless oil (33.5 mg, 0.160 mmol, 66%, 97:3 er).

¹H NMR (500 MHz, CDCl₃) δ 4.09 (apparent t, *J* = 6.6 Hz, 2H, AcOCH₂), 3.68 (apparent d, *J* = 12.0 Hz, 1H, CH₂OH), 3.58 (dd, *J* = 12.0 Hz, *J* = 6.9 Hz, 1H, CH₂OH), 3.04 (apparent t, *J* = 5.6 Hz, 1H, CHO_{epox}), 2.85 (minor diastereomer, apparent t, *J* = 6.1 Hz, 1H, CHO_{epox}), 2.06 (s, 3H, CH₃CO₂), 2.01 (br s, 1H, OH), 1.74-1.48 (m, 6H, CH₂), 1.29 (s, 3H, CH₃).

¹³C NMR (125 MHz, CDCl₃) major diastereomer: δ 171.3, 65.3, 64.2, 60.9, 59.9, 28.4, 27.8, 23.0, 21.0, 14.2; minor diastereomer (not all peaks detected): 64.6, 64.2, 63.9, 27.7, 23.2, 20.2;

FTIR (thin film) 3447, 2955, 2868, 2250, 17365, 1458, 1433, 1387, 1367, 1240, 1035, 911, 868, 729 cm⁻¹

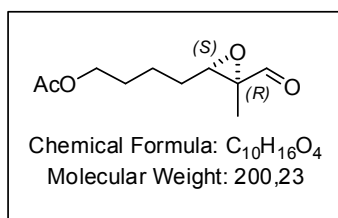
7. Experimental Section

HRMS (m/z) calcd for $C_{10}H_{18}O_4Na$ $[M+Na]^+$: 225.1097. Found 225.1099.

$[\alpha]_D^{25}$: -17.7 (c 0.362, $CHCl_3$).

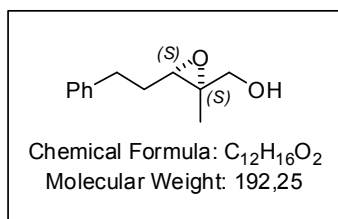
Chiral GC (Lipodex G, 60 min at 120 °C, 15 °C/min until 220 °C, 5 min at 220 °C, 0.5 bar H_2): t_r 37.9 min (minor enantiomer, major diastereomer), t_r 39.1 min (major enantiomer, major diastereomer), t_r 41.0 min (major enantiomer, minor diastereomer), t_r 42.2 min (minor enantiomer, minor diastereomer).

The absolute configuration was assigned by analogy.



4-((2S,3R)-3-formyl-3-methyloxiran-2-yl)butyl acetate (54f):

Chiral GC (BGB-174/BGB-1701, 40 min at 155 °C, 10 °C/min until 220 °C, 5 min at 220 °C, 0.5 bar H_2): t_r 22.1 min (major enantiomer, minor diastereomer), t_r 23.8 min (minor enantiomer, minor diastereomer), t_r 31.6 min (minor enantiomer, major diastereomer), t_r 32.5 min (major enantiomer, major diastereomer).



((2S,3S)-2-methyl-3-phenethyloxiran-2-yl)methanol (149g):

Prepared according to the general **Procedure B** using (*E*)-2-methyl-5-phenylpent-2-enal **53g** (*E/Z* = 20:1, 0.25 mmol) followed by reduction with $NaBH_4$. Purification by flash chromatography (50% Et_2O in pentane) afforded **149g** as a colourless oil (36.2 mg, 0.19 mmol, 75%, 95:5 dr, 98.5:1.5 er).

1H NMR (500 MHz, $CDCl_3$) δ 7.31-7.28 (m, 2H, CH_{Ar}), 7.22-7.19 (m, 3H, CH_{Ar}), 3.63 (dd, $J = 12.3$ Hz, $J = 3.9$ Hz, 1H, CH_2OH), 3.52 (dd, $J = 12.3$ Hz, $J = 8.8$ Hz, 1H, CH_2OH), 3.48 (minor diastereomer, dd, $J = 11.7$ Hz, $J = 5.8$ Hz, 1H, CH_2OH), 3.38 (minor diastereomer, dd, $J = 11.7$ Hz, $J = 6.2$ Hz, 1H, CH_2OH), 3.09 (t, $J = 6.2$ Hz, 1H, CHO_{epox}), 2.89-2.83 (m, 1H, $PhCH_2$), 2.76-2.70 (m, 1H, $PhCH_2$), 2.06-1.94 (m, 1H, $PhCH_2CH_2$), 1.88-1.81 (m, 1H, $PhCH_2CH_2$), 1.65 (br s, 1H, OH), 1.12 (s, 3H, CH_3).

^{13}C NMR (125 MHz, $CDCl_3$) major diastereomer: δ 141.2, 128.49, 128.47, 126.2, 65.3, 61.2, 59.6, 32.7, 30.1, 14.1; minor diastereomer (not all signals detected): 142.4, 128.75, 128.6, 126.3, 64.3, 63.7, 20.1.

FTIR (thin film) 3427, 3027, 2928, 2861, 1604, 1496, 1454, 1073, 1039, 908, 749, 700 cm^{-1}

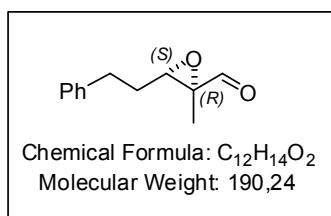
HRMS (m/z) calcd for $C_{12}H_{16}O_2$ $[M]^+$: 192.1150. Found 192.1151.

7. Experimental Section

$[\alpha]_D^{25}$: -27.6 (*c* 0.521, CHCl₃).

Chiral HPLC: Diastereomer separation: Zorbax XDB/C18, acetonitrile/water = 25:75, flow rate 1.0 mL/min, 22.2 MPa, 210 nm. Upon separation, each diastereomer was switched to a chiral column at 5.57 min till 5.62 min for the minor diastereomer and 6.06 min till 6.11 min for the major diastereomer: Chiralpak AS-RH, acetonitrile/water = 30:70, flow rate 1.0 mL/min, 10.1 MPa, 210 nm). Minor diastereomer (*cis*-**149g**): t_r 10.9 min (major enantiomer), t_r 11.6 min (minor enantiomer). Major diastereomer (*trans*-**149g**): t_r 11.5 min (minor enantiomer), t_r 12.21 min (major enantiomer).

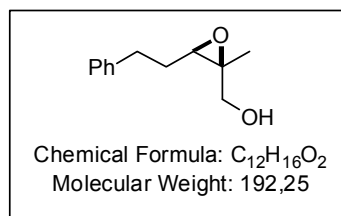
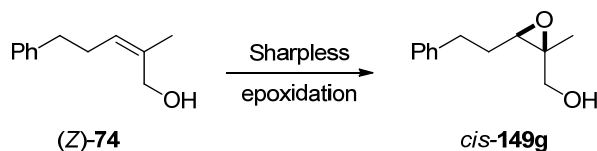
The absolute stereochemistry was assigned by analogy. The minor (*2S*, *3R*) diastereomer *cis*-**149g** has been described.^[134a]



(2*R*,3*S*)-2-methyl-3-phenethyloxirane-2-carbaldehyde (54g):

Chiral GC (BGB-177/BGB-15, 60 min at 120 °C, 10 °C/min until 230 °C, 5 min at 230 °C, 0.7 bar H₂) t_r 40.0 min (major enantiomer, minor diastereomer), t_r 40.6 min (minor enantiomer, minor diastereomer), t_r 45.1 min (major enantiomer, major diastereomer), t_r 45.6 min (minor enantiomer, major diastereomer).

Preparation of an authentic sample for the determination of the absolute stereochemistry of *cis*-149g (cf. Section 4.1.5.2):



((2*S*,3*R*)-2-methyl-3-phenethyloxiran-2-yl)methanol (*cis*-149g**):** Following the procedure of *Prévost* and *Woerpel*,^[134a] a

solution of (+)-diisopropyl tartrate (13.2 μL, 0.0625 mmol, 0.22 equiv) in dichloromethane (1 mL) with 4Å molecular sieves (16 mg) was cooled to -20 °C. Ti(O^{*i*}Pr)₄ (4.6 μL, 0.0129 mmol, 0.16 equiv) was added, followed by *tert*-butylhydroperoxide (77.5 μL, 5.5 M in decanes, 0.426 mmol, 1.5 equiv). A solution of (*Z*)-**74** (50 mg, 0.28 mmol, 1 equiv) in dichloromethane (0.2

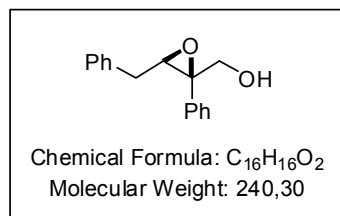
7. Experimental Section

mL) was added. The reaction mixture was stirred at $-20\text{ }^{\circ}\text{C}$ for 16 h, warmed up to room temperature at treated with H_2O (0.3 mL) and 30% NaOH (0.1 mL). After stirring the biphasic solution for 1h at room temperature, the mixture was extracted with dichloromethane three times, dried over Na_2SO_4 , filtered and concentrated. Flash column chromatography eluting with 35% diethyl ether in pentane afforded *cis*-**149g** as a colourless oil (43.6 mg, 0.23 mmol, 80%).

$^1\text{H NMR}$ (500 MHz, CDCl_3) δ 7.31-7.28 (m, 2H, CH_{Ar}), 7.23-7.19 (m, 3H, CH_{Ar}), 3.47 (d, $J = 12.0$ Hz, 1H, CH_2OH), 3.38 (d, $J = 12.0$ Hz, 1H, CH_2OH), 2.89-2.84 (m, 2H, PhCH_2), 2.75-2.67 (m, 1H, CHO_{epox}), 2.05-1.98 (m, 1H, PhCH_2CH_2), 1.87-1.81 (m, 1H, PhCH_2CH_2), 1.60 (br s, 1H, OH), 1.32 (s, 3H, CH_3).

Chiral HPLC: Chiralpak AS-RH, acetonitrile/water = 30:70, flow rate 1.0 mL/min, 10.1 MPa, 210 nm). t_r 5.55 min (major enantiomer), t_r 6.26 min (minor enantiomer). *Since no diastereomer separation was required in this case, the sample was not pre-eluted on an achiral HPLC column.*

The physical data are identical in all respects to those previously reported.^[134a]



((2S,3S)-2-methyl-3-phenethyloxiran-2-yl)methanol (149h):

Prepared according to the general **Procedure B** using (*E*)-2,4-diphenylbut-2-enal **53h** (*E/Z* > 20:1, 0.25 mmol) followed by reduction with NaBH_4 . Purification by flash chromatography (50% Et_2O in pentane) afforded **149h** as a colourless oil (29.4

mg, 0.12 mmol, 49%, 56:44 dr, 95:5 er).

$^1\text{H NMR}$ (500 MHz, CDCl_3) δ 7.46-7.05 (m, 10H, major + minor diast, CH_{Ar}), 4.32 (dd, $J = 12.3$ Hz, $J = 4.8$ Hz, 1H, major diast, CH_2OH), 4.14 (dd, $J = 12.3$ Hz, $J = 5.8$ Hz, 1H, major diast, CH_2OH), 4.06-3.91 (m, 2H, minor diast, CH_2OH), 3.61 (t, $J = 6.2$ Hz, 1H, minor diast, CHO_{epox}), 3.22 (t, $J = 6.4$ Hz, 1H, major diast, CHO_{epox}), 3.16 (dd, $J = 14.7$ Hz, $J = 6.4$ Hz, 1H, major diast, PhCH_2), 3.10 (dd, $J = 14.7$ Hz, $J = 6.3$ Hz, 1H, major diast, PhCH_2), 2.58 (dd, $J = 14.7$ Hz, $J = 6.8$ Hz, 1H, minor diast, PhCH_2), 2.52 (dd, $J = 14.7$ Hz, $J = 5.8$ Hz, 1H, minor diast, PhCH_2) 1.82 (br s, 1H, minor diast, OH), 1.73 (br s, 1H, major diast, OH).

$^{13}\text{C NMR}$ (125 MHz, CDCl_3 , mixture of 2 diastereomers) δ 138.9, 137.44, 137.40, 135.6, 128.9, 128.8, 128.7, 128.6, 128.5, 128.4, 128.1, 127.9, 127.4, 127.0, 126.8, 128.6, 125.9, 68.7, 66.2, 64.4, 64.1, 63.2, 61.4, 34.9, 34.8.

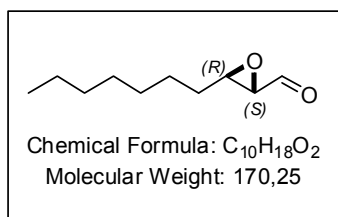
FTIR (thin film) 3432, 3062, 3029, 2923, 1603, 1496, 1453, 1085, 1031, 939, 861, 762 cm^{-1}

7. Experimental Section

HRMS (m/z) calcd for $C_{16}H_{16}O_2Na$ $[M+Na]^+$: 263.1042. Found 263.1040.

Chiral HPLC: *Diastereomer separation:* Zorbax XDB/C18, elution gradient 0-9.5 min: methanol/water = 55:45, 9.5-12.5 min: methanol/water = 80:20, 12.5-20 min: methanol/water = 55:45, flow rate 1.0 mL/min, 32.8 MPa, 210 nm. Upon separation, each diastereomer was switched to a chiral column at 7.38 min till 7.42 min for the minor diastereomer and 8.28 min till 8.33 min for the major diastereomer: CelluCoat RP, acetonitrile/water = 40:60, flow rate 1.0 mL/min, 18.2 MPa, 210 nm). Minor diastereomer: t_r 18.2 min (minor enantiomer), t_r 19.4 min (major enantiomer). Major diastereomer: t_r 18.1 min (major enantiomer), t_r 18.6 min (minor enantiomer).

The absolute stereochemistry was assigned by analogy.



(2S,3R)-3-heptyloxirane-2-carbaldehyde (54i): Prepared according to the general **Procedure A** using commercial (*E*)-dec-2-enal. The yield (30%) was determined by GC analysis (95:5 dr, 70:30 er).

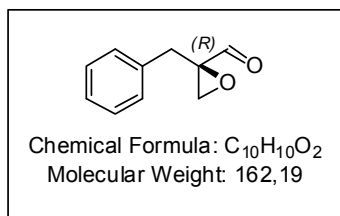
1H NMR (300 MHz, $CDCl_3$) δ = 9.01 (d, J = 6.2 Hz, 1H), 3.18 - 3.15 (m, 1H), 3.09 (dd, J = 6.2 Hz, 1H), 1.23 - 1.63 (m, 10H), 0.86 (t, J = 5.3 Hz, 3H)

Chiral GC: (BGB-176, 90 °C iso, 0.5 bar H_2): t_r 12.1 min (major enantiomer, major diastereomer), t_r 12.9 min (minor enantiomer, major diastereomer), t_r 5.4 min (major enantiomer, minor diastereomer), t_r 1.12 min (minor enantiomer, minor diastereomer).

The physical data are identical in all respects to those previously reported.^[36] The absolute stereochemistry was assigned by comparison of the chiral GC spectra with an authentic sample of (*2R,3S*)-**54i** which was prepared using the procedure of Wang and List.^[36]

7. Experimental Section

7.2.3.2 α -Substituted Epoxyaldehydes 67



(R)-2-benzylloxirane-2-carbaldehyde (67a): Prepared according to the general **Procedure C** using 2-benzylacrylaldehyde **66a** (0.25 mmol). Purification by flash chromatography (20% Et₂O in pentane) afforded **67a** as a colourless oil (31.7 mg, 0.195 mmol, 78%, 99:1 er).

¹H NMR (400 MHz, CDCl₃) δ 8.94 (s, 1H, CHO), 7.31-7.20 (m, 5H, CH_{Ar}), 3.21 (d, J = 1.4 Hz, 2H, PhCH₂), 3.00 (d, J = 4.6 Hz, 1H, CH₂O_{epox}), 2.85 (d, J = 4.6 Hz, 1H, CH₂O_{epox}).

¹³C NMR (100 MHz, CDCl₃): δ 198.6, 134.8, 129.9, 128.4, 127.0, 61.4, 48.9, 33.1.

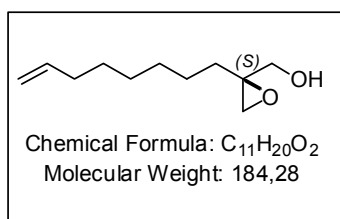
FTIR (thin film) 3064, 3032, 2826, 1726, 1497, 1454, 1077, 1010, 907, 730 cm⁻¹

HRMS (m/z) calcd for C₁₀H₁₀O₂ [M]⁺: 162.0681. Found 162.0682.

$[\alpha]_D^{25}$: + 47.0 (c 0.502, CHCl₃).

Chiral GC (BGB-178/BGB-15, 35 min at 115 °C, 8 °C/min until 220 °C, 0.6 bar H₂) t_r 26.0 min (major enantiomer), t_r 27.0 min (minor enantiomer).

The physical data are identical in all respects to those previously reported.^[88] The absolute stereochemistry was assigned by analogy.



(S)-2-(2-(oct-7-enyl)oxiran-2-yl)methanol (150b): Prepared according to the general **Procedure C** using 2-methylenedec-9-enal **66b** (0.25 mmol) followed by reduction with NaBH₄. Purification by flash chromatography (30% Et₂O in pentane) afforded **150b** as a colourless oil (33.9 mg, 0.184 mmol, 74%,

98.5:1.5 er).

¹H NMR (300 MHz, CDCl₃) δ 5.80 (ddt, J = 17.4 Hz, J = 10.2 Hz, J = 6.7 Hz, CH=CH₂), 5.03-4.99 (m, 2H, CH=CH₂), 3.77 (dd, J = 12.2, J = 4.2 Hz, 1H, CH₂OH), 3.64 (dd, J = 12.2 Hz, J = 8.6 Hz, 1H, CH₂OH), 2.88 (d, J = 4.7 Hz, 1H, CH₂O_{epox}), 2.66 (d, J = 4.7 Hz, 1H, CH₂O_{epox}), 2.07-2.00 (m, 2H, CH₂=CHCH₂), 1.82-1.26 (m, 11H, CH₂).

¹³C NMR (75 MHz, CDCl₃): δ 139.0, 114.3, 62.8, 59.7, 49.8, 33.7, 32.0, 29.6, 28.9, 28.8, 24.6;

FTIR (thin film) 3429, 3077, 2928, 2857, 2249, 1641, 1464, 1415, 1046, 908, 730 cm⁻¹

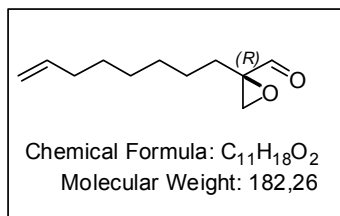
HRMS (m/z) calcd for C₁₁H₂₁O₂ [M+H]⁺: 185.1542. Found 185.1540.

$[\alpha]_D^{25}$: - 10.8 (c 0.574, CHCl₃).

7. Experimental Section

Chiral GC (Hydrodex- β TBDAc, 25 min at 150 °C, 10 °C/min until 220 °C, 0.5 bar H₂) t_r 14.5 min (major enantiomer), t_r 15.4 min (minor enantiomer).

The absolute stereochemistry was assigned by analogy.



(R)-2-(oct-7-enyl)oxirane-2-carbaldehyde (67b):

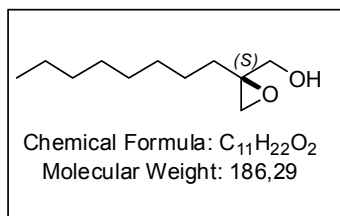
¹H NMR (500 MHz, CDCl₃) δ 8.88 (s, 1H, CHO), 5.80 (ddt, $J = 17.09$ Hz, $J = 10.2$ Hz, $J = 6.6$ Hz, CH=CH₂), 5.03-4.90 (m, 2H, CH=CH₂), 3.02 (br s, 2H, CH₂O_{epox}), 2.09-1.88 (m, 3H, CH₂), 1.76-1.66 (m, 1H, CH₂), 1.46-1.21 (m, 8H, CH₂).

¹³C NMR (100 MHz, CDCl₃): δ 199.1, 139.0, 114.3, 61.4, 49.6, 33.7, 29.5, 28.8, 28.7, 27.6, 24.3.

FTIR (thin film) 3077, 2929, 2857, 1730, 1641, 1464, 1438, 1144, 910, 731 cm⁻¹

HRMS (m/z) calcd for C₁₁H₁₉O₂ [M+H]⁺: 183.13851. Found 183.13831.

Chiral GC (BGB-174/BGB-1701, 130 °C isocratic, then baked out at 8 °C/min until 220 °C, 5 min at 220 °C, 0.5 bar H₂): t_r 27.8 min (major enantiomer), t_r 29.3 min (minor enantiomer).



(S)-(2-octyloxiran-2-yl)methanol (150d): Prepared according to the general procedure **B** using 2-methylenedecanal **5c** (0.25 mmol) followed by reduction with NaBH₄. Purification by flash chromatography (50% Et₂O in pentane) afforded **150d** as a colourless oil (36.4 mg, 0.196 mmol, 78%, 99:1 er).

¹H NMR (500 MHz, CDCl₃) δ 3.78 (dd, $J = 12.1$, $J = 3.8$ Hz, 1H, CH₂OH), 3.64 (dd, $J = 12.1$ Hz, $J = 8.4$ Hz, 1H, CH₂OH), 2.89 (d, $J = 4.7$ Hz, 1H, CH₂O_{epox}), 2.67 (d, $J = 4.7$ Hz, 1H, CH₂O_{epox}), 1.80-1.75 (m, 1H, CH₂), 1.68 (br s, 1H, OH), 1.53-1.47 (m, 1H, CH₂), 1.39-1.23 (m, 12H, CH₂), 0.88 (t, $J = 6.7$ Hz, 3H, CH₃).

¹³C NMR (125 MHz, CDCl₃): δ 62.7, 59.8, 49.8, 32.0, 31.8, 29.7, 29.2, 24.6, 22.6, 14.1.

FTIR (thin film) 3421, 2927, 2857, 2251, 1466, 1364, 1197, 1053, 908, 808, 731 cm⁻¹

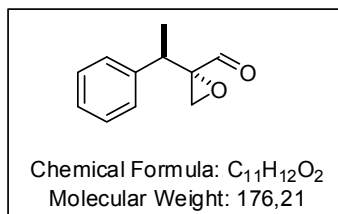
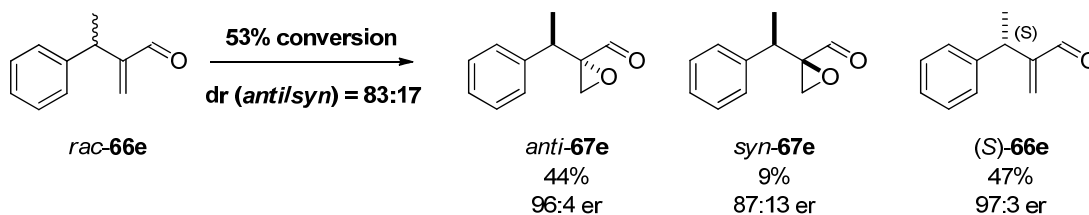
$[\alpha]_D^{25}$: -14.8 (c 0.595, CHCl₃); Lit^[130] $[\alpha]_D^{20}$: -11.7 (c 1.0, CHCl₃, 72% ee).

HRMS (m/z) calcd for C₁₁H₂₃O₂ [M+H]⁺: 187.1698. Found 187.1699.

Chiral GC (BGB-177/BGB-15, 140 °C isocratic, then baked out at 220 °C, 0.6 bar H₂) t_r 19.75 min (major enantiomer), t_r 20.8 min (minor enantiomer).

The physical data are identical in all respects to those previously reported.^[130]

7. Experimental Section



(S)-2-((R)-1-phenylethyl)oxirane-2-carbaldehyde (*anti*-67e):

Prepared according to the general **Procedure C** using racemic 2-methylene-3-phenylbutanal *rac*-66e (0.25 mmol). Analysis of the crude reaction mixture after 24 h showed 53% conversion of the starting material and two diastereomers *anti*-67e and *syn*-67e with dr = 83:17. Purification by flash chromatography (5% EtOAc in pentane) afforded *anti*-67e as a colourless oil (13.0 mg, 0.074 mmol, 30%, lowered yield due to incomplete separation from (S)-66e, 96:4 er).

¹H NMR (500 MHz, CDCl₃) δ 8.95 (s, 1H, CHO), 7.31-7.28 (m, 2H, CH_{Ar}), 7.26-7.21 (m, 3H, CH_{Ar}), 3.68 (q, *J* = 7.2 Hz, 1H, PhCH), 2.87 (d, *J* = 4.6 Hz, 1H, CH₂O_{epox}), 2.58 (d, *J* = 4.6 Hz, 1H, CH₂O_{epox}), 1.38 (d, *J* = 6.9 Hz, 3H, CH₃).

¹³C NMR (125 MHz, CDCl₃): δ 199.0, 140.4, 128.5, 128.2, 127.1, 64.6, 48.9, 35.8, 16.2.

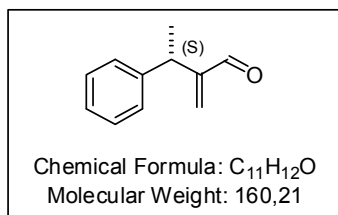
FTIR (thin film) 30314, 2979, 2940, 2821, 2255, 1733, 1496, 1454, 907, 865, 729 cm⁻¹

HRMS (*m/z*) calcd for C₁₁H₁₂O₂ [M]⁺: 176.0837. Found 176.0839.

[α]_D²⁵: +41.5 (*c* 0.65, CHCl₃).

Chiral GC (G-BP, 40 min at 110 °C, 14 °C/min until 220 °C, 5 min at 220 °C, 0.6 bar H₂): t_r 25.3 min (minor enantiomer, major diastereomer *anti*-67e), t_r 27.0 min (major enantiomer, major diastereomer *anti*-67e), t_r 34.0 min (minor enantiomer, minor diastereomer *syn*-67e), t_r 36.3 min (major enantiomer, minor diastereomer *syn*-67e).

The physical data are identical in all respects to those previously reported.^[88]



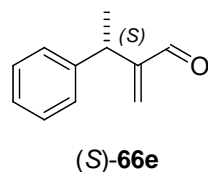
(S)-2-methylene-3-phenylbutanal (S)-66e: The physical data of this compound are identical in all respects to *rac*-66e. This compound was isolated by flash chromatography (5% EtOAc in pentane) as a colourless oil (8.79 mg, 0.055 mmol, 22%, lowered yield due to incomplete separation from *anti*-67e, 97:3 er).

[α]_D²⁵: +48.6 (*c* 0.44, CHCl₃), Lit (*R* enantiomer)^[135]: [α]_D²⁵: -38.7 (*c* 1.01, CHCl₃).

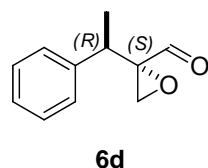
7. Experimental Section

Chiral GC (G-BP, 40 min at 110 °C, 14 °C/min until 220 °C, 5 min at 220 °C, 0.6 bar H₂) t_r 13.9 min (major enantiomer), t_r 14.4 min (minor enantiomer).

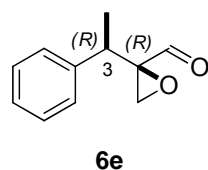
Assignment of the absolute configuration:



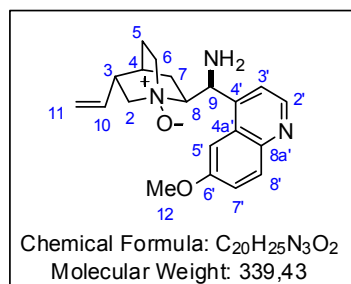
(S)-66e: The absolute configuration was established by comparison of the optical rotation with the literature value.^[135]



anti-67e: The relative *anti*-configuration was assigned by comparison of the chemical shifts in ¹H and ¹³C NMR spectra with the literature values.^[88] The absolute configuration was assigned based on the configuration of the recovered enantioenriched starting material (S)-66e.



syn-67e: The relative *syn*-configuration was assigned by comparison of the chemical shifts in ¹H and ¹³C NMR spectra with the literature values.^[88] The absolute configuration was *tentatively* assigned based on the observed *dr* and *er* values of all components of the reaction, such that the stoichiometry of the (R) and (S) enantiomers at C-3 is balanced. GC and NMR analyses of the crude reaction mixture indicated that (S)-66e, *anti*-67e and *syn*-67e were the only components of the reaction.

7.2.4 Studies on the *N*-oxidation of catalyst **9**7.2.4.1. Synthesis of 9-amino(9-deoxy)*epi*quinine *N*-oxide (**78**)

9-amino(9-deoxy)*epi*quinine *N*-oxide (78**):** 9-Amino-(9-deoxy)*epi*quinine (**9**) (100 mg, 0.31 mmol) was dissolved in dichloromethane (3 mL) and cooled to $-78\text{ }^{\circ}\text{C}$. Under ambient atmosphere, *m*-CPBA (60 mg, 0.27 mmol, 0.87 equiv, 77% purity) was added, and the reaction mixture was stirred for 1 h at $-78\text{ }^{\circ}\text{C}$. The crude reaction mixture was then directly loaded

onto a silica gel column packed with a 900:100:6.5 solvent mixture of CH₂Cl₂:MeOH:NH₃ *conc.* and eluted with the same solvent mixture. The first eluted product corresponds to the excess starting material (**9**). Further elution yielded the title compound **78** as an oil which becomes a highly hygroscopic amorphous white foam after washing with ether and evaporating the solvent under reduced pressure (92.8 mg, 0.27 mmol, quant.).

¹H NMR (500 MHz, MeOD) δ 8.71 (d, $J = 4.6$ Hz, 1H, H-2'), 7.98 (d, $J = 9.2$ Hz, 1H, H-8'), 7.73 (br s, 1 H, H-5'), 7.64 (d, $J = 4.6$ Hz, 1H, H-3'), 7.48 (dd, $J = 9.2$ Hz, $J = 2.5$ Hz, 1H, H-7'), 5.92 (ddd, $J = 17.2$ Hz, $J = 10.5$ Hz, $J = 6.8$ Hz, 1H, H-10), 5.38-5.08 (m, 3H, H-9 + H-11), 4.08 (c. m, 1H, H-6b), 4.03 (s, 3H, C-12), 3.89 (br s, 1H, H-8), 3.70 (dd, $J = 12.9$ Hz, $J = 10.6$ Hz, 1H, H-2a), 3.53-3.37 (m, 2H, H-2b + H-6a), 2.99-2.88 (m, 1H, H-3), 2.15-1.79 (m, 3H, H-5 + H-7b), 1.76 (c. m, 1H, H-4), 1.09-0.99 (m, 1H, H-7a).

¹³C NMR (150 MHz, MeOD) δ 160.3 (C-6'), 148.4 (C-2'), 147.6 (C-8a'), 144.9 (C-4'), 139.3 (C-10), 131.5 (C-8'), 129.7 (C-4a'), 124.15 (C-7'), 121.8 (C-3'), 117.2 (C-11), 102.0 (C-5'), 74.7 (C-8), 71.7 (C-2), 58.5 (C-6), 56.3 (C-12), 52.0 (C-9), 41.6 (C-3), 28.8 (C-7), 28.0 (C-4), 27.8 (C-5).

¹⁵N-NMR (60 MHz, MeOD, $\delta_{\text{NH}_3} = 0$ ppm) δ 296.5 (quinoline N), 117.5 (N-oxide), primary amine could not be detected.

FTIR (thin film) 3264, 2943, 2216, 1620, 1590, 1507, 1474, 1432, 1359, 1309, 1263, 1236, 1175, 1135, 1083, 1028, 987, 909, 856, 830, 725.

LRMS (EI): $m/z = 339$ [M], 322, 305, 214, 187, 156, 136, 108, 98, 81, 67, 56, 41.

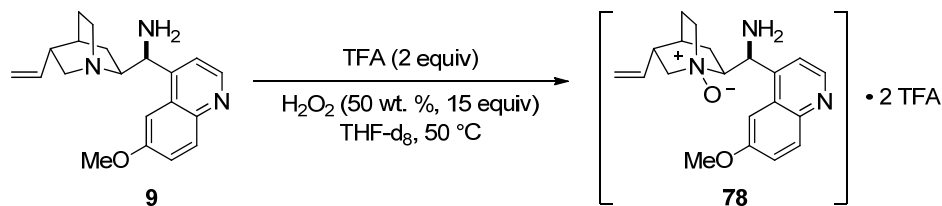
HRMS (m/z) calcd for C₂₀H₂₆N₃O₂ [M+H]⁺: 340.20195. Found: 340.20190.

7. Experimental Section

7.2.4.2 Kinetic studies

Kinetic studies on the oxidation of the amine salt [9·2TFA] to [78·2TFA] were performed by taking aliquots of the reaction over 18 h (Table 7.1). Two methods were employed to determine the reaction conversion: aliquots diluted in THF-d₈ (approx. 0.1 mL sample + 0.3 mL THF-d₈) were analyzed by ¹H NMR spectrometry, and aliquots diluted in MeOH (0.2 -1 μL in 1 mL MeOH) were analyzed by ion pair chromatography (IPC, 50 mm Zorbax Eclipse Plus C18, 1.8 μm, 4.6 mm i.D.; mobile phase: methanol/5 mM DiKGA pH 4.6 = 50:50, 1.0 mL/min, 220 nm, 308K). The conversion vs. time graph (Figure 7.1) was plotted using the average conversion obtained from both methods. This graph shows no apparent autocatalytic effect.

Table 7.1 Conversion of the amine salt [9·2TFA] to [78·2TFA] in the presence of excess aq. H₂O₂, monitored over 18 h.



Reaction time, h	Conv., % (NMR)	Conv., % (IPC)	Reaction time, h	Conv., % (NMR)	Conv., % (IPC)
0.5	4	4	5	43	37
1	6	12	7	64	59
2	17	18	9	62	72
3	24	25	18	100	90
4	37	35			

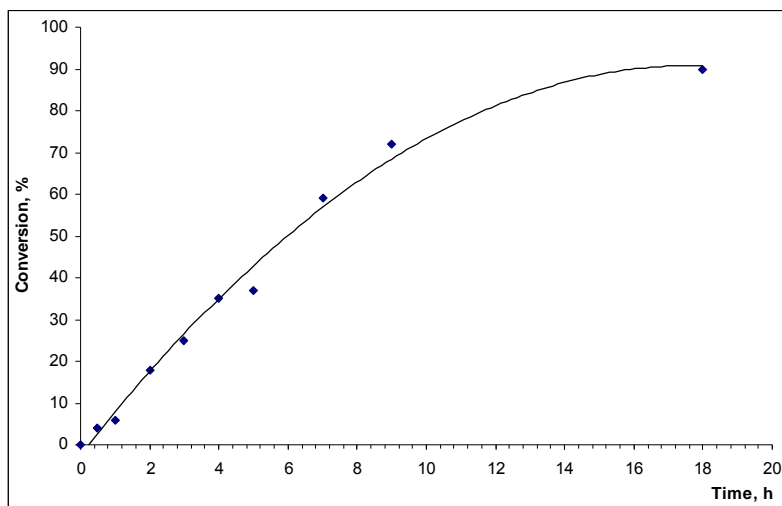
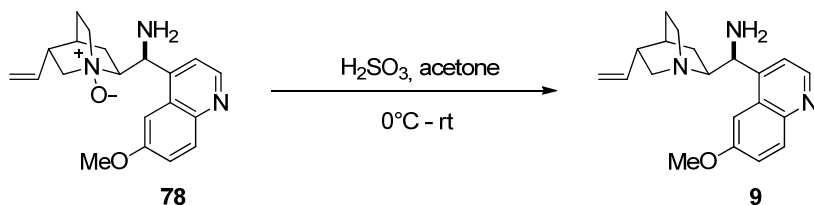


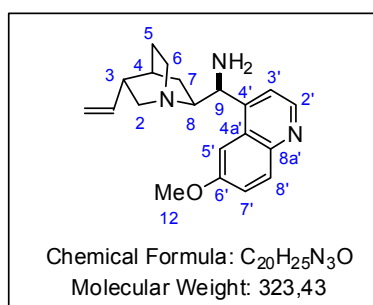
Figure 7.1 Kinetic plot of oxidation of the amine salt [9·2TFA] to [78·2TFA] in the presence of excess aq. H₂O₂.

7. Experimental Section

7.2.4.3 Reduction of 9-amino(9-deoxy)*epi*quinine *N*-oxide **78** to 9-amino(9-deoxy)*epi*quinine **9**



9-Amino(9-deoxy)*epi*quinine *N*-oxide (**78**) (20.6 mg, 0.061 mmol) was dissolved in acetone (0.8 mL) and H₂SO₃ (6% wt, 0.1 mL, 0.073 mmol, 1.2 equiv) was added dropwise at 0 °C. The reaction mixture was stirred for 17 h, dissolved in dichloromethane, washed with sat. aq. NaHCO₃, dried over MgSO₄, filtered and the solvent was removed under reduced pressure. The resulting white amorphous foam (11.1 mg, 0.034 mmol, 56%) was obtained as a spectroscopically pure compound, whose physical data was identical in all respects to 9-amino(9-deoxy)*epi*quinine (**9**).



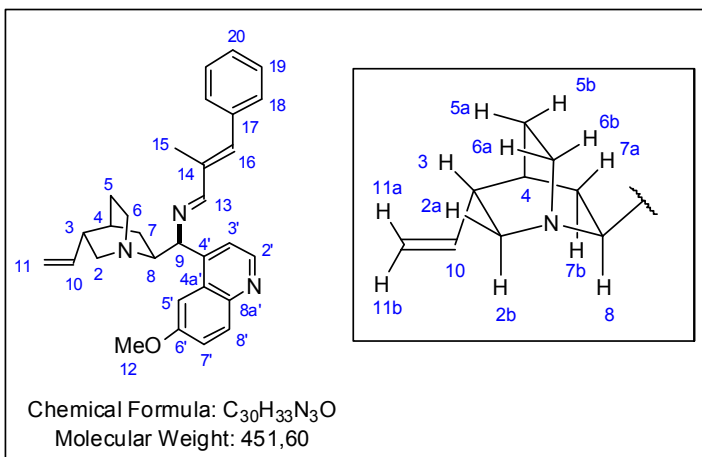
¹H NMR (500 MHz, CDCl₃) δ 8.73 (d, *J* = 4.5 Hz, 1H, H-2'), 8.01 (d, *J* = 9.2 Hz, 1H, H-8'), 7.64 (br s, 1 H, H-5'), 7.43 (br d, *J* = 4.2 Hz, 1H, H-3'), 7.36 (dd, *J* = 9.1 Hz, *J* = 2.8 Hz, 1H, H-7'), 5.78 (ddd, *J* = 17.3 Hz, *J* = 10.1 Hz, *J* = 7.3 Hz, 1H, CH=CH₂), 5.00-4.93 (m, 2H, CH=CH₂), 4.57 (br d, *J* = 9.7 Hz, 1H, H-9), 3.94 (s, 3H, C-12), 3.26 (dd, *J* = 13.8 Hz, *J* = 10.0 Hz, 1H, H-2), 3.21-3.15 (m, 1H, H-6), 3.11-3.02 (m, 1H, H-8), 2.82-2.75 (m, 2H, H-6, H-2), 2.30-2.23 (m, 1H, H-3), 1.94 (br s, 2H, NH₂), 1.62-1.58 (m, 1H, H-4), 1.57-1.50 (m, 2H, H-5), 1.45-1.36 (m, 1H, H-7), 0.75 (ddt, *J* = 13.6 Hz, *J* = 7.5 Hz, *J* = 1.9 Hz, 1H, H-7).

¹³C NMR (150 MHz, MeOD) δ 157.6 (C-6'), 147.8 (C-2'), 147.0 (C-8a'), 144.7 (C-4'), 141.7 (CH=CH₂), 131.8 (C-8'), 128.7 (C-4a'), 121.2 (C-7'), 119.9 (C-3'), 114.3 (CH=CH₂), 102.0 (C-5'), 61.9 (C-8), 56.3 (C-2), 55.5 (C-12), 52.5 (C-9), 40.9 (C-6), 39.8 (C-3), 28.2 (C-5), 27.5 (C-4), 26.0 (C-7).

7. Experimental Section

7.2.5 NMR Investigations of Imine Salts 80

(*S,E*)-1-(6-methoxyquinolin-4-yl)-*N*-((*E*)-2-methyl-3-phenylallylidene)-1-((1*S*,2*S*,4*S*,5*R*)-5-vinylquinuclidin-2-yl)methanamine (80): 9-Amino-(9-deoxy)*epi*quinine (**9**) (400 mg, 1.24



mmol) and (*E*)-2-methyl-3-phenylacrylaldehyde (183 μ L, 1.30 mmol, 1.05 equiv) were dissolved in methanol (4 mL) and activated 4 Å molecular sieves (0.5 g) were added. After stirring the reaction mixture overnight, TLC control (CH_2Cl_2 : MeOH: NH_3 conc.9:1:0.065) showed the disappearance of the starting

material. The mixture was filtered through a pad of Celite washing with dichloromethane, and the solvent was evaporated under reduced pressure to afford the title compound in quantitative yield, containing 5% of the excess (*E*)-2-methyl-3-phenylacrylaldehyde. This compound was found to be fairly stable to hydrolysis and could be handled in the air and with non-dried solvents. For long-term storage, it was kept under argon at 4 °C as a solid and in a vacuum-sealed NMR tube as a solution.

1H NMR (600 MHz, $CDCl_3$) δ 8.64 (d, $J = 4.5$ Hz, 1H, H-2'), 7.96 (s, 1H, H-13), 7.92 (d, $J = 9.2$ Hz, 1H, H-8'), 7.87 (d, $J = 2.8$ Hz, 1H, H-5'), 7.39 (d, $J = 4.5$ Hz, 1H, H-3'), 7.28 (dd, $J = 9.2$ Hz, $J = 2.8$ Hz, 1H, H-7'), 7.25-7.16 (m, 5H, H-18 + H-19 + H-20), 6.67 (br s, 1H, H-16), 5.69 (ddd, $J = 17.3$ Hz, $J = 10.3$ Hz, $J = 7.4$ Hz, 1H, H-10), 4.88 (ddd, $J = 17.3$ Hz, $J < 2$ Hz, $J < 2$ Hz 1H, H-11a), 4.84 (ddd, $J = 10.3$ Hz, $J < 2$ Hz, $J < 2$ Hz, 1H, H-11b), 4.69 (d, $J = 9.5$ Hz, 1H, H-9), 3.89 (s, 3H, H-12), 3.53 (ddd, $J = 10$ Hz, $J = 9.5$ Hz, $J = 8$ Hz 1H, H-8), 3.15 (dd, $J = 13.8$ Hz, $J = 10.3$ Hz, 1H, H-2a), 3.13 (dddd, $J = 14$ Hz, $J = 9$ Hz, $J = 2.5$ Hz, 1H, H-6b), 2.69 (ddd, $J = 14$ Hz, $J = 10.5$ Hz, $J = 5.9$ Hz, 1H, H-6a), 2.67 (dd, $J = 13.8$ Hz, $J = 6.0$ Hz, 1H, H-2b), 2.15 (c. m, 1H, H-3), 2.07 (d, $J < 2$ Hz, 3H, H-15), 1.56 (c. m, 1H, H-4), 1.47 (c. m, 2H, H-5a + H-5b), 1.26 (dddd, $J = 13.7$ Hz, $J = 10$ Hz, $J = 3.7$ Hz, 1H, H-7b), 0.81 (dddd, $J = 13.7$ Hz, $J = 8$ Hz, $J < 2$ Hz, 1H, H-7a).

^{13}C NMR (150 MHz, $CDCl_3$) δ 165.7 (C-13), 157.3 (C-6'), 147.7 (C-2'), 146.1 (C-4'), 145.1 (C-8a'), 142.0 (C-10), 139.44 (C-16), 137.15 (C-14), 136.7 (C-17), 131.7 (C-8'), 129.3 (C-19), 128.3 (C-18), 128.0 (C-4a'), 127.6 (C-20), 121.5 (C-3'), 121.3 (C-7'), 114.2 (C-11), 103.3 (C-

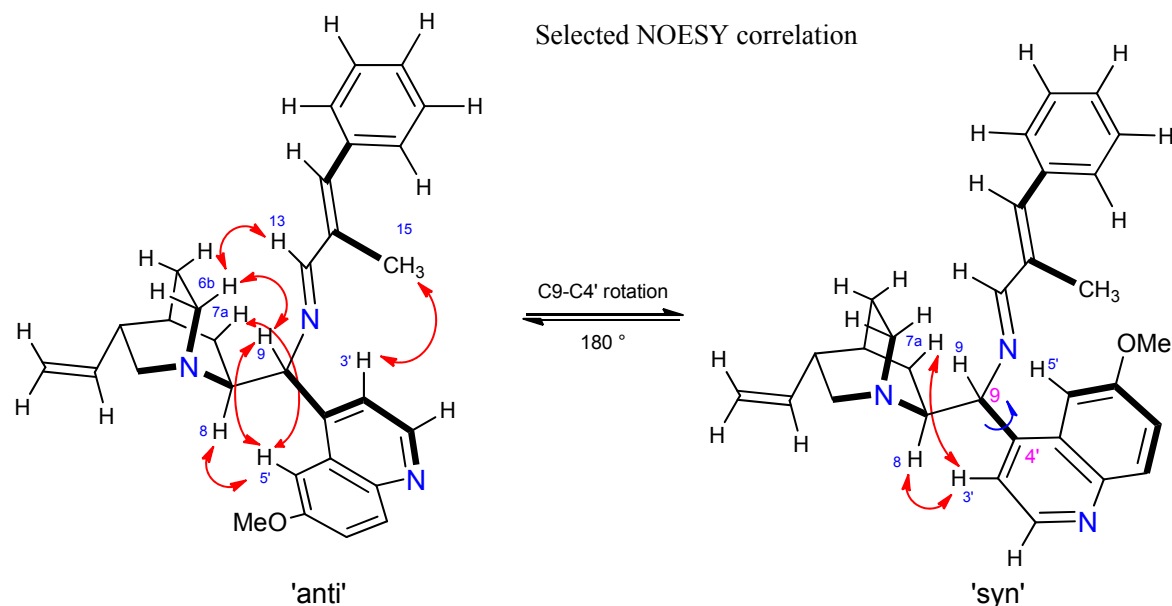
7. Experimental Section

5'), 74.8 (C-9), 60.4 (C-8), 56.6 (C-2), 55.5 (C-12), 41.0 (C-6), 40.0 (C-3), 28.35 (C-5), 28.0 (C-4), 26.0 (C-7), 13.5 (C-15).

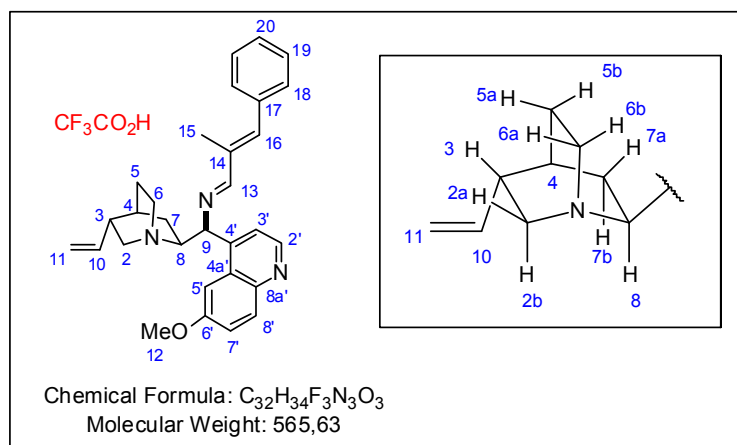
$^{15}\text{N-NMR}$ (60 MHz, CDCl_3 , $\delta_{\text{NH}_3} = 0$ ppm) δ 333.8 (imine N), 305.2 (quinoline N), 24.3 (quinuclidine N).

LRMS (EI): $m/z = 451$ [M], 308, 293, 266, 225, 199, 173, 160, 136, 81, 42.

HRMS (m/z) calcd for $\text{C}_{30}\text{H}_{33}\text{N}_3\text{ONa}$ [M+H] $^+$: 474.2516. Found: 474.2519.



(*S,E*)-1-(6-methoxyquinolin-4-yl)-*N*-((*E*)-2-methyl-3-phenylallylidene)-1-((1*S*,2*S*,4*S*,5*R*)-5-vinylquinuclidin-2-yl)methanamine trifluoroacetic acid salt (80a**):** Imine **80** (20 mg, 0.044



mmol) was dissolved in dry CDCl_3 in a flame-dried two-necked flask containing 20 mg activated 4 Å molecular sieves. To this suspension, trichloroacetic acid (3.3 μL , 0.044 mmol, 1 equiv) was added. After stirring for 5 min, the solution was transferred

into a flame-dried NMR tube using an HPLC syringe filter to remove molecular sieves and sealed under vacuum.

7. Experimental Section

^1H NMR (600 MHz, CDCl_3) δ 12.5 (br s, 1H, NH), 8.73 (d, $J = 4.4$ Hz, 1H, H-2'), 8.02 (d, $J = 9.4$ Hz, 1H, H-8'), 7.99 (s, 1H, H-13), 7.75 (br s, 1H, H-5'), 7.38 (dd, $J = 9.4$ Hz, $J = 2.8$ Hz, 1H, H-7'), 7.35 (br s, 1H, H-3'), 7.31-7.22 (m, 5H, H-18 + H-19 + H-20), 6.68 (br s, 1H, H-16), 5.68 (ddd, $J = 17.2$ Hz, $J = 10.2$ Hz, $J = 6.6$ Hz, 1H, H-10), 5.16-5.07 (m, 2H, H-11a + H-11b), 4.90 (br s, 1H, H-9), 4.28 (br s, 1H, H-8), 3.98 (s, 3H, H-12), 3.72 (dd, $J = 14$ Hz, $J = 10$ Hz, 1H, H-2a), 3.52 (c. m, 1H, H-6b), 3.35 (c. m, 1H, H-6a), 3.27 (c. m, 1H, H-2b), 2.65 (dt, $J = 10$ Hz, $J = 5.2$ Hz, 1H, H-3), 2.18 (d, $J = 1.2$ Hz, 3H, H-15), 2.00 (c. m, 1H, H-4), 1.96 (c. m, 2H, H-5a + H-5b), 1.71 (dd, $J = 13.2$ Hz, $J = 10.8$ Hz, 1H, H-7b), 1.35 (d, $J = 13.2$, 1H, H-7a).

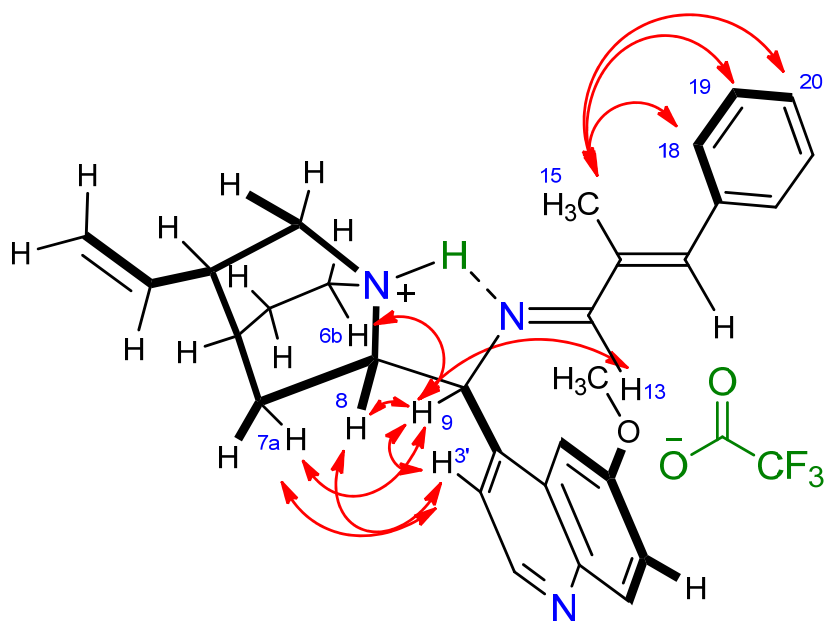
^{13}C NMR (150 MHz, CDCl_3) δ 169.6 (C-13), 162.3 (q, $J = 34.3$ Hz, COCF_3), 158.3 (C-6'), 147.2 (C-2'), 145.4 (C-4'), 142.1 (2C, C-8a' + 16), 137.1 (2C, C-14 + C-10), 136.1 (C-17), 132.3 (C-8'), 129.5 (C-18), 128.3 (C-19), 128.1 (C-20), 127.1 (C-4a'), 122.5 (C-7'), 122.1 (C-3'), 117.3 (C-11), 116.9 (q, $J = 293.7$ Hz, COCF_3), 103.7 (C-5'), 74.4 (C-9), 60.0 (C-8), 56.1 (C-12), 53.8 (C-2), 40.5 (C-6), 36.9 (C-3), 27.0 (C-4), 24.9 (C-5), 24.3 (C-7), 12.7 (C-15);

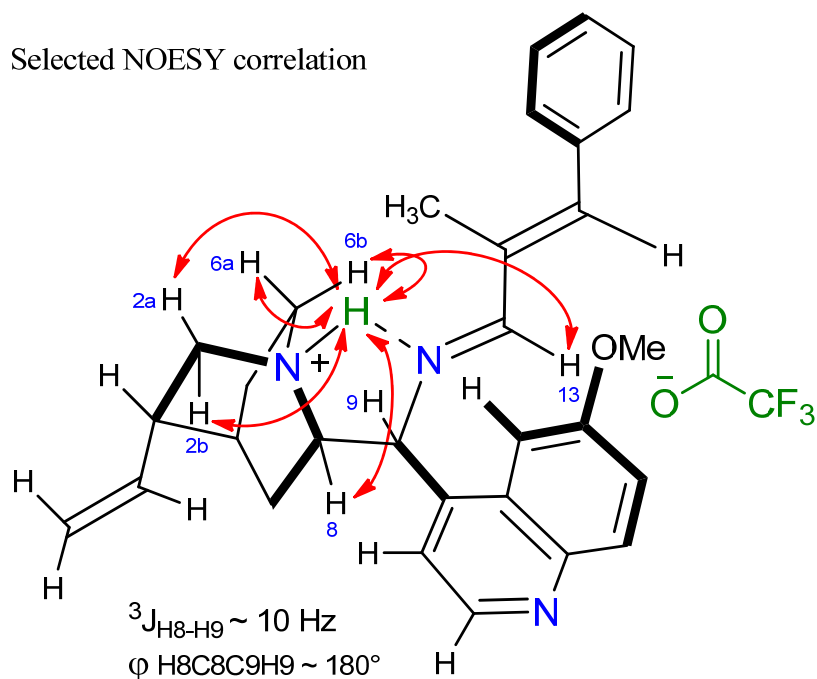
^{15}N -NMR (60 MHz, CDCl_3 , $\delta_{\text{NH}_3} = 0$ ppm,) δ 318.3 (imine N), 310.4 (quinoline N), 40.5 (quinuclidine N).

^{19}F -NMR (376 MHz, CDCl_3) δ -79.5.

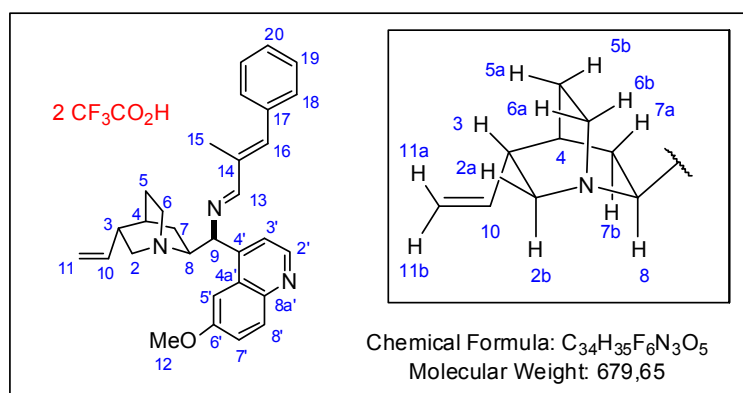
LRMS or **HRMS** were not performed due to extreme sensitivity of the title compound to hydrolysis.

Selected NOESY correlation





(*S,E*)-1-(6-methoxyquinolin-4-yl)-*N*-((*E*)-2-methyl-3-phenylallylidene)-1-((1*S*,2*S*,4*S*,5*R*)-5-vinylquinuclidin-2-yl)methanamine bis-trifluoroacetic acid salt (80b**):** Imine **80** (19.9 mg,



0.044 mmol) was dissolved in dry CDCl_3 in a flame-dried two-necked flask containing 20 mg activated 4 Å molecular sieves. To this suspension trichloroacetic acid (6.5 μL , 0.088 mmol, 2 equiv) was added. After stirring for 5 min,

this solution was transferred to a flame-dried NMR tube using an HPLC syringe filter to remove molecular sieves and sealed under vacuum.

$^1\text{H NMR}$ (600 MHz, CDCl_3) δ 12.0 (br s, 1H, NH), 8.88 (d, $J = 5.0 \text{ Hz}$, 1H, H-2'), 8.23 (d, $J = 9.3 \text{ Hz}$, 1H, H-8'), 8.13 (s, 1H, H-13), 7.98 (br s, 1H, H-5'), 7.77 (d, $J = 5.0 \text{ Hz}$, 1H, H-3'), 7.50 (dd, $J = 9.2 \text{ Hz}$, $J = 2.4 \text{ Hz}$, 1H, H-7'), 7.30-7.18 (m, 5H, H-18 + H-19 + H-20), 6.74 (s, 1H, H-16), 5.66 (ddd, $J = 17.2 \text{ Hz}$, $J = 10.4 \text{ Hz}$, $J = 6.4 \text{ Hz}$, 1H, H-10), 5.15 (c. m, 1H, H-9), 5.13 (dd, $J = 10.2 \text{ Hz}$, $J = 1.2 \text{ Hz}$, 1H, H-11a), 5.10 (dd, $J = 17.2 \text{ Hz}$, $J = 1.2 \text{ Hz}$, 1H, H-11b),

7. Experimental Section

4.34 (dt, $J = 9.6$ Hz, $J = 6.0$ Hz, 1H, H-8), 4.03 (s, 3H, H-12), 3.67 (c. m, 1H, H-6b), 3.65 (dd, 1H, $J = 13.8$ Hz, $J = 10.6$ Hz, H-2a), 3.34 (c. m, 1H, H-6a), 3.31 (ddd, $J = 13.8$ Hz, $J = 6.0$ Hz, $J = 1.6$ Hz, 1H, H-2b), 2.65 (dt, $J = 10.8$ Hz, $J = 6.0$ Hz, 1H, H-3), 2.15 (d, $J = 1.2$ Hz, 3H, H-15), 2.12-1.90 (m, 3H, H-4 + H-5a + H-5b), 1.74 (ddd, $J = 13.6$ Hz, $J = 9.6$ Hz, $J = 2.0$ Hz, 1H, H-7b), 1.40 (d, $J = 13.6$ Hz, 1H, H-7a).

^{13}C NMR (150 MHz, CDCl_3) δ 171.2 (C-13), 162.1 (q, $J = 35.7$ Hz, COCF_3), 159.7 (C-6'), 147.7 (C-4'), 143.4 (C-16), 143.0 (C-2'), 139.5 (C-8a'), 136.6 (C-10), 136.5 (C-14), 135.7 (C-17), 129.5 (C-19), 128.4 (C-20), 128.36 (C-18), 128.0 (C-4a'), 127.3 (C-8'), 125.6 (C-7'), 122.5 (C-3'), 117.6 (C-11), 116.6 (q, $J = 291.4$ Hz, COCF_3), 103.6 (C-5'), 73.2 (br, C-9), 59.8 (C-8), 56.4 (C-12), 53.8 (C-2), 40.9 (C-6), 36.6 (C-3), 26.8 (C-4), 24.4 (C-5), 23.9 (C-7), 12.6 (C-15).

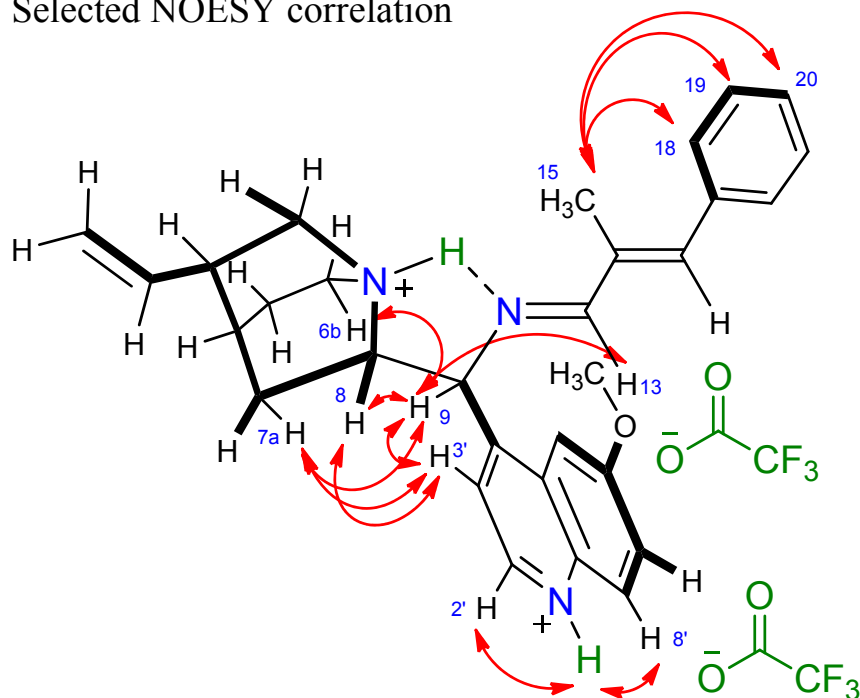
^{15}N -NMR (60 MHz, CDCl_3 , $\delta_{\text{NH}_3} = 0$ ppm) δ 313.9 (imine-N), quinoline N could not be detected, quinuclidine N could not be detected.

^{15}N -NMR (60 MHz, CDCl_3 , $T = 296$ K, $\delta_{\text{NH}_3} = 0$ ppm) δ 294 (quinoline N), 103 (N-oxide), amide N not detected under these conditions.

^{19}F -NMR (376 MHz, CDCl_3) δ -79.5.

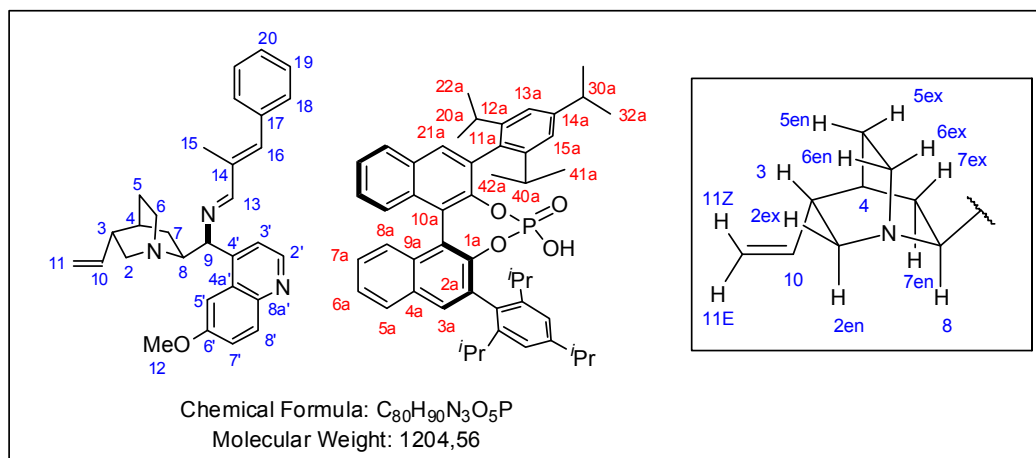
HRMS was not performed due to extreme sensitivity of the title compound to hydrolysis.

Selected NOESY correlation



7. Experimental Section

(*S,E*)-1-(6-methoxyquinolin-4-yl)-*N*-((*E*)-2-methyl-3-phenylallylidene)-1-((1*S*,2*S*,4*S*,5*R*)-5-vinylquinuclidin-2-yl)methanamine (*R*)-TRIP salt (80c**) :**



Imine **80** (20 mg, 0.044 mmol) was dissolved in dry CDCl₃ in a flame-dried two-necked flask containing 20 mg activated 4 Å molecular sieves. To this suspension, (*R*)-TRIP (**3**) (31 mg, 0.044 mmol, 1 equiv) was added. After stirring for 5 min, this solution was transferred to a flame-dried NMR tube using an HPLC syringe filter to remove molecular sieves and sealed under vacuum.

¹H NMR (600 MHz, CDCl₃, 223K, 2 conformers in 3:1 ratio, only major conformer described) δ 12.72 (br s, 1H, NH), 8.83 (d, *J* = 4.7 Hz, 1H, H-2'), 8.08 (d, *J* = 9.3 Hz, 1H, H-8'), 7.88 (d, *J* = 8.4 Hz, 2H, H-5a), 7.85 (s, 2H, H-3a), 7.49 (dd, *J* = 8.2 Hz, *J* = 5.4 Hz, 2H, H-6a), 7.45 (dd, *J* = 9.4 Hz, *J* = 2.2 Hz, 1H, H-7'), 7.35 (d, *J* = 8.5 Hz, 2H, H-8a), 7.30 (dd, *J* = 8 Hz, *J* = n.d., 2H, H-7a), 7.22-7.16 (m, 3H, H-19 + H-20), 7.08 (c. m, 1H, H-13), 7.075 (s, 2H, H-15a), 7.073 (d, *J* = 4.3 Hz, 1H, H-3'), 6.99 (br s, 3H, H-5' + H-13a), 6.63 (br s, 2H, C-18), 6.05 (s, 1H, H-16), 5.61 (ddd, *J* = 16.7 Hz, *J* = 10.4 Hz, *J* = 6.2 Hz, 1H, H-10), 5.12 (d, *J* = 10.8 Hz, 1H, H-9), 5.06 (d, *J* = 10.5 Hz, 1H, H-11E), 4.99 (d, *J* = 17.1 Hz, 1H, H-11Z), 4.18 (c. m, 1H, H-2ex), 3.91 (s, 3H, H-12), 3.41 (t, *J* = 10.3 Hz, 1H, H-8), 3.08 (br s, 2H, H-40a), 2.91 (sept, *J* = 6.8 Hz, 2H, H-30a), 2.75 (t, *J* = 11.5 Hz, 1H, H-6ex), 2.60 (c. m, 1H, H-6en), 2.62 (sept, *J* = 6.6 Hz, 2H, H-20a), 2.43 (c. m, 2H, H-3 + H-2en), 1.80 (c. m, 1H, H-4), 1.77 (t, *J* = 12.0 Hz, 1H, H-7en), 1.54 (c. m, 2H, H-5), 1.29 (c. m, 6H, H-31a), 1.28 (c. m, 6H, H-32a), 1.20 (s, 3H, H-15), 1.18 (c. m, 6H, H-42a), 1.05 (s, 6H, H-22a), 1.04 (s, 6H, H-41a), 0.96 (c. m, 1H, H-7ex), 0.88 (d, *J* = 6.7 Hz, 6H, H-21a).

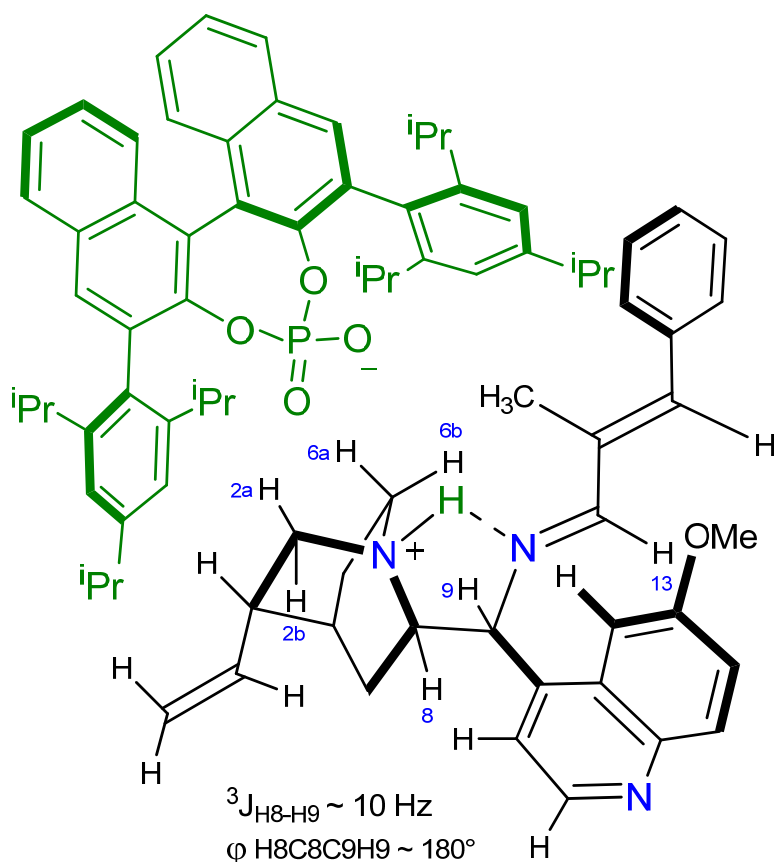
¹³C NMR (150 MHz, CDCl₃) δ 169.4 (C-13), 158.7 (C-6'), 148.75 (d, *J*_{P-C} = 9.1 Hz, C-1a), 148.5 (C-16a), 147.6 (C-12a), 147.7 (C-2'), 147.3 (C-14a), 145.1 (C-4'), 133.7 (C-11a), 141.8

7. Experimental Section

(C-8a'), 141.3 (C-16), 137.6 (C-10 + C-14), 136.1 (C-17), 133.7 (C-11a), 133.45 (d, $J_{P-C} = 2.4$ Hz, C-2a), 132.9 (C-9a), 132.5 (C-8'), 131.2 (C-3a), 130.3 (C-4a), 129.3 (C-18), 128.2 (C-19 + C-4a'), 128.0 (C-5a), 127.6 (C-20), 126.9 (C-8a), 125.5 (C-7a), 124.3 (C-6a), 122.82 (d, $J_{P-C} = 2$ Hz, C-10a), 121.8 (C-7'), 121.6 (br, C-3'), 120.6 (C-15a), 119.6 (C-13a), 116.7 (C-11), 102.0 (C-5'), 64.0 (br, C-9), 61.2 (C-8), 55.7 (C-12), 54.0 (C-2), 39.3 (C-6), 36.6 (C-3), 34.2 (C-30a), 31.1 (C-40a), 30.7 (C-20a), 26.8 (C-4), 26.4 (C-41a), 25.1 (C-5), 24.3 (C-7), 24.7 (C-21a), 24.3 (C-31a), 24.1 (C-32a), 23.8 (C-22a), 23.69 (C-42a), 11.9 (C-15).

$^{15}\text{N-NMR}$ (60 MHz, CDCl_3 , T = 223 K, $\delta_{\text{NH}_3} = 0$ ppms) δ 320.5 (imine N), 307.5 ($^2J_{\text{NH}_2\text{I}} = 10.3$ Hz, quinoline N), 40.5 ($^1J_{\text{NH}^+} = 70$ Hz, quinuclidine N).

$^{31}\text{P-NMR}$ (202 MHz, CDCl_3 , T = 223K, 2 species in a 3:1 ratio) δ 6.2 (3:1), 5.6 (3:1) LRMS or HRMS was not performed due to extreme sensitivity of the title compound to hydrolysis.



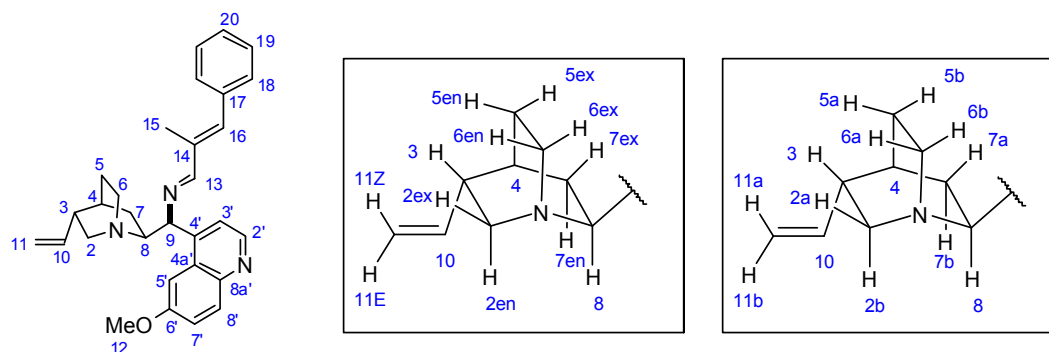
7. Experimental Section

Summary of ^{15}N NMR data for salts **80**

Acid partner HX (salt)	Equiv HX	Imine-N ₂₁ , ppm	Quinoline-N ₂₂ , ppm	Quinuclidine-N ₁ , ppm
None (80)	-	333.8	305.2	24.3
TFA (80a)	1	318.3	310.4	40.5
(<i>R</i>)-TRIP (80b)	1	320.5	307.5	40.5
(<i>R</i>)-TRIP (80b) ^a	1	319.1	297.5	not detected
TFA (80c)	2	313.9	not detected	not detected
(<i>R</i>)-TRIP (80d)	2	not detected	not detected	40.6

^a in MeOD as solvent

Summary of ^1H NMR data for salts **80**



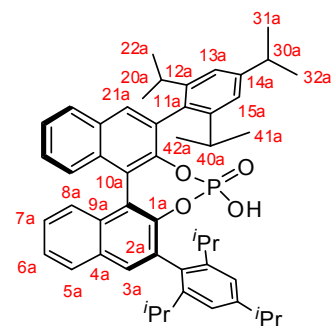
Proton assignment	80 Shift, ppm	80a (1 TFA) Shift, ppm	80b (2 TFA) Shift, ppm	80c (1 TRIP) Shift, ppm	80c (1 TRIP) Shift, ppm in CD ₃ OD
N-H	-	12.5	12.0	12.7	(exchangeable)
2a (ex)	3.15	3.72	3.65	4.18	
2b (en)	2.67	3.27	3.31	2.43	
3	2.15	2.65	2.65	2.43	
4	1.56	2.00	2.12-1.90	1.80	
5	1.47	1.96	2.12-1.90	1.54	
6a (en)	2.69	3.35	3.34	2.60	
6b (ex)	3.13	3.52	3.67	2.75	
7a (ex)	0.81	1.35	1.40	0.96	

7. Experimental Section

7b (en)	1.26	1.71	1.74	1.77	
8	3.53	4.28	4.34	3.41	
9	4.69	4.90	5.15	5.12	
10	5.69	5.68	5.66	5.61	
11a (Z)	4.88	5.16-5.07	5.13	4.99	
11b (E)	4.84	5.16-5.07	5.10	5.06	
12	3.89	3.98	4.03	3.91	
13	7.96	7.99	8.13	7.08	
15	2.07	2.18	2.15	1.20	
16	6.67	6.68	6.74	6.05	
18	7.25-7.16	7.31-7.22	7.30-7.18	6.63	
19	7.25-7.16	7.31-7.22	7.30-7.18	7.22-7.16	
20	7.25-7.16	7.31-7.22	7.30-7.18	7.22-7.16	
2'	8.64	8.73	8.88	8.83	8.71
3'	7.39	7.35	7.77	7.07	
5'	7.87	7.75	7.98	6.99	
7'	7.28	7.38	7.50	7.45	7.48
8'	7.92	8.02	8.23	8.08	8.00

Comparison of ^1H NMR data for (*R*)-TRIP as counteranion in salts **80c** and free acid (*R*)-TRIP

Proton assignment	(<i>R</i>)-TRIP acid Shift, ppm ^[186]	(<i>R</i>)-TRIP counterion in 80c Shift, ppm
3a	7.76	7.85
5a	7.88	7.88
6a	7.45-7.49	7.49
7a	7.22-7.30	7.30
8a	7.22-7.30	7.35
13a	6.91	6.99
15a	6.94	7.07
20a	2.49	2.62
21a	0.69	0.88
22a	0.94	1.05
30a	2.56	2.91
31a	1.19	1.29
32a	1.19	1.28
40a	2.81	3.08
41a	0.87	1.04
42a	1.01	1.18



7. Experimental Section

NMR-derived model: computational details

The NMR-derived model for the iminium structures **80** and $[\mathbf{80}+\text{H}]^+$ structures were calculated using XPLOR-NIH Ver. 2.9.7.^[149] The low-level force-field defined in the parameter for **80** was simply generated by PRODRG. Distance restraints derived from NOE cross peaks integrals over 5 different mixing time of 0, 100, 200, 300, 500 and 750 ms were applied using the “RELAXATION”^[187] function of XPLOR to account for spin-diffusion effect while *J*-coupling-derived restraints were imposed by using the “DIHEDRAL”^[149] function of the XPLOR-program. The simulated annealing computation operated in the following way: an initial molecular model was first minimized with a gradient criterion of less than 0.5 kcal/mol. The molecule is then set to a temperature of 2000K over a period of 8.1 ps, in steps of 1.25 fs. The molecule evolves at this temperature for 8.1 ps (6500 steps), thus sampling conformational space extensively. This is followed by a first cooling period lasting 6.25 ps down to 1000 K then by a second cooling period of 2.5ps down to 100K, both followed by Powell energy minimisation. This protocol was repeated 500 times and the 20 resulting conformers with lowest energy were preserved. During the first cooling period (5000 steps), NOE and *J*-coupling-derived dihedral angle terms are gradually raised from their initial weighting (0.02 kcal mol⁻¹Å⁻² and 1.0 kcal mol⁻¹deg⁻²) to their final weighting of (20.0 kcal mol⁻¹Å⁻² and 1000 kcal mol⁻¹deg⁻²) respectively.

List of NOE integrals (no units) used in XPLOR simulated annealing:

Atom 1	Atom 2	Mixing times (ms)					
		0	100	200	300	500	750
H2'	H3'	0	-6807000	-15103500	-25131000	-37046000	-48903000
H8'	H7'	0	8207850	-8459250	-21682500	-42346000	-57675500
H1	H8	0	-6149300	-10252100	-14155000	-16756000	-15819000
H1	H2	0	-7559450	-12609000	-16183000	-17430000	-14698000
H1	H6b	0	-4736050	-7431050	-9396900	-9726150	-7619650
H1	H6a	0	-5977750	-9125550	-12143000	-12764500	-10202850
H1	H2b	0	-6204550	-9743400	-13305000	-13483500	-10478500
H13	H16	0	-21701500	-39821500	-56816500	-81254000	-99154000
H13	H9	0	-12194500	-21131500	-28413500	-36035000	-39313000
H13	H8	0	-618255	-586175	-911640	-1900950	-1395505
H13	H6b	0	-1236095	-2643150	-3856950	-3041650	-3036050
H13	H15	0	-1407100	-1780650	-1700650	-4389350	-3098900
H5'	H9	0	-8837850	-16086000	-21475500	-27603000	-30311500
H5'	H8	0	-10018650	-17517000	-23850000	-31637500	-34836500
H5'	H12	0	-12781500	-21535000	-30516000	-43310500	-49277000
H5'	H15	0	-961760	-2261500	-4519400	-5648400	-6149000
H7'	H12	0	-3922550	-2969250	-6618150	-8045500	-11616200
H3'	H7a	0	-3547400	-6404900	-9760500	-9691200	-11085500

7. Experimental Section

H3'	H9	0	-10134600	-17499500	-23422500	-30685500	-32522000
H3'	H8	0	-4793400	-8332300	-10757850	-14911000	-17589500
H3'	H15	0	979860	99365	-1440910	-1061450	-1022205
H18/19	H16	0	486050	-9185900	-13371000	-22705000	-29305000
H18/19	H15	0	-7812650	-11562500	-16143000	-26825000	-32687500
H16	H15	0	1639900	-1197150	-2683100	-2021925	-3798650
H10	H2b	0	-3443950	-6522900	-8862550	-11840000	-13120500
H10	H3	0	-4004650	-4982800	-7616550	-11123500	-13869500
H10	H4	0	-1786550	-4483350	-6601850	-7872050	-9796100
H10	H7b	0	-4638900	-8361050	-12106500	-15515500	-17732000
H11a/11b	H2b	0	-3399550	-5443400	-7592050	-9246050	-10791000
H11a/11b	H3	0	-2860450	-5766450	-7578300	-11750000	-14224000
H9	H7a	0	-6351200	-10245000	-12966950	-14218600	-12979250
H9	H6b	0	-11422500	-18934000	-22933000	-25371500	-22709000
H9	H4/5a/5b	0	-6225050	-10371350	-13237550	-14085550	-12890300
H8	H2b	0	-16207500	-25480000	-32718500	-36934000	-35192500
H8	H7b	0	-13375500	-21747000	-28232000	-32881500	-32498000
H12	H15	0	-2142455	-4660900	-6600150	-8739450	-9921050

List of dihedral angles used in XPLOR simulated annealing

Atom1	Atom2	Atom3	Atom4	Dihedral (°)	±
H8	C8	C9	H9	180	40
C9	N21	C13	C14	180	1
N21	C13	C14	C16	180	40
C13	C14	C16	C17	180	1

List of additional distance restraint used in XPLOR simulated annealing

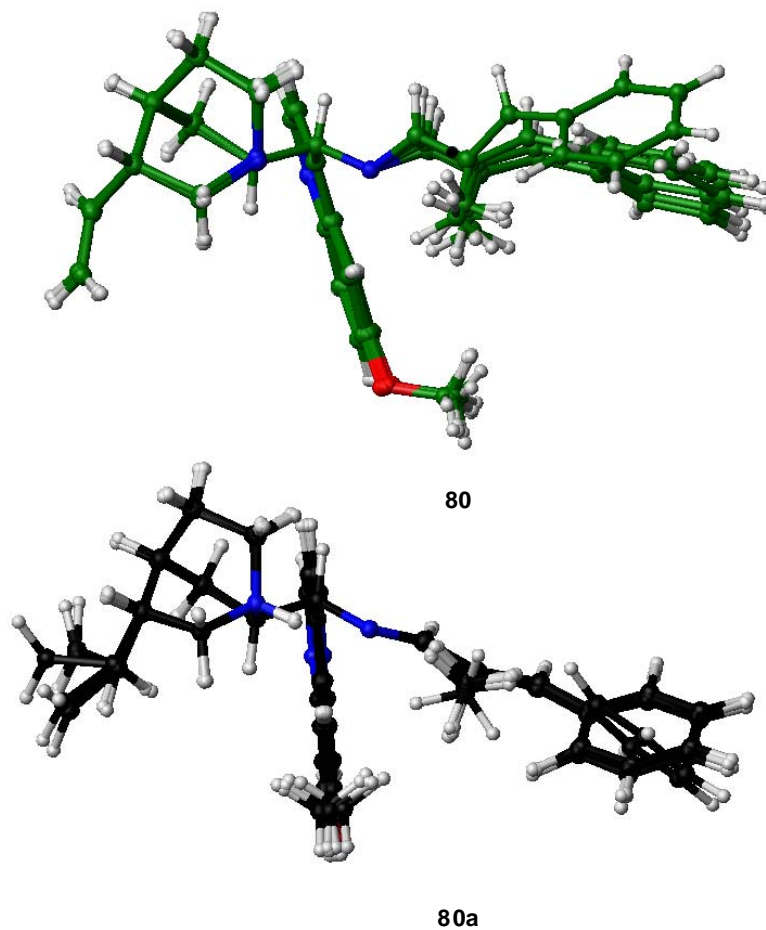
Atom 1	Atom 2	lower	Upper
H1	N21	1.5Å	2.5Å

XPLOR-based structure calculations: experimental summary

Results for structural models of 80 and [80+H]⁺ (20 best of 500)	80	[80+H]⁺
Average Energy	641 kcal/mol	564 kcal/mol
RMSD	<0.1 Å	<0.1 Å
Full Relaxation Matrix violations		
% of peak volumes with deviations within range 0.5-1.5	94%	94%
Other violations		
dihedral angles >5° (>7°)	1 (0)	0 (0)
bond angles >5° (>7°)	6 (0)	3 (0)
bond lengths >0.05 Å (>0.07 Å)	5 (0)	5 (0)

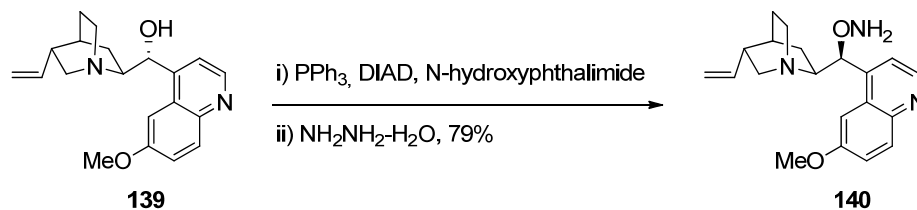
7. Experimental Section

Overlay of the resulting five lowest energy structures derived from the NMR data (*NOE* and *J* couplings) are depicted in green for the free imine **80** and in black for the protonated species **80a**. These structures are in overall agreement with the applied restraints with very low levels of violations and with relatively low residual energy. The flexibility of certain moieties such as in the phenyl group or in the ethylene group is present due to the lack of restraints measured by NMR.

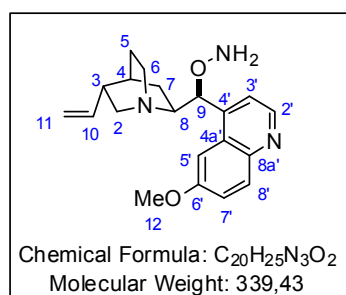


7. Experimental Section

7.2.6 Synthesis of 9-hydroxylamino(9-deoxy)epiquinine **140**



In a flame-dried round bottom flask under argon, quinine **139** (266 mg, 0.82 mmol, 1 equiv), triphenyl phosphine (258 mg, 1.97 mmol, 2.4 equiv) and *N*-hydroxyphthalimide (160.7 mg, 1.97 mmol, 2.4 equiv) were dissolved in dry THF (5 mL). The resulting orange solution was cooled to 0 °C and diisopropyl azadicarboxylate (DIAD, 195.2 μ L, 1.97 mmol, 2.4 equiv) was added dropwise. The solution was allowed to warm up to room temperature and stirred for 4 h. Hydrazine monohydrate (152.5 μ L, 3.77 mmol, 4.6 mmol) was added and the reaction was stirred for 30 min. The crude reaction mixture was diluted in ethyl acetate and water, and extracted with diethyl acetate three times. The combined organic layers were washed with sat. aq. NaCl, dried over MgSO₄, filtered and the solvent was removed under reduced pressure. Column chromatography eluting with a gradient of 20%-50% MeOH in EtOAc afforded **140** as an off-white amorphous foam (221.4 mg, 0.65 mmol, 79%).



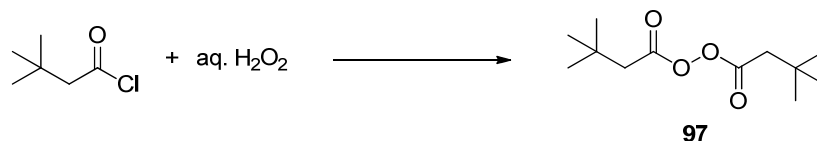
¹H NMR (500 MHz, CDCl₃) δ 8.78 (d, J = 4.5 Hz, 1H, H-2'), 8.06 (d, J = 9.3 Hz, 1H, H-8'), 7.77 (br s, 1 H, H-5'), 7.42 (d, J = 2.8 Hz, 1H, H-3'), 7.40 (br d, J = 2.9 Hz, 1H, H-7'), 5.74 (ddd, J = 17.2 Hz, J = 10.5 Hz, J = 7.5 Hz, 1H, H-10), 5.47 (br s, 1H, H-9), 4.95 (c. m, 2H, H-11), 3.96 (s, 3H, C-12), 3.42-3.26 (m, 3H), 2.95-2.83 (m, 1H), 2.78 (dq, J = 13.9 Hz, J = 2.2 Hz, 1H), 2.29 (br s, 1H), 1.71-1.55 (m, 3H), 0.83 (dd, J = 13.5 Hz, J = 7.5 Hz, 1H).

¹³C NMR (125 MHz, CDCl₃) δ 157.8, 147.3, 144.8, 143.3 (br), 141.5, 131.7, 128.2, 121.7, 121.2 (br), 114.4, 101.8, 84.7 (br), 58.9, 55.7, 55.5, 41.1, 39.5, 27.9, 27.4, 25.0.

HRMS (m/z) calcd for C₂₀H₂₅N₃O₂Na [M+Na]⁺: 362.18389. Found: 362.18414.

7.3 Catalytic Asymmetric α -Benzoyloxylation of Carbonyl Compounds

7.3.1 Preparation of the Starting Materials

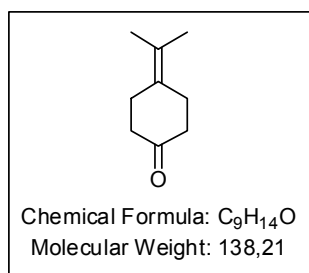
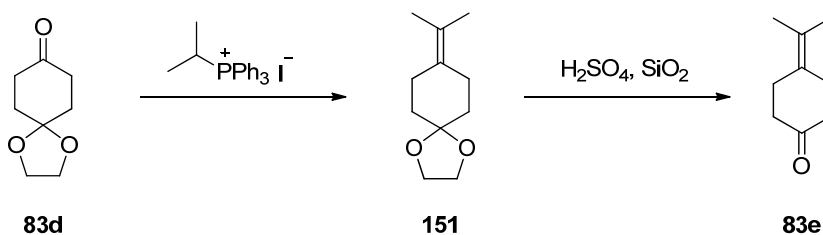


According to the procedure of *Kochi*,^[152] to a solution of pyridine (4.9 mL, 36 mmol, 2.4 equiv) in diethyl ether (15 mL) at 0 °C was added 50 wt. %, aqueous hydrogen peroxide (2.05 mL, 33 mmol, 2.2 equiv) dropwise with rapid stirring. Neopentyl chloride (4.17 mL, 30 mmol, 2 equiv) was added dropwise, so that the temperature did not exceed 4 °C. The reaction was stirred vigorously for 2 h, and 100 mL of ether were added, followed by a chilled solution of H₂SO₄ (50 mL in 200 mL water). The phase were separated and the aqueous solution washed with diethyl ether (100 mL). The combined organic phases were washed with chilled 10% H₂SO₄, water and NaHCO₃ (twice) and dried over Na₂SO₄. The solvent was removed under reduced pressure to afford **97** as a white solid (2.12g, 9.2 mmol, 61%).

¹H NMR (500 MHz, THF-d₈) : δ 2.43 (s, 4H), 1.20 (s, 18H).

The physical data are identical in all respects to those previously reported.^[152]

Ketones **83a-d** and **83f-k** were obtained from commercial sources (Sigma-Aldrich, Alfa Aesar) and used without purification.



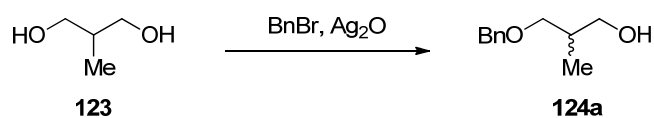
4-Isopropylidencyclohexanone (83e): Following the literature method of *Reviel et al.*^[188] NaH (616 mg, 15.4 mmol, 1.2 equiv, 60% suspension in oil) was dissolved in dry DMSO (8 mL), and the solution was stirred at 50 °C until it was red in colour. Ketone **83d** (2g, 12.8 mmol, 1 equiv) in DMSO (8 mL) was added and the reaction was stirred at 50 °C for 16 h. It was then cooled to room

7. Experimental Section

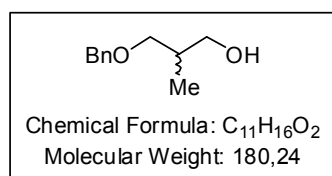
temperature, diluted with water (8 mL) and extracted with diethyl ether three times. Triphenyl phosphine oxide was repeatedly precipitated and filtered off by the addition of hexanes. The crude product **151** was dissolved in dichloromethane (10 mL), and 15% aq. H₂SO₄ (10 mL) and silica gel (1 spatula) and stirred at room temperature for 2 days. Column chromatography eluting with a gradient of 10% diethyl ether in pentane afforded **83e** as a colourless oil (1.17 g, 8.5 mmol, 55%, 2 steps).

¹H NMR: (500 MHz, CDCl₃) δ 2.54 (apparent t, *J* = 6.5 Hz, 4H, CH₂C(O)CH₂), 2.39 (apparent t, *J* = 7.4 Hz, 4H, CH₂C=C(Me₂)CH₂), 1.72 (s, 6H, CH₃).

The physical data are identical in all respects to those previously reported.^[188]



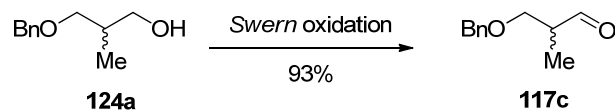
3-(benzyloxy)-2-methylpropan-1-ol (124a): To the diol **123** (4.9 mL, 55.5 mmol, 1 equiv) in dichloromethane (250 mL) was added Ag₂O (1.9 g, 83 mmol, 1.5 equiv) and benzyl bromide (7.3 mL, 61 mmol, 1.1 equiv). The mixture was stirred at room temperature for 2 days, after which incomplete conversion was still observed. The crude reaction mixture was diluted with water, extracted with dichloromethane three times, dried over MgSO₄ and the solvent was removed under reduced pressure. Column chromatography eluting with 30% EtOAc in hexanes afforded spectroscopically pure **124a** as a colourless oil (2.53 g, 14 mmol, 25%).



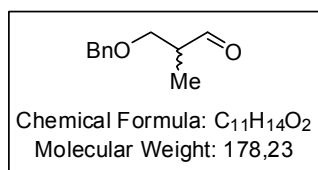
¹H NMR: (500 MHz, CDCl₃) δ 7.40-7.28 (m, 5H, CH_{Ar}), 4.53 (br s, 2H, PhCH₂), 3.67-3.59 (m, 2H, CH₂OH), 3.57 (dd, *J* = 9.2 Hz, *J* = 4.8 Hz, 1H, BnOCH₂), 3.44 (dd, *J* = 9.2 Hz, *J* = 8.2 Hz, 1H, BnOCH₂), 2.55 (br s, 1H, OH), 2.09 (c.m, 1H, MeCH), 0.89 (d, *J* = 7.2 Hz, 3H, CH₃).

The physical data are identical in all respects to those previously reported.^[189]

7. Experimental Section



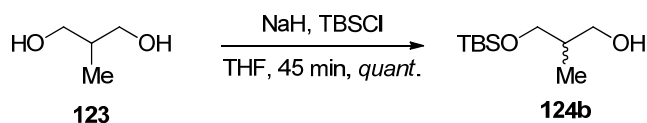
3-(benzyloxy)-2-methylpropanal (117c): To a solution of oxalyl chloride (0.98 mL, 11.1 mmol, 2 equiv) in dry dichloromethane (5 mL) at $-78\text{ }^{\circ}\text{C}$ under argon was added DMSO (0.8 mL, 11.1 mmol, 2 equiv) in dry dichloromethane (5 mL). The mixture was stirred for 10 min, and the alcohol **124a** (1.0 g, 5.55 mmol, 1 equiv) in dry dichloromethane (15 mL) was added dropwise at $-78\text{ }^{\circ}\text{C}$. The mixture was stirred at this temperature for 25 min and triethyl amine (3 mL, 21.6 mmol, 3.9 equiv) was added. After stirring the reaction at $-78\text{ }^{\circ}\text{C}$ for an additional 15 min, the reaction was allowed to warm up to r.t., diluted with 100 mL of dichloromethane, and washed with 1M HCl and water. The aqueous layer was washed with dichloromethane three times, and the combined organic layers washed with sat. aq. NaCl, dried over MgSO_4 and the solvent was removed under reduced pressure. Column chromatography eluting with 20% EtOAc in hexanes afforded spectroscopically pure **117c** as a colourless oil (0.92 g, 5.16 mmol, 93%).



$^1\text{H NMR}$: (500 MHz, CDCl_3) δ 9.74 (d, $J = 8.2$ Hz, 1H, CHO), 7.39-7.28 (m, 5H, CH_{Ar}), 4.54 (s, 2H, PhCH_2), 3.70 (dd, $J = 9.4$ Hz, $J = 6.8$ Hz, 1H, BnOCH_2), 3.65 (dd, $J = 9.4$ Hz, $J = 5.2$ Hz, 1H, BnOCH_2), 2.68 (c. m, 1H, MeCH), 1.15 (d, $J = 7.0$ Hz, 3H, CH_3).

HRMS (m/z) alcd for $\text{C}_{11}\text{H}_{15}\text{O}_2$ $[\text{M}+\text{H}]^+$: 179.10720. Found: 179.10712

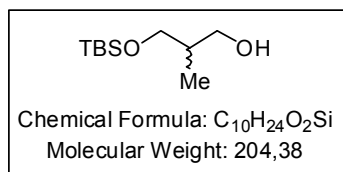
The physical data are identical in all respects to those previously reported.^[189]



In a flame-dried round bottom flask equipped with a dropping funnel under argon, NaH (1.78 g, 44.4 mmol, 1 equiv, 60% suspension in oil) was suspended in dry THF (84 mL), and the diol **123** (3.9 mL, 44.4 mmol, 1 equiv) was added dropwise. The reaction mixture was stirred at r.t. for 45 min and TBSCl (6.7 g, 44.4 mmol, 1 equiv) was added in several portions. The reaction was stirred for another 45 min and quenched with 10% aq. Na_2CO_3 and water to dissolve all insoluble material. The crude reaction extracted with diethyl ether three times, the combined organic layers washed with sat. aq. NaCl, dried over MgSO_4 and the solvent was removed under

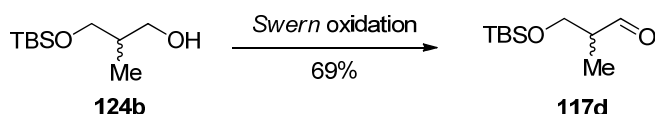
7. Experimental Section

reduced pressure. Compound **124b** was obtained in a spectroscopically pure form and quantitative yield (9,1 g, 44.4 mmol) without any further purification.

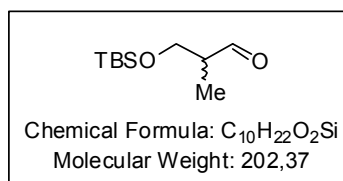


¹H NMR: (500 MHz, CDCl₃) δ 3.75 (ddd, *J* = 9.8 Hz, *J* = 4.4 Hz, *J* = 0.4 Hz, 1H, TBSOCH₂), 3.68-3.58 (m, 2H, CH₂OH), 3.55 (dd, *J* = 9.7 Hz, *J* = 7.9 Hz, 1H, TBSOCH₂), 2.86 (br s, 1H, OH), 1.95 (c. m, 1H, MeCH), 0.91 (s, 9H, (CH₃)₃CSi), 0.84 (d, *J* = 6.9 Hz, 3H, CH₃), 0.08 (s, 6H, Si(CH₃)₂).

The physical data are identical in all respects to those previously reported.^[190]



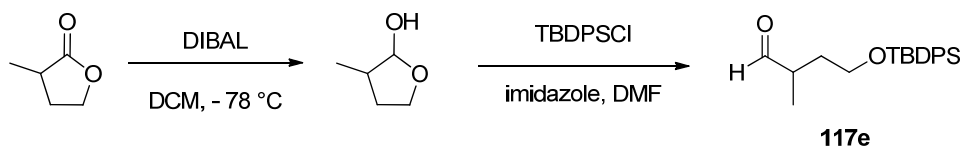
3-((tert-butyldimethylsilyloxy)-2-methylpropanal (117d): To a solution of oxalyl chloride (0.91 mL, 10.6 mmol, 2 equiv) in dry dichloromethane (18 mL) at -78 °C under argon was added DMSO (1.5 mL, 21.2 mmol, 4 equiv). The mixture was stirred for 30 min, and the alcohol **124b** (1.0 g, 5.3 mmol, 1 equiv) in dry dichloromethane (18 mL) was added dropwise at -78°C. The mixture was stirred at this temperature for 30 min and triethyl amine (4.4 mL, 31.9 mmol, 6 equiv) was added. After stirring the reaction at -78 °C for an addition 30 min, the reaction was allowed to warm up to r.t., quenched with sat. aq. NH₄Cl, diluted with 100 mL of dichloromethane, and washed with sat. aq. NH₄Cl and water. The aqueous layer was washed with dichloromethane three times, and the combined organic layers washed with sat. aq. NaCl, dried over MgSO₄ and the solvent was removed under reduced pressure. Column chromatography eluting with 15% EtOAc in hexanes afforded spectroscopically pure **117d** as a colourless oil (0.74 g, 3.66 mmol, 69%).



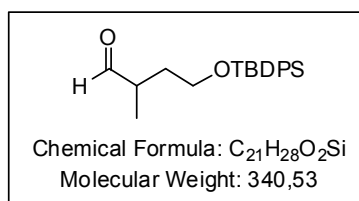
¹H NMR: (500 MHz, CDCl₃) δ 9.73 (d, *J* = 1.6 Hz, 1H, CHO), 3.83 (dd, *J* = 10.5, *J* = 5.1 Hz, 1H, TBSOCH₂), 3.81 (dd, *J* = 10.2, *J* = 6.3 Hz, 1H, TBSOCH₂), 2.53-2.50 (m, 1H, MeCH), 1.05 (d, *J* = 7.0 Hz, 3H, CH₃), 0.83 (s, 9H, (CH₃)₃CSi), 0.04 (s, 6H, Si(CH₃)₂).

The physical data are identical in all respects to those previously reported.^[189]

7. Experimental Section



4-((tert-butyldiphenylsilyl)oxy)-2-methylbutanal (117e): α -Methyl- γ -butyrolactone (1 g, 9.99 mmol, 1 equiv) was dissolved in anhydrous dichloromethane (12 mL) and cooled to $-78\text{ }^{\circ}\text{C}$. To this solution was added DIBAL (1 M in dichloromethane, 11 mL, 1.1 equiv) and the reaction was stirred at $-78\text{ }^{\circ}\text{C}$ for 1 h, at which point TLC control showed complete conversion of the starting material. The crude reaction mixture was quenched with ethyl acetate and sodium potassium tartrate (Rochelle's salt) at $-78\text{ }^{\circ}\text{C}$ and allowed warm up to room temperature over 1 h while stirring. The reaction was then extracted with dichloromethane three times, washed with brine, dried over MgSO_4 , filtered and carefully evaporated under reduced pressure (this product is very volatile) to afford the crude lactol as clear liquid, which was used in the next step without purification. The crude lactol was dissolved in anhydrous DMF (10 mL). To this solution was added TBDPSCl (2.74 g, 9.99 mmol, 1 equiv) and imidazole (1.02 g, 15 mmol, 1.5 equiv), and the reaction was stirred at room temperature for 20 h. The crude reaction mixture was diluted with dichloromethane, washed with sat. aq. NH_4Cl , extracted with dichloromethane three times, washed with brine, dried over MgSO_4 , filtered and evaporated under reduced pressure. Column chromatography eluting with 3% diethyl ether in pentane afforded pure **117e** as a colorless oil (1.93 g, 5.67 mmol, 57% over 2 steps).



$^1\text{H NMR}$: (500 MHz, CDCl_3) δ 9.69 (d, $J = 1.6\text{ Hz}$, 1H, CHO), 7.69-7.63 (m, 4H, CH_{Ar}), 7.47-7.36 (m, 6H, CH_{Ar}), 3.78-3.67 (m, 2H, TBDPSOCH_2), 2.59 (dpent, $J = 6.9\text{ Hz}$, $J = 1.4\text{ Hz}$, 1H, MeCH), 2.06-1.97 (m, 1H, $\text{TBDPSOCH}_2\text{CH}_2$), 1.67-1.59 (m, 1H, $\text{TBDPSOCH}_2\text{CH}_2$), 1.09 (d, $J = 7.2\text{ Hz}$, 3H, CH_3), 1.05 (s, 9H, $(\text{CH}_3)_3\text{CSi}$).

The physical data are identical in all respects to those previously reported.^[191]

7.3.2 General α -Benzoyloxylaton Procedures

Anhydrous benzoyl peroxide is available commercially (98% anhydrous) or can be prepared from the commercially available 70-75% hydrate on a large scale using a simple procedure as follows. To benzoyl peroxide (10 g, 75%, remainder water, Sigma-Aldrich) was added dichloromethane (100 mL) and stirred for 5 min at room temperature until most of the solid dissolved. This slightly opaque solution was cooled to 0 °C and $\text{MgSO}_4 \cdot x\text{H}_2\text{O}$ or Na_2SO_4 (10 g, Sigma-Aldrich) was added slowly. This suspension was thoroughly swirled, filtered through a sintered glass filter, evaporated under reduced pressure (keeping the water bath temperature below 30 °C) and dried under vacuum to obtain a fine free-flowing white solid. Anhydrous benzoyl peroxide prepared in this manner was stored at 4 °C and its purity was checked by ^1H NMR in THF-d_8 .

CAUTION: Although we handled this compound without any special precautions, and never experienced any shock or heat related explosions, care should be taken when using this chemical. Anhydrous benzoyl peroxide should never be heated above 40 °C or exposed to sparks, shock or strong reducing agents. This compound is known to explode spontaneously when heated above its melting point at 103 °C.

7.3.2.1 α -Benzoyloxylaton of Cyclic Ketones **83**

Procedure A: *α -Benzoyloxylation of 6-membered cyclic ketones **83a-h** and cholestanone **83l***

A 2 mL vial, equipped with a magnetic stirring bar, was charged with 2,6-di-tert-butyl-4-methylphenol (BHT) (9.0 mg, 0.0408 mmol, 10 mol%), cinchona primary amine derivative **9**, **11** or **12** (0.408 mmol, 10 mol%), trichloroacetic acid (6.6 mg, 0.0408 mmol, 10 mol%), ketone **1** (0.408 mmol) and 1,4-dioxane (0.4 mL) and stirred for 5 min before adding anhydrous benzoyl peroxide (147 mg, 0.612 mmol, 1.5 equiv). The reaction mixture was stirred at 30 °C for 24 h (48 h for 2 mmol scale), diluted with dichloromethane, treated with a saturated aqueous solution of NaHCO_3 , extracted three times with dichloromethane, washed with brine, dried over Na_2SO_4 , filtered, concentrated to approx. 1 mL (approx. 5 mL on 2 mmol scale) and purified by either flash column chromatography eluting with a specified mixture of pentane and Et_2O , or preparative TLC. The enantioselectivity was determined by chiral-phase HPLC analysis. Although most ketones **84** could be purified by regular silica-gel chromatography without any, or with only slight ($\leq 3\%$ ee), racemization, compounds **84e** and **84f** were found to be particularly sensitive to racemization. Preparative TLC-grade silica (Macherey-Nagel, SIL 193

7. Experimental Section

G-25 UV₂₅₄) was found to reproducibly preserve the enantiomeric excess for all purified ketones **84**, whereas other types of silica and alumina diminished the enantioselectivity after flash column chromatography for some products. A rapid plug of regular silica or alumina eluting with diethyl ether without a prior aqueous workup was found to be effective in preventing racemization but failed to remove excess benzoyl peroxide.

Procedure B: α -Benzoyloxylation of *n*-membered cyclic ketones (*n* = 7,8) **83j-k**

A 2 mL vial, equipped with a magnetic stirring bar, was charged with 2,6-di-tert-butyl-4-methylphenol (BHT) (4.5 mg, 0.0204 mmol, 10 mol% w.r.t. benzoyl peroxide), 9-amino(9-deoxy)*epi*quinine **9** (6.6 mg, 0.0204 mmol, 10 mol% w.r.t. benzoyl peroxide), phosphoric acid diphenyl ester (5.1 mg, 0.0204 mmol, 10 mol% w.r.t. benzoyl peroxide), ketone **1** (0.408 mmol, 2 equiv w.r.t. benzoyl peroxide) and 0.2 mL of dioxane and stirred for 5 min before adding anhydrous benzoyl peroxide (49 mg, 0.208 mmol). The reaction mixture was stirred at 30 °C for 20 h, diluted with dichloromethane, then treated with a saturated aqueous solution of NaHCO₃, extracted three times with dichloromethane, washed with brine, dried over Na₂SO₄, filtered, concentrated to approx. 1 mL and purified by either flash column chromatography eluting with a specified mixture of pentane and Et₂O, or preparative TLC. The enantioselectivity was determined by chiral-phase HPLC analysis.

7.3.2.2 α -Benzoyloxylation of α -Branched Aldehydes **117**

A 2 mL vial, equipped with a magnetic stirring bar, was charged with 2,6-di-tert-butyl-4-methylphenol (BHT) (9.0 mg, 0.0408 mmol, 10 mol%), cinchona primary amine derivative **9** or **15** (0.408 mmol, 10 mol%), (*R*) or (*S*)-TRIP **3** (29 mg, 0.0408 mmol), aldehyde **117** (0.408 mmol) and THF (0.4 mL) before adding anhydrous benzoyl peroxide (119 mg, 0.490 mmol, 1.2 equiv). The reaction mixture was stirred at room temperature for 15 h, diluted with dichloromethane, then treated with a saturated aqueous solution of NaHCO₃, extracted three times with dichloromethane, washed with brine, dried over Na₂SO₄, filtered, concentrated and purified by either flash column chromatography eluting with a specified mixture of pentane and Et₂O. The enantioselectivity of the resulting aldehydes **118** was determined by chiral-phase HPLC analysis.

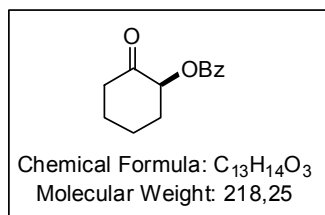
7. Experimental Section

Procedure C: in-situ reduction of aldehydes 118 to diols 154

To the crude reaction mixture containing aldehyde **118** was added ethanol (2 mL) and NaBH₄ (2 equiv) at room temperature. The reaction mixture was stirred at room temperature for 10 min, diluted with ethyl acetate, and treated with a saturated aqueous solution of NH₄Cl, extracted three times with ethyl acetate, washed with brine, dried over Na₂SO₄, filtered, concentrated to approximately 1 mL and purified by either flash column chromatography eluting with a specified mixture of ethyl acetate/hexane or diethyl ether/pentane, or preparative TLC. The enantioselectivity was determined by chiral-phase HPLC analysis. **IMPORTANT**: stirring the reaction for longer times (> 10 min) at room temperature results in the transfer of the benzoyl group to the primary alcohol moiety (complete within 2 hr) to form the more thermodynamically stable product^[192] (cf. compounds **156** and **157**). This process can be effectively suppressed by short reaction time (10 min or less, *vide supra*) or by running the reaction at – 78 °C and monitoring the reaction by TLC.

7.3.2.3 α -Benzoyloxylaton of α -Branched Enals 53b-c

A 2 mL vial, equipped with a magnetic stirring bar, was charged with 2,6-di-tert-butyl-4-methylphenol (BHT) (4.4 mg, 0.020 mmol, 10 mol%), 9-amino(9-deoxy)*epi*quinine **9** (6.5 mg, 0.020 mmol, 10 mol%), trichloroacetic acid (9.8 mg, 0.060 mmol, 30 mol%), aldehyde **53** (0.20 mmol) and THF (0.2 mL) before adding anhydrous benzoyl peroxide (72.7 mg, 0.30 mmol, 1.5 equiv). The reaction mixture was stirred at room temperature for 18 h, diluted with dichloromethane, then treated with a saturated aqueous solution of NaHCO₃, extracted three times with dichloromethane, washed with brine, dried over Na₂SO₄, filtered, concentrated and purified by either flash column chromatography eluting with a specified mixture of pentane and Et₂O. The enantioselectivity of the resulting aldehydes **128** and **129** was determined by chiral-phase HPLC analysis.

7.3.3 Scope of Enantioenriched α -Benzoyloxylated Carbonyl Compounds7.3.3.1 α -Benzoyloxylated Cyclic Ketones 84

(S)-2-Benzoyloxycyclohexanone (84a): Prepared according to the general procedure A (Section 7.3.2.1) using commercial cyclohexanone **83a** (21 μ L, 0.204 mmol) and 9-amino-9-deoxyepiquinine **9** (6.6 mg, 0.0204 mmol). Purification by flash chromatography (20% Et₂O in pentane) afforded **84a** as a white solid (29.7 mg, 0.14 mmol, 67%, 97:3 er). A single recrystallization from hot pentane/diethyl ether increased the enantiomeric ratio of **84a** to >99.5:0.5 er.

¹H NMR (400 MHz, CDCl₃) δ 8.09 (dd, $J = 8.4$ Hz, $J = 1.1$ Hz, 2H, CH_{Ar}), 7.57 (tt, $J = 7.4$ Hz, $J = 1.2$ Hz, 1H, CH_{Ar}), 7.44 (t, $J = 7.8$ Hz, 2H, CH_{Ar}), 5.41 (dd, $J = 12.0$ Hz, $J = 6.3$ Hz, 1H, CHOBz), 2.57 (dq, $J = 13.7$ Hz, $J = 2.2$ Hz, 1H), 2.48 (ddd, $J = 13.6$ Hz, $J = 6.2$ Hz, $J = 0.8$ Hz, 1H), 2.48-2.39 (m, 1H), 2.12 (dsept, $J = 13.4$ Hz, $J = 3.0$ Hz, 1H), 2.03 (c.m, 1H), 1.94 (qd, $J = 12.5$ Hz, $J = 3.6$ Hz, 1H), 1.83 (qt, $J = 12.4$ Hz, $J = 3.1$ Hz, 1H), 1.69 (qt, $J = 13.2$ Hz, $J = 4.0$ Hz, 1H).

¹³C NMR (100 MHz, CDCl₃) δ 204.35, 165.53, 133.12, 129.83, 129.62, 128.30, 76.94, 40.71, 33.15, 27.16, 23.74.

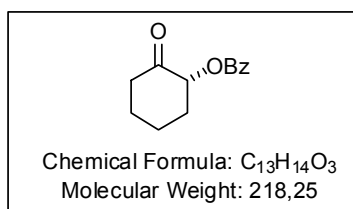
FTIR (thin film) 2947, 2869, 1716, 1451, 1316, 1269, 1112, 1071, 909, 730 cm⁻¹

HRMS (m/z) calcd for C₁₃H₁₄O₃Na [M+Na]⁺: 241.0835. Found 241.0833.

m.p.: 87.9-88.1 °C.

$[\alpha]_D^{25}$: -16.3° (c 0.295, CHCl₃) [For the opposite enantiomer, Lit:^[108] $[\alpha]_D^{25} = +19.9$ ($c = 0.87$, CHCl₃)].

Chiral HPLC (OD-3, nHept/iPrOH 90:10, 1 mL/min, 25 °C) t_r 4.5 min (minor enantiomer), t_r 6.19 min (major enantiomer).



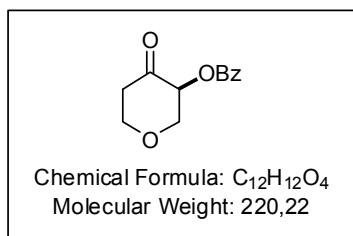
(R)-2-Benzoyloxycyclohexanone (ent-84a): Prepared according to the general procedure A (Section 7.3.2.1) using commercial cyclohexanone **84a** (21 μ L, 0.204 mmol) and 9-amino-9-deoxyepicinchonine **12** (6.6 mg, 0.0204 mmol). Purification by flash chromatography (20% Et₂O in pentane) afforded **ent-4a** as a white solid (64.9 mg, 0.30 mmol, 73%, 89:11 er).

¹H and ¹³C NMR spectra were identical to those of compound (S)-**84a**.

7. Experimental Section

$[\alpha]_D^{25}$: + 7.4° (*c* 0.296, CHCl₃) [Lit: *Error! Bookmark not defined.* $[\alpha]_D^{25}$ = + 19.9 (*c* = 0.87, CHCl₃)]

Chiral HPLC (OD-3, nHept/iPrOH 90:10, 1 mL/min, 25 °C) *t_r* 4.5 min (major enantiomer), *t_r* 6.19 min (minor enantiomer).



(S)-2-Benzoyloxytetrahydro-4H-pyran-4-one 4c (84b):

Prepared according to the general procedure A (Section 7.3.2.1) using commercial tetrahydro-4H-pyran-4-one **83b** (36.9 μL, 0.408 mmol) and 9-amino-9-deoxyepiquinine **9** (13.2 mg, 0.0408 mmol), except that (PhO)₂PO₂H (10.2 mg, 0.0408 mmol) was used as the acid co-catalyst. Purification by flash chromatography (25% Et₂O in pentane) afforded **84b** as a white solid (59.3 mg, 0.27 mmol, 66%, 93:7 er, purified by prep. TLC: 95:5 er).

¹H NMR (400 MHz, CDCl₃) δ 8.07 (d, *J* = 8.4 Hz, *J* = 1.3 Hz, 2H, CH_{Ar}), 7.59 (t, *J* = 7.5 Hz, *J* = 1.3 Hz, 1H, CH_{Ar}), 7.45 (t, *J* = 7.7 Hz, 2H, CH_{Ar}), 5.52 (ddd, *J* = 10.5 Hz, *J* = 6.9 Hz, *J* = 0.6 Hz, 1H, CHOBz), 4.46 (ddd, *J* = 10.5 Hz, *J* = 7.0 Hz, 1.5 Hz, 1H, OCH₂CHOBz), 4.31 (ddt, *J* = 11.4 Hz, *J* = 7.2 Hz, *J* = 1.5 Hz, 1H, OCH₂CHOBz), 3.72 (c.m, 2H, OCH₂CH₂), 2.85 (c.m, 1H, OCH₂CH₂), 2.60 (dt, *J* = 14.2 Hz, *J* = 2.1 Hz, 1H, OCH₂CH₂).

¹³C NMR (100 MHz, CDCl₃) δ 200.47, 165.09, 133.53, 129.99, 129.05, 128.48, 74.07, 70.59, 68.55, 42.29.

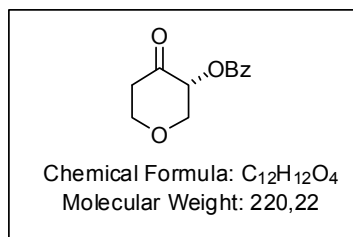
FTIR (thin film) 2976, 2864, 1723, 1694, 1452, 1317, 1279, 1206, 1124, 1100, 1072, 973 cm⁻¹;

HRMS (*m/z*) calcd for C₁₂H₁₂O₄Na [M+Na]⁺: 243.0628. Found 243.0625.

m.p.: 78.3-78.5 °C.

$[\alpha]_D^{25}$: - 16.2° (*c* 0.260, CHCl₃).

Chiral HPLC (OD-3, nHept/iPrOH 90:10, 1 mL/min, 25 °C) *t_r* 6.20 min (minor enantiomer), *t_r* 8.18 min (major enantiomer).



(R)-2-Benzoyloxytetrahydro-4H-pyran-4-one (ent-84b):

Prepared according to the general procedure A (Section 7.3.2.1) using commercial tetrahydro-4H-pyran-4-one **83b** (36.9 μL, 0.408 mmol) and 9-amino-9-deoxyepicinchonine **12** (12 mg, 0.0408 mmol), except that (PhO)₂PO₂H (10.2 mg, 0.0408 mmol) was used as the acid co-catalyst. Purification by flash chromatography (25% Et₂O in

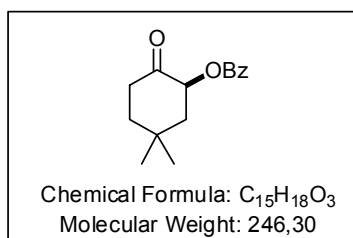
7. Experimental Section

pentane) afforded **ent-84b** as a white solid (56.6 mg, 0.26 mmol, 63%, 93:7 er, purified by prep. TLC: 95:5 er).

^1H and ^{13}C NMR spectra were identical to those of compound (*S*)-**84b**.

m.p.: 78.3-78.5 °C.

Chiral HPLC (OD-3, nHept/iPrOH 98:2, 1 mL/min, 25 °C) t_r 11.07 min (major enantiomer), t_r 16.65 min (minor enantiomer).



(*S*)-2-Benzoyloxy-4,4-dimethylcyclohexanone (**84c**):

Prepared according to the general procedure A (Section 7.3.2.1) using commercial 4,4-dimethylcyclohexanone **83c** (51.5 mg, 0.408 mmol) and 9-amino-9-deoxyepiquinine **9** (13.2 mg, 0.0408 mmol). Purification by flash chromatography (20%

Et_2O in pentane) afforded **84c** as a colorless oil (78.3 mg, 0.32 mmol, 78%, 94.5:5.5 er).

^1H NMR (400 MHz, CDCl_3) δ 8.07 (d, $J = 7.9$ Hz, $J = 1.1$ Hz, 2H, CH_{Ar}), 7.55 (t, $J = 7.6$ Hz, $J = 1.2$ Hz, 1H, CH_{Ar}), 7.42 (t, $J = 7.8$ Hz, 2H, CH_{Ar}), 5.55 (dd, $J = 13.2$ Hz, $J = 6.5$ Hz, 1H, CHOBz), 2.63 (apparent td, $J = 14.2$ Hz, $J = 6.3$ Hz, 1H, C(O)CH_2), 2.41 (ddd, $J = 14.2$ Hz, $J = 4.5$ Hz, $J = 2.5$ Hz, 1H, C(O)CH_2), 2.11 (ddd, $J = 12.6$ Hz, $J = 6.5$ Hz, 3.3 Hz, 1H, CHOBzCH_2), 1.89 (apparent t, $J = 12.9$ Hz, 1H, CHOBzCH_2), 1.82-1.74 (m, 1H, $\text{C(Me)}_2\text{CH}_2$), 1.69 (td, $J = 13.9$ Hz, $J = 4.5$ Hz, 1H, $\text{C(Me)}_2\text{CH}_2$), 1.31 (s, 3H, CH_3), 1.10 (s, 3H, CH_3).

^{13}C NMR (100 MHz, CDCl_3) δ 204.93, 165.71, 133.18, 129.89, 129.71, 128.36, 74.18, 45.27, 39.58, 36.98, 32.08, 31.40, 24.69.

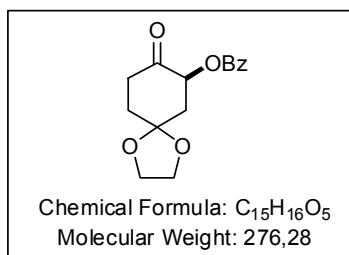
FTIR (thin film) 2959, 2932, 2865, 1737, 1717, 1451, 1367, 1315, 1296, 1279, 1262, 1176, 1115, 1070, 1026, 996 cm^{-1}

HRMS (m/z) calcd for $\text{C}_{15}\text{H}_{18}\text{O}_3\text{Na}$ $[\text{M}+\text{Na}]^+$: 269.1148. Found 269.1145.

$[\alpha]_{\text{D}}^{25}$: -20.2° (c 0.317, CHCl_3).

Chiral HPLC (AD-3, nHept/iPrOH 97:3, 1 mL/min, 25 °C) t_r 7.13 min (minor enantiomer), t_r 8.68 min (major enantiomer).

7. Experimental Section



(S)-7-Benzoyloxy-1,4-dioxaspiro[4.5]decane-8-one (**84d**):

Prepared according to the general procedure A (Section 7.3.2.1) using commercial 1,4-dioxaspiro[4.5]decan-8-one **83d** (63.7 mg, 0.408 mmol) and 9-amino-9-deoxyepiquinine **9** (13.2 mg, 0.0408 mmol). Purification by flash chromatography (40% Et₂O in pentane) afforded **84d** as a white solid (58.6 mg, 0.21 mmol,

52%, 95.5:4.5 er).

¹H NMR (400 MHz, CDCl₃) δ 8.08 (d, *J* = 7.6 Hz, 2H, CH_{Ar}), 7.57 (t, *J* = 7.4 Hz, 1H, CH_{Ar}), 7.44 (t, *J* = 7.7 Hz, 2H, CH_{Ar}), 5.68 (dd, *J* = 13.0 Hz, *J* = 6.5 Hz, 1H, CHOBz), 4.16-3.99 (m, 4H, OCH₂CH₂O), 2.79 (td, *J* = 14.1 Hz, *J* = 6.6 Hz, 1H, C(O)CH₂), 2.56-2.41 (m, 2H, C(O)CH₂ and CHOBzCH₂), 2.26 (apparent t, *J* = 12.8 Hz, 1H, CHOBzCH₂), 2.14-1.97 (m, 2H).

¹³C NMR (100 MHz, CDCl₃) δ 203.32, 165.33, 133.24, 129.88, 129.49, 128.37, 107.31, 73.64, 64.97, 64.88, 40.28, 35.83, 34.56.

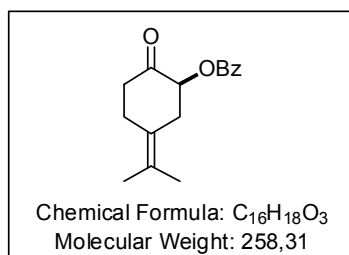
FTIR (thin film) 2965, 2891, 1740, 1720, 1603, 1452, 1315, 1295, 1272, 1247, 1178, 1146, 1109, 1071, 1042, 989, 930 cm⁻¹

HRMS (*m/z*) calcd for C₁₅H₁₆O₅Na [M+Na]⁺: 299.0890. Found 299.0890.

m.p.: 84.8-85.0 °C.

[α]_D²⁵: -31.6° (*c* 0.450, CHCl₃).

Chiral HPLC (OD-3, nHept/iPrOH 90:10, 0.5 mL/min, 25 °C) *t*_r 12.19 min (minor enantiomer), *t*_r 13.48 min (major enantiomer).



(S)-2-Benzoyloxy-4-isopropylidencyclohexanone (**84e**):

Prepared according to the general procedure A (Section 7.3.2.1) using 4-isopropylidencyclohexanone **83e** (56.4 mg, 0.408 mmol) and 9-amino-9-deoxyepiquinine **9** (13.2 mg, 0.0408 mmol). Purification by flash chromatography (10% Et₂O in pentane) afforded **84e** as a colorless oil (66.4 mg, 0.26 mmol,

63%, 86:14 er, purified by prep. TLC: 93:7 er).

¹H NMR (400 MHz, CDCl₃) δ 8.10 (dd, *J* = 8.3 Hz, *J* = 1.4 Hz, 2H, CH_{Ar}), 7.57 (tt, *J* = 7.4 Hz, *J* = 1.2 Hz, 1H, CH_{Ar}), 7.45 (t, *J* = 7.8 Hz, 2H, CH_{Ar}), 5.39 (dd, *J* = 12.7 Hz, *J* = 6.5 Hz, 1H, CHOBz), 3.26 (ddd, *J* = 13.5 Hz, *J* = 6.5 Hz, *J* = 2.1 Hz, 1H, CHOBzCH₂), 2.92 (c.m, 1H, CH₂), 2.56 (dt, *J* = 14.6 Hz, *J* = 4.9 Hz, 1H, CH₂), 2.51-2.37 (m, 2H, CH₂), 2.26 (c.m, 1H, C=CCH₂CH₂), 1.79 (s, 6H, CH₃).

7. Experimental Section

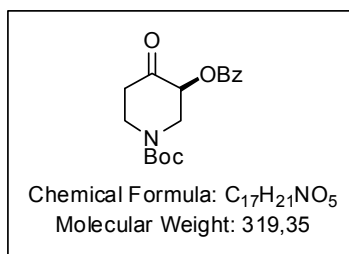
^{13}C NMR (100 MHz, CDCl_3) δ 204.60, 165.60, 133.22, 129.91, 129.69, 128.39, 128.12, 123.89, 76.05, 39.59, 34.94, 28.46, 20.58, 20.52.

FTIR (thin film) 2988, 2919, 2857, 1737, 1719, 1451, 1364, 1315, 1269, 1110, 1071, 1027 cm^{-1}

HRMS (m/z) calcd for $\text{C}_{16}\text{H}_{18}\text{O}_3\text{Na}$ $[\text{M}+\text{Na}]^+$: 281.1148. Found 281.1147.

$[\alpha]_{\text{D}}^{25}$: -20.9° (c 0.316, CHCl_3).

Chiral HPLC (OD-3, nHept/iPrOH 99.5:0.5, 1 mL/min, 25 °C) t_{r} 15.83 min (minor enantiomer), t_{r} 18.83 min (major enantiomer).



(S)-2-Benzoyloxy-N-Boc-4-Piperidone (84f): Prepared according to the general procedure A (Section 7.3.2.1) using commercial *N*-Boc-4-Piperidone **83f** (83.0 mg, 0.408 mmol) and 9-amino-9-deoxyepiquinine **9** (13.2 mg, 0.0408 mmol). Purification by flash chromatography (gradient from 20% to 35% Et_2O in pentane) afforded **84f** as a pale yellow oil (58.3 mg, 0.18 mmol, 45%, 88:12 er, purified by prep. TLC: 92:8 er).

^1H NMR (400 MHz, CDCl_3) δ 8.07 (dd, $J = 8.0$ Hz, $J = 1.2$ Hz, 2H, CH_{Ar}), 7.59 (tt, $J = 7.4$ Hz, $J = 1.2$ Hz, 1H, CH_{Ar}), 7.45 (t, $J = 7.8$ Hz, 2H, CH_{Ar}), 5.36 (dd, $J = 10.4$ Hz, $J = 6.6$ Hz, 1H, CHOBz), 4.84-4.39 (br m, 1H, CH_2), 4.39-4.15 (br s, 1H, CH_2), 3.37 (br s, 1H, CH_2), 3.22 (ddd, $J = 13.5$ Hz, $J = 11.1$ Hz, $J = 3.9$ Hz, 1H, CH_2), 2.72-2.52 (m, 2H, $\text{NBocCH}_2\text{CH}_2$), 1.49 (s, 9H, $\text{C}(\text{CH}_3)_3$).

^{13}C NMR (100 MHz, CDCl_3) δ 201.47, 165.12, 154.22, 133.52, 129.98, 129.10, 128.48, 81.24, 73.93, 48.14 (br), 43.61 (br), 40.52, 28.30.

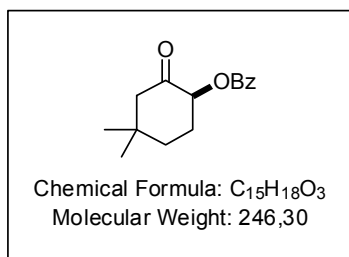
FTIR (thin film) 2977, 2932, 2873, 1724, 1699, 1477, 1452, 1420, 1367, 1312, 1297, 1273, 1237, 1165, 1112, 1072, 1026, 969, 891, 863, 770 cm^{-1}

HRMS (m/z) calcd for $\text{C}_{17}\text{H}_{21}\text{O}_5\text{Na}$ $[\text{M}+\text{Na}]^+$: 342.1312. Found 342.1312

$[\alpha]_{\text{D}}^{25}$: -30.7° (c 0.254, CHCl_3)

Chiral HPLC (AD-3, nHept/iPrOH 95:5, 1 mL/min, 25 °C) t_{r} 7.47 min (minor enantiomer), t_{r} 8.77 min (major enantiomer).

7. Experimental Section



(S)-2-Benzoyloxy-5,5-dimethylcyclohexanone (84g): Prepared according to the general procedure **A** (Section 7.3.2.1) using commercial 2,2-dimethylcyclohexanone **84g** (28.3 μ L, 0.184 mmol) and 9-amino-9-deoxyepiquinine **9** (5.95 mg, 0.0184 mmol). Purification by flash chromatography (20% Et₂O in pentane) afforded **84g** as a white solid (34.7 mg, 0.141 mmol, 77%, 96:4 er).

¹H NMR (400 MHz, CDCl₃) δ 8.09 (d, J = 8.5 Hz, J = 1.3 Hz, 2H, CH_{Ar}), 7.56 (t, J = 7.6 Hz, J = 1.2 Hz, 1H, CH_{Ar}), 7.44 (t, J = 7.7 Hz, 2H, CH_{Ar}), 5.37 (dd, J = 12.2 Hz, J = 6.9 Hz, 1H, CHOBz), 2.42 (d, J = 13.0 Hz, 1H, C(O)CH₂), 2.34-2.26 (m, 1H, C(Me)₂CH₂CH₂), 2.26 (dd, J = 13.0 Hz, J = 2.9 Hz, 1H, C(O)CH₂), 2.09 (qd, J = 13.2 Hz, J = 4.2 Hz, 1H, C(Me)₂CH₂CH₂), 1.85 (td, J = 13.8 Hz, J = 4.1 Hz, 1H, C(Me)₂CH₂CH₂), 1.71 (dq, J = 13.8 Hz, J = 3.3 Hz, 1H, C(Me)₂CH₂CH₂), 1.12 (s, 3H, CH₃), 0.97 (s, 3H, CH₃).

¹³C NMR (100 MHz, CDCl₃) δ 203.99, 165.68, 133.19, 129.91, 129.70, 128.37, 76.60, 53.36, 36.80, 36.66, 31.51, 28.58, 25.19.

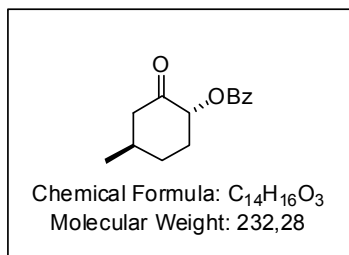
FTIR (thin film) 2959, 1736, 1719, 1452, 1315, 1281, 1218, 1177, 1119, 1071, 909 cm⁻¹

HRMS (m/z) calcd for C₁₅H₁₈O₃Na [M+Na]⁺: 269.1148. Found 269.1148.

m.p.: 77.5-77.7 °C.

[α]_D²⁵: -28.6° (c 0.336, CHCl₃).

Chiral HPLC (AD-3, nHept/iPrOH 97:3, 1 mL/min, 25 °C) t_r 6.83 min (minor enantiomer), t_r 9.71 min (major enantiomer).



(1R,4R)-4-methyl-2-oxocyclohexyl benzoate (84h): Prepared according to the general procedure **A** (Section 7.3.2.1) using commercial (*R*)-3-methylcyclohexanone **83h** (44.8 μ L, 0.408 mmol) and 9-amino-9-deoxyepiquinidine **11** (13.2 mg, 0.0408 mmol). Purification by flash chromatography (gradient from 5% to 10% Et₂O in pentane) afforded **84h** as a white solid (56.7 mg, 0.24 mmol, 60%, 12.3:1 rr, 18:1 dr).

¹H NMR (400 MHz, CDCl₃) δ 8.09 (dd, J = 8.0 Hz, J = 1.3 Hz, 2H, CH_{Ar}), 7.57 (tt, J = 7.4 Hz, J = 1.1 Hz, 1H, CH_{Ar}), 7.44 (t, J = 7.8 Hz, 2H, CH_{Ar}), 5.40 (dd, J = 12.6 Hz, J = 6.6 Hz, 1H, CHOBz), 2.53 (ddd, J = 13.0 Hz, J = 3.8 Hz, J = 2.7 Hz, 1H, C(O)CH₂), 2.40 (dq, J = 12.6 Hz,

7. Experimental Section

$J = 3.3$ Hz, 1H, CHOBzCH₂), 2.22 (td, $J = 13.0$ Hz, $J = 0.9$ Hz, 1H, C(O)CH₂), 2.06-1.87 (m, 3H, CH₂ and CH), 1.58 (c.m, 1H, CHMeCH₂CH₂), 1.09 (d, $J = 6.3$ Hz, 3H, CH₃).

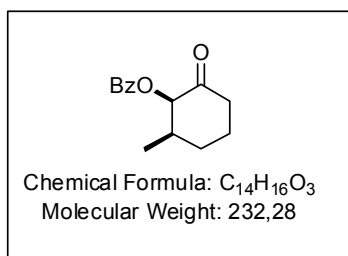
¹³C NMR (100 MHz, CDCl₃) δ 203.76, 165.68, 133.18, 129.90, 129.71, 128.37, 76.64, 48.75, 35.07, 32.27, 31.76, 20.06.

FTIR (thin film) 2956, 2929, 2872, 1736, 1720, 1452, 1315, 1298, 1271, 1114, 1073, 1027 cm⁻¹

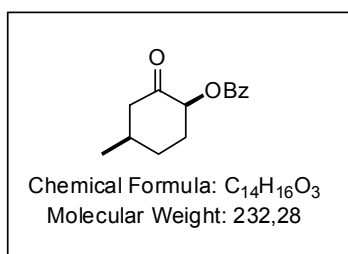
HRMS (m/z) calcd for C₁₄H₁₆O₃Na [M+Na]⁺: 255.0992. Found 255.0992.

m.p.: 87.0-87.3 °C.

$[\alpha]_D^{25}$: + 23.0° (c 0.252, CHCl₃).



(1R,2R)-2-methyl-6-oxocyclohexyl benzoate (152): Selected data for the minor regioisomer. ¹H NMR (400 MHz, CDCl₃) δ 5.47 (dd, $J = 5.3$ Hz, $J = 0.9$ Hz, 1H, CHOBz). ¹³C NMR signals could not be detected. A diastereomer of this compound could not be detected.



(1S,4R)-4-methyl-2-oxocyclohexyl benzoate (84i): Prepared according to the general procedure A (Section 7.3.2.1) using commercial (*R*)-3-methylcyclohexanone **83h** (44.8 μ L, 0.408 mmol) and 9-amino-9-deoxyepiquinine **11** (13.2 mg, 0.0408 mmol). Purification by flash chromatography (gradient from 0% to 10% Et₂O in pentane) afforded **84i** as a mixture with the minor regioisomer (27%) (53.9 mg, 0.23 mmol, 57%, 2.2:1 rr, 18.5:1 dr).

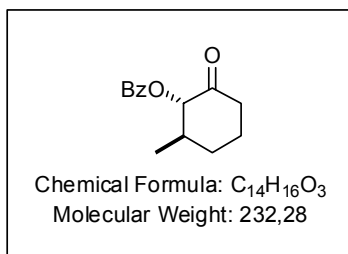
¹H NMR (400 MHz, CDCl₃): δ 8.13-8.06 (m, 2H, CH_{Ar}), 7.58 (tt, $J = 7.5$ Hz, $J = 1.2$ Hz, 1H, CH_{Ar}), 7.45 (t, $J = 7.8$ Hz, 2H, CH_{Ar}), 5.33 (dd, $J = 9.5$ Hz, $J = 8.2$ Hz, 1H, CHOBz), 2.63 (dd, $J = 12.9$ Hz, $J = 5.2$ Hz, 1H, C(O)CH₂), 2.45-2.33 (m, 2H, CH₂), 2.25-2.18 (m, 2H, CH₂ and CH), 2.04-1.98 (m, 1H, CHMeCH₂CH₂), 1.78 (dq, $J = 14.0$ Hz, $J = 4.6$ Hz, $J = 2.1$ Hz, 1H, CHMeCH₂CH₂), 1.03 (d, $J = 7.0$ Hz, 3H, CH₃).

¹³C NMR (100 MHz, CDCl₃) δ 204.84, 165.57, 133.22, 129.68, 129.88, 128.40, 76.83, 46.90, 32.34, 29.24, 28.76, 19.15.

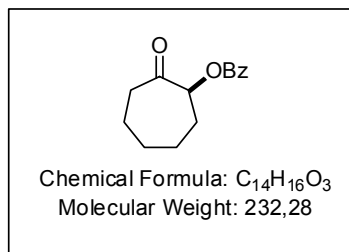
LRMS (m/z) EI: 232 [M⁺], 127, 110, 105, 77, 51, 41, 29.

HRMS (m/z) calcd for C₁₄H₁₆O₃Na [M+Na]⁺: 255.0992. Found 255.0991.

7. Experimental Section



(1S,2R)-2-methyl-6-oxocyclohexyl benzoate (153): Selected data for the minor regioisomer. ¹H NMR (400 MHz, CDCl₃) δ 5.47 (d, *J* = 11.7 Hz, 1H, CHOBz), 1.16 (d, *J* = 6.4 Hz, 3H, Me); ¹³C NMR (100 MHz, CDCl₃) δ 203.89, 165.93, 133.15, 129.88, 128.39, 82.27, 40.42, 39.55 (CHMe), 32.73, 25.70, 19.05. A diastereomer of this compound could not be detected.



(S)-2-Benzoyloxycycloheptanone (84j): Prepared according to the general procedure **B** (Section 7.3.2.1) using commercial cycloheptanone **83j** (48.2 μL, 0.408 mmol) and 9-amino-9-deoxyepiquinine **9** (13.2 mg, 0.0408 mmol). Purification by flash chromatography (gradient from 2% to 10% Et₂O in pentane) afforded **84j** as a white solid (35.1 mg, 0.15 mmol, 74%, 95:5 er, purified by prep. TLC: 98:2 er).

¹H NMR (400 MHz, CDCl₃) δ 8.08 (d, *J* = 8.3 Hz, *J* = 1.3 Hz, 2H, CH_{Ar}), 7.57 (t, *J* = 7.5 Hz, 1.2 Hz, 1H, CH_{Ar}), 7.45 (t, *J* = 7.5 Hz, 2H, CH_{Ar}), 5.46 (dd, *J* = 9.7 Hz, *J* = 3.3 Hz, 1H, CHOBz), 2.71 (c.m, 1H, C(O)CH₂), 2.51 (ddd, *J* = 16.5 Hz, *J* = 9.8 Hz, *J* = 4.6 Hz, 1H, C(O)CH₂), 2.13 (c.m, 1H, CH₂), 1.99-1.67 (m, 6H, CH₂), 1.50-1.40 (m, 1H, CH₂).

¹³C NMR (100 MHz, CDCl₃) δ 207.41, 165.82, 133.22, 129.85, 129.67, 128.40, 79.03, 40.75, 30.42, 28.42, 26.46, 23.04.

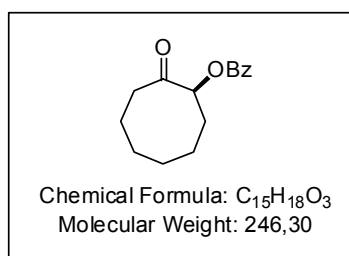
FTIR (thin film) 2933, 2860, 1714, 1602, 1452, 1316, 1303, 1272, 1114, 1071, 1027, 933 cm⁻¹;

HRMS (*m/z*) calcd for C₁₄H₁₆O₃Na [M+Na]⁺: 255.0992. Found 255.0992.

m.p.: 79.8-80.3 °C.

[α]_D²⁵: + 46.7° (*c* 0.262, CHCl₃).

Chiral HPLC (OD-3, nHept/iPrOH 90:10, 1 mL/min, 25 °C) t_r 4.10 min (minor enantiomer), t_r 4.87 min (major enantiomer).



(S)-2-Benzoyloxycyclooctanone (84k): Prepared according to the general procedure **B** (Section 7.3.2.1) using commercial cyclooctanone **83k** (51.5 mg, 0.408 mmol) and 9-amino-9-deoxyepiquinine **9** (13.2 mg, 0.0408 mmol). Purification by flash chromatography (gradient from 5% to 10% Et₂O in pentane) afforded **84k** as a white solid containing 11% of the

7. Experimental Section

bis-benzoyloxyated product (40.6 mg, 0.16 mmol, 81%, 98:2 er).

¹H NMR (400 MHz, CDCl₃) δ 8.08 (d, *J* = 8.3 Hz, *J* = 1.3 Hz, 2H, CH_{Ar}), 7.58 (t, *J* = 7.6 Hz, *J* = 1.1 Hz, 1H, CH_{Ar}), 7.45 (t, *J* = 7.8 Hz, 2H, CH_{Ar}), 5.43 (dd, *J* = 8.7 Hz, *J* = 3.6 Hz, 1H, CHOBz), 2.75 (ddd, *J* = 14.1 Hz, *J* = 9.6 Hz, *J* = 3.2 Hz, 1H, C(O)CH₂), 2.44 (ddd, *J* = 14.1 Hz, *J* = 9.2 Hz, *J* = 3.5 Hz, 1H, C(O)CH₂), 2.34 (ddt, *J* = 14.2 Hz, *J* = 9.6 Hz, *J* = 3.5 Hz, 1H, CHOBzCH₂), 2.12-2.00 (m, 2H, CH₂), 2.00-1.82 (m, 2H, CH₂), 1.77-1.62 (m, 2H, CH₂), 1.62-1.49 (m, 2H, CH₂), 1.34-1.23 (m, 1H, CH₂).

¹³C NMR (100 MHz, CDCl₃) δ 211.64, 165.96, 133.21, 129.80, 129.57, 128.37, 77.31, 40.44, 31.21, 27.43, 24.56, 24.42, 21.82.

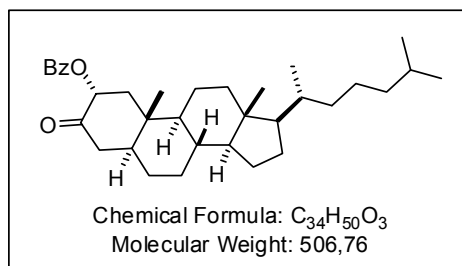
FTIR (thin film) 2931, 2861, 1714, 1451, 1316, 1275, 1111, 1098, 1070, 1026, 955 cm⁻¹

HRMS (*m/z*) calcd for C₁₅H₁₈O₃Na [M+Na]⁺: 269.1148. Found 269.1149.

m.p.: 85.5-85.8 °C.

[α]_D²⁵: + 54.0° (*c* 0.252, CHCl₃).

Chiral HPLC (OD-3, nHept/iPrOH 95:5, 1 mL/min, 25 °C) *t_r* 4.33 min (minor enantiomer), *t_r* 5.20 min (major enantiomer).



2α-Benzoyloxy-5α-cholestan-3-one (841): Prepared according to the general procedure A (Section 7.3.2.1) using commercial 5α-cholestan-3-one **831** (78.9 mg, 0.204 mmol) and 9-amino-9-deoxyepiquinidine **11** (6.6 mg, 0.0204 mmol). Purification by flash chromatography (gradient from 5% to 10% Et₂O in

pentane) afforded **841** as a white solid (91.4 mg, 0.180 mmol, 88%, 20:1 rr, >20:1 dr).

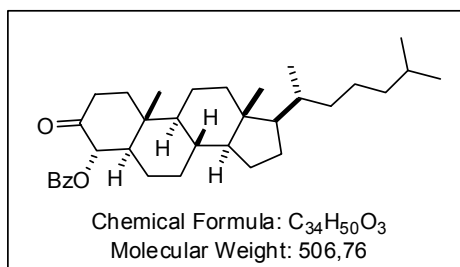
¹H NMR (300 MHz, CDCl₃): δ 8.11-8.06 (m, 2H, CH_{Ar}), 7.57 (tt, *J* = 7.4 Hz, 1.4 Hz, 1H, CH_{Ar}), 7.43 (apparent t, *J* = 7.7 Hz, 2H, CH_{Ar}), 5.54 (dd, *J* = 12.8 Hz, *J* = 6.7 Hz, 1H, CHOBz), 2.50 (t, *J* = 14.0 Hz, 1H), 2.42 (dd, *J* = 12.5 Hz, *J* = 6.6 Hz, 1H), 2.26 (dd, *J* = 14.0 Hz, *J* = 3.4 Hz, 1H), 2.00 (dt, *J* = 12.5 Hz, *J* = 3.9 Hz, 1H), 1.93-0.93 (m, 28H), 0.90 (d, *J* = 6.5 Hz, 3H), 0.88 (d, *J* = 1.4 Hz, 3H), 0.85 (d, *J* = 1.4 Hz, 3H), 0.68 (s, 3H).

¹³C NMR (75 MHz, CDCl₃) δ 204.00, 165.69, 131.11, 129.85, 129.72, 128.31, 74.91, 56.19, 56.10, 53.87, 47.88, 44.93, 43.66, 42.59, 39.75, 39.48, 37.30, 36.11, 35.75, 34.72, 31.61, 28.42, 28.21, 27.99, 24.18, 23.79, 22.80, 22.54, 21.65, 18.65, 12.82, 12.06.

HRMS (*m/z*) calcd for C₃₄H₅₀O₃Na [M+Na]⁺: 529.3652. Found 529.3654.

m.p.: 198-199 °C.

7. Experimental Section



4 α -Benzoyloxy-5- α -cholestan-3-one (84m):

Prepared according to the general procedure A (Section 7.3.2.1) using commercial 5- α -cholestan-3-one **83I** (78.9 mg, 0.204 mmol) and 9-amino-9-deoxyepiquinidine **11** (6.6 mg, 0.0204 mmol).

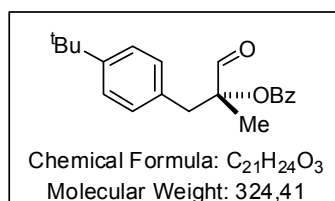
Purification by flash chromatography (gradient from 5% to 10% Et₂O in pentane) afforded **84I** as a white solid (26.1 mg, 0.051 mmol, 25%, >20:1 rr, 20:1 dr).

¹H NMR (500 MHz, CDCl₃): δ 8.11-8.06 (m, 2H, CH_{Ar}), 7.57 (t, J = 7.4 Hz, 1H, CH_{Ar}), 7.43 (apparent t, J = 7.7 Hz, 2H, CH_{Ar}), 5.33 (d, J = 12.4 Hz, 1H, CHOBz), 2.61 (dt, J = 14.5 Hz, J = 6.4 Hz, 1H), 2.48 (dq, J = 14.4 Hz, J = 2.1 Hz, 1H), 2.10 (ddd, J = 13.5 Hz, J = 6.7 Hz, J = 2.3 Hz, 1H), 2.01 (dt, J = 12.7 Hz, J = 3.1 Hz, 1H), 1.90-0.94 (m, 28H), 0.91 (d, J = 6.5 Hz, 3H), 0.88 (dd, J = 1.4 Hz, J = 1.4 Hz, 3H), 0.85 (d, J = 1.4 Hz, 3H), 0.69 (s, 3H).

¹³C NMR (125 MHz, CDCl₃) δ 204.4, 166.1, 129.85, 129.85, 129.80, 128.4, 77.8, 56.23, 56.20, 54.0, 51.7, 42.5, 39.8, 39.5, 38.9, 37.5, 37.0, 36.1, 35.8, 35.0, 31.2, 28.2, 28.0, 24.3, 24.2, 23.8, 22.8, 22.6, 21.3, 18.9, 13.0, 12.1.

HRMS (m/z) calcd for C₃₄H₅₀O₃Na [M+Na]⁺: 529.365215. Found 529.36553.

7.3.3.2 α -Benzoyloxyated α -Substituted Aldehydes 118



(R)-1-(4-(tert-butyl)phenyl)-2-methyl-3-oxopropan-2-yl

benzoate (**118a**): Prepared according to the general procedure (Section 7.3.2.2) using commercial 3-(4-(tert-butyl)phenyl)-2-methylpropanal **117a** (43.2 μ L, 0.20 mmol), 9-amino-9-deoxyepiquinine **9** (6.6 mg, 0.020 mmol) and (*S*)-TRIP ((*S*)-**3**)

(14.5 mg, 0.020 mmol) according to the general procedure C (Section 7.3.2.2). Purification by flash chromatography (10% EtOAc in hexane) afforded **118a** as a colorless oil (48.7 mg, 0.15 mmol, 75%, 70:30 er).

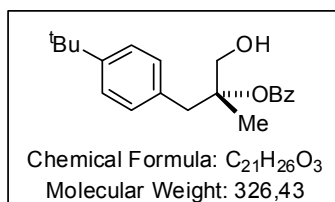
¹H NMR (500 MHz, CDCl₃) δ 9.62 (s, 1H, CHO), 8.06 (d, J = 7.9 Hz, 2H, CH_{Ar}), 7.63 (t, J = 7.3 Hz, 1H, CH_{Ar}), 7.49 (apparent t, J = 7.8 Hz, 2H, CH_{Ar}), 7.33 (d, J = 8.0 Hz, 2H, CH_{Ar}), 7.17 (d, J = 8.0 Hz, 2H, CH_{Ar}), 3.28 (d, J = 14.2 Hz, 1H, ArCH₂), 3.07 (d, J = 14.2 Hz, 1H, ArCH₂), 1.53 (s, 3H, CH₃), 1.32 (s, 9H, C(CH₃)₃).

7. Experimental Section

^{13}C NMR (125 MHz, CDCl_3) δ 199.2, 166.1, 150.0, 133.6, 131.3, 130.4, 129.9, 129.4, 128.6, 125.3, 85.0, 40.7, 34.5, 31.4, 31.2, 19.1.

HRMS (m/z) calcd for $\text{C}_{21}\text{H}_{24}\text{O}_3\text{Na}$ $[\text{M}+\text{Na}]^+$: 347.16176. Found: 347.16207.

$[\alpha]_{\text{D}}^{25}$: + 4.0° (c 0.455, CHCl_3 , 67:33 er).



(R)-1-(4-(tert-butyl)phenyl)-3-hydroxy-2-methylpropan-2-yl benzoate (154a): Prepared according to the general procedure (Section 7.3.2.2) using commercial 3-(4-(tert-butyl)phenyl)-2-methylpropanal **117a** (43.2 μL , 0.20 mmol), 9-amino-9-deoxyepiquinine **9** (6.6 mg, 0.020 mmol) and (*S*)-TRIP ((*S*)-**3**)

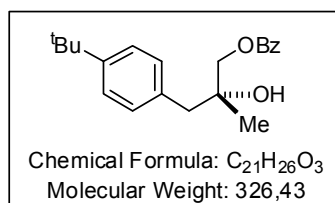
(14.5 mg, 0.020 mmol), and directly reduced according to the general procedure C (Section 7.3.2.2). Purification by flash chromatography (50% EtOAc in hexane) afforded **154a** as a colorless oil (50.9 mg, 0.16 mmol, 78%, 70:30 er).

^1H NMR (500 MHz, CDCl_3) δ 7.98 (d, J = 7.9 Hz, 2H, CH_{Ar}), 7.58 (t, J = 7.4 Hz, 1H, CH_{Ar}), 7.45 (t, J = 7.7 Hz, 2H, CH_{Ar}), 7.31 (d, J = 8.2 Hz, 2H, CH_{Ar}), 7.21 (d, J = 8.2 Hz, 2H, CH_{Ar}), 3.88 (d, J = 12.8 Hz, 2H, CH_2OH), 3.80 (d, J = 12.8 Hz, 2H, CH_2OH), 3.23 (d, J = 13.5 Hz, 1H, ArCH_2), 3.17 (d, J = 13.5 Hz, 1H, ArCH_2), 1.50 (s, 3H, CH_3), 1.31 (s, 9H, $\text{C}(\text{CH}_3)_3$).

^{13}C NMR (125 MHz, CDCl_3) δ 167.2, 149.6, 133.1, 133.0, 130.9, 130.6, 129.8, 128.4, 125.1, 87.4, 68.0, 41.8, 34.4, 31.4, 21.2.

HRMS (m/z) calcd for $\text{C}_{21}\text{H}_{26}\text{O}_3\text{Na}$ $[\text{M}+\text{Na}]^+$: 349.17741. Found: 349.17737.

Chiral HPLC (OD-3, *n*-Hept/ i PrOH 99:1, 0.5 mL/min, 25 °C) t_{r} 24.2 min (major enantiomer), t_{r} 26.3 min (minor enantiomer).



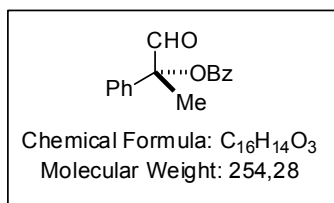
(R)-3-(4-(tert-butyl)phenyl)-2-hydroxy-2-methylpropyl benzoate (157a): This compound was obtained selectively by following the general procedure C (Section 7.3.2.2) but stirring the reaction for 2 h at r.t.

^1H NMR (500 MHz, CDCl_3) δ 8.08 (d, J = 8.1 Hz, 2H, CH_{Ar}), 7.60 (t, J = 7.2 Hz, 1H, CH_{Ar}), 7.48 (t, J = 8.1 Hz, 2H, CH_{Ar}), 7.34 (d, J = 8.4 Hz, 2H, CH_{Ar}), 7.18 (d, J = 8.4 Hz, 2H, CH_{Ar}), 4.21 (s, 2H, CH_2OH), 2.94 (d, J = 13.1 Hz, 1H, ArCH_2), 2.90 (d, J = 13.1 Hz, 1H, ArCH_2), 1.32 (s, 3H, CH_3), 1.31 (s, 9H, $\text{C}(\text{CH}_3)_3$).

7. Experimental Section

^{13}C NMR (125 MHz, CDCl_3) δ 166.4, 149.7, 133.21, 133.17, 130.1, 130.0, 129.6, 128.5, 125.4, 71.9, 70.5, 44.8, 34.4, 31.3, 24.5.

HRMS (m/z) calcd for $\text{C}_{21}\text{H}_{26}\text{O}_3\text{Na}$ $[\text{M}+\text{Na}]^+$: 349.17741. Found: 349.17733.



(R)-2-Benzoyloxy-2-phenylpropionaldehyde (118b): Prepared according to the general procedure (Section 7.3.2.2) using commercial 2-phenylpropionaldehyde **117b** (54.7 μL , 0.408 mmol), 9-amino-9-deoxyepiquinine **9** (13.2 mg, 0.0408 mmol) and (*S*)-TRIP ((*S*)-**3**) (29 mg, 0.0408 mmol). The crude product

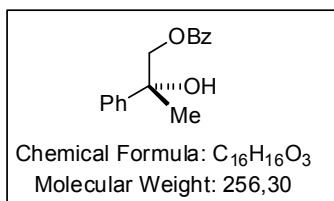
was used directly in the next step.

^1H NMR (400 MHz, CDCl_3) δ 9.56 (s, 1H, CHO), 8.18 (dd, $J = 8.2$ Hz, $J = 1.4$ Hz, 2H, CH_{Ar}), 7.65 (tt, $J = 7.5$ Hz, $J = 1.2$ Hz, 1H, CH_{Ar}), 7.59-7.49 (m, 4H, CH_{Ar}), 7.45 (t, $J = 7.8$ Hz, 2H, CH_{Ar}), 7.38 (tt, $J = 7.5$ Hz, $J = 2.0$ Hz, 1H, CH_{Ar}), 1.99 (s, 3H, CH_3).

^{13}C NMR (100 MHz, CDCl_3) δ 194.45, 165.71, 136.43, 133.86, 130.00, 129.31, 129.05, 128.72, 128.66, 125.71, 86.38, 21.02.

FTIR (thin film) 3064, 2927, 2854, 1788, 1765, 1737, 1713, 1601, 1451, 1316, 1284, 1224, 1109, 1097, 1070, 1026, 997, 831 cm^{-1}

$[\alpha]_{\text{D}}^{25}$: + 40.5° (c 0.262, CHCl_3).



(R)-2-hydroxy-2-phenylpropyl benzoate (157b): Prepared according to the general procedure C (Section 7.3.2.2) from the crude aldehyde **118b** in ethanol (2 mL) with NaBH_4 (31 mg, 0.82 mmol, 2 equiv) and stirring the reaction for 1 h at r.t., which formed the product with complete benzoyl transfer. Purification

by flash chromatography (15% Et_2O in pentane) afforded **157b** as a colorless oil (86.1 mg, 0.34 mmol, 83%, 85.5:14.5 er).

^1H NMR (400 MHz, CDCl_3) δ 7.98 (d, $J = 8.1$ Hz, 2H, CH_{Ar}), 7.60-7.50 (m, 3H, CH_{Ar}), 7.41 (c.m, 4H, CH_{Ar}), 7.30 (tt, $J = 7.2$ Hz, $J = 1.2$ Hz, 1H, CH_{Ar}), 4.53 (d, $J = 11.3$ Hz, 1H, CH_2OH), 4.48 (d, $J = 11.4$ Hz, 1H, CH_2OH), 1.67 (s, 3H, CH_3).

^{13}C NMR (100 MHz, CDCl_3) δ 166.64, 144.34, 133.24, 129.78, 129.67, 128.46, 128.43, 127.44, 125.10, 73.92, 72.31, 26.65.

FTIR (thin film) 3476, 2983, 1707, 1602, 1450, 1370, 1316, 1272, 1114, 1071, 1027, 909 cm^{-1}

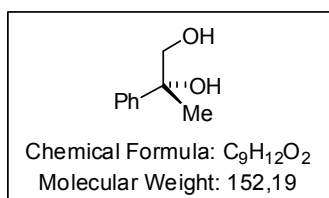
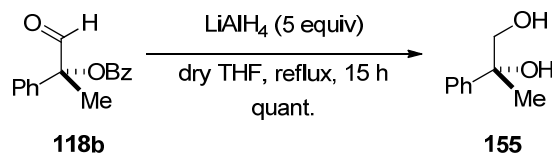
7. Experimental Section

HRMS (m/z) calcd for $C_{16}H_{16}O_3Na$ $[M+Na]^+$: 279.0992. Found: 279.0990.

$[\alpha]_D^{25}$: -5.1° (c 0.119, $CHCl_3$).

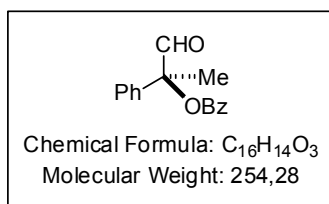
Chiral HPLC (OD-3, *n*-Hept/ⁱPrOH 97:3, 1 mL/min, 25 °C) t_r 9.78 min (major enantiomer), t_r 12.03 min (minor enantiomer).

Determination of the absolute configuration of aldehyde **118b**



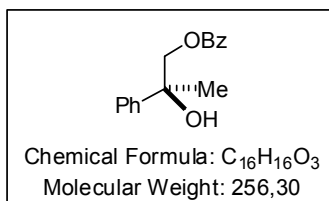
A sample of the aldehyde **118b** was reduced with excess $LiAlH_4$ to afford the diol **155** whose absolute configuration is known.^[166] 1H and ^{13}C NMR spectra were identical to those reported in the literature.^[166]

$[\alpha]_D^{25}$: -5.3° (c 0.150, EtOH) [Lit. value for the (*S*)-enantiomer^[166]: $[\alpha]_D^{25}$: $+5.7^\circ$ (c = 0.7, EtOH); (*R*)-enantiomer^[193]: $[\alpha]_D^{25}$: -5.8° (c 0.55, EtOH)].



(*S*)-2-Benzoyloxy-2-phenylpropionaldehyde (*ent*-**118b**):

Prepared according to the general procedure (Section 7.3.2.2) using commercial 2-phenylpropionaldehyde **117b** (54.7 μ L, 0.408 mmol), 9-amino-9-deoxyepicupreine **15** (12.4 mg, 0.0408 mmol) and (*R*)-TRIP ((*R*)-**3**) (29 mg, 0.0408 mmol). The crude was used directly in the next step. $[\alpha]_D^{25}$: -38.5° (c 0.571, $CHCl_3$); 1H and ^{13}C NMR spectra were identical to those of compound (*R*)-**118b**.



(*S*)-2-hydroxy-2-phenylpropyl benzoate (*ent*-**157b**): Prepared according to the general procedure C (Section 7.3.2.2) from the crude aldehyde *ent*-**118b** in ethanol (2 mL) with $NaBH_4$ (31 mg, 0.82 mmol, 2 equiv) and stirring the reaction for 1 h at r.t., which

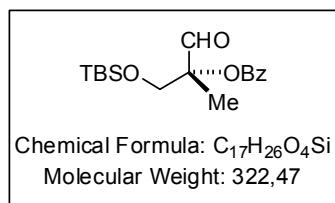
7. Experimental Section

formed the product with complete benzoyl transfer. Purification by flash chromatography (15% Et₂O in pentane) afforded *ent*-**157b** as a colorless oil (78.3 mg, 0.31 mmol, 76%, 88:12 er).

¹H and ¹³C NMR spectra were identical to those of compound (*R*)-**157b**.

[α]_D²⁵: + 5.4° (*c* 0.147, CHCl₃).

Chiral HPLC (OD-3 *n*-Hept/ⁱPrOH 97:3, 1 mL/min, 25 °C) t_r 9.80 min (minor enantiomer), t_r 11.93 min (major enantiomer).



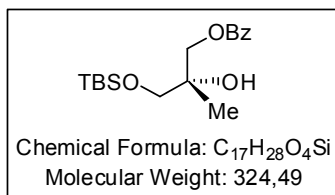
(*R*)-2-Benzoyloxy-3-((*tert*-butyldimethylsilyl)oxy)-2-methylpropionaldehyde (118d): Prepared according to the general procedure (Section 7.3.2.2) using 3-((*tert*-butyldimethylsilyl)oxy)-2-methylpropanal **117d** (83.0 mg, 0.408 mmol), 9-amino-9-deoxyepiquinine **9** (13.2 mg, 0.0408 mmol)

and (*S*)-TRIP ((*S*)-**3**) (29 mg, 0.0408 mmol). The crude was used directly in the next step. Elimination of the TBS-protected alcohol to afford methacrylaldehyde **127** was observed as a byproduct (28% yield by ¹H NMR).

¹H NMR (400 MHz, CDCl₃) δ 9.71 (s, 1H, CHO), 8.12-8.05 (m, 2H, CH_{Ar}), 7.60 (tt, *J* = 7.4 Hz, *J* = 1.1 Hz, 1H, CH_{Ar}), 7.47 (t, *J* = 7.7 Hz, 2H, CH_{Ar}), 4.03 (d, *J* = 10.7 Hz, 1H, TBSOCH₂), 3.95 (t, *J* = 10.7 Hz, 1H, TBSOCH₂), 1.50 (s, 3H, CH₃), 0.87 (s, 9H, C(CH₃)₃), 0.07 (s, 3H, Si(CH₃)₂), 0.05 (s, 3H, Si(CH₃)₂).

¹³C NMR (100 MHz, CDCl₃) δ 199.39, 166.09, 133.58, 129.88, 129.40, 128.52, 85.18, 66.36, 25.71, 18.19, 16.65, - 5.52, -5.57.

HRMS (*m/z*) calcd for C₁₇H₂₆O₄SiNa [M+Na]⁺: 345.1493. Found: 345.1496.



(*S*)-3-((*tert*-butyldimethylsilyl)oxy)-2-hydroxy-2-methylpropyl benzoate (157d): Prepared according to the general procedure C (Section 7.3.2.2) from the crude aldehyde **118d** in ethanol (2 mL) with NaBH₄ (31 mg, 0.82 mmol, 2 equiv) and stirring the reaction for 1 h at r.t., which formed the product with complete benzoyl transfer..

Purification by flash chromatography or preparative TLC (40% Et₂O in pentane) afforded **157d** as a colorless oil (34.8 mg, 0.11 mmol, 26%, 90:10 er). We found this compound to be unstable on silica gel, as reflected in the lowered yield.

7. Experimental Section

$^1\text{H NMR}$ (400 MHz, CDCl_3) δ 8.04 (dd, $J = 8.3$ Hz, $J = 1.2$ Hz, 2H, CH_{Ar}), 7.57 (tt, $J = 7.4$ Hz, $J = 1.2$ Hz, 1H, CH_{Ar}), 7.45 (t, $J = 7.6$ Hz, 2H, CH_{Ar}), 4.25 (d, $J = 1.6$ Hz, 2H, TBSOCH_2), 3.65 (d, $J = 9.8$ Hz, 1H, CH_2OH), 3.51 (d, $J = 9.8$ Hz, 1H, CH_2OH), 2.70 (s, 1H, OH), 1.26 (s, 3H, CH_3), 0.90 (s, 9H, $\text{C}(\text{CH}_3)_3$), 0.07 (s, 3H, $\text{Si}(\text{CH}_3)_2$), 0.06 (s, 3H, $\text{Si}(\text{CH}_3)_2$).

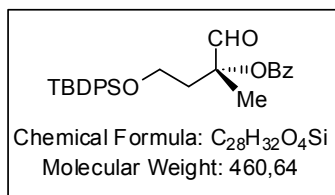
$^{13}\text{C NMR}$ (100 MHz, CDCl_3) δ 166.37, 133.05, 129.99, 129.56, 128.39, 71.69, 68.09, 67.32, 25.79, 21.12, 18.22, -5.51.

FTIR (thin film) 3488, 2955, 2930, 2886, 2858, 1722, 1471, 1464, 1452, 1269, 1095, 1027, 836, 776 cm^{-1}

HRMS (m/z) calcd for $\text{C}_{17}\text{H}_{28}\text{O}_4\text{SiNa}$ [$\text{M}+\text{Na}$] $^+$: 347.1649. Found: 347.1651.

$[\alpha]_{\text{D}}^{25}$: +2.72° (c 0.294, CHCl_3).

Chiral HPLC (OD-3, nHept/iPrOH 99:1, 1 mL/min, 25 °C) t_{r} 9.52 min (major enantiomer), t_{r} 11.10 min (minor enantiomer).



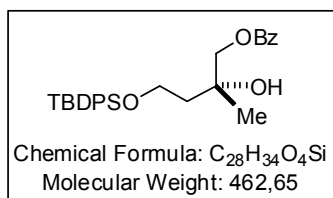
(R)-2-Benzoyloxy-4-((tert-butyldimethylsilyl)oxy)-2-methylbutanal (118e): Prepared according to the general procedure (Section 7.3.2.2) using 4-((tert-butyldimethylsilyl)oxy)-2-methylpropionaldehyde **117e** (139.0 mg, 0.408 mmol), the 9-amino-9-deoxyepiquinine **9** and (*S*)-TRIP (*S*)-**3**. The crude was used directly in the next step.

$^1\text{H NMR}$ (400 MHz, CDCl_3) δ 9.76 (s, 1H, CHO), 8.01 (dd, $J = 8.4$ Hz, $J = 1.2$ Hz, 2H, CH_{Ar}), 7.67 (tt, $J = 7.5$ Hz, $J = 1.2$ Hz, 1H, CH_{Ar}), 7.65-7.58 (m, 4H, CH_{Ar}), 7.46 (t, $J = 7.5$ Hz, 2H, CH_{Ar}), 7.44-7.33 (m, 4H, CH_{Ar}), 7.29-7.23 (m, 2H, CH_{Ar}), 3.95 (ddd, $J = 10.5$ Hz, $J = 8.6$ Hz, $J = 4.9$ Hz, 1H, TBDPSOCH_2), 3.77 (q, $J = 5.2$ Hz, 1H, TBDPSOCH_2), 2.28-2.18 (m, 1H, $\text{TBDPSOCH}_2\text{CH}_2$), 2.14 (dt, $J = 14.5$ Hz, $J = 4.8$ Hz, 1H, $\text{TBDPSOCH}_2\text{CH}_2$), 1.64 (s, 3H, CH_3), 1.01 (s, 9H, $\text{C}(\text{CH}_3)_3$).

$^{13}\text{C NMR}$ (100 MHz, CDCl_3) δ 198.88, 165.73, 135.56, 135.42, 133.52, 133.05, 132.96, 129.84, 129.71, 129.48, 128.52, 127.77, 127.72, 125.60, 84.59, 58.76, 40.31, 26.70, 20.36, 18.99.

HRMS (m/z) calcd for $\text{C}_{28}\text{H}_{32}\text{O}_4\text{SiNa}$ [$\text{M}+\text{Na}$] $^+$: 483.1962. Found: 483.1964.

7. Experimental Section



(R)-4-((tert-butyldiphenylsilyloxy)-2-hydroxy-2-methylbutyl benzoate (157e): Prepared according to the general procedure C (Section 7.3.2.2) from the crude aldehyde **118e** in ethanol (2 mL) with $NaBH_4$ (31 mg, 0.82 mmol, 2 equiv) and stirring the

reaction for 1h at r.t., which formed the product with complete benzoyl transfer. Purification by flash chromatography (30% Et_2O in pentane) afforded **157e** as a colorless oil (169 mg, 0.37 mmol, 90%, 88:12 er).

1H NMR (400 MHz, $CDCl_3$) δ 8.04 (dd, $J = 8.2$ Hz, $J = 1.2$ Hz, 2H, CH_{Ar}), 7.69 (c.m, 4H, CH_{Ar}), 7.56 (tt, $J = 7.5$ Hz, $J = 1.2$ Hz, 1H, CH_{Ar}), 7.36-7.49 (m, 8H, CH_{Ar}), 4.33 (d, $J = 11.1$ Hz, 1H, CH_2OH), 4.27 (d, $J = 11.1$ Hz, 1H, CH_2OH), 4.05 (br. s, 1H, OH), 3.95 (br. t, $J = 5.6$ Hz, 2H, $TBDPSOCH_2$), 1.95 (c.m, 1H, $TBDPSOCH_2CH_2$), 1.84 (c.m, 1H, $TBDPSOCH_2CH_2$), 1.37 (s, 3H, CH_3), 1.07 (s, 9H, $C(CH_3)_3$).

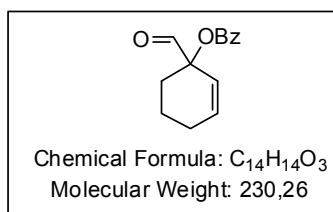
^{13}C NMR (100 MHz, $CDCl_3$) δ 166.40, 135.58, 135.57, 133.08, 132.66, 132.59, 130.09, 130.00, 129.65, 128.42, 127.90, 127.88, 127.74, 72.06, 70.97, 61.42, 39.08, 26.81, 25.00, 19.02.
FTIR (thin film) 3487, 2932, 2890, 2859, 1721, 1603, 1472, 1452, 1428, 1275, 1112, 1072, 908 cm^{-1}

HRMS (m/z) calcd for $C_{28}H_{34}O_4SiNa$ $[M+Na]^+$: 485.2119. Found: 485.2121.

$[\alpha]_D^{25}$: -7.3° (c 0.164, $CHCl_3$).

Chiral HPLC (IC-3, n -Hept/EtOH 98:2, 1 mL/min, 25 $^\circ C$, 4.3 MPa) t_r 5.35 min (major enantiomer), t_r 6.20 min (minor enantiomer).

7.3.3.3 Benzoyloxylation of Enals



1-formylcyclohex-2-en-1-yl benzoate (128b): Prepared according to the general procedure (Section 7.3.2.3) from the commercial enal **53b**. Purification by flash chromatography (10% Et_2O in pentane) afforded **128b** as a colorless oil (29.9 mg, 0.13 mmol, 65%).

1H NMR (500 MHz, $CDCl_3$) δ 9.65 (s, 1H, CHO), 8.12-8.06 (m, 2H, CH_{Ar}), 7.60 (tt, $J = 7.5$ Hz, $J = 1.3$ Hz, 1H, CH_{Ar}), 7.45 (apparent t, $J = 7.7$ Hz, 2H, CH_{Ar}), 6.26 (dt, $J = 10.2$ Hz, $J = 4.0$ Hz, 1H, $CH=CH$), 6.04 (br d, $J = 10.2$ Hz, 1H, $CH=CH$), 2.26-2.09 (m, 3H, CH_2), 2.03-1.95 (m, 1H, CH_2), 1.95-1.82 (m, 2H, CH_2).

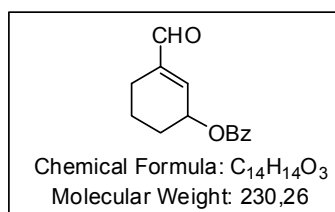
7. Experimental Section

^{13}C NMR (125 MHz, CDCl_3) δ 197.2, 165.9, 136.7, 133.5, 129.9, 129.4, 128.5, 121.9, 81.8, 28.4, 24.8, 17.8.

HRMS (m/z) calcd for $\text{C}_{14}\text{H}_{14}\text{O}_3\text{Na}$ $[\text{M}+\text{Na}]^+$: 253.08352. Found: 253.08349.

Chiral HPLC (AD-3, *n*-Hept/^{*i*}PrOH 99:1, 1 mL/min, 25 °C) t_r 7.20 min (major enantiomer), t_r 7.70 min (minor enantiomer).

Physical data for a similar compound have previously reported.^[194]



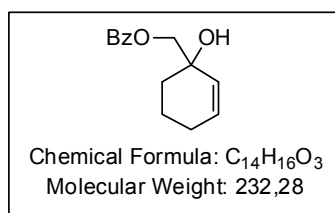
3-formylcyclohex-2-en-1-yl benzoate (129b): Prepared according to the general procedure (Section 7.3.2.3) from the commercial enal **53b** as a minor reaction component. Purification by flash chromatography (10% Et_2O in pentane) afforded **129b** as a colorless oil.

^1H NMR (500 MHz, CDCl_3) δ 9.53 (s, 1H, CHO), 8.06 (apparent d, $J = 6.7$ Hz, 2H, CH_{Ar}), 7.59 (tt, $J = 7.6$ Hz, $J = 1.3$ Hz, 1H, CH_{Ar}), 7.46 (apparent t, $J = 7.8$ Hz, 2H, CH_{Ar}), 6.79 (c. m, 1H, C=CH), 5.77 (c. m, 1H, CHOBz), 2.37-2.21 (m, 2H, CH_2), 2.16-2.08 (m, 1H, CH_2), 1.98-1.85 (m, 2H, CH_2), 1.82-1.72 (m, 1H, CH_2).

^{13}C NMR (125 MHz, CDCl_3) δ 194.0, 166.2, 145.5, 144.1, 133.3, 129.9, 129.7, 128.5, 68.5, 28.2, 21.2, 18.6.

HRMS (m/z) calcd for $\text{C}_{14}\text{H}_{14}\text{O}_3\text{Na}$ $[\text{M}+\text{Na}]^+$: 253.08352. Found: 253.08383.

Chiral HPLC (AD-3, *n*-Hept/^{*i*}PrOH 99:1, 1 mL/min, 25 °C) t_r 8.14 min, t_r 8.68 min.



(1-hydroxycyclohex-2-en-1-yl)methyl benzoate (156): Prepared according to the general procedure (Section 7.3.2.3) from the commercial enal **53b** (0.20 mmol). The crude product was analyzed by ^1H NMR to obtain the α/γ selectivity ($\alpha/\gamma = 89:11$) and directly reduced with NaBH_4 (15 mg, 0.40 mmol, 2

equiv) in ethanol (2 mL) at room temperature for 2 h to afford the rearranged, thermodynamically favoured product **156**. Purification by flash chromatography (30% Et_2O in pentane) afforded **156** as a colourless oil (30.2 mg, 0.13 mmol, 65%, 76:24 er).

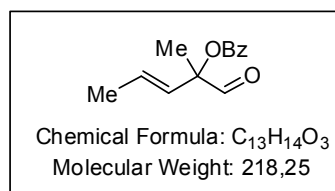
^1H NMR (500 MHz, CDCl_3) δ 8.10-8.05 (m, 2H, CH_{Ar}), 7.58 (c.m, 1H, CH_{Ar}), 7.46 (apparent t, $J = 7.9$ Hz, 2H, CH_{Ar}), 5.98 (dt, $J = 10.2$ Hz, $J = 3.6$ Hz, 1H, CH=CH), 5.73 (apparent d, $J =$

7. Experimental Section

10.2 Hz, 1H, CH=CH), 4.34 (d, $J = 11.2$ Hz, 1H, CH₂OH), 4.26 (d, $J = 11.2$ Hz, 1H, CH₂OH), 2.18-2.08 (m, 1H, CH₂), 2.14 (br. s, 1H, OH), 2.08-1.98 (m, 1H, CH₂), 1.89-1.68 (m, 4H, CH₂). ¹³C NMR (125 MHz, CDCl₃) δ 166.6, 133.2, 132.5, 130.0, 129.7, 128.5, 128.4, 71.1, 69.3, 32.9, 25.3, 18.6.

HRMS (m/z) calcd for C₁₄H₁₆O₃Na [M+Na]⁺: 255.09917. Found: 255.09914

Chiral HPLC (AD-3, *n*-Hept/ⁱPrOH 97:3, 1 mL/min, 25 °C) t_r 17.11 min (major enantiomer), t_r 18.15 min (minor enantiomer).



(E)-2-methyl-1-oxopent-3-en-2-yl benzoate (128c): Prepared according to the general procedure (Section 7.3.2.3) from the commercial enal **53c**. Purification by flash chromatography (1-5% Et₂O in pentane) afforded **128c** as a colorless oil (32.3 mg, 0.15 mmol, 74%, 76.5:23.5 er).

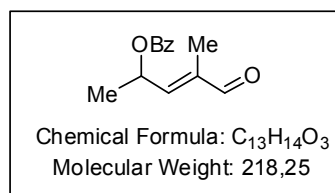
¹H NMR (500 MHz, CDCl₃) δ 9.44 (s, 1H, CHO), 8.10 (apparent d, $J = 8.0$ Hz, 2H, CH_{Ar}), 7.62 (apparent t, $J = 7.4$ Hz, 1H, CH_{Ar}), 7.49 (apparent t, $J = 7.9$ Hz, 2H, CH_{Ar}), 5.99 (dq, $J = 15.8$ Hz, $J = 6.6$ Hz, 1H, MeCH=CH), 5.62 (dq, $J = 15.8$ Hz, $J = 1.6$ Hz, 1H, MeCH=CH), 1.80 (dd, $J = 6.6$ Hz, $J = 1.6$ Hz, 3H, MeCH=CH), 2.03-1.95 (m, 1H, CH₂), 1.67 (s, 3H, CH₃). ¹³C NMR (125 MHz, CDCl₃) δ 194.2, 164.6, 132.6, 128.86, 128.79, 128.73, 127.5, 125.8, 83.8, 18.9, 17.1.

FTIR (thin film) 2927, 2854, 1717, 1692, 1451, 1266, 1110, 10701, 1044, 1026, 804, 712 cm⁻¹

HRMS (m/z) calcd for C₁₃H₁₅O₃Na [M+H]⁺: 219.10212. Found: 219.10210.

$[\alpha]_D^{25}$: + 4.6° (c 0.10, CHCl₃).

Chiral HPLC (AD-3, *n*-Hept/ⁱPrOH 99:1, 0.5 mL/min, 25 °C) t_r 6.56 min (major enantiomer), t_r 7.66 min (minor enantiomer).



(E)-4-methyl-5-oxopent-3-en-2-yl benzoate (129c): Prepared according to the general procedure (Section 7.3.2.3) from the commercial enal **53c**. Purification by flash chromatography (1-5% Et₂O in pentane) afforded **129c** as a colorless oil (2.6 mg, 0.012 mmol, 6%, 58.5:41.5 er).

¹H NMR (500 MHz, CDCl₃) δ 9.47 (s, 1H, CHO), 8.10-8.03 (m, 2H, CH_{Ar}), 7.59 (tt, $J = 7.6$ Hz, $J = 2.3$ Hz, 1H, CH_{Ar}), 7.51-7.43 (m, 2H, CH_{Ar}), 6.48 (dq, $J = 8.0$ Hz, $J = 6.6$ Hz, 1H,

7. Experimental Section

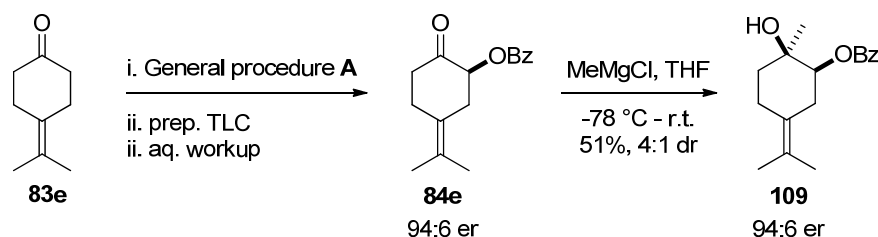
MeC=CH), 6.00 (dq, $J = 8.0$ Hz, $J = 1.3$ Hz, 1H, CHOBz), 1.90 (d, $J = 1.3$ Hz, 3H, MeC=CH), 1.55 (d, $J = 6.6$ Hz, 3H, CH₃CHOBz).

¹³C NMR (125 MHz, CDCl₃) δ 193.6, 164.7, 149.6, 138.3, 132.2, 128.8, 128.6, 127.4, 67.0, 18.5, 8.6.

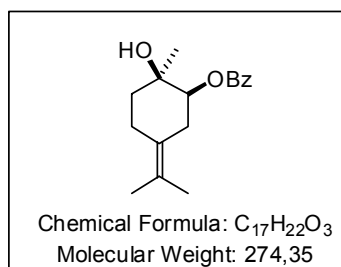
$[\alpha]_D^{25}$: + 4.6° (c 0.10, CHCl₃).

Chiral HPLC (AD-3, *n*-Hept⁺/PrOH 95:5, 1 mL/min, 25 °C) t_r 5.8 min (minor enantiomer), t_r 14.2 min (major enantiomer).

7.3.4 Asymmetric Synthesis of Cineole Derivatives 108 and 114



Compound **84e** (0.31 mmol, 94:6 er) was prepared according to the general procedure **A** on 0.5 mmol scale and purified directly using preparative TLC, followed by an aqueous workup as described in the general procedure **A**. Preparative TLC-grade silica (Macherey-Nagel, SIL G-25 UV₂₅₄) was found to preserve the enantiomeric excess of this compound, whereas other types of silica and alumina diminish the enantioselectivity after flash column chromatography to er = 86:14. The semi-crude reaction mixture obtained after a rapid plug of silica or alumina eluting with diethyl ether was found to be unracemized (er = 93:7), but gave low yields (around 30%) of the desired product in the subsequent *Grignard* reaction.



(1S,2R)-2-hydroxy-2-methyl-5-(propan-2-ylidene)cyclohexyl benzoate (109): Ketone **84e** (80 mg, 0.31 mmol, 94:6 er) was dissolved in anhydrous THF, cooled to - 78 °C, and MeMgCl (465 μ L, 3 M in THF, 4.5 equiv) was added dropwise in three 155 μ L portions over 1.5 hours. The mixture was stirred for additional 3 hours at - 78 °C, quenched with sat. aq. NH₄Cl at -

78 °C, diluted with water and diethyl ether, extracted with diethyl ether three times, washed with brine, dried over MgSO₄, filtered and evaporated under reduced pressure. Crude ¹H NMR

7. Experimental Section

showed the formation of *cis* and *trans*-configured monobenzoylated diols with dr = 4:1 (*cis:trans*), which could be readily separated by chromatography. Flash column chromatography (10% Et₂O in pentane) afforded **109** as a colourless oil (43.3 mg, 0.158 mmol, 51%, 94:6 er) along with recovered starting material.

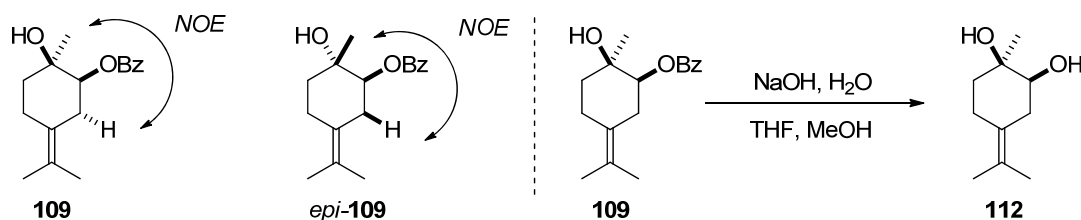
¹H NMR (400 MHz, CDCl₃): δ 8.07-8.04 (m, 2H, CH_{Ar}), 7.58 (tt, *J* = 7.4 Hz, *J* = 1.3 Hz, 1H, CH_{Ar}), 7.49-7.43 (m, 2H, CH_{Ar}), 4.86 (dd, *J* = 10.5 Hz, *J* = 4.3 Hz, 1H, CHOBz), 2.75 (dd, *J* = 13.0 Hz, *J* = 4.7 Hz, 1H, CHOBzCH₂), 2.46-2.34 (m, 2H, CHOBzCH₂ and C=CCH₂CH₂), 2.28-2.16 (m, 1H, C=CCH₂CH₂), 1.89 (dt, *J* = 13.8 Hz, *J* = 4.4 Hz, 1H, C=CCH₂CH₂), 1.70 (s, 3H, C=C(CH₃)₂), 1.68 (s, 3H, C=C(CH₃)₂), 1.47 (ddd, *J* = 13.5 Hz, *J* = 12.1 Hz, *J* = 4.6 Hz, 1H, C=CCH₂CH₂), 1.27 (s, 3H, CH₃).

¹³C NMR (100 MHz, CDCl₃) δ 165.83, 133.09, 130.28, 129.89, 129.55, 128.46, 126.85, 124.56, 78.43, 70.89, 37.65, 31.01, 26.73, 24.95, 20.26, 20.21.

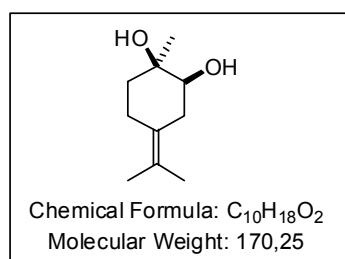
HRMS (*m/z*) calcd for C₁₇H₂₂O₃Na [M+Na]⁺: 297.1461. Found 297.1460.

Chiral HPLC (AD-3, nHept/iPrOH 95:5, 1 mL/min, 25 °C) t_r 5.13 min (minor enantiomer), t_r 6.55 min (major enantiomer).

Stereochemical assignment of **109**



The relative stereochemistry of **109** and its diastereomer *epi*-**109** was determined by *NOE* correlation.



In addition, **109** was derivatized to the literature-known^[158] diol **112** by basic hydrolysis. Alcohol **109** (21.9 mg, 0.08 mmol) was dissolved in MeOH (0.4 mL), THF (0.65 mL) and NaOH (2N, 97.5 μL) was added. The mixture was stirred for 30 min, extracted with EtOAc three times, washed with brine, dried over

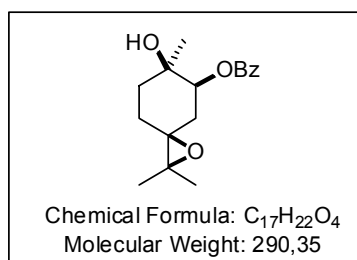
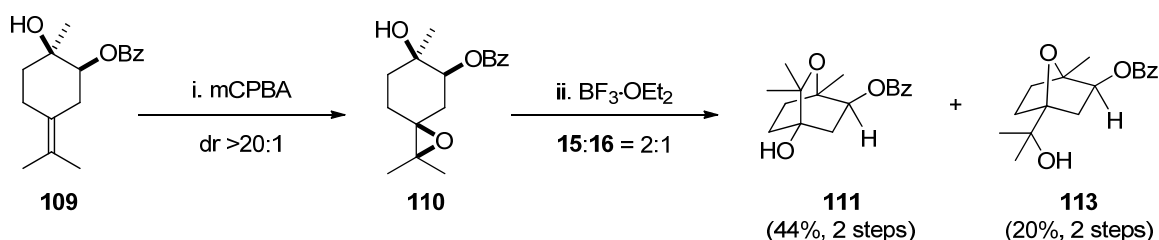
MgSO₄, filtered and evaporated under vacuum, affording spectroscopically pure **112** as a colourless oil in quantitative yield.

7. Experimental Section

^1H NMR (300 MHz, CDCl_3): δ 3.36 (dd, $J = 8.7$ Hz, $J = 4.1$ Hz, 1H, CHOH), 2.49 (dd, $J = 13.6$ Hz, $J = 4.1$ Hz, 1H, CHOHCH_2), 2.29 (dd, $J = 13.2$ Hz, $J = 8.6$ Hz, 1H, CHOHCH_2), 2.19 (dd, $J = 10.1$ Hz, $J = 4.6$ Hz, 2H, $\text{C}=\text{CCH}_2\text{CH}_2$), 1.78-1.72 (m, 1H, $\text{C}=\text{CCH}_2\text{CH}_2$), 1.69 (s, 3H, $\text{C}=\text{C}(\text{CH}_3)_2$), 1.68 (s, 3H, $\text{C}=\text{C}(\text{CH}_3)_2$), 1.48-1.35 (m, 1H, $\text{C}=\text{CCH}_2\text{CH}_2$), 1.26 (s, 3H, CH_3).

^{13}C NMR (75 MHz, CDCl_3) δ 127.02, 124.67, 75.34, 71.28, 37.12, 34.23, 25.61, 25.50, 20.24, 20.16.

The ^{13}C NMR values are in full agreement with the literature; literature values for the ^1H spectrum were found to be partly erroneous.^[158]



(5*S*,6*R*)-6-hydroxy-2,2,6-trimethyl-1-oxaspiro[2.5]octan-5-yl benzoate (**110**):

Alcohol **109** (109 mg, 0.40 mmol) was dissolved in dichloromethane (8 mL), cooled to 0 °C and *m*-CPBA (77% purity, 134.5 mg, 0.6 mmol, 1.5 equiv) was added. The mixture was stirred at this temperature for 30 min and filtered through a plug of alumina washing with diethyl ether to remove *p*-chlorobenzoic acid. ^1H NMR analysis of the crude mixture showed **110** a single diastereomer (tentative assignment shown). For purposes of characterization **110** was purified by column chromatography (35% Et_2O in pentane).

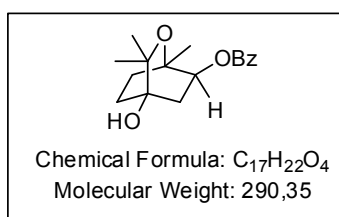
^1H NMR (300 MHz, CDCl_3): δ 8.08-8.02 (m, 2H, CH_{Ar}), 7.59 (tt, $J = 7.6$ Hz, $J = 1.2$ Hz, 1H, CH_{Ar}), 7.50-7.44 (m, 2H, CH_{Ar}), 5.23 (dd, $J = 10.8$ Hz, $J = 4.7$ Hz, 1H, CHOBz), 2.26 (dd, $J = 13.2$ Hz, $J = 10.7$ Hz, 1H, CHOBzCH_2), 2.08 (td, $J = 13.0$ Hz, $J = 4.3$ Hz, 1H, CHOBzCH_2), 1.92 (dt, $J = 14.0$ Hz, $J = 4.3$ Hz, 1H, CH_2), 1.87-1.79 (m, 2H, CH_2), 1.50-1.43 (m, 1H, CH_2), 1.35 (s, 3H, CH_3), 1.32 (s, 3H, CH_3), 1.30 (s, 3H, CH_3).

^{13}C NMR (75 MHz, CDCl_3) δ $\text{C}=\text{O}$ not detected, 133.18, 130.08, 129.57, 128.49, 77.21, 70.47, 64.95, 62.21, 34.28, 31.34, 26.68, 25.24, 20.72, 20.61.

HRMS (m/z) calcd for $\text{C}_{17}\text{H}_{22}\text{O}_4\text{Na}$ $[\text{M}+\text{Na}]^+$: 313.1410. Found 313.1411.

7. Experimental Section

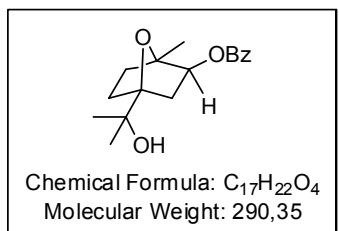
2 β -benzoyloxy, 4-hydroxy-1,8-cineole (111) and 2 β -benzoyloxy, 4-hydroxy-1,4-cineole (113): The rearrangement of **110** to **111** and **113** was performed with the crude starting material. **110** (~0.40 mmol) was dissolved in dry dichloromethane (7 mL), cooled to 0 °C and BF₃-OEt₂ (5.1 μ L, 0.04 mmol, 0.1 equiv) was added under an atmosphere of argon. The mixture was stirred overnight, letting the water bath reach ambient temperature, and dichloromethane was evaporated. ¹H NMR analysis of the crude mixture showed the formation of **111** and **113** in a 2.3:1 ratio. Flash column chromatography (gradient from 10% to 25% Et₂O in pentane) afforded **113** (22.8 mg, 0.079 mmol, 20% over 2 steps) followed by **111** (51.2 mg, 0.176 mmol, 44% over 2 steps), both as colourless oils.



¹H NMR (300 MHz, CDCl₃): δ 8.13-8.08 (m, 2H, CH_{Ar}), 7.57 (tt, $J = 7.4$ Hz, $J = 1.3$ Hz, 1H, CH_{Ar}), 7.48-7.42 (m, 2H, CH_{Ar}), 5.07 (dd, $J = 10.1$ Hz, $J = 2.9$ Hz, 1H, CHOBz), 2.26 (dd, $J = 13.8$ Hz, $J = 10.1$ Hz, 1H, CHOBzCH_{ax}), 2.13-1.94 (m, 3H, CH₂), 1.83-1.75 (m, 1H, CH₂), 1.67-1.58 (m, 1H, CH₂), 1.39 (s, 3H, CH₃), 1.34 (s, 3H, CH₃), 1.14 (s, 3H, CH₃).

¹³C NMR (100 MHz, CDCl₃) δ 166.20, 133.12, 130.26, 129.73, 128.46, 74.35, 70.95, 69.95, 39.39, 30.98, 29.56, 24.80, 23.82, 22.41.

HRMS (m/z) calcd for C₁₇H₂₂O₄Na [M+Na]⁺: 313.1410. Found 313.1408.

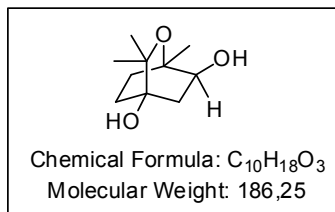
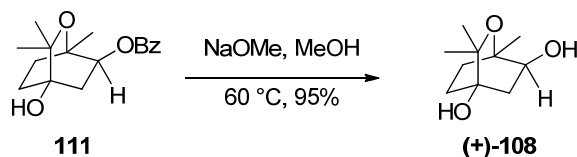


¹H NMR (400 MHz, CDCl₃): δ 8.08-8.03 (m, 2H, CH_{Ar}), 7.56 (tt, $J = 7.4$ Hz, $J = 1.3$ Hz, 1H, CH_{Ar}), 7.50-7.38 (m, 2H, CH_{Ar}), 5.15 (dd, $J = 7.3$ Hz, $J = 2.6$ Hz, 1H, CHOBz), 2.21 (dd, $J = 13.4$ Hz, $J = 7.3$ Hz, 1H, CHOBzCH_{ax}), 2.16 (br s, 1H, OH), 2.03 (ddd, $J = 13.4$ Hz, $J = 3.1$ Hz, $J = 2.9$ Hz, 1H, CHOBzCH_{eq}), 1.97-1.86 (m, 1H, CH₂), 1.78-1.66 (m, 2H, CH₂), 1.60-1.52 (m, 1H, CH₂), 1.48 (s, 3H, CH₃), 1.32 (s, 3H, CH₃), 1.28 (s, 3H, CH₃).

¹³C NMR (100 MHz, CDCl₃) δ 165.80, 132.68, 129.87, 129.29, 128.01, 90.50, 85.14, 78.61, 70.69, 41.03, 33.52, 30.75, 24.89, 16.13.

HRMS (m/z) calcd for C₁₇H₂₂O₄Na [M+Na]⁺: 313.1410. Found 313.1406.

7. Experimental Section



(+)-2β,4-dihydroxy-1,8-cineole ((+)-108): Bicyclic ether **111** (47.1 mg, 0.162 mmol) was dissolved in MeOH (3 mL) and NaOMe (17.6 mg, 0.32 mmol, 2 equiv) was added. The mixture was stirred at 60 °C for 8 h and methanol was removed by evaporation under reduced pressure. Purification by flash chromatography (20% EtOAc in hexane) afforded **(+)-108** as a white solid (28.7 mg, 0.154 mmol, 95%).

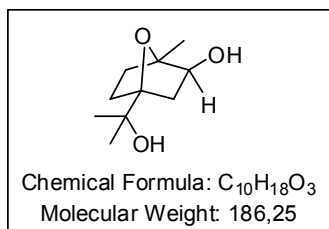
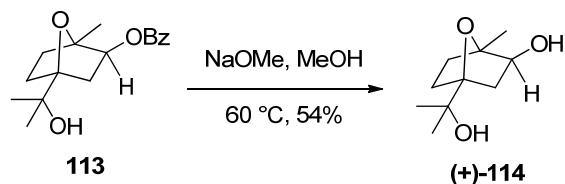
¹H NMR (400 MHz, CDCl₃): δ 3.66 (dd, *J* = 9.7 Hz, *J* = 2.6 Hz, 1H, CHOH), 2.05 (dd, *J* = 13.8 Hz, *J* = 9.8 Hz, 1H, CHOHCH_{ax}), 1.99-1.92 (m, 3H), 1.88 (br s, 2H, OH), 1.66 (c m, 1H, CH₂), 1.50-1.42 (m, 1H, CH₂), 1.28 (s, 3H, CH₃), 1.26 (s, 3H, CH₃), 1.08 (s, 3H, CH₃).

¹³C NMR (100 MHz, CDCl₃) δ 76.96, 72.37, 72.09, 70.00, 42.44, 30.31, 29.66, 24.93, 24.17, 22.31.

HRMS (*m/z*) calcd for C₁₀H₁₈O₃Na [M+Na]⁺: 209.1148. Found 209.1146.

[α]_D²⁵: + 5.67° (*c* 0.141, CHCl₃).

The physical data are identical in all respects to those previously reported.^[156]



(+)-2β,4-dihydroxy-1,4-cineole ((+)-114): Bicyclic ether **113** (22.8 mg, 0.0785 mmol) was dissolved in MeOH (2 mL) and NaOMe (8.5 mg, 0.157 mmol, 2 equiv) was added. The mixture was stirred at 60 °C for 8 h and methanol was removed by evaporation under reduced pressure. Purification by flash chromatography (20% EtOAc in hexane) afforded **18** as a white solid (7.9 mg, 0.042 mmol, 54%).

¹H NMR (400 MHz, CDCl₃): δ 3.79 (dd, *J* = 1.9 Hz, *J* = 6.9 Hz, 1H), 2.05 (dd, *J* = 13.0 Hz, *J* = 6.9 Hz, 1H, CHOHCH_{ax}), 1.88-1.73 (m, 2H), 1.80 (br s, 2H, OH), 1.61 (td, *J* = 12.2 Hz, *J* =

7. Experimental Section

3.9 Hz, 1H, CHOHCH_{eq}), 1.56-1.47 (m, 1H, CH₂), 1.47-1.39 (m, 1H, CH₂), 1.44 (s, 3H, CH₃), 1.30 (s, 3H, CH₃), 1.25 (s, 3H, CH₃).

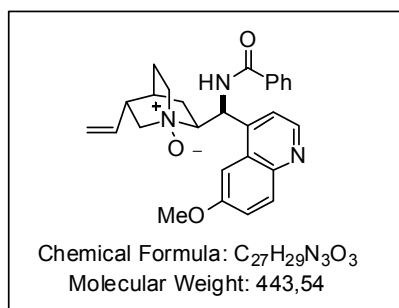
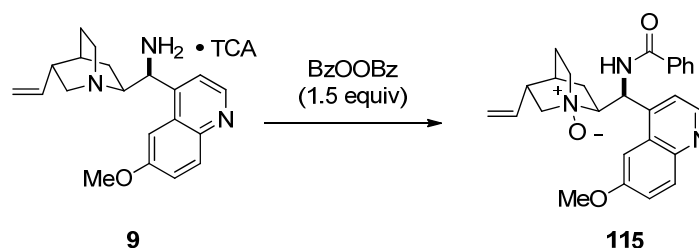
¹³C NMR (100 MHz, CDCl₃) δ 90.61, 86.42, 76.89, 71.09, 43.81, 33.01, 31.46, 25.36, 25.21, 16.22.

HRMS (*m/z*) calcd for C₁₀H₁₉O₃ [M+H]⁺: 187.1334. Found 187.1335.

[α]_D²⁵: + 4.48° (*c* 0.134, CHCl₃).

The physical data are identical in all respects to those previously reported.^[156]

7.3.5 Synthesis and Characterization of 115



9-Amino-9-deoxyepiquinine (**9**) (100 mg, 0.31 mmol) and trichloroacetic acid (50.6 mg, 0.31 mmol, 1 equiv) were dissolved in THF (0.5 mL) and anhydrous benzoyl peroxide (75.0 mg, 0.31 mmol, 1 equiv) was added. After stirring the reaction mixture for 24 h at 30 °C, the crude was washed with sat. aq. NaHCO₃, extracted with dichloromethane, dried over MgSO₄, filtered and evaporated under reduced

pressure to afford **115** as an off-white foam (127 mg, 0.29 mmol, 92%).

¹H NMR^[a] (400 MHz, CDCl₃, T = 296K) δ 8.74 (d, *J* = 4.6 Hz, 1H), 8.03 (d, *J* = 9.3 Hz, 1H), 7.90 (d, *J* = 7.5 Hz, 2H), 7.79 (br s, 1H), 7.57 (d, *J* = 4.3 Hz, 1H), 7.39-7.35 (m, 4H), 6.11-5.46 (br s, 1H)^[b], 5.66 (ddd, *J* = 17.2 Hz, *J* = 10.0 Hz, *J* = 6.9 Hz, 1H), 5.14-5.09 (m, 2H), 4.22-3.74 (m, 2H), 3.97 (br s, 3H), 3.67 (dd, *J* = 13.2 Hz, *J* = 10.6 Hz, 1H), 3.48-3.33 (m, 2H), 2.87 (c m, 1H), 2.26 (c m, 1H), 2.20-2.09 (m, 1H), 1.92 (br s, 1H), 1.88-1.71 (m, 1H), 1.69-1.42 (m, 1H).

¹³C NMR (150 MHz, CDCl₃)^[c] δ 166.35, 157.90 (br), 147.36, 144.57 (br), *Cq not detected*,^[c] 136.00, 133.35, 131.92, 131.25, 128.22, *Cq not detected*,^[c] 127.09, 121.46, 119.35 (br), 117.17, 101.37 (br), 71.55 (br), 70.85, 57.17, 55.47, 52.87 (br), 39.38, 26.46 (2C),^[c] 25.39;

7. Experimental Section

¹⁵N NMR (60 MHz, CDCl₃, T = 253 K, δ_{NH₃} = 0 ppm, 2 amide rotamers) δ 306, 308 (quinoline N), 118, 117 (N-oxide), 119, 121 (amide N). ¹⁵N-NMR (60 MHz, CDCl₃, T = 296 K, δ_{NH₃} = 0 ppm) δ 294 (quinoline N), 103 (N-oxide), amide N not detected under these conditions.

FTIR (thin film) 3045, 2959, 1651, 1621, 1603, 1590, 1578, 1507, 1474, 1432, 1328, 1264, 1227, 1176, 1158, 1101, 1081, 1028, 928, 857, 829 cm⁻¹

LRMS (EI): m/z = 443 [M⁺], 426, 386, 344, 305, 239, 213, 187, 160, 136, 105, 77, 42.

HRMS (m/z) calcd for C₂₇H₂₉N₃O₃Na [M+Na]⁺: 466.2101. Found 466.2105.

[a] At T = 253K, two conformations (presumably amide rotamers) of **115** with a ca. 2.5:1 ratio are observed by NMR (600 MHz, CDCl₃).

[b] Detected as two sharp doublets at T = 253K: ¹H NMR (600 MHz, CDCl₃, T = 253K, 2 amide rotamers) δ 5.92 (d, J = 11.5 Hz, 0.66 H), 5.31 (d, J = 11.5 Hz, 0.34 H).

[c] ¹³C NMR (150 MHz, T = 253K, CDCl₃, 2 equivalent rotamer peaks shown as two values joined by a plus sign) δ 166.16 + 165.88, 157.99 + 156.81, 147.50 + 146.82, 144.96 + 143.93, 143.85 + 139.71, 135.80 + 135.47, 132.78 + 132.71, 131.73 + 131.70, 131.33, 128.25 + 128.16, 127.86 + 125.88, 126.92 + 126.71, 121.58, 119.18, 117.29, 101.63 + 100.24, 71.33 + 66.97, 70.59 + 70.26, 62.75 + 52.43, 56.96 + 56.89, 55.40 + 55.33, 39.30 + 39.09, 26.92 + 26.23, 26.04, 26.09 + 24.81.

7.3.6 α-Chlorination and α-Fluorination of α-Branched Enal **53c**

7.3.6.1 General Procedures

Chlorination of α-Branched Enal **53b**

A 2 mL vial, equipped with a magnetic stirring bar, was charged with 9-amino(9-deoxy)*epi*quinine **9** (6.6 mg, 0.0204 mmol, 10 mol%), trichloroacetic acid (9.9 mg, 0.060 mmol, 30 mol%), aldehyde **53** (23 μL, 0.204 mmol) and THF (0.2 mL) before adding *N*-chlorosuccinimide (40.9 mg, 0.306 mmol, 1.5 equiv). The reaction mixture was stirred at room temperature for 18 h, diluted with dichloromethane, then treated with a saturated aqueous solution of NaHCO₃, extracted three times with dichloromethane, washed with brine, dried over Na₂SO₄, filtered, concentrated and purified by either flash column chromatography eluting

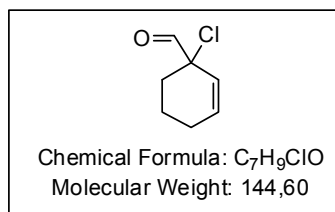
7. Experimental Section

with a specified mixture of pentane and Et₂O. A method for chiral-phase GC separation of *rac*-**135** or *rac*-**136** could not be achieved.

Fluorination of α -Branched Enal **53b**

A 2 mL vial, equipped with a magnetic stirring bar, was charged with 9-amino(9-deoxy)*epi*quinine **9** (6.6 mg, 0.0204 mmol, 10 mol%), trichloroacetic acid (9.9 mg, 0.060 mmol, 30 mol%), aldehyde **53** (23 μ L, 0.204 mmol) and THF (0.2 mL) before adding *N*-fluorobenzenesulfonamide (98.5 mg, 0.306 mmol, 1.5 equiv). The reaction mixture was stirred at room temperature for 18 h, diluted with dichloromethane, then treated with a saturated aqueous solution of NaHCO₃, extracted three times with dichloromethane, washed with brine, dried over Na₂SO₄, filtered, concentrated and purified by either flash column chromatography eluting with a specified mixture of pentane and Et₂O. The enantioselectivity of the resulting aldehyde **137** was determined by chiral-phase GC analysis.

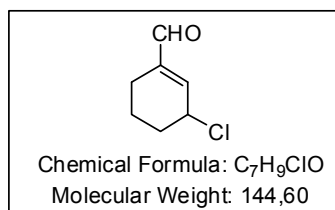
7.3.6.1 Product Characterization



1-chlorocyclohex-2-enecarbaldehyde (135): Prepared according to the general procedure (Section 7.3.2.4) from the commercial enal **53c** and analyzed by NMR as part of the crude mixture. Purification by flash chromatography (10-30% Et₂O in pentane) resulted in decomposition of this product.

Selected ¹H NMR (500 MHz, CDCl₃) δ 9.43 (s, 1H, CHO), 6.07 (dt, $J = 9.9$ Hz, $J = 4.0$ Hz, 1H, CH=CH), 5.70 (br d, $J = 10.2$ Hz, 1H, CH=CH).

This compound was found to be unstable on silica gel and could not be isolated.



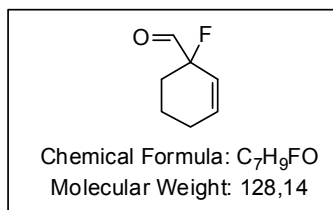
3-chlorocyclohex-1-enecarbaldehyde (136): Prepared according to the general procedure (Section 7.3.2.4) from the commercial enal **53c**. Purification by flash chromatography (10-30% Et₂O in pentane) afforded **154e** as a stable colorless oil.

¹H NMR (500 MHz, CDCl₃) δ 9.51 (s, 1H, CHO), 6.72 (c. m, 1H, CH=CH), 4.80 (c. m, 1H CH=CH), 2.36 (dt, $J = 18.4$ Hz, $J = 5.3$ Hz, 1H, CH₂), 2.22-2.01 (m, 3H, CH₂), 1.96-1.85 (m, 1H, CH₂), 1.78-1.68 (m, 1H, CH₂).

7. Experimental Section

^{13}C NMR (125 MHz, CDCl_3) δ 193.8, 146.6, 142.3, 53.5, 32.2, 21.0, 17.9.

HRMS (m/z) calcd for $\text{C}_7\text{H}_9\text{OCl}$ [M]: 144.034195. Found: 144.034050.

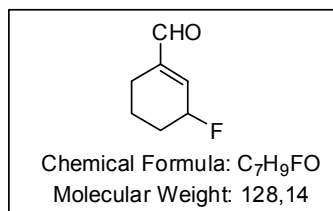


1-fluorocyclohex-2-enecarbaldehyde (137): Prepared according to the general procedure (Section 7.3.2.5) from the commercial enal **53c** and analyzed by NMR as part of the crude mixture. Purification by flash chromatography (10-30% Et_2O in pentane) resulted in decomposition of this product.

^1H NMR (500 MHz, CDCl_3) δ 9.70 (d, $J_{\text{H-F}} = 4.6$ Hz, 1H, CHO), 6.30 (c. m, 1H, CH=CH), 5.64 (c. m, 1H, CH=CH), 2.24-2.15 (m, 1H, CH_2), 2.14-2.02 (m, 1H, CH_2), 2.00-1.89 (m, 2H, CH_2), 1.83-1.76 (m, 2H, CH_2).

LRMS (EI): $m/z = 128$ [M], 109 [M-F], 99 [M-CHO], 79, 71, 59, 53, 51, 41, 39, 29, 27.

This compound was found to be unstable on silica gel and could not be isolated.



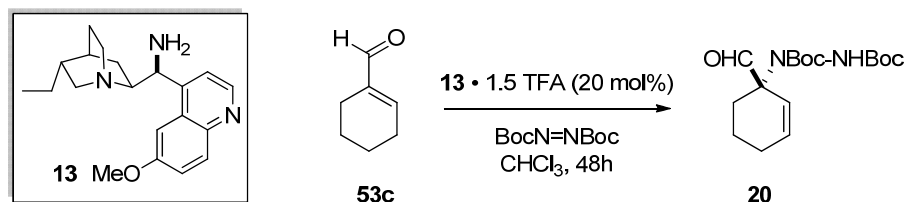
3-fluorocyclohex-1-enecarbaldehyde (137a): Prepared according to the general procedure (Section 7.3.2.4) from the commercial enal **53c**.

Selected ^1H NMR (500 MHz, CDCl_3) δ 9.57 (s, 1H, CHO), 6.71 (c. m, 1H, C=CH), 5.65 (c. m, 1H, CHF).

HRMS (m/z) calcd for $\text{C}_7\text{H}_9\text{OF}$ [M]: 128.06374. Found: 128.06362.

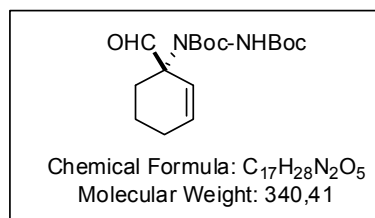
7.4 Catalytic Asymmetric α -Amination of α -Branched Enal **53c**^[25e]

7.4.1 Synthesis and Characterization



According to the procedure of *Bencivenni et al.*,^[25e] a 2 mL vial was charged with 9-amino(9-deoxy)epidihydroquinine **13** (26 mg, 0.08 mmol, 20 mol%), chloroform (0.4 mL) and TFA (9 μ L, 0.12 mmol, 30 mol%). To this solution, aldehyde **53c** (45.6 μ L, 0.4 mmol, 1 equiv) and di-*tert*-butyl-azodicarboxylate (BocN=NBoc, 110 mg, 0.48 mmol, 1.2 equiv) were added. The reaction was stirred at room temperature for 16.5 h and was found to proceed to 92% conversion. ¹H NMR analysis of the crude reaction mixture indicated >99:1 α/γ selectivity favouring the product **20**. Removal of solvent under reduced pressure and purification by flash chromatography (40% Et₂O in pentane) afforded **20** in spectroscopically pure form (yield n.d., er = 99:1).

Racemic *rac*-**20** was obtained by using the above procedure, but substituting the chiral catalyst salt [**13**·1.5TFA] with *meso*-**8** (10 mol%) and trichloroacetic acid (10 mol%).



(S)-di-tert-butyl 1-(1-formylcyclohex-2-en-1-yl)hydrazine-1,2-dicarboxylate (20): ¹H NMR (500 MHz, CDCl₃, values separated by a plus sign indicate a pair of rotamers) δ 9.54 + 9.42 (br s, 1H, CHO), 6.38 + 6.23 (br s, 1H, NH), 6.18 + 6.11 (br s, 1H, C_qCH=CH), 5.50 + 5.45 (br s, 1H, C_qCH=CH),

2.41-1.91 (m, 3H, CH₂), 1.91-1.62 (m, 3H, CH₂), 1.46 (s, 9H, C(CH₃)₃), 1.43 (s, 9H, C(CH₃)₃).

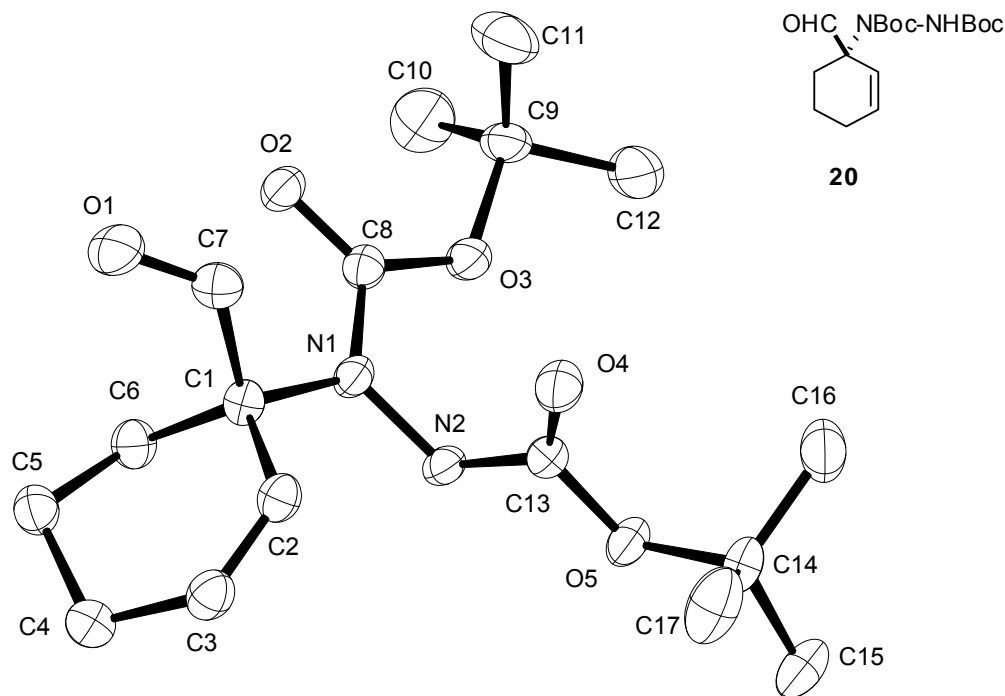
¹³C NMR (125 MHz, CDCl₃, correlated by DEPT-135, values separated by a plus sign indicate a pair of rotamers) δ 196.1 (br, CH), 155.6 (br, C_q), 154.7 (br, C_q), 135.1 + 135.0 (CH), 122.4 + 120.8 (CH), 83.7 + 82.5 (C_q), 82.0 + 81.4 (C_q), 68.9 (br, C_q), 28.2 (CH₃), 28.1 (CH₃), 26.5 + 26.1 (CH₂), 24.6 + 24.4 (CH₂), 18.5 + 18.3 (CH₂).

Chiral HPLC (OD-3, *n*-Hept/¹PrOH 97:3, 1 mL/min, 25 °C): t_r 4.53 min (major enantiomer), t_r 5.40 min (minor enantiomer). The absolute configuration was assigned by X-ray crystallography.

7. Experimental Section

7.4.2 Crystallographic Data

(*S*)-di-*tert*-butyl 1-(1-formylcyclohex-2-en-1-yl)hydrazine-1,2-dicarboxylate (**20**):



Crystal data and structure refinement

Identification code	7382	
Empirical formula	C ₁₇ H ₂₈ N ₂ O ₅	
Color	colourless	
Formula weight	340.41 g · mol ⁻¹	
Temperature	150 K	
Wavelength	1.54184 Å	
Crystal system	ORTHORHOMBIC	
Space group	P2 ₁ 2 ₁ 2 ₁ , (no. 19)	
Unit cell dimensions	a = 10.2061(6) Å	α = 90°.
	b = 10.5578(6) Å	β = 90°.
	c = 17.5556(10) Å	γ = 90°.
Volume	1891.69(19) Å ³	
Z	4	
Density (calculated)	1.195 Mg · m ⁻³	
Absorption coefficient	0.722 mm ⁻¹	
F(000)	736 e	

7. Experimental Section

Crystal size	0.40 x 0.27 x 0.16 mm ³	
θ range for data collection	4.89 to 67.17°.	
Index ranges	-11 \leq h \leq 12, -12 \leq k \leq 12, -20 \leq l \leq 20	
Reflections collected	82677	
Independent reflections	3364 [$R_{\text{int}} = 0.0415$]	
Reflections with $I > 2\sigma(I)$	3331	
Completeness to $\theta = 67.17^\circ$	99.2 %	
Absorption correction	Gaussian	
Max. and min. transmission	0.91 and 0.70	
Refinement method	Full-matrix least-squares on F^2	
Data / restraints / parameters	3364 / 0 / 223	
Goodness-of-fit on F^2	1.068	
Final R indices [$I > 2\sigma(I)$]	$R_1 = 0.0274$	$wR^2 = 0.0712$
R indices (all data)	$R_1 = 0.0275$	$wR^2 = 0.0714$
Absolute structure parameter	0.02(14)	
Largest diff. peak and hole	0.208 and -0.218 e \cdot \AA^{-3}	

Atomic coordinates and equivalent isotropic displacement parameters (\AA^2).

U_{eq} is defined as one third of the trace of the orthogonalized U_{ij} tensor.

	x	y	z	U_{eq}
O(1)	0.1543(1)	0.0858(1)	0.3570(1)	0.039(1)
O(2)	0.2532(1)	0.1707(1)	0.5201(1)	0.027(1)
O(3)	0.4430(1)	0.1418(1)	0.5868(1)	0.029(1)
O(4)	0.5563(1)	-0.0994(1)	0.4812(1)	0.033(1)
O(5)	0.7530(1)	0.0024(1)	0.4935(1)	0.028(1)
N(1)	0.4444(1)	0.1326(1)	0.4602(1)	0.024(1)
N(2)	0.5786(1)	0.1139(1)	0.4654(1)	0.023(1)
C(1)	0.3817(1)	0.1356(1)	0.3840(1)	0.023(1)
C(2)	0.4654(1)	0.0597(1)	0.3294(1)	0.026(1)
C(3)	0.4973(1)	0.0996(1)	0.2602(1)	0.031(1)
C(4)	0.4563(1)	0.2238(1)	0.2275(1)	0.033(1)
C(5)	0.3387(1)	0.2770(1)	0.2698(1)	0.030(1)
C(6)	0.3607(1)	0.2715(1)	0.3559(1)	0.027(1)
C(7)	0.2535(1)	0.0606(1)	0.3905(1)	0.029(1)
C(8)	0.3713(1)	0.1507(1)	0.5242(1)	0.024(1)
C(9)	0.3816(1)	0.1434(1)	0.6632(1)	0.033(1)

7. Experimental Section

C(10)	0.3304(2)	0.2758(2)	0.6792(1)	0.050(1)
C(11)	0.2765(2)	0.0423(2)	0.6685(1)	0.052(1)
C(12)	0.4967(2)	0.1130(2)	0.7143(1)	0.051(1)
C(13)	0.6237(1)	-0.0053(1)	0.4810(1)	0.024(1)
C(14)	0.8322(1)	-0.1137(1)	0.5031(1)	0.029(1)
C(15)	0.9699(1)	-0.0619(1)	0.5124(1)	0.040(1)
C(16)	0.7891(2)	-0.1828(2)	0.5743(1)	0.043(1)
C(17)	0.8227(2)	-0.1956(2)	0.4325(1)	0.051(1)

Table 3. Bond lengths [Å] and angles [°].

O(1)-C(7)	1.2011(16)	O(2)-C(8)	1.2256(15)
O(3)-C(8)	1.3234(14)	O(3)-C(9)	1.4809(14)
O(4)-C(13)	1.2084(15)	O(5)-C(13)	1.3396(14)
O(5)-C(14)	1.4781(14)	N(1)-N(2)	1.3866(14)
N(1)-C(1)	1.4833(14)	N(1)-C(8)	1.3640(15)
N(2)-C(13)	1.3672(15)	C(16)-C(14)	1.513(2)
C(1)-C(2)	1.5141(16)	C(1)-C(6)	1.5311(16)
C(1)-C(7)	1.5335(17)	C(2)-C(3)	1.3256(19)
C(3)-C(4)	1.4917(19)	C(4)-C(5)	1.5191(19)
C(5)-C(6)	1.5305(17)	C(9)-C(10)	1.519(2)
C(9)-C(11)	1.516(2)	C(9)-C(12)	1.5124(19)
C(14)-C(15)	1.5164(18)	C(14)-C(17)	1.515(2)
C(8)-O(3)-C(9)	121.15(9)	C(13)-O(5)-C(14)	120.51(9)
N(2)-N(1)-C(1)	119.29(9)	C(8)-N(1)-N(2)	120.42(9)
C(8)-N(1)-C(1)	120.27(9)	C(13)-N(2)-N(1)	118.48(10)
N(1)-C(1)-C(2)	108.37(9)	N(1)-C(1)-C(6)	111.73(9)
N(1)-C(1)-C(7)	106.85(9)	C(2)-C(1)-C(6)	111.83(10)
C(2)-C(1)-C(7)	104.77(10)	C(6)-C(1)-C(7)	112.89(10)
C(3)-C(2)-C(1)	123.34(11)	C(2)-C(3)-C(4)	124.31(12)
C(3)-C(4)-C(5)	110.98(11)	C(4)-C(5)-C(6)	110.65(10)
C(5)-C(6)-C(1)	111.93(10)	O(2)-C(8)-O(3)	127.22(11)
O(2)-C(8)-N(1)	120.95(11)	O(3)-C(8)-N(1)	111.82(9)
O(3)-C(9)-C(10)	108.83(11)	O(3)-C(9)-C(11)	110.27(11)
O(3)-C(9)-C(12)	101.92(10)	C(11)-C(9)-C(10)	113.18(13)
C(12)-C(9)-C(10)	110.67(13)	C(12)-C(9)-C(11)	111.37(13)

7. Experimental Section

O(4)-C(13)-O(5)	127.56(11)	O(4)-C(13)-N(2)	124.43(10)
O(5)-C(13)-N(2)	107.99(10)	O(5)-C(14)-C(16)	109.61(10)
O(5)-C(14)-C(15)	102.73(10)	O(5)-C(14)-C(17)	110.19(10)
C(16)-C(14)-C(15)	110.75(12)	C(16)-C(14)-C(17)	112.45(13)
C(17)-C(14)-C(15)	110.69(12)	O(1)-C(7)-C(1)	124.62(11)

Anisotropic displacement parameters (\AA^2).

The anisotropic displacement factor exponent takes the form:

$$-2\pi^2 [h^2 a^{*2} U_{11} + \dots + 2 h k a^* b^* U_{12}].$$

	U_{11}	U_{22}	U_{33}	U_{23}	U_{13}	U_{12}
O(1)	0.027(1)	0.056(1)	0.035(1)	0.001(1)	-0.005(1)	-0.009(1)
O(2)	0.021(1)	0.032(1)	0.028(1)	-0.001(1)	0.000(1)	0.004(1)
O(3)	0.021(1)	0.044(1)	0.023(1)	0.002(1)	0.000(1)	0.001(1)
O(4)	0.027(1)	0.027(1)	0.044(1)	0.006(1)	-0.006(1)	-0.004(1)
O(5)	0.019(1)	0.025(1)	0.041(1)	0.001(1)	-0.004(1)	0.002(1)
N(1)	0.018(1)	0.030(1)	0.023(1)	0.000(1)	-0.002(1)	0.003(1)
N(2)	0.016(1)	0.024(1)	0.029(1)	0.002(1)	0.001(1)	-0.001(1)
C(1)	0.023(1)	0.023(1)	0.024(1)	-0.001(1)	-0.002(1)	0.002(1)
C(2)	0.025(1)	0.025(1)	0.028(1)	-0.003(1)	-0.002(1)	0.004(1)
C(3)	0.027(1)	0.036(1)	0.028(1)	-0.004(1)	-0.001(1)	0.004(1)
C(4)	0.032(1)	0.039(1)	0.029(1)	0.004(1)	0.002(1)	0.001(1)
C(5)	0.031(1)	0.028(1)	0.029(1)	0.003(1)	-0.001(1)	0.002(1)
C(6)	0.029(1)	0.024(1)	0.028(1)	-0.001(1)	-0.001(1)	0.002(1)
C(7)	0.029(1)	0.030(1)	0.027(1)	-0.002(1)	0.002(1)	-0.003(1)
C(8)	0.023(1)	0.022(1)	0.026(1)	0.000(1)	-0.001(1)	0.000(1)
C(9)	0.024(1)	0.052(1)	0.021(1)	0.004(1)	0.002(1)	-0.006(1)
C(10)	0.051(1)	0.067(1)	0.032(1)	-0.013(1)	0.000(1)	0.008(1)
C(11)	0.048(1)	0.071(1)	0.039(1)	0.015(1)	-0.001(1)	-0.024(1)
C(12)	0.035(1)	0.088(1)	0.030(1)	0.015(1)	-0.004(1)	-0.004(1)
C(13)	0.021(1)	0.027(1)	0.025(1)	0.003(1)	-0.001(1)	0.000(1)
C(14)	0.026(1)	0.027(1)	0.035(1)	-0.003(1)	-0.007(1)	0.007(1)
C(15)	0.023(1)	0.041(1)	0.057(1)	-0.004(1)	-0.005(1)	0.006(1)
C(16)	0.039(1)	0.042(1)	0.048(1)	0.013(1)	-0.012(1)	0.001(1)
C(17)	0.046(1)	0.055(1)	0.051(1)	-0.022(1)	-0.014(1)	0.018(1)

8. BIBLIOGRAPHY

- [1] M. Klussmann, D. G. Blackmond, in *Chemical Evolution II: From the Origins of Life to Modern Society*, American Chemical Society, Washington, DC, **2009**.
- [2] E. Brenna, C. Fuganti, S. Serra, *Tetrahedron: Asym.* **2003**, *14*, 1.
- [3] C. Zipper, C. Bolliger, T. Fleischmann, M. J. Suter, W. Angst, M. D. Muller, H. P. Kohler, *Biodegradation* **1999**, *10*, 271.
- [4] J. A. Le Bel, *Soc. Chim. France* **1874**, *2*, 337.
- [5] J. H. van't Hoff, *Bull. Soc. Chim. France* **1875**, *2*, 295.
- [6] A. J. Hutt, J. O'Grady, *J. Antimicrob. Chemother.* **1996**, *37*, 7.
- [7] E. J. Aliens, E. W. Wuis, E. J. Veringa, *Biochem. Pharmacol.* **1988**, *37*, 9.
- [8] I. Agranat, H. Caner, J. Caldwell, *Nat. Rev. Drug Discov.* **2002**, *1*, 753.
- [9] K. C. Nicolaou, E. J. Sorensen, *Classics in Total Synthesis: Targets, Strategies, Methods*, Wiley-VCH, Weinheim, **1996**.
- [10] N. Z. Burns, P. S. Baran, R. W. Hoffmann, *Angew. Chem. Int. Ed.* **2009**, *48*, 2854.
- [11] B. List, R. A. Lerner, C. F. Barbas, *J. Am. Chem. Soc.* **2000**, *122*.
- [12] K. A. Ahrendt, C. J. Borths, D. W. C. MacMillan, *J. Am. Chem. Soc.* **2000**, *122*, 4243.
- [13] M. J. Gaunt, C. C. C. Johansson, A. McNally, N. T. Vo, *Drug Discovery Today* **2007**, *12*, 8.
- [14] K. B. Sharpless, *Angew. Chem. Int. Ed.* **2002**, *41*, 2024.
- [15] M. Marigo, J. Franzen, T. B. Poulsen, W. Zhuang, K. A. Jørgensen, *J. Am. Chem. Soc.* **2005**, *127*, 6964-6965.
- [16] B. List, *Adv. Synth. Catal.* **2004**, *346*, 1021.
- [17] J. von Liebig, *Liebigs Ann. Chem.* **1860**, *113*, 246.
- [18] G. Bredig, P. S. Fiske, *Biochem. Z.* **1913**, *46*, 7.
- [19] J. Seayad, B. List, *Org. Biomol. Chem.* **2005**, *3*, 719.
- [20] (a) P. G. Garcia, F. Lay, P. G. Garcia, C. Rabalakos, B. List, *Angew. Chem. Int. Ed.* **2009**, *48*, 4363; (b) L. Ratjen, P. García-García, F. Lay, M. E. Beck, B. List, *Angew. Chem. Int. Ed.* **2011**, *50*, 754.
- [21] T. Ooi, K. Maruoka, *Angew. Chem. Int. Ed.* **2007**, *46*, 4222.
- [22] (a) E. Knoevenagel, *Ber. Dtsch. Chem. Ges.* **1896**, *29*, 172; (b) E. Knoevenagel, *Ber. Dtsch. Chem. Ges.* **1898**, *31*, 2585; (c) E. Knoevenagel, *Ber. Dtsch. Chem. Ges.* **1898**, *31*, 738; (d) E. Knoevenagel, *Ber. Dtsch. Chem. Ges.* **1898**, *31*, 2596.
- [23] B. List, *Angew. Chem. Int. Ed.* **2010**, *49*, 1730.
- [24] B. List, *Chem. Commun.* **2006**, 819.
- [25] (a) G. Bergonzini, S. Vera, P. Melchiorre, *Angew. Chem. Int. Ed.* **2010**, *49*, 9685; (b) S. Bertelsen, M. Marigo, S. Brandes, P. Diner, K. A. Jørgensen, *J. Am. Chem. Soc.* **2006**, *128*, 12973; (c) B. Han, Y.-C. Xiao, Z.-Q. He, Y.-C. Chen, *Org. Lett.* **2009**, *11*, 4660; (d) J. Stiller, E. Marques-Lopez, R. P. Herrera, R. Fröhlich, C. Strohmam, M. Christmann, *Org. Lett.* **2011**, *13*, 70; (e) G. Bencivenni, P. Galzerano, A. Mazzanti, G. Bartoli, P. Melchiorre, *Proced. Nat. Acad. Sci.* **2010**, *107*, 20642.
- [26] (a) Z.-J. Jia, H. Jiang, J.-L. Li, B. Gschwend, Q.-Z. Li, X. Yin, J. Grouleff, Y.-C. Chen, K. A. Jørgensen, *J. Am. Chem. Soc.* **2011**, *133*, 5053; (b) Y. Liu, M. Nappi, E. Arceo, S. Vera, P. Melchiorre, *J. Am. Chem. Soc.* **2011**, *133*, 15212.
- [27] (a) S. Mukherjee, J. W. Yang, S. Hoffmann, B. List, *Chem. Rev.* **2007**, *107*, 5471; (b) A. Erikkiila, I. Majander, P. M. Pihko, *Chem. Rev.* **2007**, *107*; (c) P. Melchiorre, M. Marigo, C. Carlone, G. Bartoli, *Angew. Chem. Int. Ed.* **2008**, *47*, 6139; (d) S. Bertelsen, K. A. Jørgensen, *Chem. Soc. Rev.* **2009**, *38*, 2178; (e) J. B. Brazier, N. C. O. Tomkinson, *Top. Curr. Chem.* **2010**, *291*, 281.
- [28] T. D. Beeson, A. Mastracchio, J.-B. Hong, K. Ashton, D. W. C. MacMillan, *Science* **2007**, *316*, 582.

8. Bibliography

- [29] A. B. Northrup, D. W. C. MacMillan, *J. Am. Chem. Soc.* **2002**, *124*, 2458.
- [30] (a) C. Grondal, M. Jeanty, D. Enders, *Nat. Chem.* **2010**, *2*, 167; (b) D. Enders, C. Grondal, M. R. M. Hüttl, *Angew. Chem. Int. Ed.* **2007**, *46*, 1570.
- [31] (a) D. B. Llewellyn, D. Adamson, B. A. Arndtsen, *Org. Lett.* **2000**, *2*; (b) C. Carter, S. Fletcher, A. Nelson, *Tetrahedron: Asym.* **2003**, *14*, 1995; (c) D. B. Llewellyn, B. A. Arndtsen, *Tetrahedron: Asym.* **2005**, *16*, 1789; (d) J. Lacour, D. Monchaud, C. Marsol, *Tetrahedron Lett.* **2002**, *43*, 8257; (e) S. P. Smidt, N. Zimmermann, M. Studer, A. Pfalz, *Chem. Eur. J.* **2004**, *10*, 4685.
- [32] S. Mayer, B. List, *Angew. Chem. Int. Ed.* **2006**, *45*, 4193.
- [33] L. Ratjen, S. Müller, B. List, *Nachrichten aus der Chemie* **2010**, *58*, 640.
- [34] N. J. A. Martin, B. List, *J. Am. Chem. Soc.* **2006**, *128*, 13368.
- [35] (a) G. Bartoli, P. Melchiorre, *Synlett* **2008**, *12*, 1759; (b) C. Liu, Y. Lu, *Org. Lett.* **2010**, *12*, 2278; (c) W. Sun, L. Hong, C. Liu, R. Wang, *Tetrahedron: Asym.* **2010**, *21*, 2010.
- [36] X. Wang, B. List, *Angew. Chem. Int. Ed.* **2008**, *47*, 1119.
- [37] H. D. Dakin, *Biol. Chem.* **1910**, *7*, 49.
- [38] L. W. Xu, J. Luo, Y. Lu, *Chem. Commun.* **2009**, 1807.
- [39] L.-W. Xu, Y. Lu, *Org. Biomol. Chem.* **2008**, *6*, 2047.
- [40] H. Albrecht, J. Blecher, F. Kröhnke, *Tetrahedron Lett.* **1971**, *27*, 2169.
- [41] (a) Y.-C. Chen, *Synlett* **2008**, *13*, 1919; (b) L. Jiang, Y.-C. Chen, *Catal. Sci. Technol.* **2011**, *1*, 354; (c) F. Peng, Z. Shao, *J. Mol. Catal. A: Chem.* **2008**, *285*, 1.
- [42] (a) A. Russo, A. Capobianco, A. Peretto, A. Lattanzi, A. Peluso, *Eur. J. Org. Chem.* **2011**, 1922; (b) A. Lattanzi, *Org. Lett.* **2005**, *7*, 2579.
- [43] K. Ishihara, K. Nakano, *J. Am. Chem. Soc.* **2005**, *127*, 10504.
- [44] H. Kim, C. Yen, P. Preston, J. Chin, *Org. Lett.* **2006**, *8*, 5239.
- [45] P. Kwiatkowski, T. D. Beeson, J. C. Conrad, D. W. C. MacMillan, *J. Am. Chem. Soc.* **2011**, *133*, 1738.
- [46] C. F. Cullis, I. Isaac, *Trans. Faraday Soc.* **1952**, *48*, 1023.
- [47] (a) R. Helder, J. C. Hummelen, R. W. P. M. Laane, J. S. Wiering, H. Wynberg, *Tetrahedron Lett.* **1976**, *17*, 1831; (b) H. Wynberg, B. Greijdanus, *J. Chem. Soc. Chem. Commun.* **1978**, 427; (c) J. C. Hummelen, H. Wynberg, *Tetrahedron Lett.* **1978**, *19*, 1089.
- [48] C. E. Song, Cinchona Alkaloids in Synthesis and Catalysis, in *Cinchona Alkaloids in Synthesis and Catalysis*, (Eds., Wiley-VCH, Weinheim, **2009**
- [49] H. Brunner, J. Bügler, B. Nuber, *Tetrahedron: Asym.* **1995**, *6*, 1699.
- [50] J.-W. Xie, W. Chen, R. Li, M. Zeng, W. Du, L. Yue, Y.-C. Chen, Y. Wu, J. Zhu, J.-G. Deng, *Angew. Chem. Int. Ed.* **2007**, *46*, 389.
- [51] G. Bartoli, M. Bosco, A. Carlone, F. Pesciaioli, L. Sambri, P. Melchiorre, *Org. Lett.* **2007**, *9*, 1403.
- [52] N. Lu, S. Mi, D. Chen, G. Zhang, *Int. J. Quant. Chem.* **2011**, *111*, 2874.
- [53] (a) G. D. H. Dijkstra, R. M. Kellogg, H. Wynberg, *Recl. Trav. Chim. Pays-Bas* **1989**, *108*, 195; (b) G. D. H. Dijkstra, R. M. Kellogg, H. Wynberg, J. S. Svendsen, I. Marko, K. B. Sharpless, *J. Am. Chem. Soc.* **1989**, *111*, 8069.
- [54] T. Bürgi, A. Baiker, *J. Am. Chem. Soc.* **1998**, *120*, 12920.
- [55] J. M. Karle, I. L. Karle, L. Gerena, W. K. Milhous, *Antimicrob. Agents Chemother.* **1992**, *36*, 1538.
- [56] (a) D. Ferri, T. Bürgi, A. Baiker, *J. Chem. Soc. Perkin Trans. 2* **1999**, 1305; (b) T. H. A. Silva, A. B. Oliveira, H. F. D. Santos, W. B. D. Almeida, *Struc. Chem.* **2001**, *12*, 431.
- [57] R. A. Olsen, D. Borchardt, L. Mink, A. Agarwal, I. J. Mueller, F. Zaera, *J. Am. Chem. Soc.* **2006**, *128*, 15594.

8. Bibliography

- [58] G. K. S. Prakash, F. Wang, C. Ni, J. Shen, R. Haiges, A. K. Yudin, T. Mathew, G. A. Olah, *J. Am. Chem. Soc.* **2011**, *133*, 9992.
- [59] M. Fleischmann, D. Drettwan, E. Sugiono, M. Rueping, R. M. Gschwind, *Angew. Chem.* **2011**, *123*, 6488.
- [60] D. B. Ramachary, Y. V. Reddy, *Eur. J. Org. Chem.* **2012**, 865.
- [61] N. Utsumi, H. Zhang, F. Tanaka, C. F. Barbas III, *Angew. Chem. Int. Ed.* **2007**, *46*, 1878.
- [62] E. J. Corey, L. Kürti, *Enantioselective Chemical Synthesis*, Direct Book Publishing, LLC, Dallas, Texas, **2010**.
- [63] (a) W. Zhang, J. L. Loebach, S. R. Wilson, E. N. Jacobsen, *J. Am. Chem. Soc.* **1990**, *112*, 2801; (b) R. Irie, K. Noda, Y. Ito, N. Matsumoto, T. Katsuki, *Tetrahedron Lett.* **1990**, *31*, 7345; (c) R. Irie, K. Noda, Y. Ito, T. Katsuki, *Tetrahedron Lett.* **1991**, *32*, 1055.
- [64] Y. Tu, Z.-X. Wang, Y. Shi, *J. Am. Chem. Soc.* **1996**, *118*, 9806.
- [65] D. Enders, J. Zhu, G. Raabe, *Angew. Chem. Int. Ed. Engl.* **1996**, *35*, 1725.
- [66] C. L. Elston, R. F. W. Jackson, S. J. F. MacDonald, P. J. Murray, *Angew. Chem. Int. Ed. Engl.* **1997**, *36*, 410.
- [67] C. Lauret, S. M. Roberts, *Aldrichimica Acta* **2002**, *35*, 47.
- [68] T. Hashimoto, K. Maruoka, *Chem. Rev.* **2007**, *107*, 5656.
- [69] (a) M. Shibasaki, N. Yoshikawa, *Chem. Rev.* **2002**, *102*, 2187; (b) J. Inanaga, H. Furuno, T. Hayano, *Chem. Rev.* **2002**, *102*, 2211.
- [70] H. Pluim, H. Wynberg, *J. Org. Chem.* **1980**, *45*, 2498.
- [71] E. Weitz, A. Scheffer, *Chem. Ber.* **1921**, *54*, 2344.
- [72] C. A. Bunton, G. J. Minkoff, *J. Chem. Soc.* **1949**, 665.
- [73] (a) H. Meerwein, *J. prakt. Schem.* **1926**, *113*, 9; (b) D. Swern, *J. Am. Chem. Soc.* **1947**, *69*, 1692.
- [74] D. R. Kelly, E. Caroff, R. W. Flood, W. Heal, S. M. Roberts, *Chem. Commun.* **2004**, 2016.
- [75] P. Wright, J. Abbot, *Int. J. Chem. Kin.* **1993**, *25*, 901.
- [76] H. O. House, R. S. Ro, *J. Am. Chem. Soc.* **1958**, *80*, 2428.
- [77] C. F. Christian, T. Takeya, M. J. Szymanski, D. A. Singleton, *J. Org. Chem.* **2007**, *72*, 6183.
- [78] H. Sunden, I. Ibrahim, A. Cordova, *Tetrahedron Letters* **2006**, *47*, 99.
- [79] S. Lee, D. W. C. MacMillan, *Tetrahedron* **2006**, *62*, 11413.
- [80] X. Wang, C. M. Reisinger, B. List, *J. Am. Chem. Soc.* **2008**, *130*, 6070.
- [81] X. Lu, Y. Liu, B. Sun, B. Cindric, L. Deng, *J. Am. Chem. Soc.* **2008**, *130*, 8134.
- [82] C. M. Reisinger, X. Wang, B. List, *Angew. Chem. Int. Ed.* **2008**, *47*, 8112.
- [83] C. Zheng, Y. Li, Y. Yang, H. Wang, H. Cui, J. Zhang, G. Zhao, *Adv. Synth. Catal.* **2009**, *351*, 1685.
- [84] (a) T. Katsuki, Epoxidation of Allylic Alcohols, in *Comprehensive Asymmetric Catalysis*, (Eds.: E. N. Jacobsen, A. Pfaltz, H. Yamamoto), Springer, Berlin, **1999**; (b) X.-Y. Wu, X. She, Y. Sh, *J. Am. Chem. Soc.* **2002**, *124*, 8792.
- [85] P. J. Black, K. Jenkins, J. M. J. Williams, *Tetrahedron: Asym.* **2002**, *13*, 317.
- [86] J. Eshelby, M. Goessman, P. J. Parsons, L. Pennicott, A. Highton, *Org. Biomol. Chem.* **2005**, *3*, 2994.
- [87] (a) M. Hayashi, S. Terashima, K. Koga, *Tetrahedron* **1981**, *37*, 2797; (b) S. Terashima, M. Hayashi, K. Koga, *Tetrahedron Lett.* **1980**, *21*, 2733.
- [88] A. Erkkilä, P. M. Pihko, M.-R. Clarke, *Adv. Synth. Catal.* **2007**, *349*, 802-806.
- [89] C. Sparr, W. B. Schweizer, H. M. Senn, R. Gilmour, *Angew. Chem. Int. Ed.* **2009**, *48*, 3065.

8. Bibliography

- [90] (a) M. E. Jung, D. C. D'Amico, *J. Am. Chem. Soc.* **1995**, *117*, 7379; (b) H. D. King, Z. Meng, D. Denhart, R. Mattson, R. Kimura, D. Wu, Q. Gao, J. E. Macor, *Org. Lett.* **2005**, *7*, 3437-3440.
- [91] O. Lifchits, C. M. Reisinger, B. List, *J. Am. Chem. Soc.* **2010**, *132*, 10227.
- [92] B. P. Bondzic, T. Urushima, H. Ishikawa, Y. Hayashi, *Org. Lett.* **2010**, *12*, 5434.
- [93] J.-L. Li, N. Fu, L. Zhang, P. Zhou, S. Luo, J.-P. Cheng, *Eur. J. Org. Chem.* **2010**, *35*, 6840.
- [94] (a) R. Stürmer, *Liebigs Ann. Chem.* **1991**, 311; (b) J. E. Baldwin, P. G. Bulger, R. Marquez, *Tetrahedron* **2002**, *58*, 5441; (c) M. Morillas, J. Clotet, B. Rubi, D. Serra, J. Arino, F. G. Hegardt, G. Asins, *Biochem. J.* **2000**, *351*, 495.
- [95] (a) K. Y.-K. Chow, J. W. Bode, *J. Am. Chem. Soc.* **2004**, *126*, 8126; (b) J. L. Bilke, M. Dzuganova, R. Fröhlich, E.-U. Würthwein, *Org. Lett.* **2005**, *7*, 3267; (c) H. U. Vora, T. Rovis, *J. Am. Chem. Soc.* **2007**, *129*, 13796; (d) H. U. Vora, J. R. Moncecchi, O. Epstein, T. Rovis, *J. Org. Chem.* **2008**, *73*, 9727.
- [96] (a) J. M. Janey, *Angew. Chem. Int. Ed.* **2005**, *44*, 4292; (b) A. M. R. Smith, K. K. Hii, *Chem. Rev.* **2011**, *111*, 1637.
- [97] T. Vilaivan, W. Bhanthumnavin, *Molecules* **2010**, *15*, 917.
- [98] I. Gonzalez, G. Jou, J. M. Caba, F. Albericio, P. Lloyd-Williams, E. Giralt, *J. Chem. Soc. Perkin Trans. 1* **1996**, 1427.
- [99] (a) Y. Le Merrer, A. Dureault, C. Gravier, D. Languin, J. C. Depezay, *Tetrahedron Lett.* **1985**, *26*, 319; (b) T. Suami, K. Tadano, Y. Imura, H. Yokoo, *J. Carbohydr. Chem.* **1986**, *5*, 1; (c) E. J. Corey, A. Marfat, G. Goto, F. Brion, *J. Am. Chem. Soc.* **1980**, *102*, 7984.
- [100] (a) Y. Hayashi, J. Knayama, J. Yamaguchi, M. Shoji, *J. Org. Chem.* **2002**, *67*, 9443; (b) Y. Ito, Y. Kobayashi, T. Kawabata, M. Takase, S. Terashima, *Tetrahedron* **1989**, *45*, 5767.
- [101] (a) C. Agami, F. Couty, C. Lequesne, *Tetrahedron Lett.* **1994**, *35*, 3309; (b) A. Alexakis, J.-P. Tranchier, N. Lensen, P. Mangeney, *J. Am. Chem. Soc.* **1995**, *117*, 10767; (c) M. Asami, T. Mukaiyama, *Chem. Lett.* **1983**, 93; (d) L. Colombo, M. D. Giacomo, *Tetrahedron Lett.* **1999**, *40*, 1977; (e) M. P. Heitz, F. Gellibert, C. Mioskowski, *Tetrahedron Lett.* **1986**, *27*, 3859.
- [102] (a) D. Enders, U. Reinhold, *Synlett* **1994**, 792; (b) D. Enders, U. Reinhold, *Liebigs Ann.* **1996**, 11.
- [103] F. A. Davis, B. C. Chen, *Chem. Rev.* **1992**, *92*, 919.
- [104] (a) K. Morikawa, J. Park, P. G. Andersson, T. Hashiyama, K. B. Sharpless, *J. Am. Chem. Soc.* **1993**, *115*, 8463; (b) T. Hashiyama, K. Morikawa, K. B. Sharpless, *J. Org. Chem.* **1992**, *57*, 5067.
- [105] (a) W. Adam, R. T. Fell, C. Mock-Knoblauch, C. R. Saha-Möller, *Tetrahedron Lett.* **1996**, *37*, 6531; (b) W. Adam, R. T. Fell, V. R. Stegmann, C. R. Saha-Möller, *J. Am. Chem. Soc.* **1998**, *120*, 708.
- [106] M. Koprowski, J. Luczak, E. Krawczyk, *Tetrahedron* **2006**, *62*, 12363.
- [107] Y. Zhu, Y. Tu, H. Yu, Y. Shi, *Tetrahedron Lett.* **1998**, *39*, 7819.
- [108] Y. Zhu, L. Shu, Y. Tu, Y. Shi, *J. Org. Chem.* **2001**, *66*, 1818.
- [109] N. Momiyama, H. Yamamoto, *J. Am. Chem. Soc.* **2003**, *125*, 6038.
- [110] Y. Hayashi, J. Yamaguchi, K. Hibino, M. Shoji, *Tetrahedron Lett.* **2003**, *44*, 8293.
- [111] S. P. Brown, M. P. Brochu, C. J. Sinz, D. W. C. MacMillan, *J. Am. Chem. Soc.* **2003**, *125*, 10808.
- [112] G. Zhong, *Angew. Chem. Int. Ed.* **2003**, *42*, 4247.
- [113] (a) S. Kumarn, D. M. Shawn, D. A. Longbottom, S. V. Ley, *Chem. Commun.* **2006**, 3211; (b) L. Yang, R.-H. Liu, B. Wang, L.-L. Weng, H. Zheng, *Tetrahedron Lett.* **2009**, *50*, 2628; (c) G. Zhong, *Chem. Commun.* **2004**, 606; (d) I. K. Mangion, D. W. C.

8. Bibliography

- MacMillan, *J. Am. Chem. Soc.* **2005**, *127*, 3696; (e) G. Zhong, Y. Yu, *Org. Lett.* **2004**, *6*, 1637.
- [114] (a) S.-G. Kim, T.-H. Park, *Tetrahedron Lett.* **2006**, *47*, 9067; (b) H.-M. Guo, L. Cheng, L.-F. Cun, L.-Z. Gong, A.-Q. Mi, Y.-Z. Jang, *Chem. Commun.* **2006**, 428.
- [115] (a) A. Boegevig, H. Sunden, A. Cordova, *Angew. Chem. Int. Ed.* **2004**, *43*, 1109; (b) A. Cordova, H. Sunden, A. Boegevig, M. Johansson, F. Himo, *Chem. Eur. J.* **2004**, *10*, 3673; (c) Y. Hayashi, J. Yamaguchi, T. Sumiya, M. Shoji, *Angew. Chem. Int. Ed.* **2004**, *43*, 1112; (d) N. Momiyama, H. Torii, S. Saito, H. Yamamoto, *Proced. Nat. Acad. Sci.* **2004**, *101*, 5374; (e) Y. Hayashi, J. Yamaguchi, T. Sumiya, K. Hibino, M. Shoji.
- [116] (a) D. B. Ramachary, C. F. Barbas III, *Org. Lett.* **2005**, *7*, 1577; (b) J. Joseph, D. B. Ramachary, E. D. Jemmis, *Org. Biomol. Chem.* **2006**, *4*, 2685.
- [117] P. Jiao, H. Yamamoto, *Synlett* **2009**, *16*, 2685.
- [118] T. Kano, H. Mii, K. Maruoka, *J. Am. Chem. Soc.* **2009**, *131*, 3450.
- [119] M. J. P. Vaismaa, S. C. Y. Yau, N. C. O. Tomkinson, *Tetrahedron Lett.* **2009**, *50*, 3625.
- [120] H. Gotoh, Y. Hayashi, *Chem. Commun.* **2009**, 3083.
- [121] L.-W. Xu, L. Li, Z.-H. Shia, *Adv. Synth. Catal.* **2010**, *352*, 243.
- [122] O. Lifchits, N. Demoulin, B. List, *Angew. Chem. Int. Ed.* **2011**, *50*, 9680.
- [123] S. McCooey, S. Connon, *Org. Lett.* **2007**, *9*, 599.
- [124] L. Qin, L. Li, L. Yi, C.-S. Da, Y.-F. Zhou, *Chirality* **2011**, *23*, 527.
- [125] E. W. Colvin, A. D. Robertson, S. Wakharkar, *J. Chem. Soc., Chem. Commun.* **1983**, 312-314.
- [126] (a) F. G. Bordwell. *Bordwell pKa Table (Acidity in DMSO)*. <http://www.chem.wisc.edu/areas/reich/pkatable/>, accessed on November 9, 2011; (b) P. Christ, A. G. Lindsay, S. S. Vormittag, J.-M. Neudörfl, A. Berkessel, A. C. O'Donoghue, *Chem. Eur. J.* **2011**, *17*, 8524; (c) R. Williams. http://research.chem.psu.edu/brpgroup/pKa_compilation.pdf, accessed on November 9, 2011
- [127] L. A. Badovskaya, G. D. Krapivin, T. Y. Kalyugina, V. G. Kul'nevich, G. F. Muzychenko, *Zh. Org. Khim.* **1975**, *11*, 2446.
- [128] N. Tada, L. Cui, H. Okubo, T. Miura, A. Itoh, *Adv. Synth. Catal.* **2010**, *352*, 2383.
- [129] A. Erkkilä, P. M. Pihko, *Eur. J. Org. Chem.* **2007**, 4205.
- [130] X. Li, B. Borhan, *J. Am. Chem. Soc.* **2008**, *130*, 16126.
- [131] K. Zumbansen, A. Döhring, B. List, *Adv. Synth. Catal.* **2010**, *352*, 1135.
- [132] A. K. Chatterjee, T.-L. Choi, D. P. Sanders, R. H. Grubbs, *J. Am. Chem. Soc.* **2003**, *125*, 11360.
- [133] W. C. Still, C. Gennari, *Tetrahedron Lett.* **1983**, *24*, 4405.
- [134] (a) M. Prévost, K. A. Woerpel, *J. Am. Chem. Soc.* **2009**, *131*, 14182; (b) S. Sano, T. Takehisa, S. Ogawa, K. Yokoyama, Y. Nagao, *Chem. Pharm. Bull.* **2002**, *50*, 1300.
- [135] K. S. Yoo, C. P. Park, C. H. Yoon, S. Sakaguchi, J. O'Neill, K. W. Jung, *Org. Lett.* **2007**, *9*, 3933.
- [136] C. Reisinger, *Dissertation*. Köln University, **2010**.
- [137] B. Vakulya, S. Varga, A. Csampai, T. Soos, *Org. Lett.* **2005**, *7*, 1967.
- [138] H. Diaz-Arauzo, J. M. Cook, *J. Nat. Prod.* **1990**, *53*, 112.
- [139] S. Juila, J. Guixer, J. Masana, J. Rocas, S. Colonna, R. Annuziata, H. Molinari, *J. Chem. Soc. Perkin Trans. 1* **1982**, 1317.
- [140] Y. Wu, R. P. Singh, L. Deng, *J. Am. Chem. Soc.* **2011**, *133*, 15219.
- [141] (a) M. B. Schmid, K. Zeitler, R. M. Gschwind, *Chem. Sci.* **2011**, *2*, 1793; (b) M. B. Schmid, K. Zeitler, R. M. Gschwind, *J. Am. Chem. Soc.* **2011**, *133*, 7065; (c) M. B. Schmid, K. Zeitler, R. M. Gschwind, *J. Org. Chem.* **2011**, *76*, 3005.

8. Bibliography

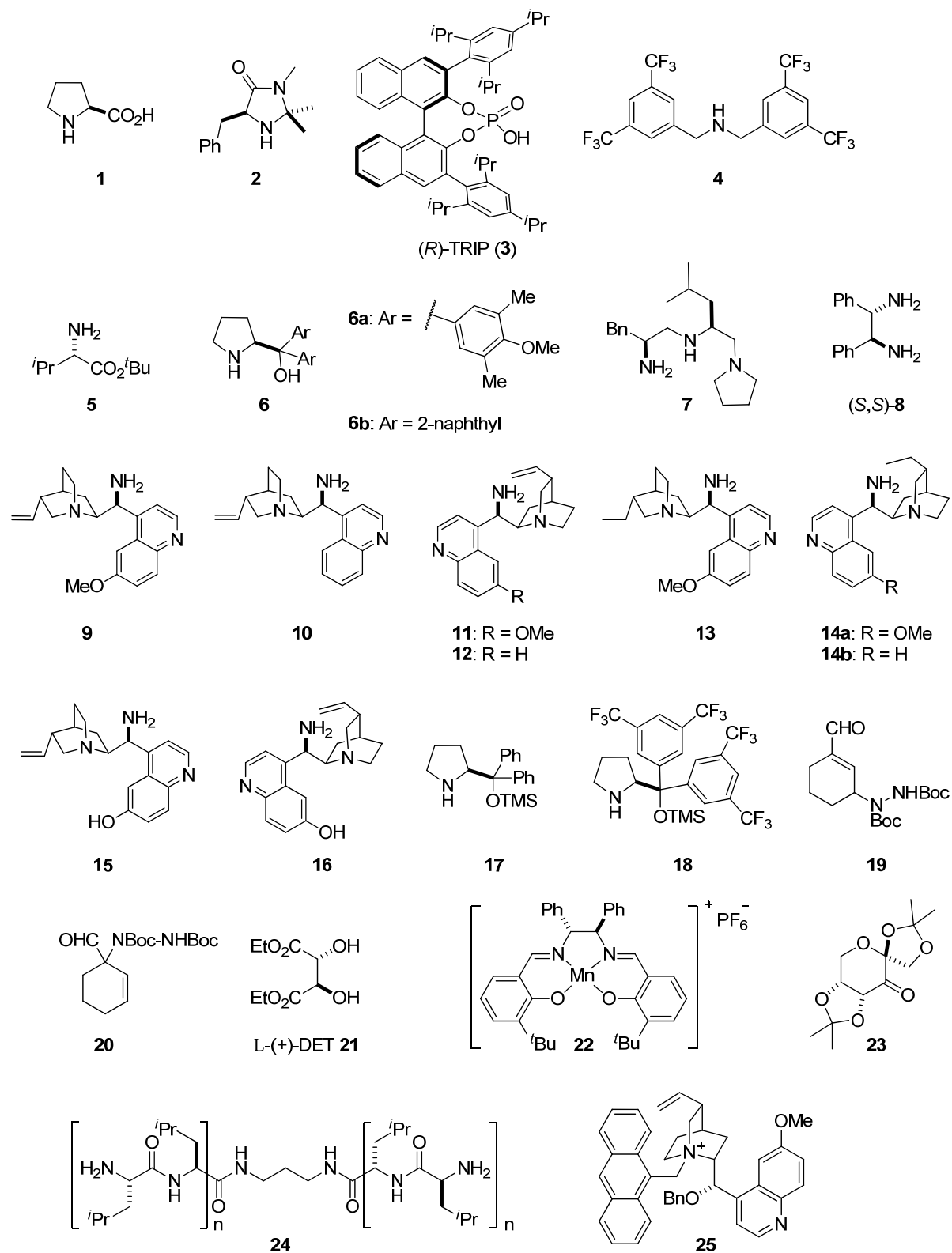
- [142] (a) D. Crepaux, J. M. Lehn, R. R. Dean, *Mol. Phys.* **1969**, *16*, 225; (b) L. Ghosez, P. Bayard, P. Nshimyumukiza, V. Gouverneur, F. Sainte, R. Beaudegnies, M. Rivera, A. M. Frisque-Hesbain, C. Wynants, *Tetrahedron* **1995**, *51*, 11021.
- [143] R. K. Harris, S. Ng, A. Connelly, *Magn. Reson. Chem.* **1991**, *29*, 1152.
- [144] U. Vogeli, W. V. Philipsborn, *Org. Magn. Reson.* **1975**, *7*, 617.
- [145] J. Schripsema, R. Verpoorte, A. B. Svendsen, C. Erkelens, *Spectr. Lett.* **1987**, *20*, 777.
- [146] (a) S. Sharif, G. S. Denisov, M. D. Toney, H.-H. Limbach, *J. Am. Chem. Soc.* **2007**, *129*, 6313; (b) S. Sharif, E. Fogle, M. D. Toney, G. S. Denisov, I. G. Shenderovich, G. Buntkowsky, P. M. Tolstoy, M. C. Huot, H.-H. Limbach, *J. Am. Chem. Soc.* **2007**, *129*, 9558; (c) S. Sharif, D. Schagen, M. D. Toney, H.-H. Limbach, *J. Am. Chem. Soc.* **2007**, *129*, 4440.
- [147] D. D. Muccio, W. G. Copan, W. W. Abrahamson, G. D. Mateescu, *Org. Magn. Reson.* **1984**, *22*, 121.
- [148] (a) R. Díaz-Torres, S. Alvarez, *Dalton Trans.* **2011**, *40*, 10742; (b) A. J. Kotlewska, F. van Rantwijk, R. A. Sheldon, I. W. C. E. Arends, *Green Chem.* **2011**, *13*, 2154.
- [149] C. D. Schwieters, J. J. Kuszewski, G. M. Clore, *Prog Nucl Mag Res Sp* **2006**, *48*, 47-62.
- [150] P. Galzerano, F. Pesciaioli, A. Mazzanti, G. Bartoli, P. Melchiorre, *Angew. Chem. Int. Ed.* **2009**, *48*, 7892-7894.
- [151] M. S. Jadhav, P. Righi, E. Marcantoni, G. Bencivenni, *J. Org. Chem.* **2011**, *ASAP*, doi: 10.1021/jo2024976.
- [152] J. K. Kochi, *J. Am. Chem. Soc.* **1963**, *85*, 1958.
- [153] X. Feng, L. Shu, Y. Shi, *J. Am. Chem. Soc.* **1999**, *121*, 11002.
- [154] G. Revial, I. Jabin, M. Pfau, *Tetrahedron Asym.* **2000**, *11*, 4975.
- [155] S. A. Snyder, E. J. Corey, *Tetrahedron Lett.* **2006**, *47*, 2083.
- [156] R. M. Carman, A. C. Rayner, *Aust. J. Chem.* **1994**, *47*, 2087.
- [157] P. Vogel, J. Cossy, J. Plumet, O. Arjona, *Tetrahedron* **1999**, *55*, 13521.
- [158] H. Becker, M. A. Soler, K. B. Sharpless, *Tetrahedron* **1995**, *51*, 1345.
- [159] I. Washington, K. N. Houk, *Angew. Chem. Int. Ed.* **2001**, *40*, 4485.
- [160] (a) A. Nemchik, V. Badescu, O. Phanstiel IV, *Tetrahedron* **2003**, *59*, 4315; (b) O. E. Ansong, S. Jansen, Y. Wei, G. Pomrink, H. Lu, S. Li, Y. Guo, *J. Mater. Chem.* **2007**, *17*, 4499.
- [161] J. A. King Jr., G. L. Bryant Jr., *J. Org. Chem.* **1992**, *57*, 5137.
- [162] N. A. Turovskii, I. A. Opeida, O. V. Kushch, *Russ. J. Org. Chem.* **2003**, *39*, 642.
- [163] W. C. Agwada, *Chem. Eng. Data* **1982**, *27*, 479.
- [164] (a) G. Jiang, B. List, *Angew. Chem. Int. Ed.* **2011**, *50*, 9471; (b) A. Lee, A. Michrowska, S. Sulzer-Mosse, B. List, *Angew. Chem. Int. Ed.* **2011**, *50*, 1707.
- [165] N. Fu, L. Zhang, J. Li, S. Luo, J.-P. Cheng, *Angew. Chem. Int. Ed.* **2011**, *50*, 11451.
- [166] B. Gourdet, H. W. Lam, *Angew. Chem. Int. Ed.* **2010**, *49*, 8733.
- [167] C. H. Cheon, H. Yamamoto, *Chem. Commun.* **2011**, *47*, 3043.
- [168] (a) J. B. Brazier, J. L. Cavill, R. L. Elliott, G. Evans, T. J. K. Gibbs, I. L. Jones, J. A. Platts, N. C. O. Tomkinson, *Tetrahedron* **2009**, *65*, 9961; (b) J. Cavill, J. Peters, N. Tomkinson, *Chem. Commun.* **2003**, 728; (c) J. L. Cavill, R. L. Elliott, G. Evans, I. L. Jones, J. A. Platts, A. M. Ruda, N. C. O. Tomkinson, *Tetrahedron* **2006**, *62*, 410.
- [169] (a) L. Y. Chen, H. He, B.-J. Pei, W. H. Chan, A. W. M. Lee, *Synthesis* **2009**, 1573; (b) H. He, B.-J. Pei, H.-H. Chou, T. Tian, W.-H. Chan, A. W. M. Lee, *Org. Lett.* **2008**, *10*, 2421; (c) Y. Langlois, A. Petit, P. Remy, M. C. Scherrmann, C. Kouklovsky, *Tetrahedron Lett.* **2008**, *49*, 5576; (d) T. Tian, B.-J. Pei, Q.-H. Li, H. He, L. Y. Chen, X. Zhou, W. K. Chan, A. W. M. Lee, *Synlett* **2009**, 2115.
- [170] (a) W. Kroutil, M. E. Lasterra-Sanchez, S. J. Maddrell, P. Mayon, P. Morgan, S. M. Roberts, S. R. Thornton, C. J. Todd, M. Tueter, *J. Chem. Soc., Perkin Trans. 1* **1996**,

8. Bibliography

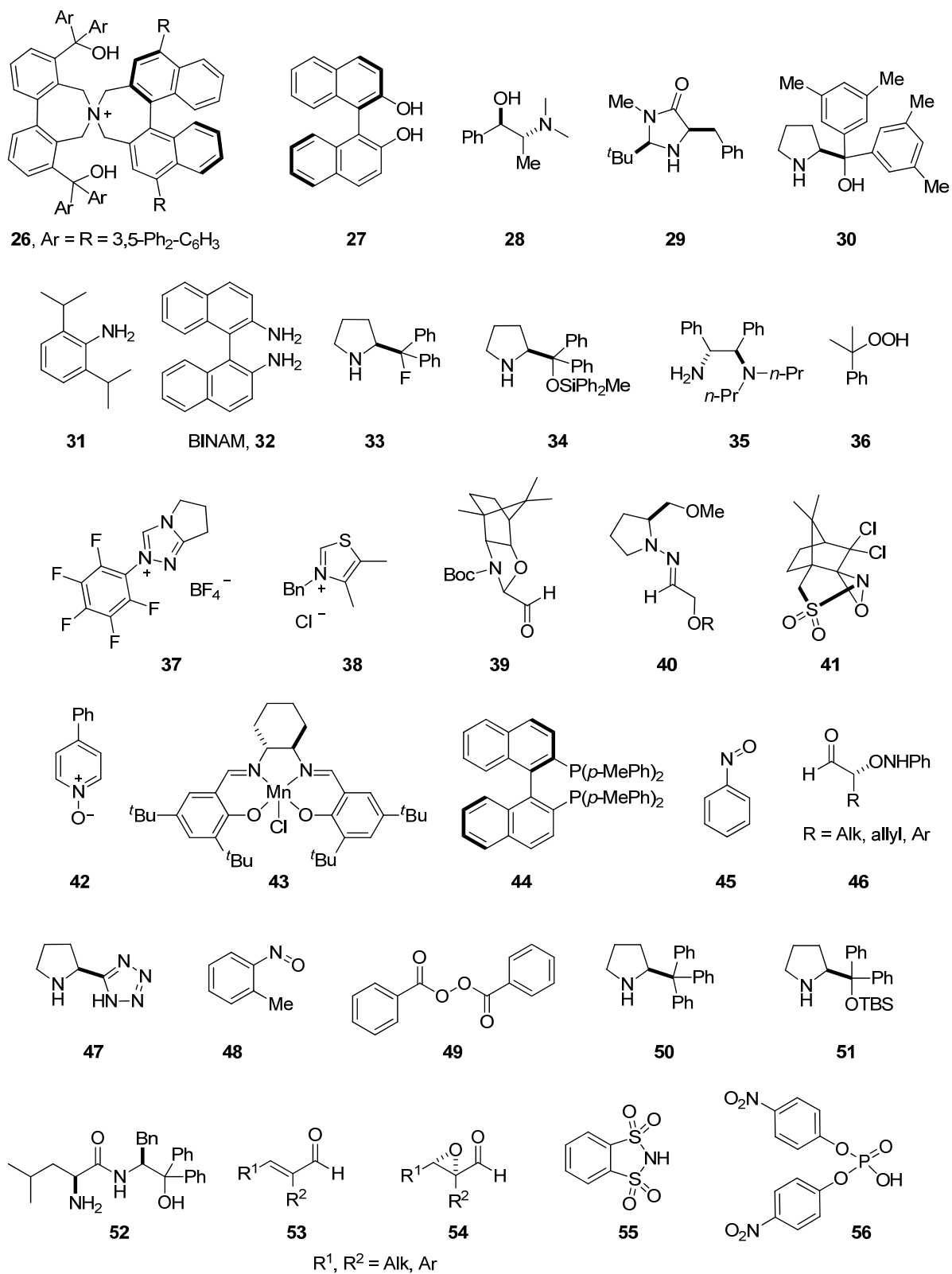
- 23, 2837; (b) B. Hauer, J. F. Bickley, J. Massue, P. C. A. Pena, S. M. Roberts, J. Skidmore, *Can. J. Chem.* **2002**, *80*, 546; (c) P. E. Coffey, K. H. Drauz, S. M. Roberts, J. Skidmore, J. A. Smith, *Chem. Commun.* **2001**, *22*, 2330; (d) P. A. Bentley, J. F. Bickley, S. M. Roberts, A. Steiner, *Tetrahedron Lett.* **2001**, *42*, 3741; (e) J. V. Allen, K. H. Drauz, R. W. Flood, S. M. Roberts, J. Skidmore, *Tetrahedron Lett.* **1999**, *40*, 5417; (f) J. V. Allen, S. Bergeron, M. J. Griffiths, S. Mukherjee, S. M. Roberts, N. M. Williamson, L. E. Wu, *J. Chem. Soc., Perkin Trans. 1* **1998**, 3171.
- [171] (a) W. Adam, P. B. Rao, H.-G. Degen, A. Levai, T. Patonay, C. R. Saha-Möller, *J. Org. Chem.* **2002**, *67*, 259; (b) S. Arai, M. Oku, M. Miura, T. Shioiri, *Synlett* **1998**, *11*, 1201; (c) S. Arai, H. Tsuge, M. Oku, M. Miura, T. Shioiri, *Tetrahedron* **2002**, *58*, 1623.
- [172] A. Lattanzi, *Adv. Synth. Catal.* **2006**, *348*, 339.
- [173] X. Tian, C. Cassani, Y. Liu, A. Moran, A. Urakawa, P. Galzerano, E. Arceo, P. Melchiorre, *J. Am. Chem. Soc.* **2011**, *133*, 17934.
- [174] R. I. Storer, D. E. Carrera, Y. Ni, D. W. C. MacMillan, *J. Am. Chem. Soc.* **2006**, *128*, 84.
- [175] X.-H. Liu, L.-L. Lin, X.-M. Feng, *Acc. Chem. Res.* **2011**, *44*, 574.
- [176] N. A. Turovskii, I. A. Opeida, O. V. Kushch, *Russ. J. Org. Chem.* **2003**, *39*, 687.
- [177] (a) T. Akiyama, J. Itoh, K. Yokota, K. Fuchibe, *Angew. Chem., Int. Ed.* **2004**, *43*, 1566; (b) T. Akiyama, H. Morita, J. Itoh, K. Fuchibe, *Org. Lett.* **2005**, *7*, 2583; (c) T. Akiyama PCT Int. Appl., WO 200409675, **2004**; (d) T. Akiyama, Y. Saitoh, H. Morita, K. Fuchibe, *Adv. Synth. Catal.* **2005**, *347*, 1523; (e) D. Uraguchi, M. Terada, *J. Am. Chem. Soc.* **2004**, *126*, 5356; (f) D. Uraguchi, K. Sorimachi, M. Terada, *J. Am. Chem. Soc.* **2004**, *126*, 11804; (g) D. Uraguchi, K. Sorimachi, M. Terada, *J. Am. Chem. Soc.* **2005**, *127*, 9360; (h) M. Terada, D. Uraguchi, K. Sorimachi, H. Shimizu, PCT Int. Appl., WO 2005070875, **2005**; (i) B. Vakulya, S. Varga, A. Csámpai, T. Soós, *Org. Lett.* **2005**, *7*, 1967.
- [178] P. García-García, F. Lay, P. García-García, C. Rabalakos, B. List, *Angew. Chem. Int. Ed.* **2009**, *48*, 4363.
- [179] T. C. Jones, N. C. O. Tomkinson, *Org. Synth.* **2007**, *84*, 70.
- [180] C. C. Browder, F. P. Marmsäter, F. G. West, *Can. J. Chem.* **2004**, *82*, 375.
- [181] D. A. Colby, R. G. Bergman, J. A. Ellman, *J. Am. Chem. Soc.* **2006**, *128*, 5604.
- [182] E. Piers, K. A. Skupinska, D. J. Wallace, *Synlett* **1999**, 1867.
- [183] V. P. Baillargeon, J. K. Stille, *J. Am. Chem. Soc.* **1986**, *108*, 452.
- [184] K. Basu, J. Richards, L. A. Paquette, *Synthesis* **2004**, 2841.
- [185] Y. Gao, R. M. Hanson, J. M. Kluder, S. Y. Ko, H. Masamune, K. B. Sharpless, *J. Am. Chem. Soc.* **1987**, *109*, 5765.
- [186] M. Klussmann, L. Ratjen, S. Hoffmann, V. Wakchaure, R. Goddard, B. List, *Synlett* **2010**, *14*, 2189.
- [187] P. Yip, D. A. Case, *J. Magn. Reson.* **1989**, *83*, 643.
- [188] G. Revial, I. Jabin, M. Pfau, *Tetrahedron: Asym.* **2000**, *11*, 4975.
- [189] T. Nishimura, T. Onoue, K. Ohe, S. Uemura, *J. Org. Chem.* **1999**, *64*.
- [190] X. Gao, H. Han, M. J. Krische, *J. Am. Chem. Soc.* **2011**, *133*, 12795.
- [191] C. Givélet, V. Bernat, M. Danel, C. Andre-Barres, H. Vial, *Eur. J. Org. Chem.* **2007**, *19*, 3095.
- [192] O. Yamada, K. Ogasawara, *Tetrahedron Lett.* **1998**, *39*, 7747.
- [193] J. R. DeBergh, K. M. Spivey, J. M. Ready, *J. Am. Chem. Soc.* **2008**, *130*, 7828.
- [194] M. Shibasaki, S. Terashima, S.-I. Yamada, *Chem. Pharm. Bull.* **1976**, *24*, 315.

9. APPENDIX

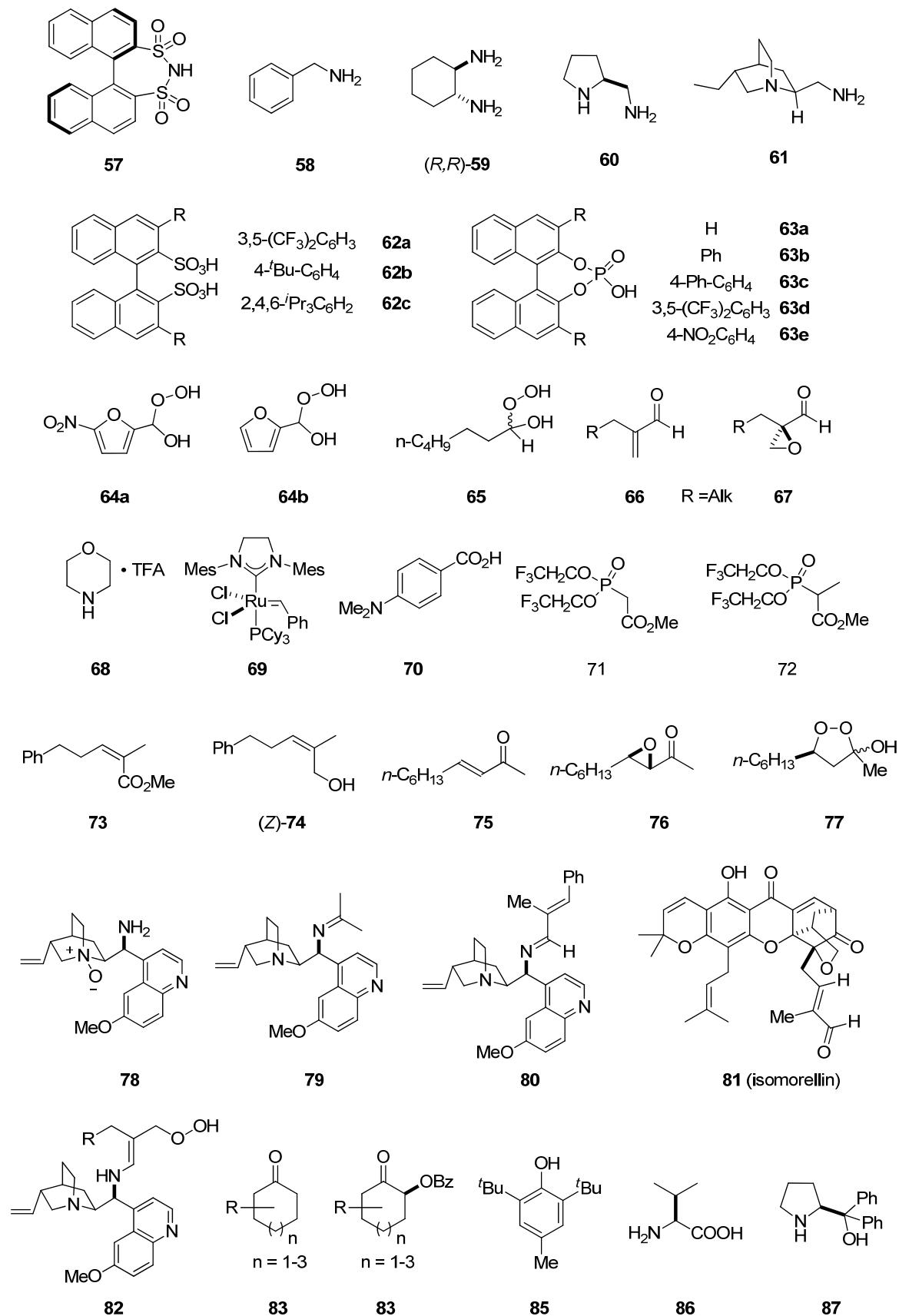
9.1 Structure Index



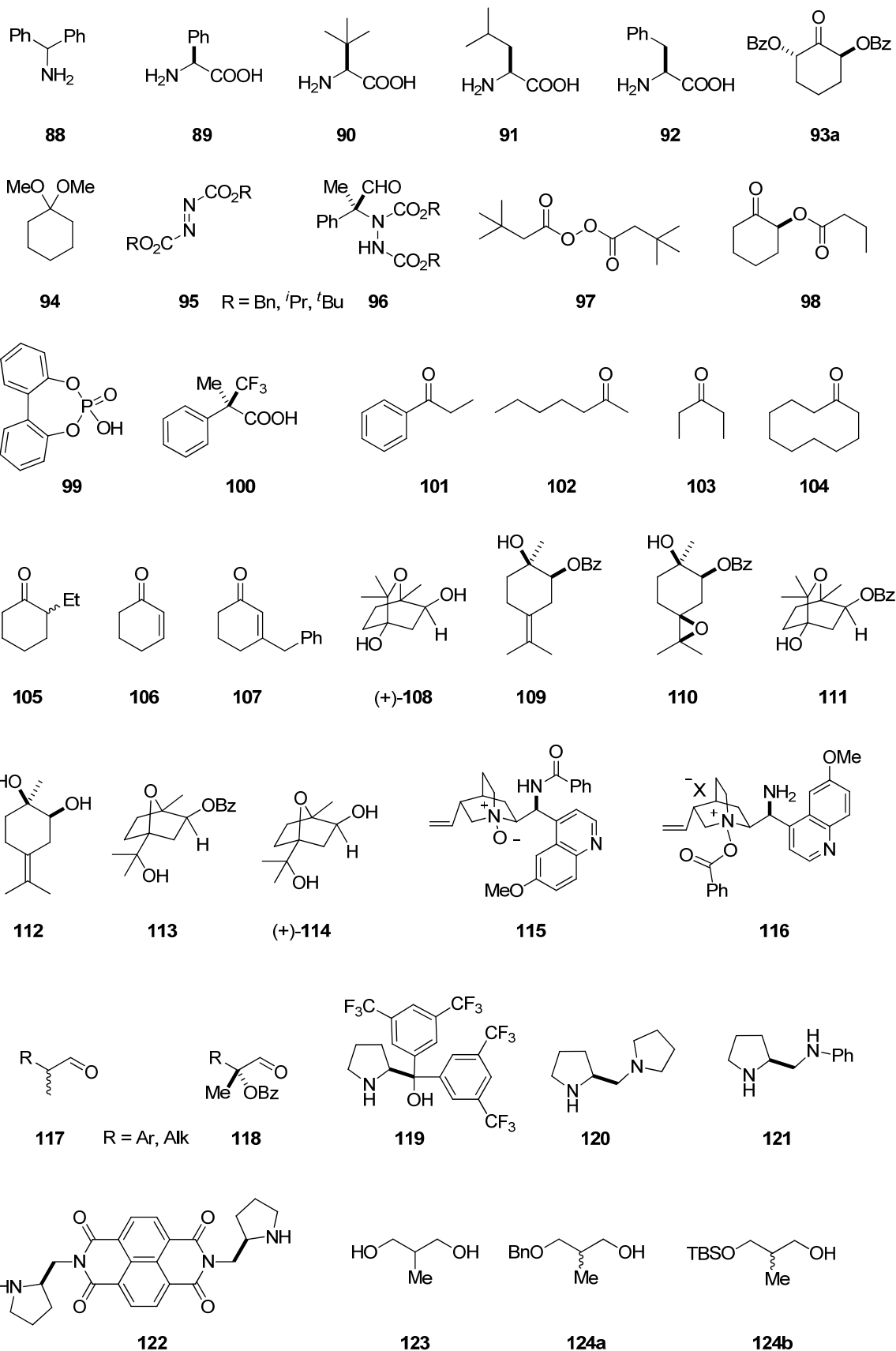
9. Appendix



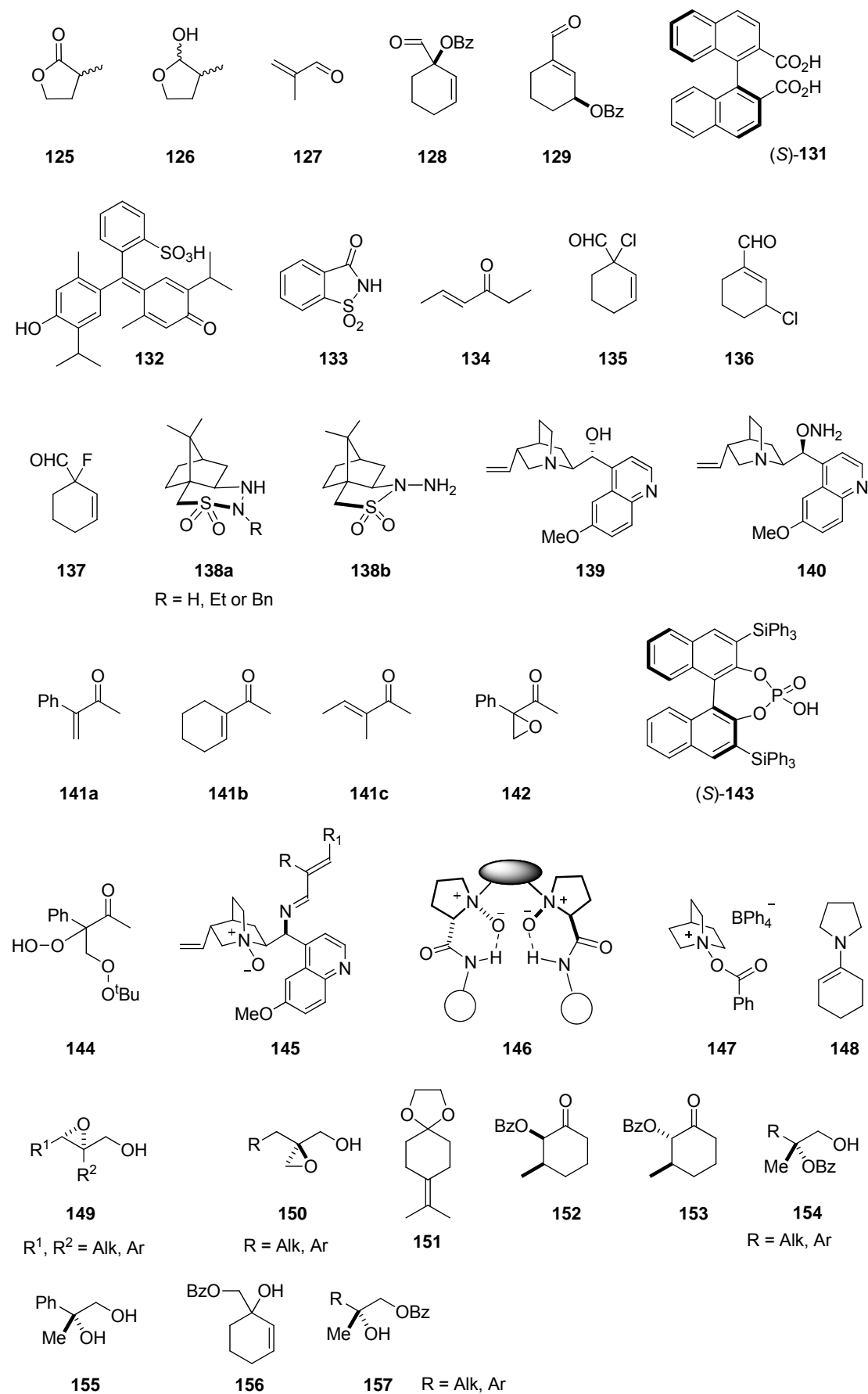
9. Appendix



9. Appendix



9. Appendix



9.2 Erklärung

“Ich versichere, dass ich die von mir vorgelegte Dissertation selbständig angefertigt, die benutzten Quellen und Hilfsmittel vollständig angegeben und die Stellen der Arbeit – einschließlich Tabellen, Karten und Abbildungen –, die anderen Werken im Wortlaut oder dem Sinn nach entnommen sind, in jedem Einzelfall als Entlehnung kenntlich gemacht habe; dass diese Dissertation noch keiner anderen Fakultät oder Universität zur Prüfung vorgelegen hat; dass sie – abgesehen von unten angegebenen Teilpublikationen – noch nicht veröffentlicht worden ist sowie, dass ich eine solche Veröffentlichung vor Abschluss des Promotionsverfahrens nicht vornehmen werde. Die Bestimmungen der Promotionsordnung sind mir bekannt. Die von mir vorgelegte Dissertation ist von Herrn Professor Dr. Benjamin List betreut worden.“

Mülheim an der Ruhr, Februar 2012

Bisher sind folgende Teilpublikationen veröffentlicht worden:

“Catalytic Asymmetric Epoxidation of α -Branched Enals”: O. Lifchits, C. M. Reisinger, B. List, *J. Am. Chem. Soc.* **2010**, *132*, 10227-10229.

“Direct Asymmetric α Benzoyloxylation of Cyclic Ketones”: O. Lifchits, N. Demoulin, B. List, *Angew. Chem.* **2011**, *123*, 9854-9857; *Angew. Chem. Int. Ed.* **2011**, *50*, 9680-9683.

9.3 Lebenslauf

Olga Lifchits

Geboren am 3. Juli 1984
in Minusinsk, Russland
Staatsangehörigkeit kanadisch

Akademischer Werdegang

Promotion

09.2008 – 02.2012 Dissertation im Arbeitskreis von Prof. Dr. Benjamin List
Max-Planck-Institut für Kohlenforschung, Mülheim an der Ruhr
mit dem Titel „Organocatalytic Approaches to Asymmetric Oxidation:
Epoxidation of α -Branched Enals and α -Benzoyloxylation of Cyclic
Ketones”

Hochschulstudium

09.2006-08.2008 M.Sc. im Arbeitskreis von Prof. André Charette
Université de Montréal, Kanada
mit dem Titel „Nucleophilic Ring-Opening of Methyl-1-Nitrocyclopro-
panecarboxylates”

09.2002-05.2008 Biochemiestudium an der University of Toronto, Canada
Abschluss: Hon. B.Sc., GPA 3.95/4.00
Senior thesis im Arbeitskreis von Prof. Mark Lautens mit dem Titel
„ $P(O^iPr)_3$ as an improved reagent for *gem*-Dibromoolefination of
Aldehydes and Ketones.”

Schulbildung

1999-2002 Midland Secondary School, Kanada
Abschluss: Ontario Secondary School Diploma
1998-1999 Forest Hill Collegiate Institute, Kanada
1996-1997 Schule no. 32, Krasnojarsk, Russland
1991-1996 Schule no. 16, Minusinsk, Russland